Shining a light on catalytic chain transfer

Document Version:
Publisher's PDF, also known as Version of Record (includes final page, issue and volume numbers)

Please check the document version of this publication:

• A submitted manuscript is the version of the article upon submission and before peer-review. There can be important differences between the submitted version and the official published version of record. People interested in the research are advised to contact the author for the final version of the publication, or visit the DOI to the publisher's website.
• The final author version and the galley proof are versions of the publication after peer review.
• The final published version features the final layout of the paper including the volume, issue and page numbers.

Link to publication

Download date: 20. Jan. 2020

Shining a Light on Catalytic Chain Transfer

Sebastiaan C.J. Pierik

Shining a Light on
Catalytic Chain Transfer

PROEFSCHRIFT

ter verkrijging van de graad van doctor aan de
Technische Universiteit Eindhoven, op gezag van de
Rector Magnificus, prof.dr. R.A. van Santen, voor
een commissie aangewezen door het College voor
Promoties in het openbaar te verdedigen
op woensdag 20 maart 2002 om 16.00 uur

door

Sebastianus Christoffel Josephus Pierik

geboren te Spaubeek

Dit proefschrift is goedgekeurd door de promotoren:

prof.dr. A.M. van Herk
en
prof.dr.ir. A.L. German

Copromotor:
prof.dr. T.P. Davis

Table of contents

Table of contents

Chapter 1

General Introduction

Synopsis: After a brief introduction in free radical polymerization in general and catalytic chain transfer polymerization in particular, the aims of the presented investigations are discussed. Next, a short outline of all chapters in this thesis is given.

1.1 Free-radical polymerization

Free-radical polymerization is a very versatile polymerization mechanism that can be applied to a wide variety of vinyl monomers. The resulting polymeric materials can be used in applications ranging from packaging materials to coatings as well as automotive parts. These different applications require different material properties, which are determined amongst others by the microstructure of the polymer chain, the interactions between the chains and the types of additives. When we focus on the microstructure, we can distinguish polymers that differ in the structure of the backbone, in molecular weight, in composition and in end groups. In Scheme 1.1 the various microstructural features are presented and for each feature some examples are provided. Furthermore, all these features can be combined in one single polymer. When a polymer consists of more than one monomer, it is called a copolymer. In this class of polymers several variations are known as well. Two linear copolymers with the same overall composition can have a different distribution of the monomers over the polymer chain resulting in random, gradient or even block copolymers.

From this short overview it is clear that in principle many very different microstructures can be obtained. However, in free-radical polymerization it is impossible to obtain a polymer in which all chains have exactly the same structure. They will differ in length, composition, end groups and backbone structure, even when all chains are initiated at exactly the same moment and in the same way. During the polymerization these structural differences will usually

Scheme 1.1 Polymer microstructure

Microstructure

| Backbone structure | + | Composition | + | Molecular weight | + End groups |

e.g.
- linear
- star-shaped
- network
- grafts

one or more monomer(s)
e.g.
- styrenes
- acrylates
- vinyl esters
- dienes
- functional monomers

varying from
10^2 to 10^7 g·mol^{-1}

e.g.
- COOH
- OH
- Br
- double bond

distribution of monomers
e.g.
random
gradient
blockwise
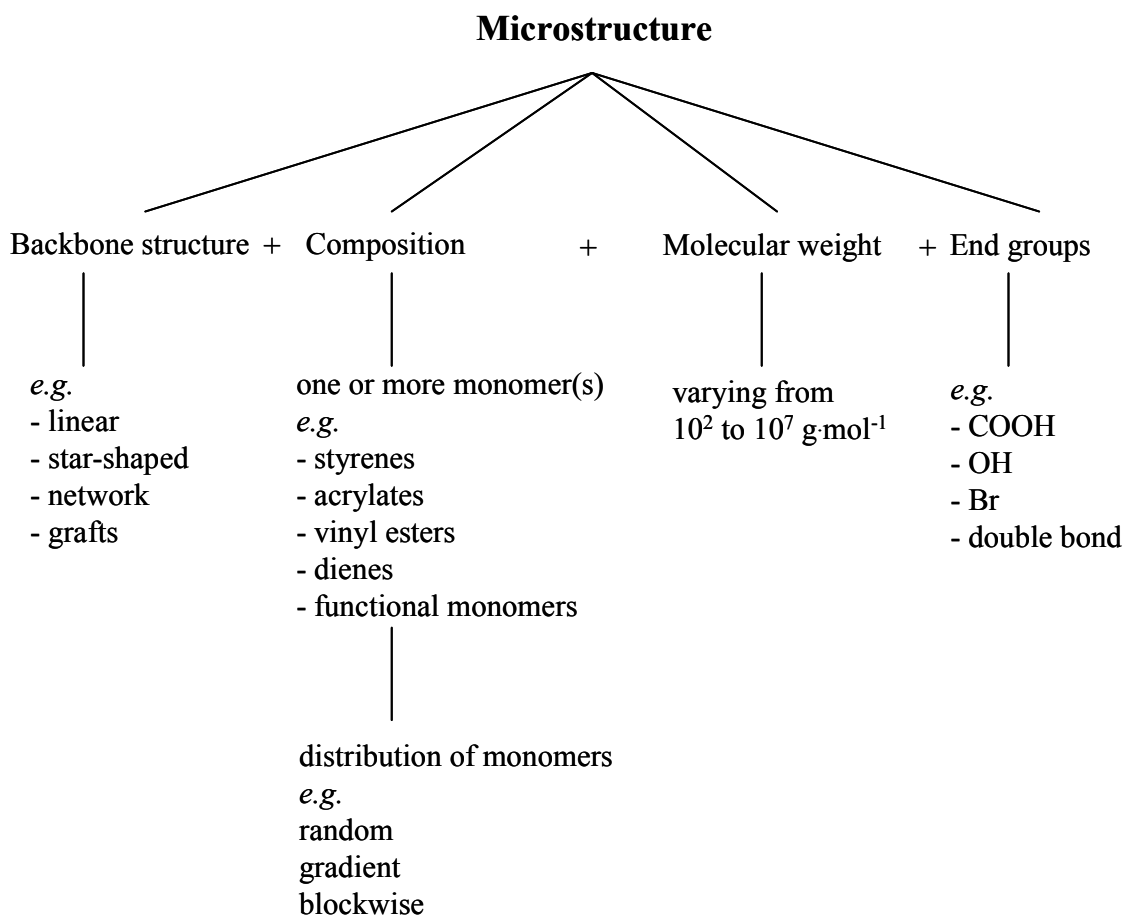
become larger as the ratios of the different components in the reaction mixture change. So it is not easy to control the polymerization and thus to obtain polymers with a predefined structure. In the past two decades several techniques have been developed to control one or more aspects of the chain structure. Many of these are aimed at producing homopolymers with narrow molecular weight distributions and eventually block copolymers. Otsu *et al.* was among the first to work in this field, using disulfides that are capable of both initiating and, after dissociation, reversibly terminating the free-radical polymerization.[1] Since then many other techniques have been developed that are based on reversibly terminating the growing polymeric radicals, like nitroxide mediated polymerization (NMP),[2] atom transfer radical polymerization (ATRP)[3,4] and reversible addition fragmentation chain transfer (RAFT).[5] Together, these form the field of controlled radical polymerization.

1.2 Catalytic chain transfer polymerization

In catalytic chain transfer (CCT) polymerization small quantities of generally an organocobalt complex are used to catalyze chain transfer for methacrylates, styrene and α-methylstyrene. In this way, polymer chain length can be varied practically independently of initiator concentration and therefore of the rate of polymerization. In the polymerization of other monomers like acrylates and vinyl acetate the same catalysts inhibit the polymerization reaction. This catalytic chain transfer behaviour was first described by a Russian research group in the early eighties.[6,7] As it was developed in the same period of time as NMP and ATRP, CCT is often included in the field of controlled radical polymerization as well, although the basic principle is different. The main difference is that in NMP and ATRP in an ideal situation, the growth-time of a single chain equals reaction time due to reversible termination of the growing chains, whereas in CCT a chain is formed within *e.g.* 1 second and cannot grow further.

CCT has several advantages over more traditional ways of controlling molecular weight. In order to obtain low molecular weight polymers no large amounts of chain transfer agents like mercaptans, which can add colour and odour to your product, are required and neither are large amounts of initiator. In addition, the process can be carried out at lower temperatures. Another advantage of CCT is that, under well-chosen conditions, nearly all polymer chains will have an unsaturated bond at the chain end, which remains available for post-reactions. These advantages make CCT a very promising technique for *e.g.* the coatings industry, which is, due to more strict environmental legislation, forced to look for ways to produce coatings with a lower solvent content, the so-called high-solid coatings, which require low molecular weights. Also in the production of water-borne systems via emulsion polymerization CCT can be readily applied. The attractiveness of CCT towards industry is also reflected by the fact that the majority of the early literature on CCT is found in patents.[8,9]

1.3 Aims of the investigations

In academia, CCT has been mostly applied in homopolymerizations of methyl methacrylate (MMA) and styrene. For MMA a general mechanism has been suggested that is now widely accepted. The focus, however, of the majority of the, mostly industry driven, research on CCT has been on novel catalysts and on the application of the macromonomers produced by CCT. That is why many aspects of the mechanism and of the interaction of the catalyst with other compounds are still matters of discussion, although catalytic chain transfer has been discovered more than twenty years ago.

As discussed before, one of the main fields of application for CCT will be in the coatings industry. For the production of polymers for coatings usually a mixture of various types of monomers is used containing *e.g.* both functional and non-functional acrylates and methacrylates and styrene. When we wish to really understand and control these more complex systems containing CCT active monomers like methacrylates and CCT inactive monomers like acrylates in solution or even emulsion, it will be necessary to first thoroughly investigate the homopolymerizations of these monomers and create a set of standard reaction procedures.

So, the aim of this investigation is three-fold:

1) to gain a better understanding of the CCT mechanism, its rate determining step and possible side-reactions involving solvents, initiator, oxygen, additives and contaminants both at low and high conversion. As a reference system the homopolymerization of MMA in the presence of cobaloxime boron fluoride (CoBF) was chosen as this is the best-studied and most straightforward system. Other monomers like styrene and *n*-butyl acrylate (BA) will be studied to investigate the effect of the α-methyl group in the methacrylates.

2) to explore the applicability of CCT in the copolymerization of CCT active and inactive monomers and to describe the process from a mechanistic point of view. Two systems will be investigated MMA - methyl acrylate (MA) and MMA - BA.

3) to describe the feasibility of CCT (co)polymerizations in (mini)emulsion polymerization focusing on the homopolymerization of MMA and the copolymerization of MMA and BA.

1.4 Outline of this thesis

In Chapter 2 a short overview is given of the research on catalytic chain transfer of the past two decades. The mechanisms involved are presented in more detail and in a few cases the effects on molecular weight and conversion are investigated via computer simulations. Finally, the applications of the macromonomers are discussed.

The investigations with respect to the first aim are presented in Chapters 3 to 5. Chapter 3 deals with the effect of reaction conditions on CCT of MMA. The effects of oxygen, initiator concentration, temperature, solvent and additives or contaminants on CCT are discussed. This chapter also discusses the possible effects of diffusion control on CCT and compares a series of homologous methacrylates in well designed experiments. All these reactions are carried out up to low conversion. The effects of higher conversion and longer reaction times, on the other hand, are presented in Chapter 4. Some mechanistic models are presented to explain deviations from free-radical polymerization theory and these models are tested using simulations. The effect of acid and peroxides on the evolution of the molecular weight distribution is discussed.

A last point of discussion with respect to the mechanism of the homopolymerizations is presented in Chapter 5. It deals with the polymerization of monomers that are less active in CCT like styrene or even inactive, like BA. The influence of UV-light on these reactions is investigated and the underlying mechanisms are discussed.

The copolymerizations of MMA and MA as well as BA are discussed in Chapter 6. A kinetic model to describe the experimental observations is developed and a theoretical expression for the experimentally accessible chain transfer coefficient is derived. Furthermore, the effect of the catalytic chain transfer agent on the reactivity ratios is investigated for the MMA – BA system. A few experiments to clarify the effects of conversion, and herewith composition drift, on the formation of copolymeric macromonomers are described. In Chapter 7, the knowledge gained in the previous chapters is used to apply to the polymerization of MMA and the copolymerization of MMA and BA in emulsion and miniemulsion.

Finally in the epilogue, Chapter 8, the aims and results are compared and evaluated, and possible directions for further research are presented.

1.5 References

[1] Otsu, T.; Yoshida, M., *Makromol. Chem., Rapid Commun.* **1982**, *3*, 127.

[2] Solomon, D.H.; Rizzardo, E., Cacioli, P., *Eur. Pat. Appl. EP135280*, **1985**

[3] Kato, M.; Kamigaito, M.; Sawamoto, M.; Higashimura, T., *Macromolecules* **1995**, *28*, 1721.

[4] Wang, J.S.; Matyjaszewski, K., *Macromolecules* **1995**, *28*, 7901.

[5] Chiefari, J.; Chong, Y.K.; Ercole, F.; Krstina, J.; Jeffery, J.; Le, T.P.T.; Mayadunne, R.T.A.; Meijs, G.F.; Moad, C.L.; Moad, G; Thang, S.H., *Macromolecules* **1998**, *31*, 5559

[6] Smirnov, B.R.; Morozova, I.S.; Marchenko, A.P.; Markevich, M.A.; Pushchaeva, L.M.; Enikolopyan, N.S., *Doklady Chemistry* **1980**, *253*, 383.

[7] Enikolopyan, N.S.; Smirnov, B.R.; Ponomarev, G.V.; Belgovskii, I.M., *J. Polym. Sci. Polym. Chem. Ed.* **1981**, *19*, 879.

[8] Carlson, G.M.; Abbey, K.J., *US Patent 4526945*, **1985**

[9] Janowicz, A.H.; Melby, L.R., *US Patent 4680352*, **1987**

Chapter 2

A review on catalytic chain transfer

Synopsis: In this chapter a short introduction into cobalt chemistry in general will be given. Before discussing several aspects of catalytic chain transfer in more detail, the determination of chain transfer coefficients, which are used to compare catalyst activities, is introduced. Emphasis in this chapter will be on the mechanisms involving catalytic chain transfer and possible side-reactions. In a few cases Predici® simulations will be carried out to clarify the effects of the mechanistic features suggested to explain various experimental observations. Finally, the application of the product macromonomers will be discussed.

2.1 Cobalt chemistry

Coenzyme B12[1], of which the structure is shown in Figure 2.1, has played an important role in the development of cobalt chemistry. It serves as a cofactor in various enzymatic reactions that proceed via radical intermediates.[2] In these reactions a hydrogen atom and another substituent X are interchanged as shown in Scheme 2.1.[2,3] This 1,2-rearrangement proceeds via the following steps. First the coenzyme homolytically dissociates into a cob(II)alamin and a 5'-deoxyadenosylradical (the group designated R in Figure 2.1). This radical R• abstracts a hydrogen from the substrate after which an
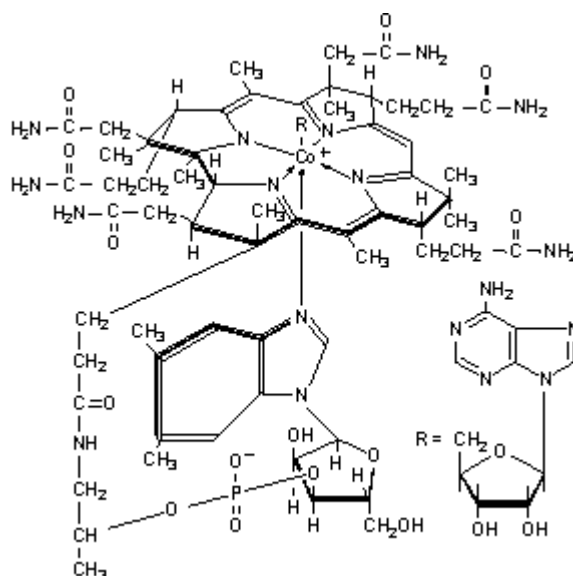
Figure 2.1 The structure of coenzyme B12.

15

Scheme 2.1 1,2-interchange of hydrogen[2]

$$B_{12}\!-\!R \rightleftharpoons B_{12r} + R\bullet$$
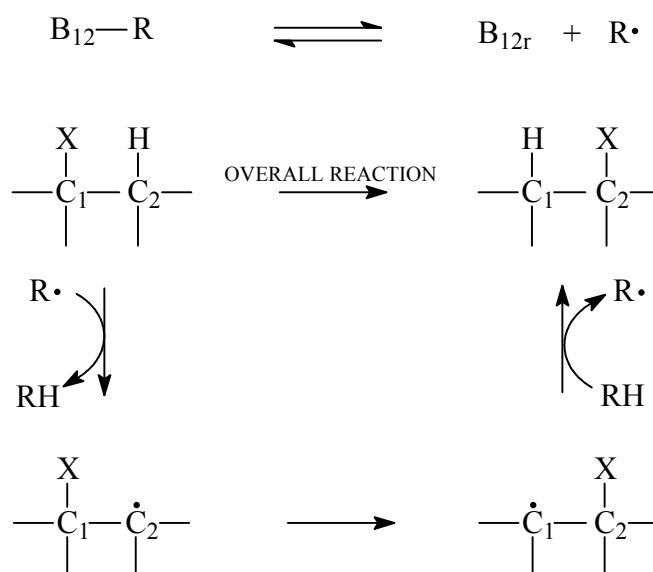
intramolecular rearrangement of the resulting substrate-radical can take place. Finally, the product substrate radical reabstracts a hydrogen from the 5'-deoxyadenosine RH and the 5'-deoxyadenosylradical R• and the cob(II)alamin recombine to reform coenzyme B12. The intermediate cob(II)alamin is a *low spin* d^7-species and therefore has one unpaired electron, just like any organic radical and so it behaves in a similar way. Beside that, the bond dissociation energy of the coenzyme is remarkably low, around 100 kJ· mol^{-1} [2] and that is why coenzyme B12 can serve as a radical source under very mild conditions, *e.g.* in mammalian systems.

Over the past forty years many research groups have been working on the elucidation of the mechanism and kinetics of coenzyme B12 dependent rearrangements.[1,2] Many model compounds like cobalt-Schiff bases and cobaloximes have been synthesized and their reactions and properties have been investigated.[4] Although vitamin B12 itself is only moderately active as a catalytic chain transfer agent[16], some of its model compounds do show high activity[3] and many of their properties can be related to various aspects of both desired and undesired reactions occurring in a catalytic chain transfer polymerization.

2.2 Determination of chain transfer coefficients

The catalytic activities of the various complexes can be compared using the chain transfer coefficient C_T. It is defined as the ratio of the reaction rate constant for transfer k_{tr} and the reaction rate constant for propagation k_p. Experimentally, it can be obtained from a series of polymerizations at different catalyst levels. For each polymerization the number average degree of polymerization is determined and its reciprocal value is plotted against the ratio of catalyst concentration, [Co(II)], and monomer concentration, [M], according to the Mayo-equation:[5]

$$\frac{1}{P_n} = \frac{<k_t>[P\bullet]}{k_p[M]} + \frac{k_{tr}[Co(II)]}{k_p[M]} = \frac{1}{P_{n0}} + C_T\frac{[Co(II)]}{[M]} \tag{2.1}$$

in which P_n is the number average degree of polymerization, P_{n0} is the number average degree of polymerization in absence of transfer agent, $<k_t>$ is the average termination rate constant and [P•] is the radical concentration. The slope of this plot equals the chain transfer coefficient, assuming all added cobalt is available for chain transfer. If this is not true an apparent chain transfer coefficient is determined. Clay and Gilbert developed an alternative method to determine C_T considering the complete molecular weight distribution and not a single average.[6] In this method, for each polymerization, the slope of a plot of the natural logarithm of the number molecular weight distribution $P(M)$ against molecular weight is determined at the high molecular weight end. This is expressed mathematically as

$$\frac{d\ln(P(M))}{dM} = -\left(\frac{<k_t>[P\bullet]}{k_p[M]} + C_T\frac{[Co(II)]}{[M]}\right)\frac{1}{M_o} \tag{2.2}$$

in which M_o is the molar mass of a monomer unit. The slopes determined according to eq 2.2 are plotted against the ratio of transfer agent and monomer concentration. The slope of this plot equals the chain transfer coefficient as well. This method, also called the chain-length distribution (CLD) method, is less sensitive to artifacts in SEC-data caused by noise or improper baseline selection.[7] Heuts *et al.*[8] compared the Mayo-method and the CLD-method. For the Mayo-method they used both number average molecular weight M_n and weight average molecular weight M_w to calculate P_n. In the CLD-method the slope around the peak

molecular weight and at the high molecular weight end was taken. Heuts *et al.*[8] concluded that the CLD-method and the Mayo-method are essentially equivalent from a theoretical point of view.[23] From an experimental point of view, *i.e.* to obtain C_T having highest accuracy, it is best to use either the Mayo-method calculating P_n from M_w or to use the CLD-method around the peak molecular weight.[8]

2.3 Catalytic chain transfer

2.3.1 General introduction

Catalytic chain transfer was first discovered in the late seventies by a Russian research group working on porphyrin chemistry.[9] In one of their first publications on this subject they suggested the mechanism that is now widely accepted (see Scheme 2.2).[10,11,12]

Scheme 2.2 Mechanism of catalytic chain transfer
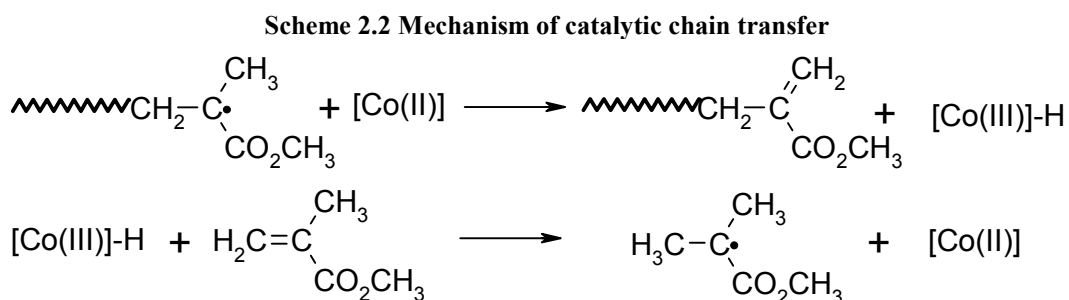
In the first step a cobalt(II)-species abstracts a hydrogen atom from the α-methyl group of the polymeric radical. As a consequence a polymer with a vinyl end group, a so called macromonomer or macromer, and a cobalt hydride are formed. In the second step the cobalt hydride reinitiates a new growing chain through transfer of the hydrogen to monomer. So, in this step the catalyst is regenerated and transfer to monomer has occurred. It was shown that catalytic chain transfer is applicable to both functional and non-functional methacrylates and styrene. Polymerizations of acrylates and vinyl acetate, however, were inhibited by the presence of a cobalt porphyrin.[11] Later, other groups reported the applicability of CCT to α-methylstyrene[13,14], ethyl α-hydroxymethacrylate[15], α-methylene butyrolactone[16] and 2-phenylallyl alcohol.[17] In a patent Janowicz gives examples of the catalytic chain transfer
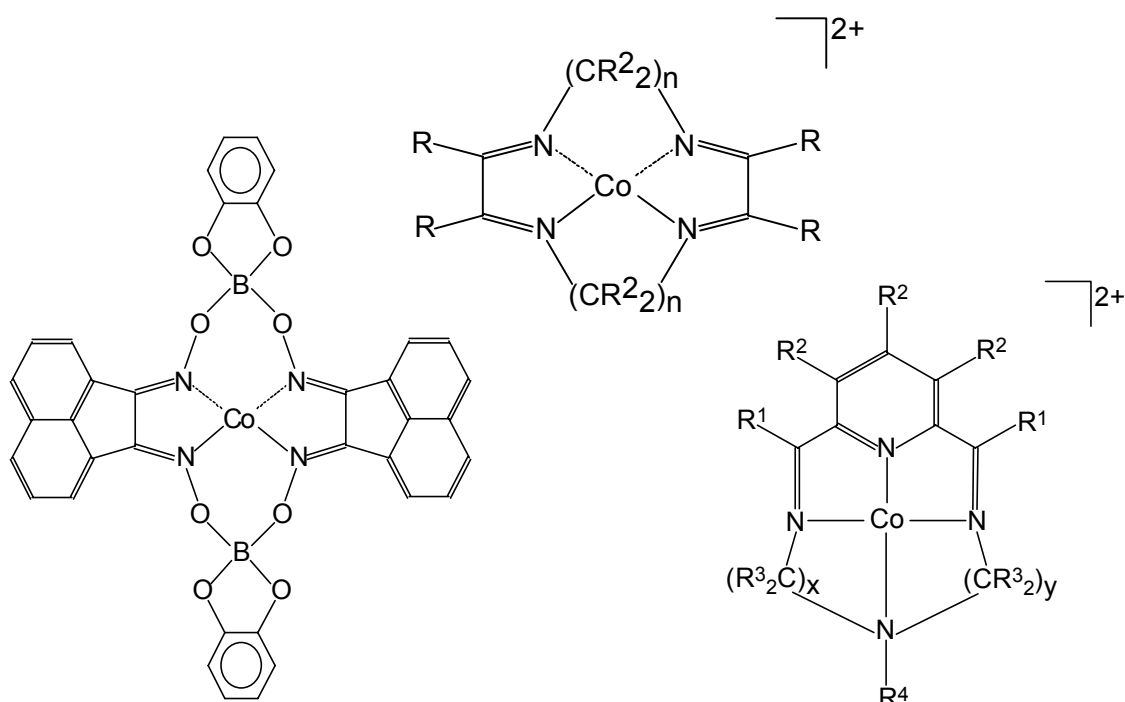
Figure 2.2 Selection of complexes patented for CCT behaviour. Left: cobaloxime-derivative[19c] ; middle: Co(II) coordinated to a tetraazatetraalkylcyclododecatetraene (for n=2)[19a]; right: Co(II) coordinated to a tetraazabicycloheptadecapentaene (for x=y=3)[19d]

polymerization of methacrylonitrile, acrylonitrile and isoprene[18], but from the available data it is not possible to determine the chain transfer activity accurately.

During the past two decades, a large number of complexes has been tested for CCT behaviour mainly by DuPont, CSIRO and Zeneca.[19] A few examples are given in Figure 2.2. In 1984 Burczyk *et al.*[20] introduced cobaloximes which proved to be an order of magnitude more active than the porphyrins that had been used before. A few years later a modified cobaloxime was reported, in which the hydrogen bridges were replaced by difluoroboron groups, which makes the complex hydrolytically more stable, see Figure 2.3. Additional advantages are that the synthesis is quite straightforward and relatively cheap. This complex and some simple derivatives are the ones
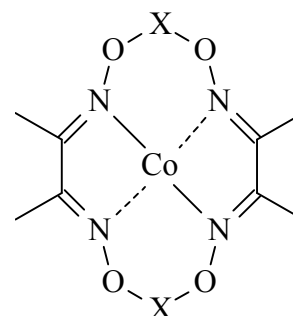
Figure 2.3 Cobaloxime. X = H: hydrogen bridges; X = BF$_2$: boron fluoride bridges

most frequently used in the academic field. Recently, Abramo and Norton[21] reported on the application of a chromium metalloradical $(\eta^5\text{-}C_5Ph_5)Cr(CO)_3$ as a catalytic chain transfer agent. Its activity is, however, an order of magnitude lower than that of cobaloximes.

A short overview of a selection of conventional and catalytic chain transfer agents and their chain transfer coefficients, C_T, for methyl methacrylate is given in Table 2.1. For comparison C_T for uncatalyzed chain transfer to monomer is shown as well. Although it is realized that the transfer and reinitiation steps in catalyzed and uncatalyzed chain transfer to monomer are not equivalent, these data are used to calculate the efficiency of the catalysts, *i.e.* the ratio of C_T with and C_T without catalyst. This ratio is found to be around 10^9, close to the range for enzymatic catalysis.[16]

In a review Davis *et al.*[22] gave some valuable rules of thumb to predict whether a cobalt complex will be active or inactive in CCT. First of all the Co(II) complex should exist in a *low spin* state. Most Co(II) complexes surrounded by two oxygen and two nitrogen atoms are in a *high spin* state and therefore inactive. In most active complexes four nitrogen atoms are directly bonded to cobalt. Secondly, when electrons in the macrocyclic ligand are only partially delocalized, the complex will be less coloured. This can be an important consideration for industrial application.

Table 2.1 Chain transfer coefficients for various transfer agents in the polymerization of MMA at 60 °C unless indicated otherwise.

Compound	C_T (-)	Reference
methyl methacrylate	1×10^{-5}	24
n-dodecanethiol	1.2	23
CBr$_4$	0.27	24
dibenzyl disulfide	0.0063	25
cobaloxime boron fluoride	$28 \times 10^3 - 40 \times 10^3$	26,27
cobalt(II)-hematoporphyrin IX, tetramethyl ether	2.4×10^3	11
$(\eta^5\text{-}C_5Ph_5)Cr(CO)_3$	984 (at 100 °C)	21
cobalt phtalocyanine	2.9×10^3	28
bis[(difluoroboryl)diphenylglyoximato]Co(II)	25×10^3	29

2.3.2 A closer look into the mechanisms of catalytic chain transfer

2.3.2.1 Investigations of the general mechanism

The mechanism as shown in Scheme 2.2 had been suggested after it was demonstrated that a hydrogen from the α-methyl group of the polymeric radical was transferred to the monomer resulting in tail addition.[11,12] The intermediate cobalt hydride was not observable, as reinitiation is very fast. However, hydrides of other cobalt complexes, such as pentacyanocobaltate are known to be catalyst for olefin hydrogenation.[10] Furthermore, Schrauzer has reported on the actual isolation of hydrides of tributylphosphine cobaloximes[30] and on the reactions of cobalt hydrides with olefins to form alkylcobaloximes.[30,31] Schrauzer[30] also succeeded in the preparation of the corresponding hydride of Vitamin B12. These findings lend support to the mechanism presented in Scheme 2.2.

A different mechanism which would also be in line with the experimental observations of the process is one according to the Michaelis-Menten kinetic scheme,[11,32] which is given in Scheme 2.3.

Scheme 2.3 Michaelis-Menten kinetic scheme

$$MMA \; + \; [Co(II)] \; \rightleftharpoons \; [MMA-[Co(II)]]$$

$$[MMA-[Co(II)]] \; + \; P_n\bullet \; \longrightarrow \; [Co(II)] \; + \; D_n \; + \; P_1\bullet$$
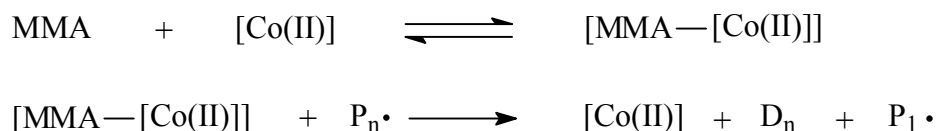
In this mechanism monomer, MMA, first forms a complex with the Co(II) catalyst resulting in [MMA-[Co(II)]]. After that the monomer-catalyst complex reacts with a polymeric radical, $P_n\bullet$ resulting in the same products as shown in Scheme 2.2, *viz.* a dead polymer chain D_n and a monomeric radical $P_1\bullet$. Heuts *et al.* elaborated on this Michaelis-Menten type mechanism, but their results contradicted the expected outcome and were in favour of the generally excepted mechanism.[33]

Furthermore, Gridnev *et al.*[34] showed a significant kinetic isotope effect of a factor of 3.5 when MMA-d^8 was polymerized in the presence of a cobalt porphyrin under CCT conditions. This led them to conclude that hydrogen transfer from the polymeric radical to the cobalt complex is the rate determining step in the CCT mechanism.

2.3.2.2 Chain-length dependent termination and catalytic inhibition

Already in the first publications, it was reported that in the presence of a catalytic chain transfer agent the rate of polymerization[9,32] decreases. Secondly, at high catalyst concentrations molecular weights are higher than predicted by the Mayo-equation using C_T determined at lower catalyst levels.[32,35] In other words, catalyst activity appears to decrease at high concentrations of Co(II) complex. Several explanations for this behaviour have been proposed, based on experimental results using different types of cobalt complexes. O' Driscoll *et al.*[36,37] concluded that the decrease in polymerization rate is caused by a decrease in degree of polymerization, resulting in a higher termination rate constant and thus in a lower radical concentration. Suddaby *et al.*[38] and Kukulj *et al.*[39] also use the increase in the average termination rate constant to explain the decrease in polymerization rate. Surprisingly O' Driscoll *et al.*[36,37] reported that the chain transfer coefficient is inversely dependent on chain length, but this inverse dependence is not related to the curved Mayo-plot. These results are contradicted by Smirnov *et al.*[35] who report an increase in chain transfer coefficient for chain lengths up to eight monomer units, which easily explains the behaviour of the Mayo-plot. The decrease in polymerization rate is explained by a process called catalytic inhibition, which is the reaction of the intermediate cobalt hydride with a polymeric radical $P_n\bullet$ forming a dead polymer chain D_n as shown in the first reaction in Scheme 2.4.[40] Smirnov *et al.* argue that if the decrease in polymerization rate would only depend on the decrease in chain length, it would be the same for all complexes at equal chain lengths and it is shown that this is not the case for cobalt phtalocyanines in the presence of various concentrations of the base quinoline.

Gridnev *et al.*[41,42] also use the principle of catalytic inhibition to explain the decrease in polymerization rates in a study of CCT behaviour of cobaloximes. It is also suggested that the

Scheme 2.4 Catalytic inhibition via three pathways

$$P_n\bullet \;+\; [Co(III)]-H \longrightarrow D_n \;+\; [Co(II)]$$

$$P_n\bullet \;+\; [Co(III)]-P_m \longrightarrow D_{n+m} \;+\; [Co(II)]$$

$$2\,[Co(III)]-H \longrightarrow 2\,[Co(II)] \;+\; H-H$$
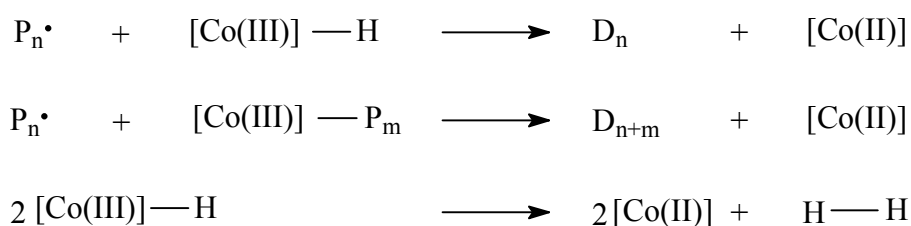
polymeric radical can form an adduct with the Co(II)-complex, similar to coenzyme B12, and this adduct can take part in inhibition (Scheme 2.4, second reaction) as well. The first inhibition reaction only occurs to a significant extent when cobalt hydride is well stabilized by the axial ligand. This stabilization will reduce the reactivity of cobalt hydride towards less reactive monomer relative to more reactive radicals.[42] A similar conclusion based on stabilization of cobalt hydride, was drawn by Suddaby *et al.*[43] for the CCT polymerization of MMA in presence of cobaloxime boron fluoride in *N,N'*-dimethyl formamide solution to explain extensive inhibition of the polymerization. This may also be the case for the cobalt phtalocyanines investigated by Smirnov.[40] A third possible inhibition reaction would be the self reaction of cobalt hydride under evolution of H_2[22], a well-known reaction within the area of vitamin B12 chemistry.[30,44]

A problem in distinguishing between the suggested mechanisms is that, using GPC, it is very difficult to determine molecular weights below a 1000 g· mol^{-1} accurately. Gridnev *et al.*[45] showed a strong dependence of both refractive index and extinction coefficient on chain length for oligomers up to six monomer units. This effect may have perturbed some of the investigations at high catalyst concentrations. Furthermore, the initiation of monomer by cobalt hydride has been shown to be reversible via scrambling experiments of MMA-H[8] and MMA-d[8] using high concentrations of catalytic chain transfer agent.[34] This reversibility was considered in some earlier papers[37,46], but discarded by others.[35] Last but not least, one must be aware that the use of different cobalt complexes in conjunction with different axial ligands may very well lead to different polymerization kinetics and products.

Computer simulations excluding chain-length dependent termination and inhibition
Polymerization kinetics were modelled using the Predici software package,[47] version 5.21.2. This software is especially designed to model polymerizations. The simulations were run on a 233 MHz Intel Pentium computer equipped with 32 MB of RAM and a Windows 98 operating system. Standard simulation settings were chosen and the relative integrator accuracy is set to 0.01. Unless otherwise stated simulations were run in moments mode, in which only the moments of the molecular weight distribution are calculated.

Using the Predici software package an attempt is made to clarify the effects of some of the proposed mechanisms. Initially the effects of the reversibility of reinitiation by cobalt hydride,

chain-length dependent termination and catalytic inhibition by cobalt hydride will be investigated. The complete model is shown in Scheme 2.5. It contains initiator decomposition, initiation, propagation, termination both by combination and disproportionation, transfer to a cobalt catalyst, monomer reinitiation via cobalt hydride and catalytic inhibition via cobalt hydride. In order to be able to show the effect of reversible reinitiation and chain-length dependent termination the reactions of the polymeric radical with chain length one have been defined separately. In this way these reactions can be monitored more easily. The standard reaction rate constants for all reactions can be found in Table 2.2. In the current version of Predici it is not possible to see how often a specific reaction has occurred, when the reaction products take part in a subsequent reaction. In order to circumvent these and other limitations of the software package a few hypothetical species are introduced. These species do not influence the actual kinetics.[*]

Table 2.2 Standard rate coefficients for the CCT polymerization of MMA at 60 °C used in Predici simulations.

Rate constant	Value	Remarks
k_d	9.7×10^{-6} s^{-1}	Taken from ref. 25. Initiator efficiency is set to 1
k_i	2530 L· mol^{-1}· s^{-1}	Recalculated from ref. 48 assuming equal activation energies for initiation and propagation
k_p	833 L· mol^{-1}· s^{-1}	Taken from ref. 49
k_{tc}, k_{tc1}, k_{td}, k_{td1}	5×10^7 L· mol^{-1}· s^{-1}	Recalculated from ref. 50
k_{tr}	3.3×10^7 L· mol^{-1}· s^{-1}	Calculated using $C_T = 39.6 \times 10^3$
k_{rein}	1×10^3 L· mol^{-1}· s^{-1}	Estimated
k_{in}	1×10^9 L· mol^{-1}· s^{-1}	Estimated

---

[*] The first hypothetical species, X, is the reaction product of initiation by initiator radicals and of reinitiation by cobalt hydride. This species X is transformed at very high rates into a polymeric radical of chain length 1 (species P_1) and a species "Counter1". (In the simulations the "rate constant" fast is set to 10^{15} L· mol^{-1}· s^{-1}.) At any point in the reaction the concentration of "Counter1" is the number of times a primary polymeric radical has been formed.

Furthermore, it is not possible to directly convert a species having a chain-length distribution into a monomeric species. So, to be able to simulate the chain transfer of polymeric radical $P_1\bullet$ to Co(II) catalyst, two more hypothetical species are introduced. CCT of $P_1\bullet$ to the cobalt catalyst results in hypothetical species MMA_1 which has a chain-length distribution. MMA_1 at its turn is transformed at very high rates into the polymeric species "Counter2" and MMA. In this way CCT of a monomeric radical is incorporated and via Counter2 it is known, how often this occurs. The actual kinetics are not influenced as the transformation reactions are very fast.

Scheme 2.5 Fundamental reaction steps in Predici simulations

$$I\!-\!I \xrightarrow{k_d} 2\ I\bullet$$

$$I\bullet + MMA \xrightarrow{k_i} X\bullet$$

$$P_n{}^\bullet + MMA \xrightarrow{k_p} P_{n+1}{}^\bullet$$

$$P_n{}^\bullet + P_m{}^\bullet \xrightarrow{k_{tc}} D_{n+m}$$

$$P_n{}^\bullet + P_m{}^\bullet \xrightarrow{k_{td}} D_n + D_m$$

$$P_n{}^\bullet + [Co(II)] \xrightarrow{k_{tr}} [Co(III)]\!-\!H + D_n$$

$$[Co(III)]\!-\!H + MMA \xrightarrow{k_{rein}} X\bullet + [Co(II)]$$

$$X\bullet \xrightarrow{fast} P_1\bullet + Counter$$

$$P_1\bullet + MMA \xrightarrow{k_p} P_2\bullet$$

$$P_1\bullet + P_1\bullet \xrightarrow{k_{tc1}} D_2$$

$$P_1\bullet + P_1\bullet \xrightarrow{k_{td1}} D_1 + D_1$$

$$P_1\bullet + P_n{}^\bullet \xrightarrow{k_{tc1}} D_{n+1}$$

$$P_1\bullet + P_n{}^\bullet \xrightarrow{k_{td1}} D_1 + D_n$$

$$P_1\bullet + [Co(II)] \xrightarrow{k_{tr}} MMA_1 + [Co(III)]\!-\!H$$

$$MMA_1 \xrightarrow{fast} Counter2 + MMA$$

$$[Co(III)]\!-\!H + P_n{}^\bullet \xrightarrow{k_{in}} D_n$$

$$[Co(III)]\!-\!H + P_1\bullet \xrightarrow{k_{in}} D_1$$
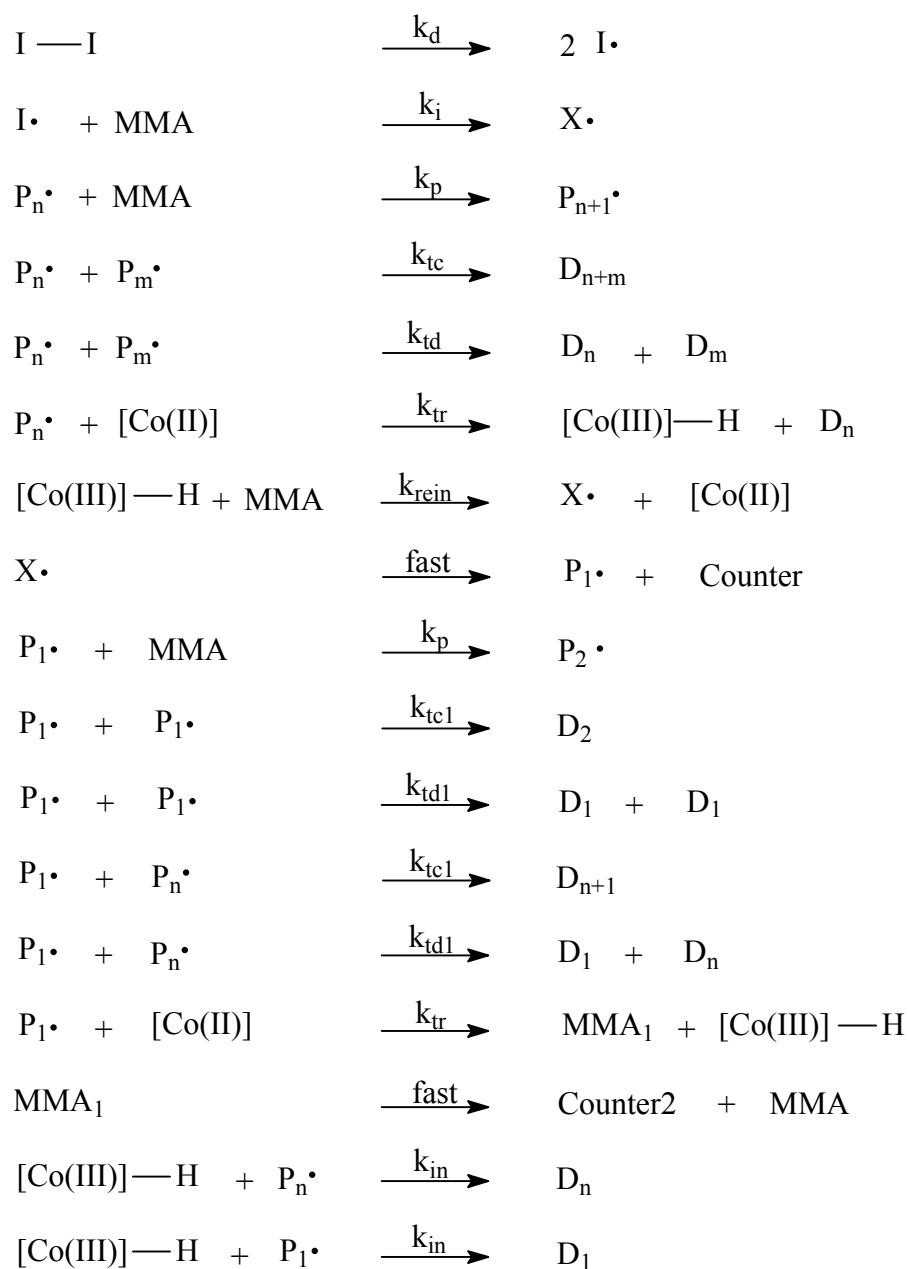
First a set of 17 simulations was carried out assuming no inhibition and equal termination rate constants for all chain lengths. The total reaction time was set at 1800 s. In Figure 2.4 both conversion and reciprocal P_n, calculated from both M_n and M_w, are shown versus the ratio of cobalt complex and monomer concentration. It can clearly be seen that at higher cobalt to monomer ratios both Mayo-plots deviate from linearity. This effect is more pronounced when
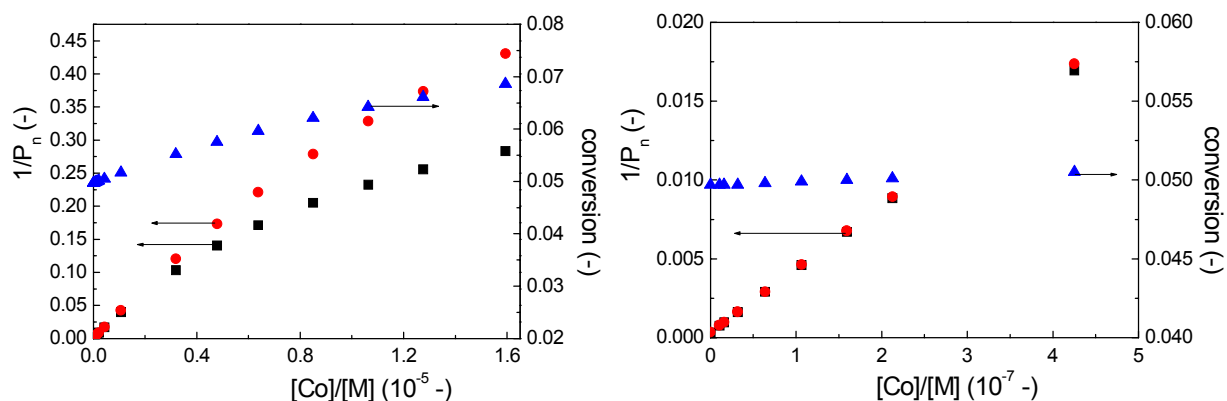
Figure 2.4 Results from computer simulations from the Predici software package using the model shown in Scheme 2.5 and the rate constants in Table 2.2 assuming no inhibition. Reaction time is 1800 s.
■: reciprocal P_n calculated from M_n (left axis); ●: reciprocal P_n calculated form M_w (left axis);
▲: conversion (right axis). The plot on the right hand side is an enlargement of the left side of the plot on the left hand side.

reciprocal P_n is calculated from M_n instead of M_w. In several experimental studies this effect has been observed as well.[32,37,40] In the model no dependence of transfer rate coefficients on chain length was invoked. So no dependence of reaction rate constants on chain length is needed to explain the deviations from linearity in the Mayo-plots. This does not mean, of course, that there can not be such a dependence. Furthermore, an increase in conversion is observed when the ratio of cobalt to monomer concentration is increased, which is in contrast with nearly all experimental reports. Here the model clearly fails to predict the experimentally observed trends. The increasing conversion observed in the simulations originates from the fact that in three reaction steps monomer is consumed, *viz.* initiation, propagation and reinitiation. In the simulations it can be seen that the cobalt hydride concentration is at steady state. This means that the rate of reinitiation will equal the rate of transfer. So the rate of monomer consumption is the sum of the rates of initiation, propagation and transfer.

$$-\frac{d[\text{M}]}{dt} = k_i[\text{I}\bullet][\text{M}] + k_p[\text{P}\bullet][\text{M}] + k_{\text{rein}}[[\text{Co(III)}] - \text{H}][\text{M}]$$

$$= k_i[\text{I}\bullet][\text{M}] + k_p[\text{P}\bullet][\text{M}] + k_{\text{tr}}[\text{P}\bullet][\text{Co(II)}]$$

(2.3)

The rate of transfer goes up with increasing cobalt concentration and therefore conversion increases as well. The magnitude of this effect will depend on the concentration of Co(II) catalyst. Suppose $[Co(II)] = 10^{-4}$ mol· L^{-1} and $[M] = 10$ mol· L^{-1}. The ratio of both falls within the limits of Figure 2.4. This results in $k_{tr}[Co(II)] = 3.3 \times 10^3$ s^{-1}, where $k_p[M] = 8.3 \times 10^3$ s^{-1}. This means that 28 % of total monomer consumption is caused by reinitiation of monomer, which clearly is a significant contribution.

It is of course important to see whether it is possible to determine the chain transfer coefficient from the results of these simulations accurately. For this reason a second set of 17 simulations was run up to 200 s instead of 1800 s. The results are shown in Table 2.3. For both sets of simulations the determination of C_T is done in five different ways using either M_n or M_w to calculate P_n and with or without correction for monomer conversion. The fifth method is based on an equation derived by Gridnev *et al.*[16,51] for conditions of intensive chain transfer and is used in the low molecular weight region.

$$P_n = 2 + \frac{k_p[M]}{k_{tr}[Co]} \tag{2.4}$$

This equation was derived as an alternative for the Mayo-equation as the long chain assumptions used in the derivation of the Mayo-equation are not valid for intensive chain transfer resulting in the formation of oligomers.

Table 2.3 C_T determined via different methods from molecular weight data obtained from Predici computer simulations.

Method	[Co]/[M]	C_T (10^3 -)	C_T (10^3 -)
	(-)	(1800 s)	(200 s)
Mayo, P_n from M_n	$0 - 4 \times 10^{-6}$	39.2	38.5
Mayo, P_n from M_w	$0 - 4 \times 10^{-6}$	40.1	39.4
Mayo, P_n from M_n, [M] corrected	$0 - 4 \times 10^{-6}$	40.2	38.6
Mayo, P_n from M_w, [M] corrected	$0 - 4 \times 10^{-6}$	41.1	39.5
Gridnev method, [M] corrected	$3 \times 10^{-5} - 15 \times 10^{-5}$	41.9	39.9
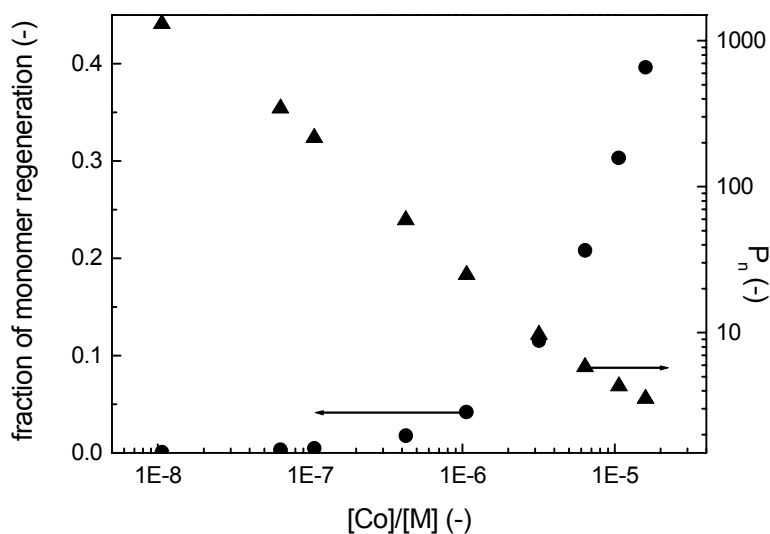
Figure 2.5 Fraction of monomer regeneration (●) and degree of polymerization (▲) determined from Predici computer simulations of the catalytic chain transfer polymerization of MMA at 60 °C.

It can be seen that when the Mayo-method is applied at lower cobalt concentrations, which is common practice nowadays[38], in all cases C_T is determined accurately with a deviation of at most 4 percent from the input value 39.6×10^3. The Mayo-method using $M_w / 2 M_o$ to determine P_n gives the best results. This is also suggested by Heuts *et al.* in an experimental study.[23] At least for these simulation results correction for monomer conversion does not improve the results. The equation proposed by Gridnev *et al.*[51] yields good results at lower conversions. It is, however, rather sensitive to changes in molecular weight and will therefore in practice be difficult to apply. However, it does show that deviations from the Mayo equation are not necessarily due to any side-reactions, but to the invalidity of the long chain assumption applied in the derivation of this equation. Regeneration of monomer from a monomeric radical is not taken into account in the Mayo-equation although this is a major reaction at high levels of cobalt catalyst as demonstrated in Figure 2.5.

The fraction of monomer regeneration is defined as the fraction of catalytic chain transfer reactions resulting in reformation of monomer. For a polymerization in which the number average degree of polymerization is about 10, more than 10 percent of the total amount of chain transfer reactions comprises transfer of a monomeric radical to Co(II) resulting in reformation of monomer. This will appear as a drop in catalytic activity calculated from the

Mayo-equation as these reactions do not result in the formation of polymer and are therefore not accounted for in the molecular weight distribution.[38]

Simulations including chain-length dependent termination

A third set of 17 simulations was carried out to see the effect of chain-length dependent termination. For simplicity this effect is restricted to the monomeric radical. The rate constants for termination between a monomeric radical and any other radical are set at 5×10^8 L· mol^{-1}· s^{-1} which is an order of magnitude higher than the termination rate constants for termination of two polymeric radicals. It is realized that this model with only two termination rate constants will not in any way accurately describe the complex dependence of termination kinetics on chain length. However, as the monomeric radical is continuously formed via reinitiation of monomer by cobalt hydride, it will contribute to a significant extent to the overall termination kinetics. Therefore, it is believed that simulations containing these simplifications with respect to actual termination kinetics will reflect realistic trends.

The results of the simulations demonstrate that the effects of chain-length dependent termination on P_n appear to be negligible. More strikingly, a strong effect on conversion rate
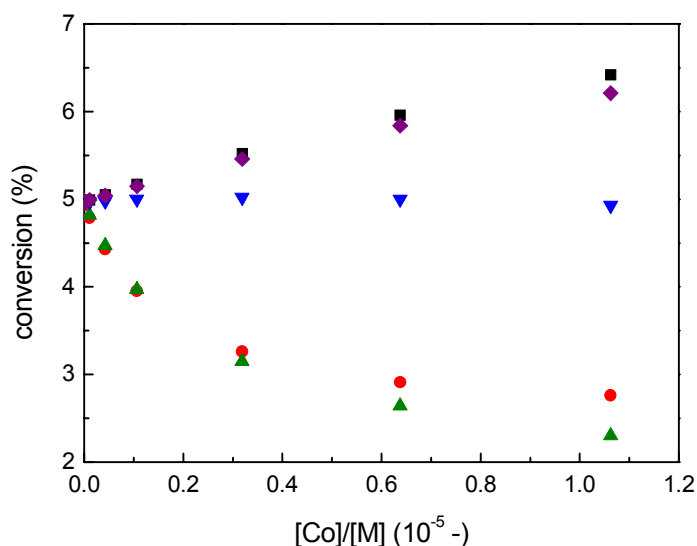
Figure 2.6 Monomer conversion results from computer simulations from the Predici software package using the model shown in Scheme 2.5 and the rate constants in Table 2.2 assuming no inhibition and chain length dependent k_t unless otherwise stated. Reaction time is 1800 s.
■: according to model; ▲: $k_{tc1} = k_{td1} = 5 \times 10^8$ L·mol^{-1}·s^{-1}; ●: $k_{in}/k_{rein} = 10^6$; ▼: $k_{in}/k_{rein} = 10^5$;
◆: $k_{in}/k_{rein} = 10^4$.

is found as shown in Figure 2.6. For the highest cobalt complex concentrations conversion decreases with almost 40 percent relative to the reactions without cobalt complex present, because of the enhanced rate of termination. The same trend is reported in experimental work[20,32,38,41], in which a decrease in conversion is observed, when catalyst concentration was increased.

Simulations including catalytic inhibition

The relative reaction rates of cobalt hydride with growing radicals and radical – radical termination determine to what extent inhibition will affect the overall polymerization kinetics. As is shown in Scheme 2.5 cobalt hydride has two possible fates, inhibition and reinitiation, respectively. When reinitiation is suppressed, the rate of inhibition will increase and *vice versa*. Reinitiation is usually assumed to be non-rate-determining and therefore very fast.[26] Estimates for k_{rein} used for computer simulation purposes range from 5×10^2 [52] to orders of magnitude higher than k_{tr}.[53] In the simulations carried out so far k_{rein} could be varied between 10^2 and 10^9 without any noticeable difference. This can also be derived mathematically assuming there is a steady state concentration of cobalt hydride and the ratio of cobalt hydride and cobalt(II) should be lower than 10^{-3}.

In order to calculate the order of magnitude of k_{in} for meaningful simulations we assume that there is no effect on conversion when the rate of inhibition is less than one percent of the rate of termination as shown in equation 2.5

$$\frac{k_{in}[[Co(III)] - H][P\bullet]}{k_t[P\bullet]^2} < 10^{-2}$$

(2.5)

Assuming a steady state for cobalt hydride it can be derived that

$$[[Co(III)] - H] = \frac{k_{tr}[Co(II)][P\bullet]}{k_{rein}[M] + k_{in}[P\bullet]}$$

(2.6)

If inhibition is not important, the rate of reinitiation will be substantially larger than the rate of inhibition and so the second term in the denominator of equation 2.6 can be neglected. In that case combining equations 2.5 and 2.6 results in

$$\frac{k_{\text{in}}}{k_{\text{rein}}} < 10^{-2} \frac{k_{\text{t}}[\text{M}]}{k_{\text{tr}}[\text{Co(II)}]} \tag{2.7}$$

Substituting the rate constants and monomer concentration used in the simulation program the following condition is obtained for absence of inhibition effects in this particular system

$$\frac{k_{\text{in}}}{k_{\text{rein}}} < \frac{0.15}{[\text{Co(II)}]} \tag{2.8}$$

To have a physically realistic set of reaction rate constants k_{rein} was set at 10^3 L· mol^{-1}· s^{-1} and k_{in} was varied between 10^7 an 10^9 L· mol^{-1}· s^{-1}. The effects of these different levels of inhibition on conversion are shown in Figure 2.6 as well. Similar to the simulations with chain-length dependent termination there is no effect on the degree of polymerization. The validity of condition 2.8 is nicely shown in Figure 2.6 for the conversion data of the simulations having $k_{\text{in}}/k_{\text{rein}} = 10^4$. For $[\text{Co(II)}] = 10^{-4}$ mol· L^{-1} we do see an effect, where this effect has disappeared for $[\text{Co(II)}] = 10^{-5}$ mol· L^{-1}. These simulations show that quite strong stabilization of the cobalt hydride towards monomer is required for catalytic inhibition to take effect. It depends on the actual reinitiation rate constant whether this is physically realistic or not.

Both chain-length dependent termination and catalytic inhibition can be used to explain the same experimentally observed trends. From recent research[54] it is known that chain-length dependent termination will play a role in free-radical polymerization. If catalytic inhibition will be part of the reaction mechanism, this will always be in addition to chain-length dependent termination.

Summary

In Table 2.4 an overview is presented of the reaction steps incorporated in the simulations, the simulation results and whether or not these simulation results are in agreement with the corresponding experimental observations. From Table 2.4 and the previous discussion, it becomes clear that the curvature of the Mayo-plot is caused by monomeric radicals undergoing chain transfer. No chain-length dependence of C_{T} is required to explain the experimental observations.

Secondly, either chain-length dependent termination or inhibition or both need to be incorporated to explain decreasing conversions with increasing [Co(II)]/[M]. As, nowadays, it is widely accepted that termination kinetics depend on chain length[54], this will at least partially explain the effect of [Co(II)]/[M] on conversion. Inhibition reactions may, but need not, contribute as well.

Table 2.4 Overview of the reaction steps incorporated in the simulations, the obtained simulation results and the agreement with experimental data.

Contents of simulations	Simulation results	Agreement with experiments?
- no chain-length dependent termination - no inhibition - monomeric radical can give transfer	-conversion increases with increasing [Co(II)]/[M] -curved Mayo-plot at high [Co)/[M]	no yes
- chain-length dependent termination - no inhibition - monomeric radical can give transfer	-conversion decreases with increasing [Co(II)]/[M] -no additional effect on molecular weight, so still curved Mayo-plot	yes yes
- no chain-length dependent termination - inhibition - monomeric radical can give transfer	-conversion decreases with increasing [Co(II)]/[M] -no additional effect on molecular weight, so still curved Mayo-plot	yes yes

2.3.2.3 Cobalt - carbon bond formation

Coenzyme B12 as shown in Figure 2.1 is the ultimate example of a compound having a cobalt - carbon bond. Many research groups in the field of cobalt chemistry have been working on the kinetics and thermodynamics of cobalt - carbon bond dissociation and

formation.[1,2,4,55,56] The stability of these organocobalt complexes seems to depend on the equatorial ligand, the axial ligand and the nature of the organic radical. Halpern[2] studied the effect of the basicity and size of the axial ligand on the bond dissociation energy (BDE) and found that it increases with increasing basicity and decreasing axial ligand size. The effect of the axial organic ligand on the bond dissociation energy is not as straightforward as is sometimes reported. Probably both steric and electronic effects play a role.[4] The thermal stability of organocobalt complexes in solution is reported to increase in the following order: *sec*-allyl < *sec*-benzyl < allyl < benzyl < *tert*-alkyl < *sec*-alkyl < *n*-alkyl.[57] The thermal stability is increased by the persistent radical effect[58] as was shown experimentally by Daikh and Finke[59] who investigated the formation of bibenzyl in the thermolysis of a benzylcobaltmacrocycle as represented in a simplified way in Scheme 2.6.

Scheme 2.6 Formation of bibenzyl
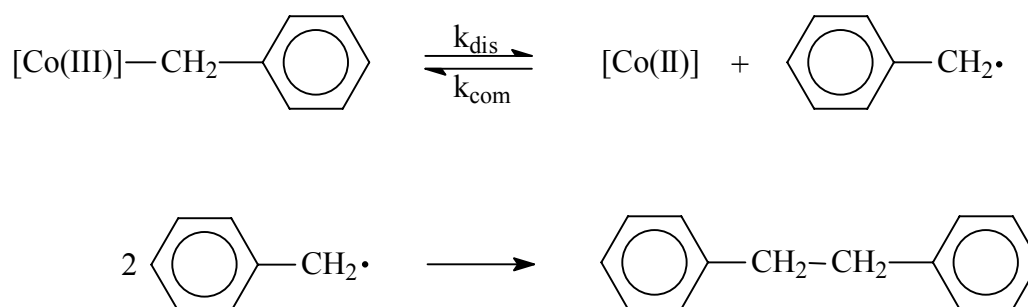
Daikh and Finke showed that only 0.18 % of bibenzyl would be formed over 1000 years. After initial bibenzyl formation and thus build-up of a Co(II)-species, combination of benzylic radicals with Co(II) is kinetically preferred over benzylic radical – benzylic radical combination. So the concentration of Co(III)-benzyl will be nearly constant as dissociation of Co(III)-benzyl is followed by recombination of Co(II) and a benzylic radical. In the presence of radical traps this stability is strongly reduced, as these will compete with Co(II) to combine with the benzylic radicals.

Wayland *et al.* apply the relative instability of *tert*-alkyl cobalt porphyrins in the synthesis of more stable primary and secondary compounds[60,61], the determination of bond dissociation activation parameters[62,63] as well as the development of kinetic models and the determination of relative reaction rates of cobalt hydride.[64]

Many authors have suggested that cobalt - carbon bond formation may influence catalytic chain transfer for MMA.[20,33,52,65] In two studies alkyl - cobalt compounds were used to initiate

the oligomerization reaction of MMA and these authors suggested a monomer insertion mechanism as they needed UV-light to keep the reactions running.[66,67] However, more recent studies show that propagation occurs via a free-radical mechanism.[68]

In the closely related field of controlled radical polymerization using cobalt complexes cobalt - carbon bond formation is of major importance. It was shown that acrylates can be polymerized in a "living" fashion using both Co(II) porphyrins[69,70] and cobaloximes.[71] Roberts *et al.*[72] recently showed that cobaloxime - polyacrylate bonds can be directly observed via MALDI-TOF mass spectrometry.

The effect of formation of cobalt-carbon bonds on the catalytic chain transfer polymerization of various monomers will be further discussed in Chapters 3 and 5.

2.3.2.4 Catalyst deactivation

Catalyst deactivation can proceed via various pathways. In catalytic chain transfer only the cobalt(II) complex can take part in the catalytic cycle. When cobalt(II) is oxidized or reduced to cobalt(III) or cobalt (I) respectively, the overall catalytic activity will decrease. The mechanism shown in Scheme 2.7 was first presented by Karmilova *et al.*[73] Scheme 2.7 demonstrates that oxidation can occur when peroxides are used as initiators.[74] A second cause of oxidation is the presence of oxygen. Some cobalt(II) complexes are known for their oxygen binding capabilities like ethylenebis(acetylacetoniminato)cobalt(II) derivatives[75],

Scheme 2.7 Possible pathways for reduction and oxidation of the cobalt catalyst in catalytic chain transfer polymerization[69]
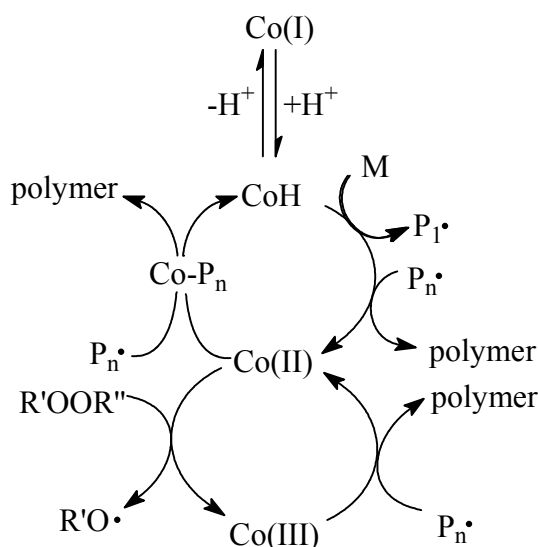
porphyrinatocobalt(II) derivatives[76] and cobaloxime derivatives.[77,78] The dioxygen affinities, however, have an inverse dependence on temperature and for porphyrins in the most favourable case only one percent will form an oxygen adduct at room temperature.[76] Therefore, oxidation by oxygen will probably occur via trapping of a polymeric radical by oxygen followed by combination of the resulting peroxo-radical and the cobalt complex.[1,79]

On the other hand cobalt hydrides of cobaloximes behave as weak acids ($pK_a \sim 10$)[30] and can be deprotonated to form a cobalt(I) species. In some solvents or in the presence of certain axial bases these can be rather stable, thereby reducing the amount of cobalt available for transfer. [60,73] A last deactivation pathway is hydrolysis or oxidation of the macrocyclic ligand. Especially for cobaloximes this is a very important side-reaction. This problem can be largely overcome by substituting the hydrogen bridges in the cobaloximes by BF_2-bridges.[78] The effect of catalyst deactivation will be further discussed in Chapters 3 and 4.

2.4 Reactivity and application of macromonomers

In order to complete this review on catalytic chain transfer, it is important to pay some attention to the reaction products of CCT, the subsequent reactions these can undergo and their applications. Several authors have studied the free-radical copolymerization of methyl methacrylate oligomers with various monomers. Cacioli *et al.*[80] studied the copolymerization of MMA oligomers with ethyl acrylate, styrene, MMA, acrylonitrile and vinyl acetate. The homopolymerization of MMA oligomers failed. For MMA no oligomer incorporation could be determined, but a reduction in molecular weight compared to a control experiment was found. In these polymerizations the MMA oligomers functioned as transfer agents. For all other monomers oligomer incorporation was achieved. Abbey *et al.*[81] studied the copolymerization behaviour of functional methacrylate dimers with styrene and also found that addition of dimer to a dimer ended radical does not occur.

Krstina *et al.*[82,83] introduced the addition-fragmentation mechanism in which a growing polymeric radical can add to the oligomeric double bond, upon which the resulting radical fragments into a new macromonomer and a growing radical as shown in Scheme 2.8. In the copolymerization of a macromonomer consisting of monomer A and a monomer B this will

Scheme 2.8 Mechanism for the addition of a methacrylic dimer to a methacrylic polymeric radical followed by fragmentation
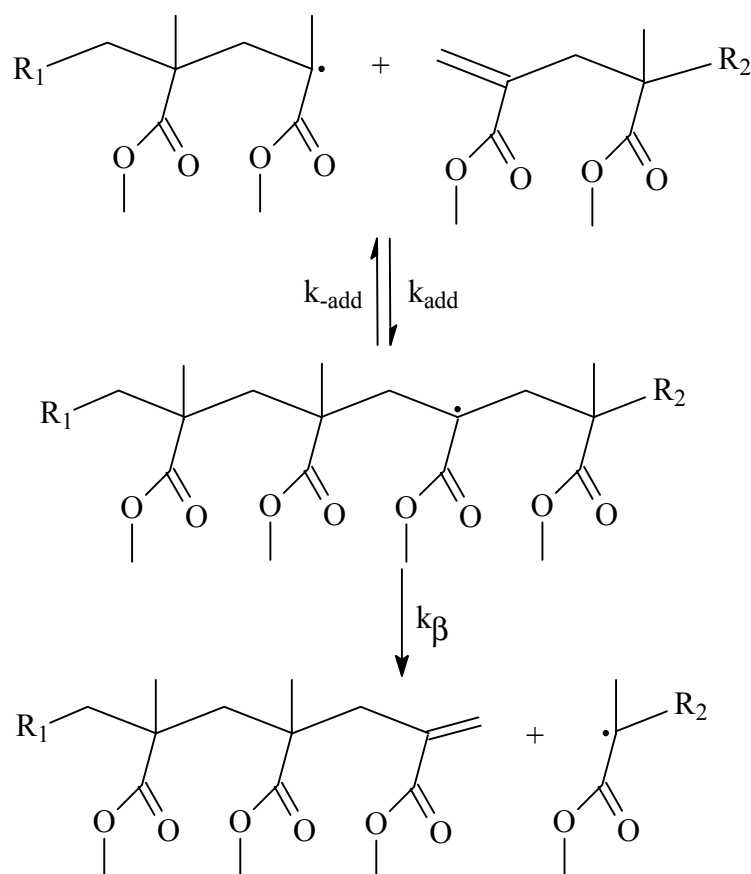
lead to the formation of a block copolymer. However, when macromonomer consisting of monomer A is copolymerized with monomer A this will lead to chain extension of the macromonomer. Reactions like these given in Scheme 2.8 can also occur during a catalytic chain transfer polymerization, complicating kinetic analysis. This will be dealt with in Chapters 4 and 6.

Chain transfer coefficients have been determined for MMA dimers,[84,85] MMA oligomers,[85] and α-methylstyrene dimers.[86] For the dimers C_T is around 0.01 and for the higher oligomers it is around 0.2. Moad *et al.*[85] suggested that this difference in C_T is caused by enhanced fragmentation of the adduct of dimer and polymeric radical back into the starting compounds, whereas for the higher oligomers the rate constants for backward and forward fragmentation are more or less equal.

Haddleton *et al.*[87] studied the copolymerization of an MMA tetramer and *n*-butyl methacrylate (BMA) in the presence of a catalytic chain transfer agent using MALDI-TOF mass

spectroscopy. In a very elegant way Haddleton *et al.* showed that the radical formed upon addition of tetramer to a growing polymethacrylate radical can only fragment. So it does not propagate to give grafting nor reacts with the cobalt complex to give chain transfer, which would result in an internal double bond. In the absence of catalytic chain transfer agent fragmentation results in the formation of a BMA-chain with one MMA unit at the chain end. The other three MMA units form a new growing radical and will add BMA. In the presence of enough macromonomer termination of this chain will occur predominantly via addition of another macromonomer followed by fragmentation. This results in a BMA-polymer with three MMA units at one end and one unit at the other. In a similar way Haddleton *et al.*[88] synthesized telechelic polymers via a 2-hydroxyethyl methacrylate tetramer.

Beside the preparation of block copolymers and telechelic polymers, macromonomers have also been used in the production of star polymers.[89] Furthermore, macromonomers consisting of methacrylic acid and BMA were used in emulsion polymerization as copolymerizable surfactants.[90] These examples show the wide applicability of macromonomers in the field of polymers and coatings.

2.5 References

[1] Dolphin, D., Ed. *B12*; Wiley: 1982

[2] Halpern, J. *Science*, **1985**, *227*, 869

[3] Davis, T.P.; Haddleton, D.M.; Richards, S.N. *J. Macromol. Sci., Rev. Macromol. Chem. Phys.* **1994**, *C34*, 234

[4] Sweany, R.L. in '*Comprehensive Organometallic Chemistry II*, *vol. 8*' (Eds. Abel, E.W.; Wilkinson, G.; Stone, F.G.A.), p. 42-, Pergamon: **1995**

[5] Mayo, F.R. *J. Am. Chem. Soc.* **1943**, *65*, 2324

[6] Clay, P.A.; Gilbert, R.G. *Macromolecules* **1995**, *28*, 552

[7] Moad, G.; Moad, C.L. *Macromolecules* **1996**, *29*, 7727

[8] Heuts, J.P.A.; Kukulj, D.; Forster, D.J.; Davis, T.P. *Macromolecules* **1998**, *31*, 2894

[9] Smirnov, B.R.; Bel'govskii, I.M.; Ponomarev, G.V.; Marchenko, A.P.; Enikolopyan, N.S. *Doklady Chemistry (English translation)* **1981**, *254*, 426

[10] Smirnov, B.R.; Morozova, I.S.; Pushchaeva, L.M.; Marchenko, A.P.; Enikolopyan, N.S. *Doklady Chemistry (English translation)* **1981**, *255*, 542

[11] Enikolopyan, N.S.; Smirnov, B.R., Ponomarev, G.V.; Bel'govskii, I.M. *J. Pol. Sci. Pol. Chem. Ed.* **1981**, *19*, 879

[12] Smirnov, B.R.; Morozova, I.S.; Marchenko, A.P.; Markevich, M.A.; Pushchaeva, L.M.; Enikolopyan, N.S. *Doklady Chemistry (Englsih Translation)* **1980**, *253*, 383

[13] Kukulj, D.; Heuts, J.P.A.; Davis, T.P. *Macromolecules* **1998**, *31*, 6034

[14] Moad, G.; Rizzardo, E.; Moad, C.L.; Ittel, S.D.; Wilczek, L.; Gridnev, A.A. *PCT Int Appl WO97/31030*, **1997**

[15] Davis, T.P.; Zammit, M.D.; Heuts, J.P.A., Moody, K. *Chem. Commun.* **1998**, 2383

[16] Gridnev, A.A *J. Polym. Sci. Part A: Polym. Chem.* **2000**, *38*, 1753

[17] Morrison, D.A.; Eadie, L.; Davis, T.P. *Macromolecules* **2001**, *34*, 7967

[18] Janowicz, A.H. *US Patent 4,694,054,* **1987**

[19] See for example a) Janowicz, A.H.; Lester, M.R. *US Patent 4,680,352,* **1987** (to DuPont), b) Hawthorne, D.G. *US Patent 5,324,879,* **1994** (to CSIRO), c) Haddleton, D.M.; Muir, A.V.G.; Leeming, S.W. *PCT Int Appl WO 95/17435,* **1995** (to Zeneca), d) Haddleton, D.M.; Muir, A.V.G. *US Patent 5,602,220,* **1997** (to Zeneca)

[20] Burczyk, A.F.; O' Driscoll, K.F.; Rempel, G.L. *J. Polym. Sci. Polym. Chem. Ed.* **1984**, *22*, 3255

[21] Abramo, G.P.; Norton, J.R. *Macromolecules* **2000**, *33*, 2790

[22] Davis, T.P.; Kukulj, D.; Haddleton, D.M.; Maloney, D.R. *Trends in Polymer Science* **1995**, *3*, 365

[23] Heuts, J.P.A.; Davis, T.P.; Russell, G.T. *Macromolecules* **1999**, *32*, 6019

[24] Berger, K.C.; Brandrup, G. in '*Polymer Handbook, 3rd Edition*' (Eds. Brandrup, J.; Immergut, E.H.), p. II/109, Wiley: **1989**

[25] Moad, G.; Solomon, D.H. *The Chemistry of Free Radical Polymerization*, 1st Ed., Pergamon, Oxford: **1995**

[26] Kukulj, D.; Davis, T.P. *Macromol. Chem. Phys.* **1998**, *199*, 1697

[27] Haddleton, D.M.; Maloney, D.R.; Suddaby, K.G.; Muir, A.V.G.; Richards, S.N. *Macromol. Symp.* **1996**, *111*, 37

[28] Smirnov, B.R.; Pushchayeva, L.M.; Plotnikov, V.D. *Polymer Science USSR* **1989**, *31*, 2607

[29] Heuts, J.P.A.; Forster, D.J.; Davis, T.P.; Yamada, B.; Yamazoe, H.; Azukizawa, M. *Macromolecules* **1999**, *32*, 2511.

[30] Schrauzer, G.N. *Angew. Chem.* **1976**, *88*, 465

[31] Schrauzer, G.N.; Windgassen, R.J. *J. Am. Chem.Soc.* **1967**, *89*, 1999

[32] Smirnov, B.R.; Marchenko, A.P.; Korolev, G.V.; Bel'govskii, I.M.; Enikolopyan, N.S. *Polymer Science USSR* **1981**, *23*, 1158

[33] Heuts, J.P.A.; Forster, D.J.; Davis, T.P. *Macromol. Rapid Commun.* **1999**, *20*, 299

[34] Gridnev, A.A.; Ittel, S.D.; Wayland, B.B.; Fryd, M. *Organometallics* **1996**, *15*, 5116

[35] Smirnov, B.R.; Marchenko, A.P.; Plotnikov, V.D.; Kuzayev, A.I.; Enikolopyan, N.S. *Polymer Science USSR* **1981**, *23*, 1169

[36] Burczyk, A.F.; O' Driscoll, K.F.; Rempel, G.L. *J. Polym. Sci. Polym. Chem. Ed.* **1984**, *22*, 3255

[37] Amin Sanayei, R.; O' Driscoll, K.F. *J. Macromol. Sci.-Chem.* **1989**, *A26*, 1137

[38] Suddaby, K.G.; Maloney, D.R.; Haddleton, D.M. *Macromolecules* **1997**, *30*, 702

[39] Kukulj, D.; Davis, T.P. *Macromol. Chem. Phys.* **1998**, *199*, 1697

[40] Smirnov, B.R.; Pushchayeva, L.M.; Plotnikov, V.D. *Polymer Science USSR* **1989**, *31*, 2607

[41] Gridnev, A.A. *Polymer Science USSR* **1989**, *31*, 2369

[42] Gridnev, A.A.; Lampeka, Ya. D.; Smirnov, B.R.; Yatsiminirskii, K.B. *Theor. Exp. Chem. (English translation)* **1987**, *23*, 293

[43] Suddaby, K.G.; O' Driscoll, K.F.; Rudin, A. *J. Polym. Sci. Part A Polym. Chem.* **1992**, *30*, 643

[44] Halpern, J. in *'B12'* (Ed. Dolphin, D.) p. 501-, Wiley: **1982**

[45] Gridnev, A.A.; Ittel, S.D.; Fryd, M. *J. Polym. Sci. Part A. Polym. Chem.* **1995**, *33*, 1185

[46] Abbey, K.J.; Carlson, G.M.; Masolaa, M.J.; Trumbo, D. *Polym. Mater. Sci. Eng.* **1986**, *55*, 235

[47] Wulkow, M. *Macromol. Theory Simul.* **1996**, *5*, 393

[48] Walbiner, M.; Wu, J.Q.; Fischer, H. *Helv. Chim. Acta* **1995**, *78*, 810

[49] van Herk, A.M. *Macromol. Theory Simul.* **2000**, *9*, 433

[50] Kowollik, C. *'Free-radical bulk copolymerization kinetics of acrylate and methacrylate monomers studied by pulsed laser techniques'* PhD.-Thesis, University of Göttingen, Cuvillier Verlag: **1999**

[51] Gridnev, A.A. Bel'govskii, I.M.; Enikolopyan, N.S. *Vysokomol. Soedin. Ser. B* **1986**, *28*, 85; (Chem. Abstr. **1986**, *105*, 6846)

[52] Davis, T.P.; Kukulj, D.; Maxwell, I.A. *Macromol. Theory Simul.* **1995**, *4*, 195

[53] Kowollik, C.; Davis, T.P. *J. Polym. Sci. Part A Polym. Chem.* **2000**, *38*, 3303

[54] See for example: de Kock, J.B.L. *"Chain-Length Dependent Bimolecular Termination in Free Radical Polymerization"* PhD-Thesis, University of Eindhoven, Eindhoven, **1999**

[55] Bakac, A.; Espenson, J.H. *J. Am. Chem. Soc.* **1984**, *106*, 5197

[56] Wolowiec, S.; Balt, S.; De Bolster, W.G. *Inorg. Chim. Acta* **1991**, *181*, 131

[57] Johnson, M.D. *Acc. Chem. Res.* **1983**, *16*, 343

[58] Fischer, H. *J. Am. Chem. Soc.* **1986**, *108*, 3925

[59] Daikh, B.E.; Finke, R.G. *J. Am. Chem. Soc.* **1992**, *114*, 2938

[60] Gridnev, A.A.; Ittel, S.D.; Fryd, M.; Wayland, B.B. *Organometallics* **1993**, *12*, 4871

[61] Gridnev, A.A.; Ittel, S.D.; Fryd, M.; Wayland, B.B. *J. Chem. Soc. Chem. Commun.* **1993**, 1010

[62] Wayland, B.B.; Gridnev, A.A.; Ittel, S.D.; Fryd, M. *Inorg. Chem.* **1994**, *33*, 3830

[63] Woska, D.C.; Zie, Z.D.; Gridnev, A.A.; Ittel, S.D.; Fryd, M.; Wayland, B.B. *J. Am. Chem. Soc.* **1996**, *118*, 9102

[64] Gridnev, A.A.; Ittel, S.D.; Fryd, M; Wayland, B.B. *Organometallics* **1996**, *15*, 222

[65] Gridnev, A.A.; Semeikin, A.S. Koifman, O.I. *Theor. Exp. Chem.* **1990**, *26*, 118

[66] Kijima, M.; Miyamori, K.; Sato, T. *J. Org. Chem.* **1987**, *52*, 706

[67] Bandaranayake, W.M.; Pattenden, G. *J. Chem. Soc. Chem. Commun.* **1988**, 1179

[68] Haddleton, D.M.; Crossman, M.C.; Hunt, K.H.; Topping, C.; Waterson, C.; Suddaby, K.G. *Macromolecules* **1997**, *30*, 3992

[69] Wayland, B.B.; Poszmik, G.; Mukerjee, S.L. *J. Am. Chem. Soc.* **1994**, *116*, 7943

[70] Wayland, B.B.; Basickes, L. Mukerjee, S.; Wei, M.; Fryd, M. *Macromolecules* **1997**, *30*, 8109

[71] Arvanitopoulos, L.D.; Greuel, M.P.; King, B.M.; Shim, A.K.; Harwood, H.J. In *Controlled Radical Polymerization*; Matyjaszewski, K. Ed.; ACS Symposium Series, vol. 685; American Chemical Society: Washington, DC, **1998**; p. 316

[72] Roberts, G.E.; Heuts, J.P.A.; Davis, T.P. *Macromolecules* **2000**, *33*, 7765

[73] Karmilova, L.V.; Ponomarev, G.V.; Smirnov, B.R.; Bel'govskii, I.M. *Russ. Chem. Rev.* **1984**, *53*, 132

[74] Gridnev, A.A. *Polymer J.* **1992**, *24*, 613

[75] Carter, M.J., Rillema, D.P.; Basolo, F. *J. Am. Chem. Soc.* **1974**, *96*, 392

[76] Walker, F.A. *J. Am. Chem. Soc.* **1973**, *95*, 1154

[77] Lance, K.A.; Goldsby, K.A.; Busch, D.H. *Inorg. Chem.* **1990**, *29*, 4537

[78] Bakac, A.; Brynildson, M.E.; Espenson, J.H. *Inorg. Chem.* **1986**, *25*, 4108

[79] Kendrick, M.J.; Al-Akhdar, W. *Inorg. Chem.* **1987**, *26*, 3972

[80] Cacioli, P.; Hawthorne, D.G.; Laslett, R.L.; Rizzardo, E.; Solomon, D.H. *J. Macromol. Sci.-Chem.* **1986**, *A23*, 839

[81] Abbey, K.J.; Trumbo, D.L.; Carlson, G.M.; Masola, M.J.; Zander, R.A. *J. Polym. Sci. Part A Polym. Chem.* **1993**, *31*, 3417

[82] Krstina, J.; Moad, G.; Rizzardo, E.; Winzor, C.L.; Berge, C.T.; Fryd, M. *Macromolecules* **1995**, *28*, 5381

[83] Krstina, J. Moad, C.L.; Moad, G.; Rizzardo, E.; Berge, C.T.; Fryd, M. *Macromol. Symp.* **1996**, *111*, 13

[84] Tanaka, H.; Kawai, H.; Sato, T.; Ota, T. *J. Polym. Sci. Part A Polym. Chem.* **1989**, *27*, 1741

[85] Moad, C.L.; Moad, G.; Rizzardo, E.; Thang, S.H. *Macromolecules* **1996**, *29*, 7717

[86] Yamada, B.; Tagahira, S.; Aoki, S. *J. Polym. Sci. Part A Polym. Chem.* **1994**, *32*, 2745

[87] Haddleton, D.M.; Maloney, D.R.; Suddaby, K.G. *Macromolecules* **1996**, *29*, 481

[88] Haddleton, D.M.; Topping, C.; Hastings, J.J.; Suddaby, K.G. *Macromol. Chem. Phys.* **1996**, *197*, 3027

[89] Antonelli, J.A.; Riverton, N.J.; Scopazzi, C. *US Patent 5,310,807* **1994**

[90] Huybrechts, J.; Bruylants, P.; Vaes, A.; De Marre, A. *Prog. Org. Coat.* **2000**, *38*, 66

Chapter 3

Mechanistic aspects of low conversion
catalytic chain transfer polymerization
of methacrylates

Synopsis: In this chapter several aspects of low conversion catalytic chain transfer polymerization of methacrylates will be investigated in more detail. First, the effects of initiator, oxygen, solvent and additives will be studied. Next, a closer look will be taken at the possibility of the occurrence of diffusion control in the transfer step. The experiments will be supported by theoretical calculations. Finally, the effect of cobalt - carbon bond formation on catalytic chain transfer will be discussed.

3.1 Introduction

In the previous chapter several aspects concerning the mechanism of catalytic chain transfer have been reviewed. So far, chain transfer coefficients for cobalt complexes have been determined with several monomers and in various solvents. The values in solution are generally lower than those in bulk.[1,2,3] In earlier literature this decrease is claimed to be caused by so-called solvent effects, interactions of solvent molecules with the active catalytic center. From studies in emulsion polymerization[4] and studies of the polymerization of methacrylic acid[5] it is known that cobaloxime boron fluoride (CoBF) (see Figure 2.3) decomposes slowly in the presence of acids. For solution polymerizations in 2-butanone, differences in catalyst activity have been reported between polymerizations in purified and unpurified solvent.[2] In the previous chapter the effect of oxygen on catalyst deactivation has been discussed briefly, as well. From these examples it is clear that various aspects of the polymerization conditions may affect catalyst activity. Therefore, we will first deal with the

influence of reaction conditions like presence of oxygen, solvent and impurities on the determination of chain transfer coefficients in order to obtain a set of standard conditions under which the experiments are performed. In this way we will be able to relate the results for different solvents and monomers.

Another recently discussed issue is whether or not the first reaction presented in Scheme 2.2 is diffusion controlled. This was suggested by several authors.[2,3,6] Heuts *et al.*[7,8,9] elaborated on this topic and concluded that the transfer reaction in catalytic chain transfer of methacrylates is indeed diffusion controlled. These conclusions were based on trends in C_T for a series of methacrylates[7,9] and on enhanced catalyst activity when polymerizations are run in supercritical CO_2.[8] We will perform experiments for different methacrylates in solution as well and we will compare our results with theoretical calculations for different levels of diffusion control and also with results reported by Heuts *et al.*[7,8,9]

A final point that will be discussed, is the possible effect of the formation of covalent bonds between the polymeric radical and the cobalt complex. The formation of cobalt – carbon bonds has been described in Chapter 2. When cobalt – carbon bond formation occurs, the amount of Co complex available for chain transfer decreases and only an apparent C_T can be determined. Equations for this apparent C_T will be derived and theoretical and experimental results will be compared.

3.2 Experimental Section

Materials. Methyl methacrylate (MMA, Merck, 99%), *n*-butyl methacrylate (BMA, Merck, 99%) and 2-ethylhexyl methacrylate (EHMA, Merck) were all distilled under reduced pressure and stored at −10 °C. Prior to use, monomers were passed over a column, containing inhibitor remover and basic alumina. Toluene and tetrahydrofuran (THF) (both Biosolve, AR) were purified using a Grubbs solvent set-up[10], purged with argon for at least three hours and stored over molsieves in a glovebox. *n*-Butyl acetate (Merck, 99%) was distilled, passed over a column of basic alumina, shaken with anhydrous $MgSO_4$, passed over a column of basic alumina, purged with argon for at least three hours and stored over molsieves in a glovebox. Azobis(methylisobutyrate) (AIBMe, Wako Chemicals) and azobis(isobutyronitrile) (AIBN,

Fluka) were recrystallized from methanol unless otherwise stated and stored in a glovebox at room temperature, as well. Methanol (Biosolve), 1-dodecanethiol (Aldrich, 98 %), benzoyl peroxide (Aldrich, 97 %) and acetic acid (Merck, 99 %) were used as received. CoBF (bis(aqua)bis((difluoroboryl)dimethylglyoximato)cobalt(II)) was prepared according to a procedure of Bakac and Espenson[11]. Two different batches were used. Both were analysed using UV-Vis spectroscopy and elemental analysis (experimental batch I: C: 23.1 %, H: 3.81 %, N: 13.3 %; batch II: C: 23.0 %, H: 3.91 %, N: 13.5 %; calculated for $C_8H_{12}N_4O_4B_2F_4Co \cdot (H_2O)_2$: C: 22.8 %, H: 3.83 %, N: 13.3 %).

General polymerization procedure. Monomers were purged with argon for at least three hours prior to transfer into the glovebox. All reaction mixtures were prepared inside a glovebox. Stock solutions of CoBF in monomer or solvent were prepared and stored for a longer period of time. AIBMe solutions in monomer were prepared immediately prior to the experiment. Reaction mixtures were made of the CoBF solution, monomer, toluene or *n*-butyl acetate and an AIBMe solution to a total volume of about 5 mL. Reactions were carried out at different solvent concentrations. For each set of conditions a total of eight polymerizations was done at different CoBF concentrations. Polymerizations were carried out in a water bath at a constant temperature of 60 °C (±0.2 °C). Reactions were stopped by addition of hydroquinone and cooling. Monomer was evaporated and the polymer was dried under reduced pressure at 60 °C. For EHMA, polymers were precipitated from methanol, redissolved in THF and precipitated before being dried. Conversion was determined gravimetrically. Experiments to investigate the effect of oxygen and impurities in initiator were carried out using CoBF batch II and AIBN. All other experiments were carried out with CoBF batch I and AIBMe.

Analyses. Size exclusion chromatography (SEC) was carried out using THF as an eluent at a flow rate of 1 mL·min⁻¹. Two Polymer Laboratories PLgel 5 μm Mixed-C columns (300 × 7.5 mm) and PLgel 5 μm guard column (50 × 7.5 mm) were used and calibrated with Polymer Laboratories narrow MWD polystyrene standards. The Mark-Houwink parameters used in universal calibration are: $K_{MMA} = 9.44 \times 10^{-5}$ dL·g⁻¹, $a_{MMA} = 0.719$, $K_S = 1.14 \times 10^{-4}$ dL·g⁻¹, $a_S = 0.716$.[12]

Viscosity measurements were conducted using a stress-controlled rheometer (AR-1000N, TA Instruments), equipped with an extended temperature module. Measurements were performed with a parallel plate geometry (2 cm diameter, 0.5 mm gap) at shear rates varying from 10 to 300 s^{-1}.

3.3 Effects of initiator impurities and oxygen

In literature it is frequently mentioned that initiator is recrystallized before use. In order to find out if recrystallization is essential for carrying out a CCT polymerization, several series of polymerizations were performed to determine C_T at different concentrations of non-recrystallized initiator. The results are collected in Figure 3.1. The Mayo-plots are offset for clarity. At lower AIBN concentrations a linear Mayo-plot is observed as expected. When the initiator concentration is increased a deviation from linearity occurs at lower CoBF concentrations. Below a threshold concentration of CoBF hardly any effect on chain length is observed, but at higher concentrations molecular weights start to decrease. The threshold Co(II) concentration, at which no catalytic chain transfer behaviour is observed, increases
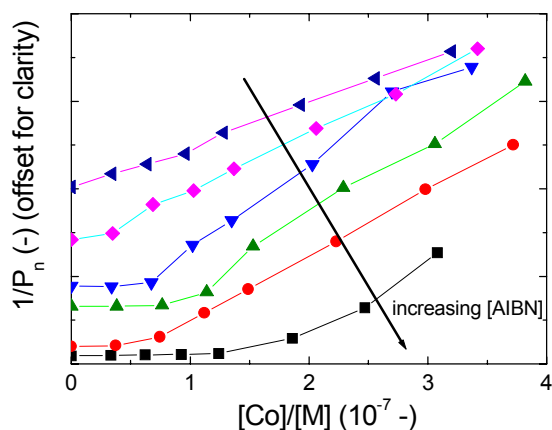
Figure 3.1 Mayo-plots for the bulk homopolymerization of MMA with CoBF at 60 ^{o}C at different [AIBN]. ◀0.015 M; ◆ 0.030 M; ▼0.044 M; ▲ 0.059 M; ● 0.073 M; ■ 0.087 M
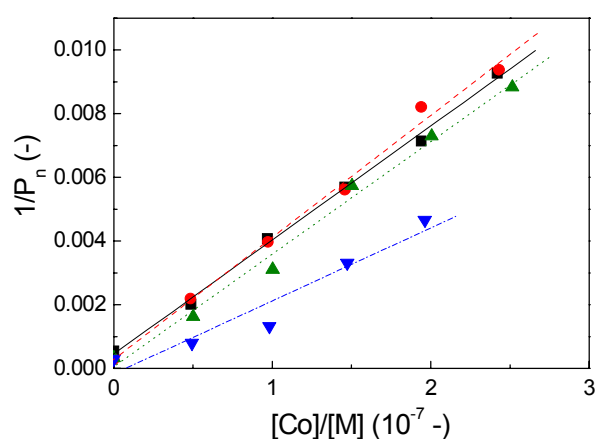
Figure. 3.2 Mayo-plots for the bulk homopolymerization of MMA with CoBF at 60 ^{o}C at different [O₂]. ■, solid line: 1 ppm; ●, dashed line: 4 ppm; ▲ , dotted line: 8 ppm; ▼ , dashed-dotted line 16 ppm

with initiator concentration and reaches about 1×10^{-6} M CoBF at 0.087 M AIBN. As this effect is absent when the initiator is recrystallized, this deactivation is probably caused by an impurity in the initiator. Assuming the impurity reacts with CoBF on a one to one basis, it can be calculated that the fraction of impurity in AIBN is less than 0.002 mol%. After recrystallization this impurity could not be reintroduced via heating of the AIBN in air or prolonged storage inside the glovebox. Therefore, it is expected that the impurity is introduced during manufacturing.

For CCT polymerizations in the presence of oxygen, deactivation is expected as well, which has been discussed in Section 2.3.2.4. Therefore, the effect of oxygen on the polymerization was tested. MMA was oxygenated by bubbling with air for over one hour. After that MMA was sealed and brought into a glovebox. The initiator was dissolved in various mixtures of oxygenated and oxygen-free MMA. The initiator solution was added to the CoBF solution just before reaction. The resulting Mayo-plots are shown in Figure 3.2. Oxygen concentrations were calculated from the oxygen saturation concentration in a solvent similar to MMA, the fraction of oxygen in air and the ratio of oxygenated and deoxygenated MMA. For the lower oxygen concentrations no effects are observed and C_T is around 37×10^3. In the presence of 16 ppm of oxygen catalytic activity is decreased by a factor of two. The effects are not as large as expected. The limited time, during which CoBF is exposed to oxygen may play a role. In addition, the reactivity of oxygen towards radicals resulting in termination or copolymerization[36], may be larger than the reactivity towards the Co(II) complex and most of the oxygen could be consumed in that way. However, when there is a continuous exposure to oxygen catalytic activity disappears completely.

3.4 Effects of solvents and solvent impurities

3.4.1 Solvent effects

In both toluene and *n*-butyl acetate the chain transfer coefficient for the polymerization of MMA was determined at several solvent concentrations in both purified and unpurified
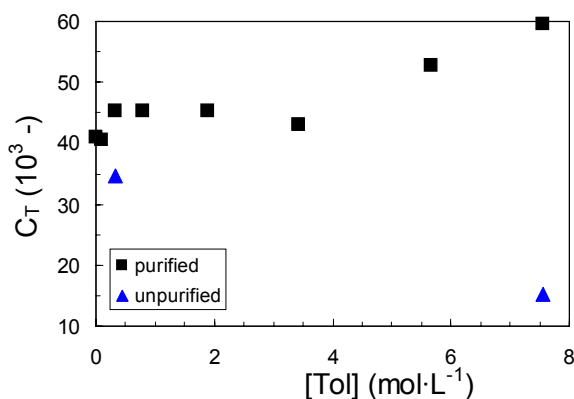
Figure 3.3 Determination of chain transfer coefficient of CoBF for the catalytic chain transfer polymerization of MMA in toluene at 60 °C. Toluene was used as received (▲) and after purification with a Grubbs-type purification set-up (■).
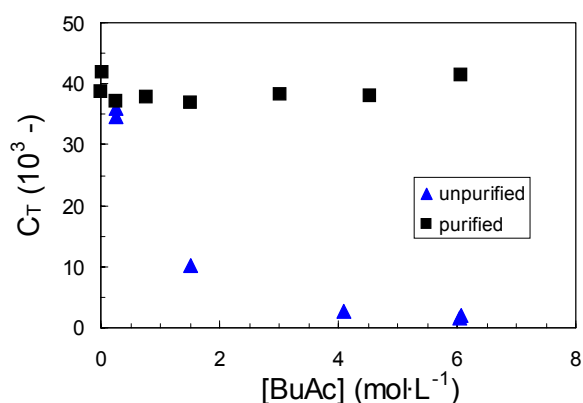
Figure 3.4 Determination of chain transfer coefficient of CoBF for the CCT polymerization of MMA in *n*-butyl acetate at 60 °C. *n*-Butyl acetate was used as received (▲) and after purification by distillation, subsequently passed over a column of basic alumina, shaken with anhydrous MgSO₄ and passed over a column of basic alumina once more (■).

solvent. The chain transfer coefficients were determined from the weight average molecular weight data to give the most reliable results.[13] The results are presented in Figures 3.3 and 3.4 and in Tables 3.1 and 3.2 for toluene and *n*-butyl acetate, respectively. For the bulk polymerization of methyl methacrylate C_T was determined to be 39.8×10^3, which is in good agreement with earlier reports.[1,2,14] It can be clearly seen that within experimental error for the purified solvents the chain transfer coefficient remains constant over almost the whole concentration range at a value determined for the bulk polymerization of methyl methacrylate.

Note that for high concentrations of purified toluene the chain transfer coefficient surprisingly increases towards 60×10^3. This effect is not seen for the solvent *n*-butyl acetate, so it is not expected to be related to dilution. The origin of this effect is unclear. So far, in reports on CCT of MMA solvent effects have only been used to explain a decrease in C_T. However, solvent effects can also enhance reaction rates when the solvent is changed. This depends on the changes, for both solvents, in Gibbs energy going from the initial state to the transition state.[15] This is presented schematically in Figure 3.5. In the particular case presented here, the difference in Gibbs energy for the two solvents is smaller in the transition state than in the initial state. This means that for the reaction in the solvent represented by the dotted curve, the

rate constant will be smaller than for the reaction in the solvent represented by the solid curve. So the increase in C_T may be due to a solvent effect.
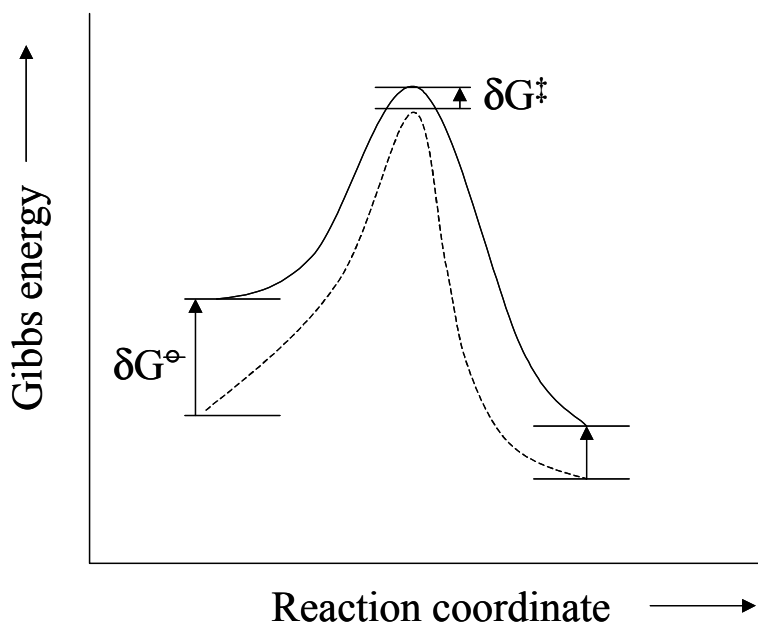
Figure 3.5 Reaction profile for the Gibbs energy in two different solvents.[15] The initial state is marked with ⊖ and the transition state is marked with ‡.

Table 3.1 Chain transfer coefficients for CoBF in the CCT polymerization of MMA determined in both purified and unpurified toluene at 60 °C.

Purified solvent		Unpurified solvent	
[Toluene]	C_T	[Toluene]	C_T
$(mol \cdot L^{-1})$	$(10^3 -)$	$(mol \cdot L^{-1})$	$(10^3 -)$
0	39.8 [a]		
9.9×10^{-2}	41.0		
0.10	40.6		
0.32	45.3	0.32	34.6
0.8	45.3		
1.9	45.3		
3.4	43.1		
5.7	52.8		
7.6	59.6	7.55	15.1

[a] C_T averaged over three experiments.

For the reactions in unpurified solvent it was shown that C_T decreases rapidly with increasing solvent concentration to around 15×10^3 for toluene and to 2×10^3 for *n*-butyl acetate. For comparison, some earlier data for both bulk and solution polymerization are shown in Table 3.3. For both toluene and butanone the chain transfer coefficients in solution are lower than in bulk.

Table 3.2 Chain transfer coefficients for CoBF in the CCT polymerization of MMA determined in both purified and unpurified *n*-butyl acetate at 60 °C.

Purified solvent		Unpurified solvent	
[*n*-Butyl acetate]	C_T	[*n*-Butyl acetate]	C_T
(mol· L^{-1})	(10^3 -)	(mol· L^{-1})	(10^3 -)
0.0016	38.6		
0.020	41.8	0.26	34.6
0.26	37.0	0.26	36.0
0.76	37.9		
1.52	36.9	1.52	10.2
3.03	38.2	4.09	2.70
4.53	38.0	6.05	1.48
6.07	41.4	6.06	2.00

Table 3.3 Chain transfer coefficients for CoBF and Co(Ph)$_4$BF in the CCT polymerization of MMA determined both in solution and in bulk.

Solvent	Concentration (mol· L^{-1})	Catalyst	C_T (-)	C_T (-) (bulk)	Ref.
Butanone (undistilled)	unknown	CoBF	8020	40900	9
Butanone (distilled)	unknown	CoBF	26500	40900	9
Toluene (distilled)	6.3	CoBF	24870	34780	8
Toluene (distilled)	6.64	CoBF	6000	24500	10
Toluene (undistilled)	6.3	Co(Ph)$_4$BF	23000	20000	15

Haddleton *et al.* demonstrated[2] that solvent purification can lead to increased chain transfer coefficients in butanone, but still found a difference between bulk and solution values.

Only for Co(Ph)$_4$BF, a tetraphenyl cobaloxime derivative, values in bulk and solution were found to be almost the same.[8] In that study both toluene and *tert*-butyl acetate were chosen as solvents as no solvent effects were expected.[8] In the other studies for both butanone and toluene, this decrease in chain transfer coefficients was at least partially explained by the occurrence of a solvent effect, the competition of monomer and solvent for the active catalytic site. As can be seen from our experiments in toluene and in *n*-butyl acetate a decrease in chain transfer coefficients can be prevented by thorough solvent purification. Therefore, we believe that the observed effects are not solvent effects, but effects of solvent impurities. So the effects of impurities, first shown by Haddleton *et al.*[2], are even stronger and fully account for observed solvent effects. This confirms recent results obtained by Heuts *et al.*[16] who only found a significant solvent effect, when pyridine was used as solvent. The question remains what these impurities can be. At least part of the decomposition will most probably be caused by traces of acid in the organic solvents. However, other compounds may also be of importance.

3.4.2 Effects of solvent impurities

In order to try and quantify the nature of the impurities, we deliberately added 1-dodecanethiol, acetic acid, THF, methanol and benzoyl peroxide to the bulk polymerization of MMA. This group of compounds is chosen to represent a range of impurities that either are known to be present in toluene or *n*-butyl acetate or that are known in literature to affect Co(II) catalysts. The effect of these impurities on low conversion polymerizations is small when these are present in low concentrations, see Figure 3.6. From studies of CCT in emulsion polymerization[17] and on the polymerization of methacrylic acid[18] it is known that at low pH CoBF is prone to decomposition. That is why we would have expected to see an effect of acetic acid, but even at 1 mol· L^{-1} no clear decrease in C_T can be seen. Peroxides are known to oxidize cobalt complexes from Co(II) into Co(III) and in that way reduce the rate of transfer with respect to the rate of propagation[19], but here we did not observe any effect either. Maybe impurities in technical peroxides are responsible for deactivation reported earlier.
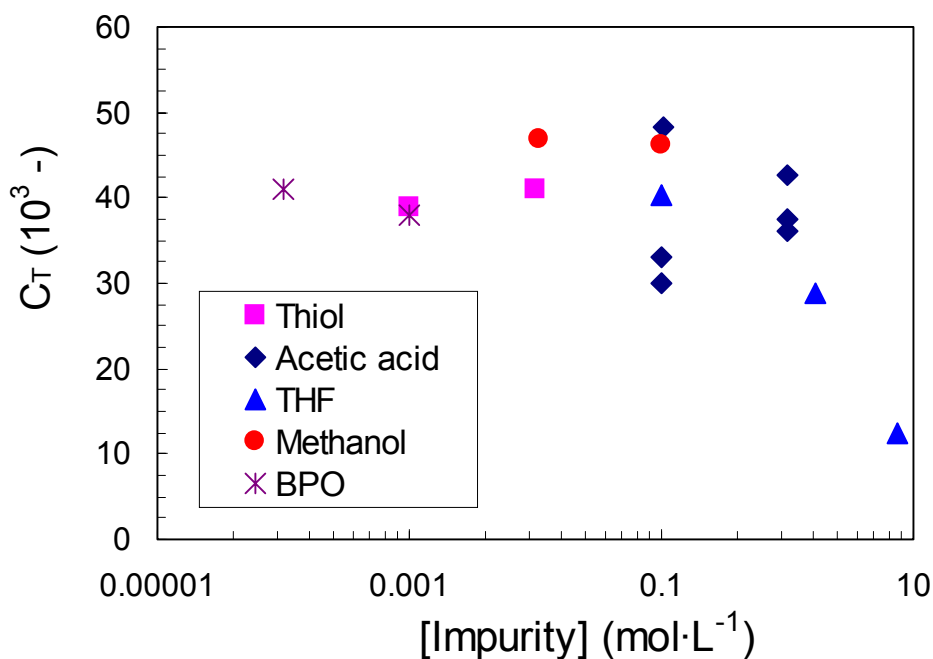
Figure 3.6 C_T of CoBF for the bulk polymerization of MMA at 60 ^oC at various impurity concentrations.

As alcohols are present in alkyl esters, methanol was tested as well, but it did not change the obtained transfer coefficients and neither did 1-dodecanethiol. Only in THF C_T decreased quite drastically but only at concentrations of THF over 1 mol· L^{-1}. This decrease may be due to the presence of peroxides despite thorough purification or due to coordination to the catalyst as THF has stronger coordinating capabilities as toluene and *n*-butyl acetate. Similar observations have been made for ATRP polymerizations, where a whole range of polar compounds such as 2-propanol[20] and water[21,22] have been found to enhance polymerization rate.

However, the exact nature of the impurities present in both toluene and *n*-butyl acetate that cause strong reductions in C_T remains unclear. This is an important question to be resolved for practical application of CCT in an industrial environment. This work will be continued in Chapter 4, where the effect of acetic acid and BPO on high conversion CCT polymerizations is studied.

3.5 Diffusion control

When we wish to determine whether diffusion plays a role in a chemical reaction, two pathways can be chosen. The first approach will be from a process technological point of view and is presented in Section 3.5.1. This approach is commonly used for two-phase systems and is adapted for the situation of CCT in a homogeneous system. In Section 3.5.2 an approach reported by North[24] for homogeneous systems is taken. This second approach is more common to chemists.

3.5.1 Diffusion control from a process technological point of view

First of all a length-scale for diffusion has to be estimated. In this approach it is assumed that the rate of diffusion is determined by the diffusion of the Co(II) catalyst. The long polymeric chains are assumed to diffuse only very slowly. Suppose the radical concentration is 1×10^{-8} mol$\cdot$L^{-1}, the Co(II) catalyst concentration is 1×10^{-6} mol$\cdot$L^{-1} and the system is perfectly mixed. In that case the volume (V_1) available to a catalyst molecule equals

$$V_1 = \frac{1}{[\text{Co(II)}]N_A}$$

(3.1)

in which N_A is the Avogadro number. Imagine the total volume is subdivided into spheres of equal size, which have a closest packing. The polymeric radical will be located in between the Co(II) catalyst molecules. The spheres will occupy 74 % of the total volume. The diameter of such a sphere is chosen as the length-scale for diffusion of a catalyst molecule to a polymeric radical. The diameter (d) of these spheres is calculated according to

$$d = \sqrt[3]{\frac{6 \times 0.74}{\pi[\text{Co(II)}]N_A}} = 1.33 \times 10^{-7}\,\text{m}$$

(3.2)

The Damköhler number (Da) is a dimensionless number that compares the rates of reaction and mass transport. In the case of mass transport via diffusion the Damköhler number is defined as

$$Da = \frac{k_{tr}[P_n\bullet]d^2}{D_{Co}} \qquad (3.3)$$

in which D_{Co} is the diffusion coefficient for the Co(II) catalyst. For *Da* numbers smaller than one, the reaction is chemically controlled. On the other hand, for *Da* numbers larger than one the reaction is diffusion controlled.

The diffusion coefficient of a cobalt compound similar to CoBF has been determined by Bon *et al.*[23] using 2D-NMR. They reported that the diffusion coefficient for the cobalt species was about half the diffusion coefficient of acetone, resulting in $D_{Co} = 1 \times 10^{-9}$ m$^2\cdot$ s^{-1}. The transfer rate constant can be calculated from $C_T = 40 \times 10^3$ and $k_p = 833$ L$\cdot$ mol$^{-1}\cdot$ s^{-1}, which results in $k_{tr} = 3.3 \times 10^7$ L$\cdot$ mol$^{-1}\cdot$ s^{-1}. Now all required parameters are known, the Damköhler number can be calculated, resulting in $Da = 10^{-6}$. According to this analysis the transfer step is not diffusion controlled. The radical and Co(II) complex can approach and separate several times before reaction occurs.

3.5.2 Diffusion control according to North

3.5.2.1 Derivation of an expression for C_T incorporating diffusion rate constants

In this section diffusion is presented as an additional reaction step, which represents the

Scheme 3.1

$$P_n\bullet \quad + \quad [Co(II)] \quad \underset{k_{-1}}{\overset{k_1}{\rightleftharpoons}} \quad [P_n\bullet\, Co(II)]$$

$$[P_n\bullet\, Co(II)] \quad \xrightarrow{k_{tr}} \quad D_n \quad + \quad [Co(III)]-H$$

$$[Co(III)]-H \quad + \quad M \quad \xrightarrow{k_{rein}} \quad P_1\bullet \quad + \quad [Co(II)]$$
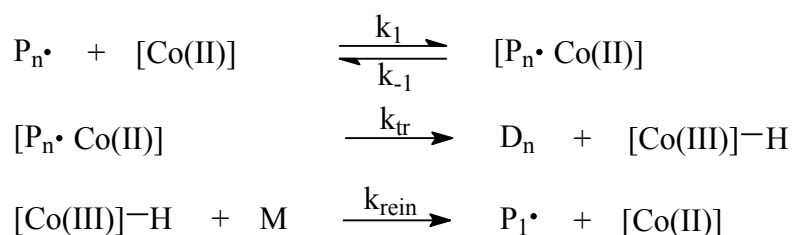
encounter and separation of a polymeric radical, $P_n\bullet$, and the cobalt(II) complex, [Co(II)], as shown in Scheme 3.1. Here [$P_n\bullet$Co(II)] represents a diffusion encounter pair. The length-scales considered are equal to those presented in the previous section. In a diffusion controlled regime the time constant for diffusion is larger than or has the same order of magnitude as the time constant for chemical reaction.

As has been discussed in Chapter 2, the second reaction in Scheme 3.1 is rate determining.

Assuming a steady state in $[P_n \bullet Co(II)]$ it can be easily derived from the corresponding rate equations that the rate of transfer, R_{tr}, can be expressed as[24]

$$R_{tr} = \frac{k_{tr} k_1}{k_{tr} + k_{-1}}[Co(II)][P\bullet]$$ (3.4)

where k_{tr} is the chain transfer rate constant and k_1 and k_{-1} are the respective rate constants for diffusional encounter and separation. When the rate constant for diffusion is large compared to the rate constant for chemical reaction ($k_{-1} >> k_{tr}$) the unpaired and paired reactants are in equilibrium, resulting in

$$R_{tr} = \frac{k_1}{k_{-1}}k_{tr}[Co(II)][P\bullet] = K_1 k_{tr}[Co(II)][P\bullet]$$ (3.5)

in which K_1 is the equilibrium constant for the formation of paired reactants.[24] In this case K_1 and k_{tr} are usually taken together as one parameter $k_{tr,overall}$. On the other hand, eq 3.4 reduces to

$$R_{tr} = k_1[Co(II)][P\bullet]$$ (3.6)

when the rate constant for chain transfer is much larger than the rate constant for diffusive separation ($k_{tr} >> k_{-1}$). So the experimentally determined transfer rate constant will actually be equal to the rate constant for bimolecular diffusion. This rate constant can be expressed as the von Smoluchowski equation[25]

$$k_1 = 4\pi\sigma_r N_A p(D_{Co} + D_{P\bullet})$$ (3.7)

in which σ_r is the radius of the solute, N_A is Avogadro's number, p is the statistical spin factor and D_{Co} and $D_{P\bullet}$ are the respective diffusion coefficients. As the diffusion coefficient for the Co(II) species will be larger than for most polymeric radicals the sum of both diffusion coefficients can be approximated by the diffusion coefficient of the Co(II) species alone, which will always result in an underestimation of the diffusion rate constant. Various theoretical and empirical expressions are used to estimate values for diffusion coefficients.[26] In most of these the following proportionality can be found

$$D \propto \frac{kT}{\eta r} \tag{3.5}$$

where k is the Boltzmann constant, T is absolute temperature, η is the dynamic viscosity of the solvent and r the solute radius. When all experiments are carried out at the same temperature the diffusion rate constants can be expressed as

$$k_1 = \frac{k_1'}{\eta} \qquad \text{and} \qquad k_{-1} = \frac{k_{-1}'}{\eta} \tag{3.9}$$

in which k_1' and k_{-1}' are constants containing all contributions to the diffusion rate constants k_1 and k_{-1} except dynamic viscosity. The rate of polymerization can be expressed as

$$R_p = k_p [M][P\bullet] \tag{3.10}$$

in which k_p is the propagation rate constant. Eqs 2.1, 3.4, 3.9 and 3.10 can be combined to give the following expression for the chain transfer coefficient.

$$C_T = \frac{k_{tr}}{k_p} \frac{k_1'}{k_{-1}' + \eta_{sol} k_{tr}} \tag{3.11}$$

This clearly shows that in a diffusion controlled regime the chain transfer coefficient will depend on solution viscosity η_{sol}. For viscous reaction mixtures the solution viscosity can be easily changed by dilution with solvent. Dilution will consequently change the extent of diffusion control. In a bulk polymerization the extent of diffusion control is defined as

$$\frac{k_{-1}}{k_{tr}} = \lambda \Rightarrow \frac{k'_{-1}}{k_{tr}} = \lambda \eta_{bulk} \tag{3.12}$$

in which λ is the diffusion control parameter. As a consequence, in a solution polymerization the ratio of k_{-1} and k_{tr} can be written as

$$\frac{k_{-1}^{sol}}{k_{tr}} = \lambda \frac{\eta_{bulk}}{\eta_{sol}} \tag{3.13}$$

A small λ (<1) indicates a diffusion controlled bulk polymerization and *vice versa*.

Furthermore, the ratio of rate constants for diffusional encounter k_1 and separation k_{-1} is defined as χ. The ratio of k_{tr} and k_p is independent of mixture composition. For a particular monomer having a specific λ, the ratio of k_{tr} and k_p is calculated from the chain transfer coefficient determined for the bulk polymerization. Combining eq 3.11 and 3.12 this results in

$$\frac{k_{tr}}{k_p} = C_T^{bulk} \frac{\lambda + 1}{\lambda \chi} \tag{3.14}$$

Substituting eq 3.14 into eq 3.11 gives

$$C_T = C_T^{bulk} \frac{\lambda + 1}{\lambda + \dfrac{\eta_{sol}}{\eta_{bulk}}} \tag{3.15}$$

It can be seen that χ, the ratio of k_1 and k_{-1}, does not influence the relative change in C_T. So, no knowledge of χ is required to establish whether or not the reaction is diffusion controlled. A moderately diffusion controlled system can be assumed to have $\lambda = 1$ and a strongly diffusion controlled one to have $\lambda = 0.1$. These values are applied in the next section.

3.5.2.2 Comparison of experimental results and theoretical calculations

As was shown in the first part of this chapter toluene does hardly affect the chain transfer coefficient for CoBF in MMA. However, MMA has approximately the same viscosity as toluene and, therefore, no change is expected. Recently, Heuts[27] also reported that changing solution viscosity, via dilution or addition of high molecular weight polymer, did not affect the chain transfer coefficient. That is why we performed polymerizations of *n*-BMA and 2-EHMA at different toluene concentrations to see whether or not the chain transfer coefficient would change. The experimental results are shown in Figures 3.7 and 3.8. Also shown in Figures 3.7 and 3.8 are theoretical curves for moderately and strongly diffusion controlled systems calculated according to eq 3.15. These are calculated in the following way. Both systems are given the same C_T-value at zero solvent concentration being 28×10^3 for BMA and 11.9×10^3 for 2-EHMA. The dynamic viscosity of the mixtures is calculated as follows

$$\ln \eta_{sol} = \sum_i w_i \ln \eta_i \tag{3.16}$$

in which w_i is the weight fraction of component i in the solution and η_i the bulk viscosity of component i. This equation generally gives a good approximation of the solution viscosity.[28] Bulk viscosity data for 2-EHMA were determined from rheological measurements. The results are shown in Figure 3.9. For the other compounds viscosities were calculated using the parameters from Yaws[28]. All values are shown in Table 3.4.
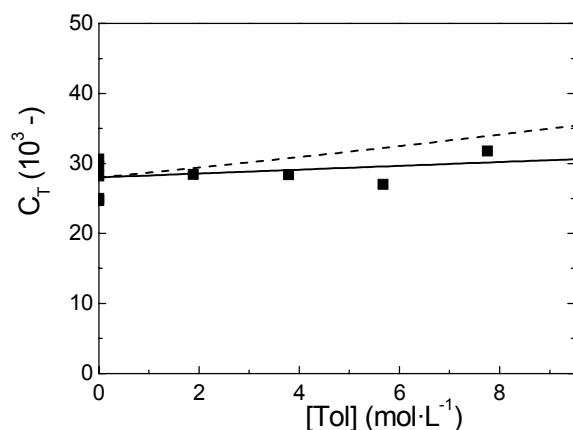
Figure 3.7 Determination of chain transfer coefficient of CoBF for the catalytic chain transfer polymerization of *n*-BMA in toluene at 60 °C. Experimental data (■) and theoretical calculations based on a model taking into account the effect of monomer viscosity on the chain transfer coefficient assuming moderate (solid line) and strong (dashed line) diffusion control in the transfer step.
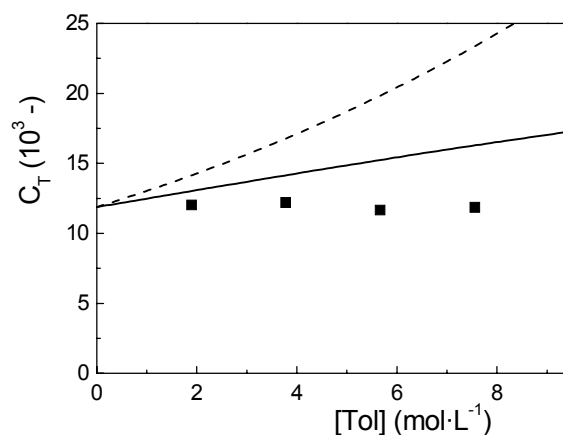
Figure 3.8 Determination of chain transfer coefficient of CoBF for the catalytic chain transfer polymerization of 2-EHMA in toluene at 60 °C. Experimental data (■) and theoretical calculations based on a model taking into account the effect of monomer viscosity on the chain transfer coefficient assuming moderate (solid line) and strong (dashed line) diffusion control in the transfer step.

Table 3.4 Viscosity data for toluene and the methacrylic monomers at 60 °C.

Monomer or solvent	viscosity (10^{-3} Pa· s)
toluene	0.387
methyl methacrylate	0.382
n-butyl methacrylate	0.515
2-ethylhexyl methacrylate	1.03
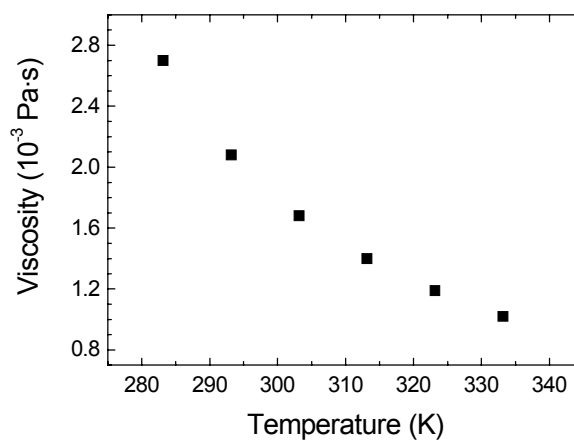
Figure 3.9 Viscosities (Pa· s) for 2-EHMA measured at different temperatures.

For *n*-BMA the chain transfer coefficient hardly changes with increasing toluene concentration in contrast to what has been observed for MMA, but the theoretical increase in chain transfer coefficient at moderate diffusion control is too small compared with experimental inaccuracies to distinguish whether the system is moderately or not diffusion controlled. We can conclude, however, that the system is not strongly diffusion controlled. For 2-EHMA the chain transfer coefficient is independent of solvent concentration. In Figure 3.9 we can see a clear distinction between the theoretical curves for moderate and strong diffusion control and the experimental values. Therefore, this indicates that the chain transfer step for 2-EHMA is not diffusion controlled. As the viscosity for 2-EHMA is higher than for n-BMA and for MMA it is very likely that the transfer steps for these monomers are not diffusion controlled either. If this is true, the transfer constants can be calculated using known data for the propagation rate constants[29]. These are all shown in Table 3.5. It can be seen that with increasing size of the ester group k_{tr} decreases. Heuts *et al.*[7] found a similar trend in a series methyl, ethyl, butyl methacrylate, although the decrease in k_{tr} in their data is around 45 percent going from MMA to *n*-BMA, where it is only 18 percent in the data presented here. Heuts *et al.* concluded that the decrease in chain transfer constant was caused by the increase in monomer viscosity and, therefore, supported their main conclusion that the chain transfer step is diffusion controlled.

Table 3.5 Chain transfer coefficients, propagation rate constants and transfer rate constants for MMA, *n*-BMA and 2-EHMA.

Monomer	C_T (average)	$k_p{}^a$ (L· mol^{-1}· s^{-1})	k_{tr} (L· mol^{-1}· s^{-1})
MMA	39.8×10^3	833	3.3×10^7
n-BMA	28.0×10^3	976	2.7×10^7
2-EHMA	11.9×10^3	1190	1.4×10^7

^{a} All k_p data are taken from van Herk[25]

As we have indications that the transfer step is not diffusion controlled we have to look for an alternative explanation. We suppose that the transition state in the transfer step is sterically hindered by the increasing size of the ester group. The *n*-butyl group is not that large and has some flexibility and so only a small decrease in C_T is found going from MMA to *n*-BMA. The 2-ethylhexyl group on the other hand is very bulky, causing a larger reduction in k_{tr} with

respect to the transfer constants for MMA and *n*-BMA. Mironychev *et al.* [30] studied the catalytic chain transfer behaviour of a cobalt porphyrin for a series of eight methacrylates differing in the length of the ester chain. They found a similar decrease in k_{tr} and concluded as well that steric hindrance was one of the reasons.

The conclusion that the transfer step is not diffusion controlled also contradicts very interesting findings of Forster *et al.*[8] who conducted a catalytic chain transfer polymerization of MMA in supercritical CO_2. and obtained very low molecular weight polymer. C_T is estimated to be over 1×10^5, which is nearly an order of magnitude higher than what is found in bulk or solution. Unfortunately, no results for polymerizations in supercritical CO_2 without transfer agent were presented, so it is not completely clear what the effect of the CO_2 itself is. Furthermore, for *e.g.* k_p solvent effects have been reported in supercritical CO_2.[31] It cannot be excluded that solvent effects have a significant influence on k_{tr} as well. Therefore, it is hard to say what the reason for the discrepancy is between the results presented here and those obtained in CO_2.

3.6 Cobalt – carbon bond formation

In Section 2.3.2.3 we briefly discussed the formation of cobalt – carbon bonds. Investigations on the effects Co – C bond formation may have on catalytic chain transfer polymerizations in general and for the polymerization of MMA in particular will be reported from both a theoretical and an experimental point of view.

3.6.1 Derivation of an expression for C_T incorporating Co – C bond formation

In Scheme 3.2 the reactions that are taken into account are shown. In comparison to Scheme 3.1 only the formation and dissociation of a cobalt – polymer species P_n-Co(III) has been added. For this set of reactions the rate of transfer will be equal to

$$R_{tr} = k_{tr}[[P \bullet Co(II)]] \tag{3.17}$$

Scheme 3.2

$$P_n{}^\bullet \;\; + \;\; [Co(II)] \qquad \underset{k_{-1}}{\overset{k_1}{\rightleftharpoons}} \qquad [P_n^\bullet\, Co(II)]$$

$$[P_n^\bullet\, Co(II)] \qquad \underset{k_{dis}}{\overset{k_{com}}{\rightleftharpoons}} \qquad [Co(III)] - P_n$$

$$[P_n^\bullet\, Co(II)] \qquad \xrightarrow{k_{tr}} \qquad D_n \;\; + \;\; [Co(III)] - H$$

$$[Co(III)] - H \;\; + \;\; M \qquad \xrightarrow{k_{rein}} \qquad P_1{}^\bullet \;\; + \;\; [Co(II)]$$
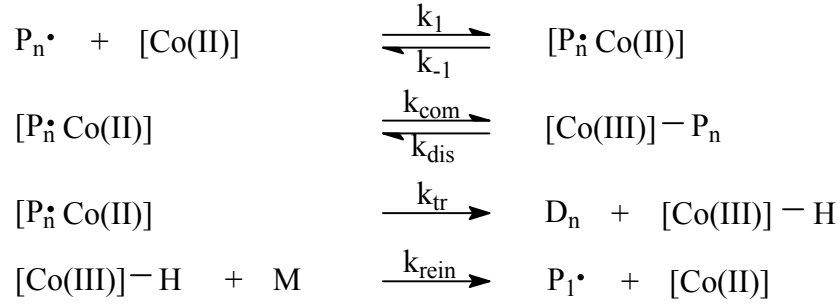
So we need to express the concentration of $[P{\bullet}Co(II)]$ as a function of the total amount of cobalt present in the system. This can be done using the differential equations for Co(II) and P-Co(III) in a steady state situation and a mass balance for all cobalt species. The reinitiation is assumed to be fast enough to prevent build-up of substantial amounts of Co(III)-H as discussed in Chapter 2.

$$\frac{d[Co(II)]}{dt} = (k_{tr} + k_{-1})[P \bullet Co(II)] - k_1[Co(II)][P \bullet] = 0 \tag{3.18}$$

$$\frac{d[P - Co(III)]}{dt} = k_{com}[P \bullet Co(II)] - k_{dis}[P - Co(III)] = 0 \tag{3.19}$$

$$[Co(II)] + [P \bullet Co(II)] + [P - Co(III)] = [Co]_0 \tag{3.20}$$

Equation 3.18 and 3.19 can be rewritten as respectively,

$$[Co(II)] = \frac{(k_{tr} + k_{-1})[P \bullet Co(II)]}{k_1[P\bullet]} \tag{3.21}$$

and

$$[P - Co(III)] = \frac{k_{com}}{k_{dis}}[P \bullet Co(II)] \tag{3.22}$$

which combined with mass balance eq 3.20 results in

$$[P \bullet Co(II)] = \frac{1}{1 + \dfrac{k_{com}}{k_{dis}} + \dfrac{k_{-1} + k_{tr}}{k_1[P\bullet]}}[Co]_0 \tag{3.23}$$

Together with eq 3.17 we obtain the transfer rate

$$R_{\text{tr}} = \frac{k_{\text{tr}}}{[\text{P}\bullet] + \dfrac{k_{\text{com}}}{k_{\text{dis}}}[\text{P}\bullet] + \dfrac{k_{-1} + k_{\text{tr}}}{k_1}}[\text{Co}]_0[\text{P}\bullet] \tag{3.24}$$

When this expression is used in combination with the Mayo-equation 2.1, this results in an apparent chain transfer coefficient that depends on radical concentration.

$$C_{\text{T}} = \frac{1}{[\text{P}\bullet] + \dfrac{k_{\text{com}}}{k_{\text{dis}}}[\text{P}\bullet] + \dfrac{k_{-1} + k_{\text{tr}}}{k_1}}\frac{k_{\text{tr}}}{k_{\text{p}}} \tag{3.25}$$

3.6.2 Theoretical calculations for C_{T}

In order to make meaningful calculations for C_{T}, valid estimates of the rate constants in eq 3.25 have to be made. These rate constants are not generally available. For some systems only overall rate constants are known, combining diffusion rate constants and either combination or dissociation rate constants. The overall rate constants for combination and dissociation can be derived using Scheme 3.2 resulting in

$$k_{\text{dis,overall}} = k_{\text{dis}}\frac{k_{-1}}{k_{-1} + k_{\text{com}}} \tag{3.26}$$

and

$$k_{\text{com,overall}} = k_1\frac{k_{\text{com}}}{k_{\text{com}} + k_{-1}} \tag{3.27}$$

Koenig and Finke[32] suggested that k_{com} is expected to be larger than k_1, and that k_1 and k_{-1} are not expected to be numerically equal. From computer simulations of the homolytic dissociation of a benzyl Co(III) macrocycle, as presented in Scheme 2.6, Daikh and Finke[33] obtained estimates for $k_1 = 1 \times 10^{10}$ L· mol^{-1}· s^{-1} and $k_{-1} = 2 \times 10^9$ s^{-1}. Koenig *et al.*[34] studied cage-effects in the recombination of phenylthiyl radicals and argued that the rate constant for diffusive encounter will be expected to be smaller than the rate constant for diffusive separation, which is in contrast to the simulation results from Daikh and Finke. However, both rate constants are expected to be numerically in the same range from 10^8 to 10^{10}. Therefore, in all calculations using eq 3.25 k_{-1}/k_1 is set to 1 mol· L^{-1}.

Wayland *et al.*[35] determined overall combination and dissociation rate constants for cyanoisopropyl radicals and tetraanisylporphyrinato Co(II). They obtained $k_{\text{com,overall}}$ =

1.0×10^9 L· mol^{-1}· s^{-1}, $k_{dis,overall} = 236$ s^{-1} and $K_{overall} = 4.2 \times 10^6$ L· mol^{-1} at 60 °C. From eq 3.26 it can be seen that k_{dis} will be larger than $k_{dis,overall}$ by definition. From eq 3.27 it can be seen that $k_{com,overall}$ is smaller than k_1. If Koenig and Finkes suggestion[32] that k_{com} is expected to be larger than k_1, is indeed correct, than k_{com} will be larger than $k_{com,overall}$ as well. As k_{com} and k_{dis} are larger than $k_{com,overall}$ and $k_{dis,overall}$, respectively, no significant difference in the ratios of k_{com} and k_{dis}, on the one hand, and $k_{com,overall}$ and $k_{dis,overall}$, on the other hand, is to be expected.

For a polymethacrylate radical the combination – dissociation equilibrium will be shifted more towards the dissociated side as compared with a cyanoisopropyl radical. This can be expressed in a smaller combination rate constant or a larger dissociation rate constant or both. A first estimate for the equilibrium between a polymethacrylate radical and CoBF could be $k_{com}/k_{dis} = 10^6$.

The chain transfer coefficient at zero radical concentration was arbitrarily chosen to be 40,000. This does not affect the trends shown in Figures 3.10 and 3.11. In Figure 3.10 C_T is shown as a function of radical concentration for different values of k_{com}/k_{dis}. It is assumed that the rate constant for diffusion is large as compared with the rate constant for transfer, so

Figure 3.10 The dependence of C_T on radical concentration [P•] assuming a reversible formation of covalent bonds between the polymeric radicals and the Co(II) species. C_T is arbitrarily set at 40,000 at [P•] = 0. k_{com}/k_{dis}: solid line 10^5; dashed line 10^6; dotted line 10^7.

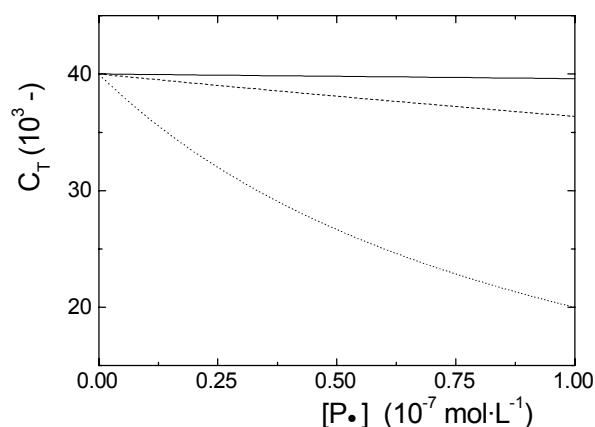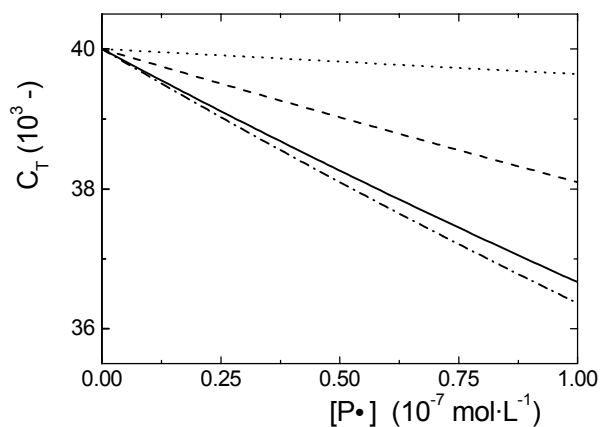**Figure 3.11** The dependence of C_T on radical concentration [P•] assuming a reversible formation of covalent bonds between the polymeric radicals and the Co(II) species at different levels of diffusion control. C_T is arbitrarily set at 40,000 at [P•] = 0. $k_{com}/k_{dis} = 10^6$. k_{-1}/k_{tr}: dashed dotted line ∞; solid line 10; dashed line 1; dotted line 0.1 mol· L^{-1}.

$k_{-1} \gg k_{tr}$. For $k_{com}/k_{dis} \geq 10^6$ a measurable decrease in chain transfer coefficient with increasing radical concentration can be seen.

For the calculation of the plots in Figure 3.10 it was assumed that the diffusive encounter and separation of the Co(II) species and the polymeric radical is faster than the transfer process. In Figure 3.11, on the other hand the effect of different degrees of diffusion control is shown when the ratio k_{com}/k_{dis} is set at 10^6. For C_T to equal 40,000 at zero radical concentration k_{tr} and k_{-1} have to be adjusted for each degree of diffusion control. In practice this means that k_{tr} is increased when stronger diffusion control is assumed. When the rate constants for diffusion are much smaller than the rate constants for transfer, the effect of cobalt − carbon bond formation on the chain transfer coefficient is strongly reduced. This can be explained as follows. When the ratio of the rate constants for diffusion and transfer is decreased, the concentration of [P•Co(II)] and as a result the concentration of P-Co(III) will diminish. So almost all of the initially added Co species will be in the form of Co(II). Although an increase in radical concentration leads to an increase in P-Co(III) concentration, that will in this case hardly effect the Co(II) concentration and thus the apparent chain transfer coefficient. In summary, we can say that if the ratio of the rate constants for combination and dissociation is large enough, an effect of radical concentration on the apparent chain transfer coefficient can be seen. However, this effect is counteracted by diffusion control.

3.6.3 Experimentally observed effects of initiator concentration on C_T

In order to relate the experimental observations to eq 3.25, a relation between radical and initiator concentration is required. The total radical concentration can be expressed according to normal free-radical polymerization kinetics as[36]

$$[P•] = \sqrt{\frac{f k_d [I]}{< k_t >}} \tag{3.28}$$

in which f is initiator efficiency, k_d is the initiator decomposition rate constant and [I] is initiator concentration. Combining eqs 3.25 and 3.28 and neglecting the first term [P•] in eq 3.25, we can directly relate the chain transfer coefficient to the experimental quantity [I] as in eq 3.29

$$C_{\mathrm{T}} = \cfrac{1}{\cfrac{k_{\mathrm{com}}}{k_{\mathrm{dis}}} \sqrt{\cfrac{fk_{\mathrm{d}}}{<k_{\mathrm{t}}>}} \sqrt{[\mathrm{I}]} + \cfrac{k_{-1}+k_{\mathrm{tr}}}{k_1}} \cfrac{k_{\mathrm{tr}}}{k_{\mathrm{p}}} \qquad (3.29)$$

In absence of diffusion control the rate of transfer is negligible compared to rate of diffusive separation ($k_{-1} \gg k_{\mathrm{tr}}$). In that case multiplying both nominator and denominator of eq 3.29 with k_1 / k_{-1} results in

$$C_{\mathrm{T}} = \cfrac{1}{\cfrac{k_1}{k_{-1}} \cfrac{k_{\mathrm{com}}}{k_{\mathrm{dis}}} \sqrt{\cfrac{fk_{\mathrm{d}}}{<k_{\mathrm{t}}>}} \sqrt{[\mathrm{I}]} + 1} \cfrac{\cfrac{k_1}{k_{-1}} k_{\mathrm{tr}}}{k_{\mathrm{p}}} \qquad (3.30)$$

When the products of k_1/k_{-1} with respectively k_{tr} and k_{com} are taken as one eq 3.31 is obtained.

$$C_{\mathrm{T}} = \cfrac{1}{\cfrac{k_{\mathrm{com,overall}}}{k_{\mathrm{dis,overall}}} \sqrt{\cfrac{fk_{\mathrm{d}}}{<k_{\mathrm{t}}>}} \sqrt{[\mathrm{I}]} + 1} \cfrac{k_{\mathrm{tr,overall}}}{k_{\mathrm{p}}} \qquad (3.31)$$

In Figure 3.12 the results for the catalytic chain transfer polymerization of MMA at different levels of initiator are shown at 50, 60 and 70 $^{\mathrm{o}}$C. The first thing to be noticed is that the results of replicate experiments can differ up to 15 %, which renders it more difficult to draw straightforward conclusions from these data. The data at 60 $^{\mathrm{o}}$C are most clear. The chain transfer coefficient does not depend on initiator concentration. At 50 $^{\mathrm{o}}$C a slight increase may be seen, which effect could not be explained by either cobalt – carbon bond formation or diffusion control, whereas at 70 $^{\mathrm{o}}$C even a minor decrease could be observed. The general trend, however, seems to be that the chain transfer coefficient does not depend on initiator concentration and therefore, not on radical concentration. Looking at the theoretical calculations this leaves two possible options. First that cobalt – carbon bond formation does not take place to any extent affecting the reaction kinetics, due to a small ratio of combination and dissociation rate constants, or secondly that cobalt – carbon bond formation does take place, but is counteracted by a strong diffusion control. As it was shown in this discussion that diffusion control is unlikely to be present in these reactions it can be concluded that the formation of cobalt – carbon bonds does not take place in the catalytic chain transfer polymerization of MMA in the temperature range 50 to 70 $^{\mathrm{o}}$C. The latter is in contrast to what

is observed in copolymerizations with acrylates.[37]

These conclusions are in line with observations that radicals larger than cyanoisopropyl do not form cobalt – carbon bonds to any observable extent[38] and in agreement with the conclusions of Heuts *et al.* using ESR-experiments in a study of styrene and MMA polymerizations.[39] The model outlined above may also be a useful tool to describe experiments performed at lower temperature or to describe polymerizations of styrene and acrylates where covalent bond formation is more likely to play a role. The above model will be applied in Chapter 5 as well.
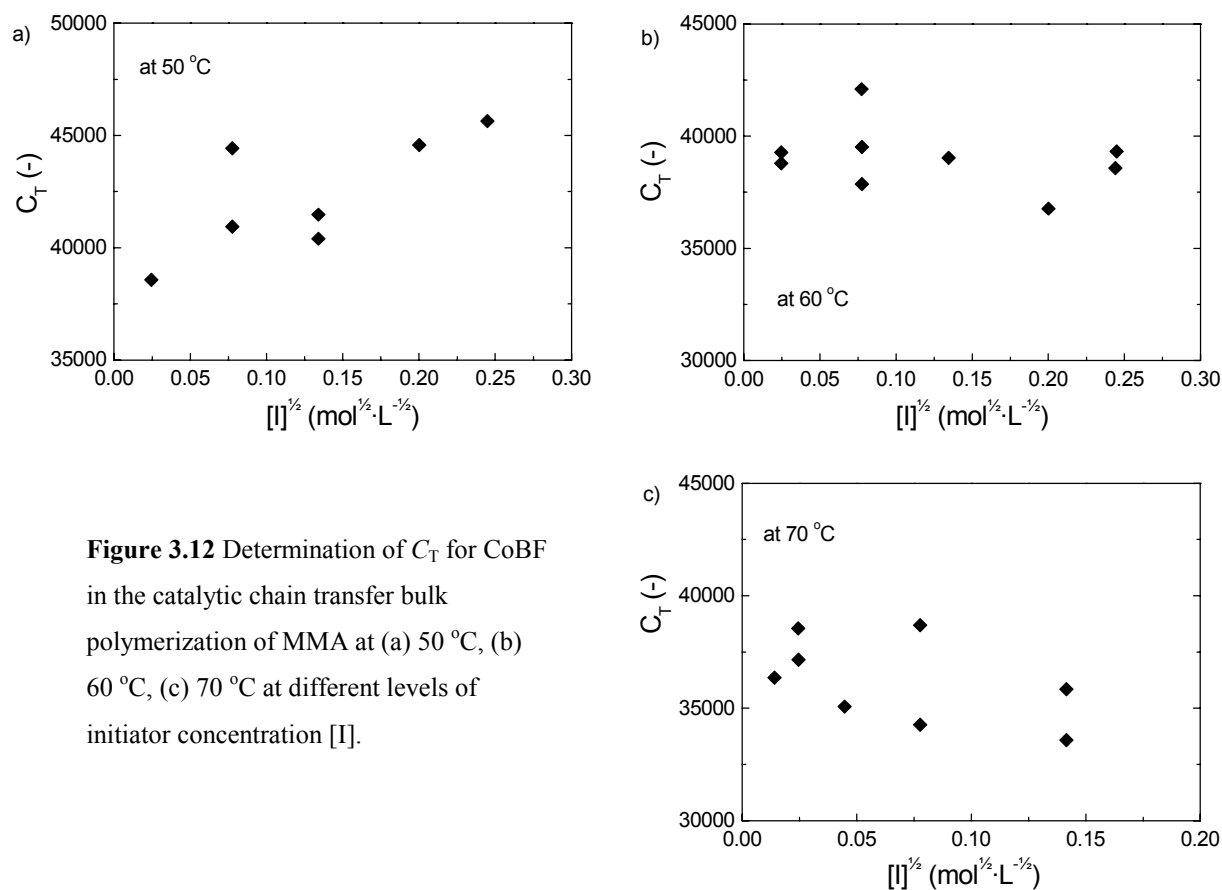

Figure 3.12 Determination of C_T for CoBF in the catalytic chain transfer bulk polymerization of MMA at (a) 50 ^{o}C, (b) 60 ^{o}C, (c) 70 ^{o}C at different levels of initiator concentration [I].

3.7 Conclusions

In this work it is clearly demonstrated that solvent effects in catalytic chain transfer polymerization in non-coordinating solvents can be fully attributed to solvent impurities in contrast to what was implied in early studies and confirming recent results from other authors. Most probably part of these impurities will be acids as these are known to decompose CoBF. Surprisingly, low conversion experiments to test this hypothesis did not show the same effects. Whatever the impurities may be, they can be efficiently removed by the Grubbs solvent purification technique. Furthermore, it was shown that small amounts of oxygen do not exert large effects on catalytic chain transfer.

The second main conclusion is that diffusion limitation is unlikely to play a role in the catalytic chain transfer polymerization of 2-ethylhexyl methacrylate and *n*-butyl methacrylate. As methyl methacrylate is less viscous than these two monomers it is likely that diffusion control is not of importance in the polymerization of MMA either. The question of diffusion control has also been assessed from a process technological point of view. Analysis of the Damköhler number confirmed the conclusion that diffusion limitation does not occur. This contradicts conclusions from other authors.

Thirdly, the effects of cobalt - carbon bond formation were investigated both from a theoretical and an experimental point of view. It was made plausible that in the catalytic chain transfer polymerization of MMA cobalt – carbon bond formation does not play a role in the kinetics, which is in agreement with results from other authors. The model, however, may also be useful in describing catalytic chain transfer of styrene or acrylates.

With the results gathered in this chapter sufficient knowledge has been obtained to be able to investigate more complicated aspects of catalytic chain transfer polymerizations, like effects of conversion, homo- and copolymerization of monomers that show reduced activity towards CoBF and the application of CCT in emulsion. These will be dealt with in the next chapters.

3.8 References

[1] Suddaby, K.G.; Maloney, D.R.; Haddleton, D.M. *Macromolecules*, **1997**, *30*, 702

[2] Haddleton, D.M.; Maloney, D.R.; Suddaby, K.G.; Muir, A.V.G.; Richards, S.N. *Macromol. Symp.* **1996**, *111*, 37

[3] Kukulj, D.; Davis, T.P. *Macrol. Chem. Phys.* **1998**, *199*, 1697

[4] Suddaby, K.G.; Haddleton, D.M.; Hastings, J.J.; Richards, S.N.; O'Donnell, J.P. *Macromolecules*, **1996**, *29*, 8083

[5] Haddleton, D.M.; Kelly, E.J.; Kukulj, D.; Morsley, S.M.; Steward, A.G. *Pol. Preprints (ACS)*, **1999**, *40(1)*, 381

[6] Davis, T.P.; Haddleton, D.M.; Richards, S.N. *J. Macromol. Sci., Rev. Macromol. Chem. Phys.* **1994**, *C34*, 234

[7] Heuts, J.P.A.; Forster, D.J.; Davis, T.P. *Macromolecules* **1999**, *32*, 3907

[8] Forster, D.J.; Heuts, J.P.A.; Lucien, F.P.; Davis, T.P. *Macromolecules* **1999**, *32*, 5514

[9] Forster, D.J.; Heuts, J.P.A.; Davis, T.P. *Polymer* **2000**, *41*, 1385

[10] Pangborn, A.B.; Giardello, M.A.; Grubbs, R.H.; Rosen, R.K.; Timmers, F.J. *Organometallics* **1996**, *15*, 1518

[11] Bakac, A.; Espenson, J.H. *J. Am. Chem. Soc.*, **1984**, *106*, 5197

[12] Hutchinson, R.A.; Paquet, D.A.; McMinn, J.H.; Beuermann, S.; Fuller, R.E.; Jackson, C. *Dechema Monographs* **1995**, *131*, 467

[13] Heuts, J.P.A.; Davis, T.P.; Russell, G.T. *Macromolecules,* **1999**, *32*, 6019

[14] Amin Sanayei, R.; O' Driscoll, K.F. *J. Macromol. Sci.-Chem.* **1989**, *A26*, 1137

[15] van Herk, A.M. *'Medium effects on axial ligand substitution reactions at vitamin B_{12} and model compounds'* PhD Thesis, Vrije Universteit Amsterdam, Amsterdam: **1986**

[16] Heuts, J.P.A.; Forster, D.J.; Davis, T.P. In *Transition Metal Catalysis in Macromolecular Design*; Boffa, L.S.; Novak, B.M. Ed.; ACS Symposium Series, vol. 760; American Chemical Society: Washington, DC, **2000**; p. 254

[17] Suddaby, K.G.; Haddleton, D.M.; Hastings, J.J.; Richards, S.N.; O'Donnell, J.P. *Macromolecules*, **1996**, *29*, 8083

[18] Haddleton, D.M.; Kelly, E.J.; Kukulj, D.; Morsley, S.M.; Steward, A.G. *Pol. Preprints (ACS)*, **1999**, *40(1)*, 381

[19] Karmilova, L.V.; Ponomarev, G.V.; Smirnov, B.R.; Belgovskii, I.M. *Russian Chemical Reviews*, **1984**, *53*, 132

[20] Xia, J.; Zhang, X.; Matyjaszewski, K. *Macromolecules* **2000**, *33*, 255

[21] Haddleton, D.M.; Hemig, A.M.; Kukulj, D.; Duncalf, D.J.; Shooter, A.J. *Macromolecules* **1998**, *31*, 2016

[22] Chambard, G.; de Man, P.A.; Klumperman, B. *Macromol. Symp.* **2000**, *150*, 45

[23] Bon, S.A.F.; Morsley, D.R.; Waterson, J.; Haddleton, D.M. *Macromol. Symp.* **2001**, *165*, 29

[24] North, A.M. *Q. Rev. Chem. Soc.* **1966**, *20*, 421

[25] Von Smoluchowski, M. *Z. Phys. Chem., Sotechiom. Verwandtschatsl.* **1917**, *92*, 129

[26] Cussler, E.L. *Diffusion: Mass Transfer in Fluid Systems*, 2nd ed.; Cambridge University Press: Cambridge, 1997

[27] Heuts, J.P.A. *Results presented on a poster during the SML 2001: Free radical polymerization, kinetics and mechanism*

[28] Yaws, C.L. *Handbook of transport property data: viscosity, thermal conductivity and diffusion coefficients of liquids and gases.* Gulf Publishing Company, London, **1995**

[29] van Herk, A.M. *Macromol. Theory Simul.* **2000**, *9*, 433

[30] Mironychev, V.Ye.; Mogilevich, M.M.; Smirnov, B.R.; Shapiro, Yu. Ye.; Golikov, I.V. *Polymer Science USSR* **1986**, *A28*, 2103

[31] Quadir, M.A.; DeSimone, J.M.; van Herk, A.M.; German, A.L. *Macromolecules* **1998**, *31*, 6481

[32] Koenig, T.; Finke, R.G.; *J. Am. Chem. Soc.* **1998**, *110*, 2657

[33] Daikh, B.E.; Finke, R.G. *J. Am. Chem. Soc.* **1992**, *114*, 2938

[34] Koenig, T.; Scott, T.W.; Franz, J.A. in *'Bonding Energetics in Organometallic Compounds'* Marks, T.J. Ed.; ACS Symposium Series 428; American Chemical Society: Washington, DC, **1990**, 113.

[35] Wayland, B.B.; Gridnev, A.A.; Ittel, S.D.; Fryd, M. *Inorg. Chem.* **1994**, *33*, 3830

[36] Moad, G.; Solomon, D.H.; *The chemistry of Free Radical Polymerization*, 1st ed., Pergamon, Oxford, 1995

[37] Pierik, B.; Masclee, D.; van Herk, A. *Macromol. Symp.* **2001**, *165*, 19

[38] Gridnev, A.A.; Ittel, S.D.; Fryd, M.; Wayland, B.B. *Organometallics* **1996**, *15*, 222

[39] Heuts, J.P.A.; Forster, D.J.; Davis, T.P.; Yamada, B.; Yamazoe, H.; Azukizawa, M. *Macromolecules* **1999**, *32*, 2511

Chapter 4

High conversion CCT polymerization
of methyl methacrylate

Synopsis: In this chapter we will focus on the effects of conversion on the apparent catalyst activity. Several mechanisms will be discussed that may explain the experimental observations. The discussion will be supported with computer simulations using Predici software. Furthermore, the effect of acid and peroxides on the evolution of the molecular weight distribution will be investigated.

4.1 Introduction

Most kinetic studies on catalytic chain transfer polymerization are focused on low conversion polymerizations. For practical applications, on the other hand, it is very important and interesting to study these polymerizations up to high conversions. From literature, some studies aiming at the production of larger amounts of macromers are known. Suddaby *et al.*[1] described a continuous process for the production of macromers in a tubular reactor. A similar set-up was applied by Grady.[2] However, steady state conversion only reached 14 % and mean residence times were below 25 minutes. So, although continuous operation can be a good alternative, it does not resemble high conversion batch reactions and cannot be used as a point of reference. Some other studies were mainly focused on the production of dimer at high catalyst concentrations and subsequent copolymerization with other monomers.[3,4] Most kinetic studies were carried out in the group of Davis and Heuts.[5,6,7,8,9,10,11] For all but one[9] studies, molecular weight distributions did not or hardly change with conversion, whereas a decrease would be expected according to the Mayo-equation, which relates the degree of polymerization to monomer concentration. Several explanations have been suggested like catalyst deactivation and catalyst – solvent interactions that change with conversion and compensate for a decrease in monomer concentration. In this chapter various mechanisms will

be discussed and related to new experiments as well as Predici simulations in order to find an explanation for the discrepancy between the predictions according to the Mayo-equation and most experimental results. Furthermore, it will be investigated whether added contaminants like acetic acid and benzoyl peroxide do affect molecular weight in high conversion polymerizations, although no effects were observed in low conversion polymerizations as reported in Chapter 3.

All investigations in this chapter are based on observations of the polymerization kinetics combined with Predici computer simulations. An alternative or complementary approach could be to directly monitor the Co(II) concentration. Although some reports are known in which the concentration of cobalt catalyst was followed by ESR-measurements[6], it is very difficult to measure Co(II) concentration in a polymerizing system by ESR or any other technique, due to the very small amounts of cobalt complex present. Therefore, it was chosen to focus on polymerization kinetics in the investigation of CCT polymerizations up to high conversion.

4.2 Experimental Section

Materials. Methyl methacrylate (MMA, Merck, 99%) was distilled under vacuum, and stored at -10 ^{o}C. Prior to use, MMA was passed over a column, containing inhibitor remover and basic alumina. Toluene (Biosolve, AR) was purified using a Grubbs solvent set-up[12], purged with argon for at least three hours and stored over molsieves in a glovebox. Azobis(methylisobutyrate) (AIBMe, Wako Chemicals) was recrystallized once from methanol and stored in a glovebox. Benzoyl peroxide (Aldrich, 97 %) and acetic acid (Merck, 99 %) were used as received. CoBF (bis(aqua)bis((difluoroboryl)dimethylglyoximato)cobalt(II)) was prepared according to a procedure of Bakac and Espenson[13]. One batch was used throughout all experiments. It was analysed using UV-Vis spectroscopy and elemental analysis (experimental: C: 22.9 %, H: 3.79 %, N: 13.2 %; calculated for $C_8H_{12}N_4O_4B_2F_4Co \cdot (H_2O)_2$: C: 22.8 %, H: 3.83 %, N: 13.3 %).

General polymerization procedure. Monomer and solvent were purged with argon for at

least three hours prior to transfer into a glovebox. All reaction mixtures were prepared inside a glovebox. Stock solutions of CoBF in monomer or solvent were prepared and stored for a longer period of time. AIBMe solutions in monomer were prepared immediately prior to the experiment. Reaction mixtures were made of the CoBF-solution, monomer, toluene and an AIBMe solution to a total volume of about 50 mL in a three-necked round-bottom flask. Polymerizations were carried out in a sand bath at a constant temperature of 60 $^{\circ}$C ($\pm$ 1.5 $^{\circ}$C). The thermo-couple was immersed into the reaction mixture for optimal control. The mixtures were stirred with a magnetic stirrer. Polymerizations were carried out inside a glovebox to prevent oxygen from entering the reaction mixture during sampling. Samples were withdrawn by a syringe to monitor conversion and molecular weight distribution. Reactions were stopped by addition of hydroquinone and cooling. Monomer was evaporated at room temperature and the polymer dried under vacuum at 60 $^{\circ}$C. Conversion was determined gravimetrically.

Analyses. Size exclusion chromatography (SEC) was carried out using tetrahydrofuran (THF) as an eluent at a flow rate of 1 mL$\cdot$ min^{-1}. Two Polymer Laboratories PLgel 5 µm Mixed-C columns (300 $\times$ 7.5 mm) and PLgel 5 µm guard column (50 $\times$ 7.5 mm) were used and calibrated with Polymer Laboratories narrow MWD polystyrene standards. The Mark-Houwink parameters used in universal calibration are: $K_{MMA} = 9.44 \times 10^{-5}$ dL$\cdot$ g^{-1}, a$_{MMA} =$ 0.719, $K_{S} = 1.14 \times 10^{-4}$ dL$\cdot$ g^{-1}, a$_{S} = 0.716$.[14]

Computer simulations.

Polymerization kinetics were modelled using the Predici software package, version 5.21.2. This software is especially designed to model polymerizations. The simulations were run on a 233 MHz Intel Pentium computer equipped with 32 MB of RAM and a Windows 98 operating system. Standard simulation settings are chosen and the relative integrator accuracy is set to 0.01. Unless otherwise stated simulations are run in moments mode.

4.3 High conversion experiments in bulk and solution

4.3.1 Possible mechanisms

In Chapters 2 and 3 several mechanistic aspects of catalytic chain transfer polymerization have been discussed in detail. However, all polymerizations were run up to conversions less than about 5 %. At higher conversions and longer reaction times other factors come into play. Depending on solvent concentration and polymer molecular weight, viscosity increases with conversion. Although no diffusion control was observed at low conversions, it may be present at high conversion. Furthermore, as the reactions are carried out over a longer time-span, the effects of catalyst deactivation, if present, are more likely to be observable. Another aspect that has to be taken into consideration is that the resulting macromers can, in principle, take part in subsequent reaction steps. In order to get a general idea about the effects of conversion, first two typical high conversion polymerizations will be discussed.
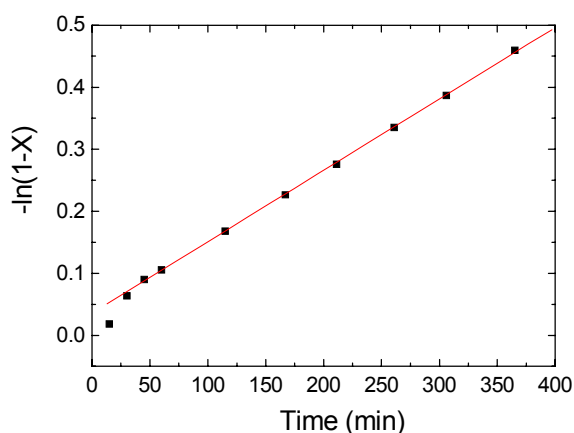
Figure 4.1 First order kinetic plot of the CCT polymerization of MMA in bulk at 60 °C.
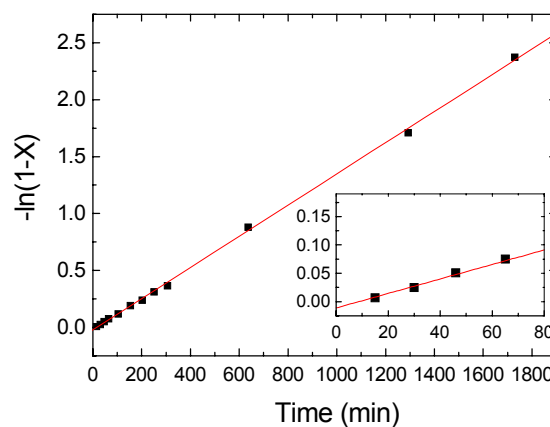
Figure 4.2 First order kinetic plot of the CCT polymerization of MMA in toluene at 60 °C. In the insert the first order kinetic plot at short reaction times is shown.

The first experiment (I) is a bulk polymerization of MMA, whereas the second (II) is a solution polymerization in toluene at 41.5 % of MMA. At regular time intervals samples were withdrawn and analyzed for conversion and molecular weight distribution. First order kinetic plots for both polymerizations are shown in Figure 4.1 and 4.2. The subsequent MWDs, in

which the areas under the curves are proportional to the conversions determined for the corresponding samples are presented in Figures 4.3 and 4.4 for experiments I and II, respectively. In Figure 4.5 the evolution of M_w can be found. M_w is preferred over M_n as it is less sensitive to SEC artifacts.

The first order kinetic plots shown in Figure 4.1 and 4.2 are straight up to high conversions, which means that the radical concentration remains constant. Theoretically the linear fits are expected to go through the origin, but this is not observed. This can be explained by temperature effects.[*]

As can be seen from Figures 4.3, 4.4 and 4.5 for both polymerizations, when looking at the whole conversion range, the MWD shifts to lower molecular weights in spite of a slight increase at lower conversions. In a polymerization similar to experiment II, Kukulj *et al.*[5]
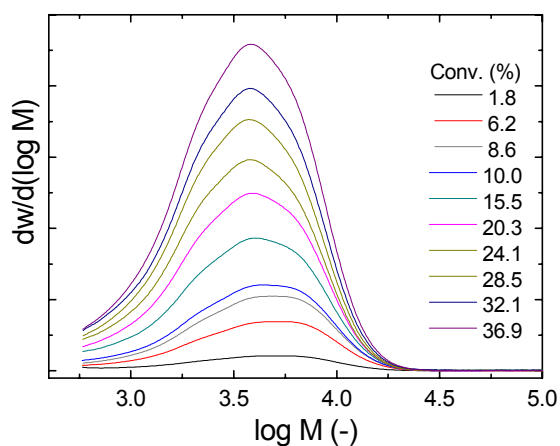
Figure 4.3 Molecular weight distributions measured at increasing conversions for the CCT polymerization of MMA in bulk at 60 $^{\circ}$C. The relative areas under the plots correspond to the monomer conversions. Conversions range from 1.8 to 36.9 %.
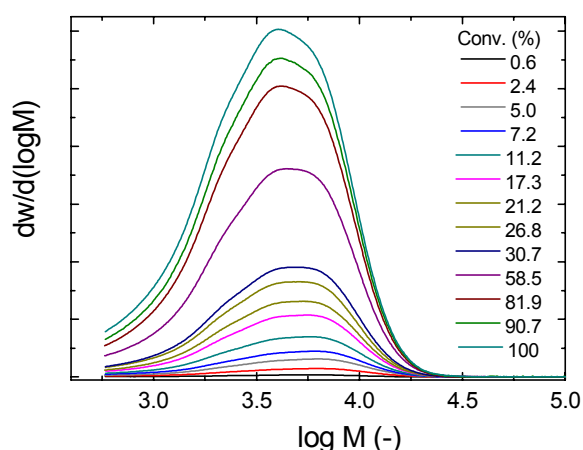
Figure 4.4 Molecular weight distributions measured at increasing conversions for the CCT polymerization of MMA in toluene at 60 $^{\circ}$C. w_{MMA} = 0.419. The relative areas under the plots correspond to the monomer conversions. Conversions range from 0.6 to 100 %.

---

[*] For the bulk polymerization the first two conversion points do not fit the linear plot, as there was a 10 $^{\circ}$C temperature overshoot during the first half hour of the reaction resulting in higher reaction rates. For the solution polymerization the linear fit bisects the time axis at about 15 minutes, as the reaction mixture was heated a bit more gradually to prevent a temperature overshoot, but resulting in an apparent inhibition period.

obtained slightly increasing molecular weights. Heuts *et al.*[11] recently also reported a slight decrease in molecular weight in the terpolymerization of styrene, MMA and 2-hydroxyethyl methacrylate, but it is very hard to interpret these data in a straightforward way, as the presence of three monomers considerably complicates the system. Kowollik *et al.*[9] reported a experimentally determined decrease of 45 % in M_w going from 10 % to 100 % conversion. Simulations showed that such a decrease corresponds to what is expected when the Co(II) concentration remains unchanged and monomer is consumed.[9] The decrease in M_w in the experiments presented here is only about 20 %. So, it seems that the effect of monomer consumption on M_w is in some way counteracted.

Simulations similar to those of Kowollik *et al.*[9] were performed using the model presented in Chapter 2, Scheme 2.4 and Table 2.2 to see the effect of conversion on molecular weight. In these particular simulations inhibition was excluded and the termination rate constants for primary radicals were set to 1.5×10^8 L·mol^{-1}·s^{-1}. The chain transfer coefficients for both simulations were calculated from the second sample of the corresponding experiments. In the calculation the term in the Mayo-equation expressing the contribution of polymer formed in
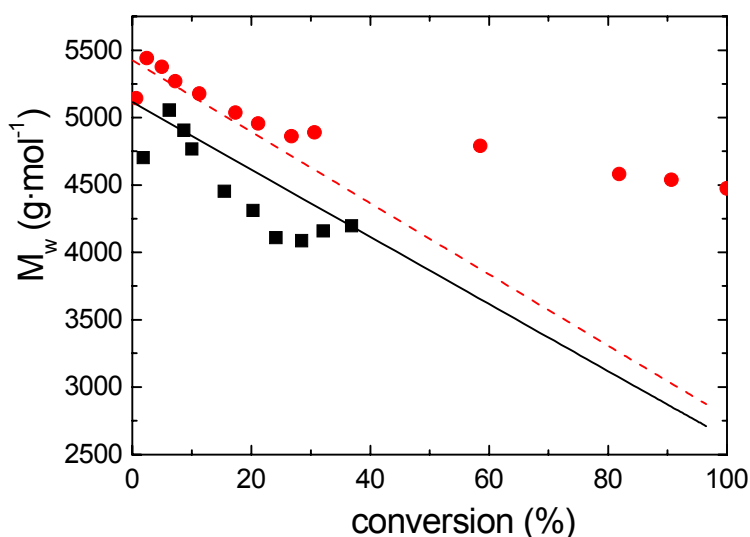
Figure 4.5 Evolution of M_w for the CCT polymerization of MMA at 60 ^{o}C. ■ : bulk MMA; ● : solution in toluene with $w_{MMA} = 0.415$. The curves are predictions from computer simulations using Predici. The model in Scheme 2.4 was used. Inhibition was assumed to be absent. k_{tr} was calculated from the second experimental data point. The dashed line represents the solution polymerization, the solid line the bulk polymerization.

the absence of chain transfer agent is neglected. This results in $C_T = 40.8 \times 10^3$ for the bulk polymerization and $C_T = 46.1 \times 10^3$ for the solution polymerization. Considering that both are determined from a single point the results are in quite good agreement and compare well with results presented in Chapter 3.

The simulation results are shown in Figure 4.5 as well. For the bulk polymerization the general trend in the experimental data and the simulation data is the same. For the solution polymerization at about 25 % conversion the experimental data start to deviate from the simulation results. So, the molecular weights produced experimentally do not decrease as much as predicted by model simulations. There can be several general explanations for the discrepancy between the results presented here, on the one hand, and those of Kowollik *et al.*[9] and the Predici computer simulations, on the other hand. This can be due to 1) a decrease in intrinsic activity of the catalyst due to changing reaction conditions, 2) a decrease in the concentration of the active form of the catalyst, 3) additional growth of polymer chains formed at lower conversions. In the next sections all three possibilities will be considered.

4.3.1.1 Changes in catalyst activity

Kukulj *et al.*[5] suggested that the continuously changing ratio of monomer to solvent may be a possible explanation for decreasing catalyst activity. However, Heuts *et al.*[7] tested this hypothesis by determining the chain transfer coefficients by keeping catalyst concentrations constant and varying the monomer concentration and did not obtain any evidence in support of this hypothesis. Results on solvent effects, in which C_T proved to be independent of toluene concentration, as discussed in Chapter 3 point in the same direction. So the explanation that changes in the ratio of monomer concentration and solvent concentration affect C_T can be discarded.

A second possibility is that due to the formation of polymer, the viscosity of the reaction mixture increases. Although it was shown in Chapter 3 that diffusion control is not expected to play a role at lower conversions, it may affect the catalytic chain transfer step at higher conversions. The molecular weights, however, are not that high and therefore no excessive viscosity increase is expected. When viscosity would affect the chain transfer rate constant, it would most probably also affect the termination rate constants. In that case the first order

kinetic curves shown in Figures 4.1 and 4.2 would show an upward deviation from linearity. This is not observed. Furthermore, Heuts[15] reported that adding polymer to a catalytic chain transfer polymerization in order to increase viscosity did not affect the obtained chain transfer coefficients. Therefore, it is expected that at least in these experiments restricted diffusion cannot explain the limited molecular weight shift. In conclusion, the explanation for the development of the MWDs in the CCT polymerizations presented here, cannot be found in changes in intrinsic catalytic activity of the chain transfer agent.

4.3.1.2 Catalyst deactivation

As discussed in Section 2.3.2.4, catalyst deactivation can proceed via various pathways. Most likely are spontaneous temperature or acid induced decomposition of the catalyst complex, oxidation by oxygen or oxygen-centered radicals or the formation of thermodynamically or kinetically stable Co(III)-R compounds. However, other deactivation pathways cannot be ruled out at this stage. In order to be able to model deactivation it is useful to obtain experimental plots of the change in concentration of active Co(II) in time. Kukulj *et al.*[5] carried out similar calculations to calculate the change in C_T. Assuming C_T is constant, it is possible to calculate the fraction of active cobalt(II). Kukulj *et al.* chose to do this via subtraction of the scaled molecular weight distributions. This results in scattered data caused by errors in the subtraction of the low molecular weight tails of the molecular weight distribution. Therefore, it was decided to calculate the fraction of cobalt(II) via the instantaneous weight average molecular weight, $M_{w,in}$, which can be calculated from the cumulative weight average molecular weight, $M_{w,cum}$. The M_w of a polymer formed in a time period Δt is defined as

$$M_{w,\Delta t} = \frac{\sum W_{i,\Delta t} M_{i,\Delta t}}{\sum W_{i,\Delta t}} \tag{4.1}$$

in which $W_{i,\Delta t}$ is the mass of polymer chains with chain-length i formed in time period Δt and $M_{i,\Delta t}$ is the molecular weight of a chain with length i. The nominator can be rewritten as the difference of the sum at time t+Δt and the sum at time t, whereas the denominator can be

rewritten as the amount of monomer converted into polymer during time period Δt, resulting in:

$$M_{w,\Delta t} = \frac{\sum W_{i,t+\Delta t} M_{i,t+\Delta t} - \sum W_{i,t} M_{i,t}}{m_o \Delta X} \qquad (4.2)$$

in which m_o is the initial amount of monomer and ΔX is the conversion in time period Δt, *i.e.* $\Delta X = X_{t+\Delta t} - X_t$. Both terms in the nominator of eq 4.2 can be rewritten as the product of conversion and M_w at their specific times giving

$$M_{w,\Delta t} = \frac{m_0 X_{t+\Delta t} M_{w,t+\Delta t} - m_0 X_t M_{w,t}}{m_o \Delta X} \qquad (4.3)$$

For a time period Δt corresponding to relatively small changes in conversion, $M_{w,\Delta t}$ will approximate $M_{w,in}$ which can be used in the Mayo-equation. So

$$M_{w,in} = \frac{\Delta(X M_{w,cum})}{\Delta X} \qquad (4.4)$$

Now, it is possible to relate the cobalt(II) concentration at time t_2 to the cobalt(II) concentration at time t_1 via the respective Mayo equations at those times.

$$\frac{[Co(II)]_{t_2}}{[Co(II)]_{t_1}} = \frac{\left(\dfrac{1}{P_{n,t_2}} - \dfrac{1}{P_{n,o,t_2}}\right)\dfrac{[M]_{t_2}}{C_T}}{\left(\dfrac{1}{P_{n,t_1}} - \dfrac{1}{P_{n,o,t_1}}\right)\dfrac{[M]_{t_1}}{C_T}} \qquad (4.5)$$

Neglecting the contributions of the inverse degree of polymerization in absence of catalyst and assuming that for the first sample, taken relatively shortly after the start of reaction, the amount of Co(II) still equals the initial amount, this results in

$$f_{Co} = \frac{(1 - X_{t_2}) P_{n,t_1}}{(1 - X_{t_1}) P_{n,t_2}} \qquad (4.6)$$

In this way the fraction of Co(II) available for chain transfer, f_{Co}, can be estimated from the experimental results. In these calculations average times and conversion are used. In Figures 4.6 and 4.7 the results of these calculations are shown for experiments I and II, respectively.
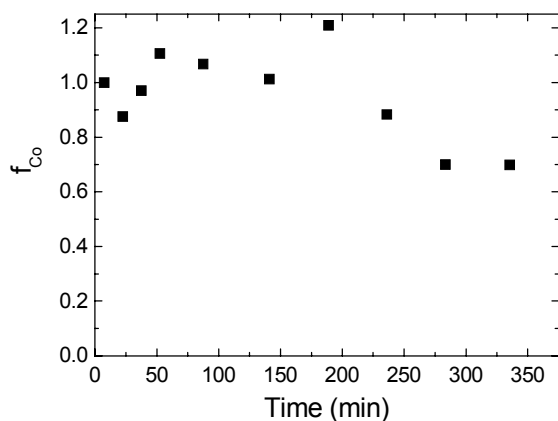

Figure 4.6 The evolution of the fraction of cobalt present as Co(II) in the CCT polymerization of MMA in bulk at 60 °C (experiment I).
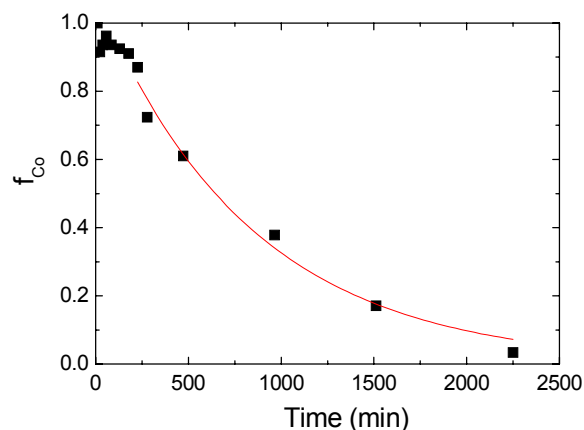
Figure 4.7 The evolution of the fraction of cobalt present as Co(II) in the CCT polymerization of MMA in toluene solution at 60 °C (experiment II).

As can be seen in Figure 4.6 especially, the data for f_{Co} still show some scatter. This is most probably the reason that in some cases f_{Co} is larger than one, which is of course physically unrealistic, unless the initially added cobalt complex was not completely present as Co(II) and is regenerated during polymerization. So during the first few hours of the reaction the amount of Co(II) is fairly constant, after which deactivation sets in. For the solution polymerization less than 10 percent of the initially added amount is still active after about 35 hours. A similar trend can be seen in the work of Kukulj *et al.*[5]

In the beginning of this section a few possible causes for deactivation were mentioned. Oxidation by oxygen is unlikely as all solvents and monomers were freed from oxygen and taken into a glovebox having a nitrogen atmosphere containing less than 1 ppm of oxygen. Furthermore, both reaction mixture preparation and polymerization are performed inside a glovebox. As was shown in Chapter 3.3 small amounts of oxygen that may still be present in spite of all precautions taken do hardly influence the polymerization. So oxygen is most probably not causing deactivation. The second pathway, spontaneous or acid induced

decomposition can not be excluded beforehand. The third pathway, formation of Co(III)-R compounds, could in principle proceed via chain transfer to solvent as shown for toluene in Scheme 4.1. Transfer to solvent results in a radical that can reinitiate or terminate polymerization, but which can also combine with Co(II). This may cause, depending on the rate of transfer to solvent and the dissociation rate of the Co(III)-R compound, a substantial build-up of Co(III), thereby reducing the amount of Co(II). Both spontaneous decomposition and deactivation via solvent-derived radicals will be modelled using Predici. The model presented in Chapter 2 is extended with these reactions. Spontaneous decomposition will be assumed to be a first order process. Reaction rate constants are shown in Table 4.1.

Scheme 4.1 Co(II) deactivation via solvent-derived radicals
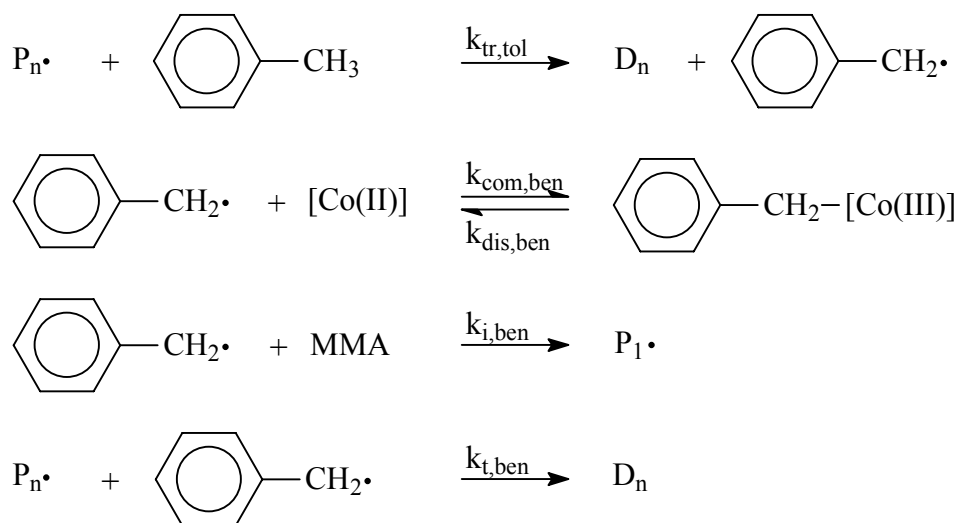
The simulation results for deactivation via transfer derived radicals are shown in Figure 4.8 together with experimental data for experiment II. Two simulated curves are shown. The solid line represents simulation results according to the data in Table 4.1. The dashed line shows results for stronger Co(III) – benzyl formation, originating from either 1) an increased transfer to toluene rate constant or 2) an increased Co(II) – benzyl combination rate constant or 3) a decreased rate constant for addition of benzyl radicals to MMA. It can be clearly seen that the experimental data and the simulation results do not agree in either case. This does not necessarily mean Co(III) – benzyl formation does not take place but it is clearly not the major mechanism responsible for the experimental observations.

Table 4.1 Additional reaction rate constants to be used in computer simulations using Predici software.

Description	Rate constant	Value	Reference / Remarks
- transfer to toluene	$k_{tr,tol}$	2.1×10^{-2} L· mol^{-1}· s^{-1}	16
- initiation of MMA by benzyl radical	$k_{i,ben}$	8×10^3 L· mol^{-1}· s^{-1}	Extrapolated from 17
- termination by benzyl radical	$k_{t,ben}$	1.5×10^8 L· mol^{-1}· s^{-1}	Estimated
- benzyl – Co(III) formation	$k_{com,ben}$	6×10^8 L· mol^{-1}· s^{-1}	Extrapolated from 18
- benzyl – Co(III) dissociation	$k_{dis,ben}$	1.4×10^{-3} s^{-1}	Extrapolated from 18
- spontaneous decomposition	k_{dec}	$1 \times 10^{-4} - 1 \times 10^{-6}$ s^{-1}	Estimated

In Figure 4.9 the simulation results for a first order decomposition of the Co(II) complex are shown. Bakac and Espenson[13] report a first order deactivation rate constant of 6.9×10^{-4} s^{-1} in a 0.1 M aqueous solution of HClO$_4$, most probably at ambient temperature. Although the

Figure 4.8 Simulation results and experimental data for the CCT polymerization of MMA in toluene at 60 ºC. In the simulations deactivation is assumed to occur via transfer to solvent derived radicals. Rate constants are given in Tables 2.2 and 4.1.except for $k_{i,ben} = 8 \times 10^3$ L· mol^{-1}· s^{-1} (solid curve); $k_{i,ben} = 8 \times 10^2$ L· mol^{-1}· s^{-1} (dashed curve)
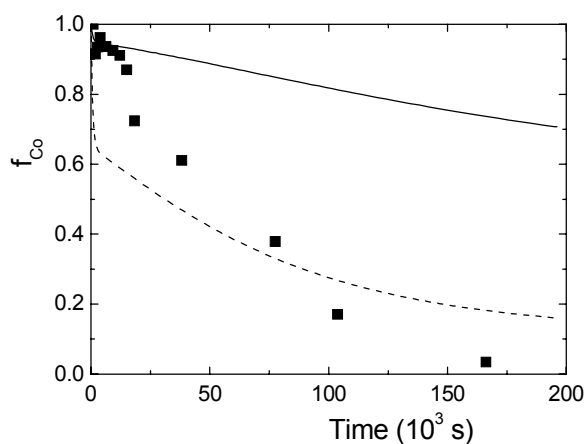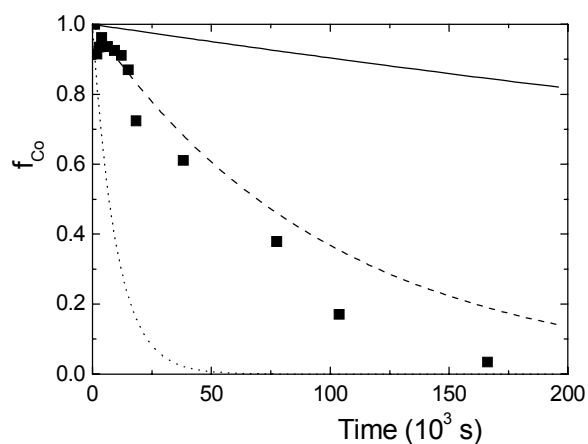
Figure 4.9 Simulation results and experimental data for the CCT polymerization of MMA in toluene at 60 ºC. In the simulations deactivation is assumed to occur spontaneously. Rate constants are given in Table 2.2 except for $k_{dec} = 1 \times 10^{-6}$ s^{-1} (solid curve); $k_{dec} = 1 \times 10^{-5}$ s^{-1} (dashed curve); $k_{dec} = 1 \times 10^{-4}$ s^{-1} (dotted curve)

polymerization reaction conditions differ widely from those described in Bakac and Espenson's experiment, a first order deactivation process with a rate constant of 1×10^{-4} s^{-1} seems a good starting point. It can be seen in Figure 4.9 that a spontaneous decomposition process can provide a better fit to the experimental data than deactivation via transfer derived radicals. Unfortunately, this does not result in any concrete information regarding the mechanism of decomposition.

In summary, it can be said that if catalyst deactivation is the reason for the deviations in M_w between simulations and experiments, spontaneous deactivation is more likely to occur than oxidation by oxygen or formation of stable Co(III)-R compounds.

4.3.1.3 Additional growth of polymer chains

Polymer chains can be reinitiated in various ways. In CCT polymerization the growing radical chains can add to macromonomer resulting in transfer of the radical to the macromonomer as shown in Scheme 2.6. Furthermore, Cacioli *et al.*[19] have shown that macromer copolymerization does not occur. Kowollik *et al.*[9] included the mechanism for transfer to

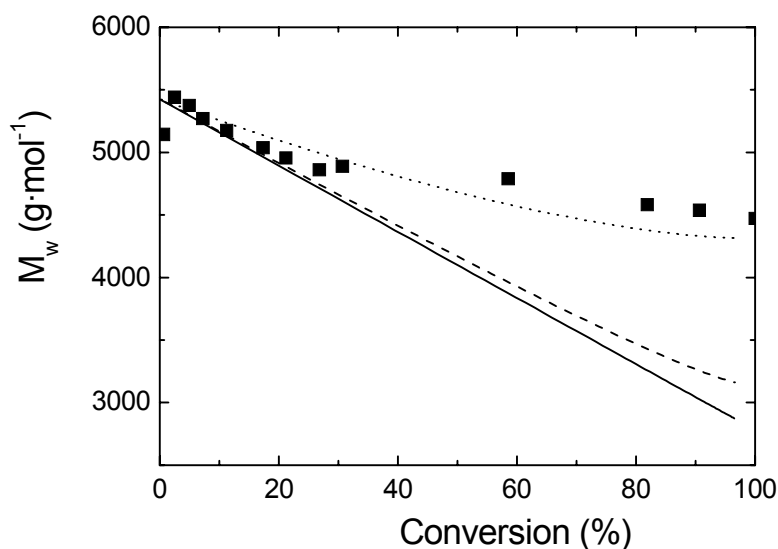**Figure 4.10** Experimental and simulation results for the CCT polymerization of MMA in toluene at 60 °C. Solid line: simulation according to Scheme 2.1 excluding inhibition; dashed line: similar including macromonomer reinitiation with $k_{macro} = 1 \times 10^3$ L· mol^{-1}· s^{-1}; dotted line: similar including macromonomer reinitiation with $k_{macro} = 1 \times 10^4$ L· mol^{-1}· s^{-1}.

macromer in their simulations and found hardly any effects on the MWD. This can be explained from the low concentration of macromer with respect to monomer in combination with a low chain transfer constant for macromer of about 0.2.[20]

A second possibility for additional growth of polymer chains is intermolecular chain transfer to polymer. For PMMA chain transfer to polymer mainly occurs to the double bond originating from disproportionation.[21] This is a process analogous to chain transfer to macromonomer. As no reports on chain transfer to the polymer backbone were found it is assumed to be negligible for MMA. A third option is reinitiation of macromonomer by cobalt hydride as suggested by Gridnev[22]. In Figure 4.10 the results are shown for simulations incorporating macromonomer reinitiation. The macromonomer reinitiation rate constant k_{macro} is set at 1×10^3 L· mol^{-1}· s^{-1}, equal to reinitiation of monomer and at 1×10^4 L· mol^{-1}· s^{-1} which is an order of magnitude larger. In the latter case a quite reasonable fit with the experimentally observed values of M_w is obtained, but this would contradict the results obtained by Kowollik *et al.*[9] and, furthermore, there is no reason to expect reinitiation of macromonomer to proceed that much faster than reinitiation of monomer.

4.3.1.4 Preliminary conclusions

In the previous three sections some possible mechanisms have been discussed that may explain the evolution of molecular weight during a high conversion catalytic chain transfer polymerization. Though it is hard to pinpoint the right mechanism or mechanisms, some can be excluded or described as unlikely. Changes in intrinsic catalyst activity due to changes in composition or viscosity do not seem to play an important role. Additional growth of macromonomer can also be excluded as this would contradict results of Kowollik *et al.*[9], although in principle a model including reinitiation of macromonomer by cobalt hydride would explain the experimental observations. Deactivation of cobalt(II) by solvent derived radicals is unlikely as well, but it may occur in other solvents. This leaves decomposition of the Co(II) complex to be most probably responsible for the fact that the decrease in molecular weight with conversion is less than expected. So far, it is not clear what induces this decomposition.

4.3.2 Effects of catalyst and solvent concentration

Two additional experiments were carried out to see whether the catalyst concentration and the solvent concentration affect the previous experimental observations. For comparison the experimental data for the previous and the present experiments are gathered in Table 4.2.

Table 4.2 Experimental data for the high conversion CCT polymerization of MMA in bulk and toluene at 60 °C.

Exp.	w_{MMA}	[CoBF]	$-\Delta M_w/M_w{}^*$	[P•]	C_T
	(-)	(10^{-6} mol· L^{-1})	(-)	(10^{-8} mol· L^{-1})	(10^3 -)
1	1	9.1	0.17	2.3	40.8
2	0.42	3.0	0.18	2.7	46.1
3	0.42	1.0	0.37	2.9	42.7
4	0.17	1.0	0.45	2.5	43.7

* Fractional decrease in M_w over the complete conversion range.

The chain transfer coefficients for all experiments, determined from the second sample, are similar. The evolution of M_w with conversion for experiments 2 to 4 is shown in Figure 4.11. Although the fractional decrease in M_w in percentage terms over the complete conversion range in experiments 3 and 4 approximates the theoretical predictions of Kowollik *et al.*[9], the experimentally observed decrease predominantly occurs during the first stage of the polymerization, whereas theory predicts a nearly linear decrease, see Figure 4.5.

The radical concentrations are all in the same range. Although the molecular weights for experiments 2 and 3 differ by a factor of 3, the radical concentrations differ only 7 percent, which is somewhat less than predicted by a combination of eq 3.28

$$[P\bullet] = \sqrt{\frac{fk_d[I]}{< k_t >}} \tag{3.28}$$

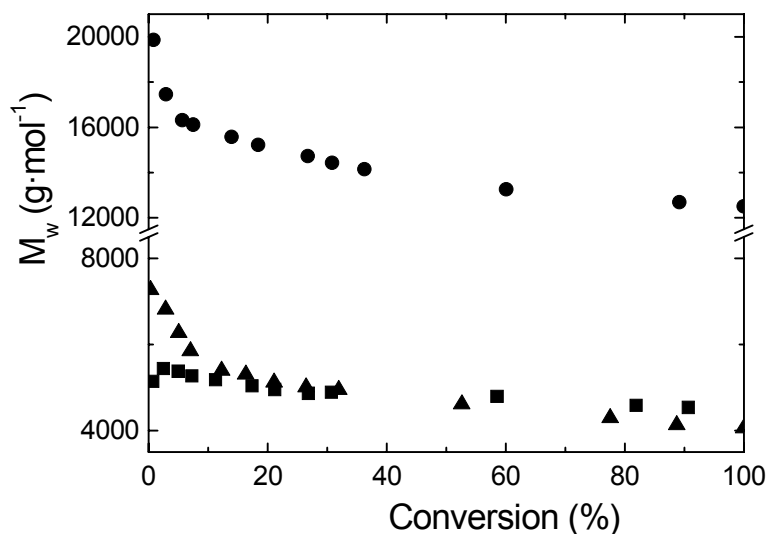and the following expression

$$< k_t > \sim P_n^{-\alpha} \tag{4.7}$$

Figure 4.11 The evolution of M_w with conversion in the CCT polymerization of MMA in toluene at 60 °C. ■: exp. 2, $w_{MMA} = 0.419$, $[CoBF] = 3.0 \times 10^{-6}$ mol· L^{-1}; ●: exp. 3, $w_{MMA} = 0.419$, $[CoBF] = 1.0 \times 10^{-6}$ mol· L^{-1}; ▲: exp. 4, $w_{MMA} = 0.170$, $[CoBF] = 1.0 \times 10^{-6}$ mol· L^{-1}

in which the average termination rate constant is related to the number average degree of polymerization and some coefficient α. Suddaby *et al.*[23] and Kukulj *et al.*[5] predict values in the range 0.12 to 0.19 for α resulting in about a 15 % decrease in M_w. Heuts *et al.*[6] recently showed an even larger increase in radical concentration. However, the experiments of Heuts *et al.*[6] were carried out at catalyst concentrations resulting in polymers having M_w's less than one thousand, which may very well result in a change in the chain-length dependence of $<k_t>$ with respect to the chain-length dependence of $<k_t>$ for higher molecular weight polymers.[24] The changes in the fraction of active cobalt(II) calculated according to equation 4.6 are shown in Figure 4.12. The first aspect to be noticed is the 40 percent increase in active CoBF during the first 7 percent of conversion in experiment 4, the one having the lower monomer content. It is unlikely that this increase can be attributed to scatter only. If the chain transfer coefficient would be calculated from the fourth point in stead of the second, this would give a value around 59×10^3, which is in agreement with the results for low conversion polymerizations at high toluene concentrations as shown in Chapter 3, although conversions were in between 2.4 and 3.6 % in the latter case. The origin of the increase in C_T at high concentrations of toluene, however, remains unclear.

In experiment 4, the fraction of active cobalt (II) starts decreasing after it has reached its peak after one hour. In experiments 2 and 3, during the first 4 to 5 hours of polymerization the fraction of active catalyst decreases only slowly after which a faster decomposition or deactivation sets in. In experiment 3, in which the highest molecular weights are produced, also the fastest deactivation occurs. For longer reaction times the radical concentration in experiment 3, determined from the slope of a first order kinetic plot, increases with time. As can be seen in eq 3.28, an increase in radical concentration may very well originate from a decrease in $<k_t>$. A decrease in $<k_t>$ is more likely to be observed in experiment 3 than in experiments 2 and 4, as the M_w in experiment 3 is a factor of 3 larger than in the other experiments. This results in a stronger increase in viscosity in experiment 3 and thus a larger decrease in $<k_t>$ with respect to experiments 2 and 4. When $<k_t>$ is controlled by diffusion, depending on conversion and molecular weight, k_{tr} may also become partially diffusion controlled. In the calculation of f_{Co} no distinction can be made between a decrease in C_T and a decrease in catalyst concentration. Therefore, a decrease in k_{tr} would appear as enhanced deactivation. The fact that it is not possible to distinguish between changes in C_T and [Co(II)] further complicates analysis.
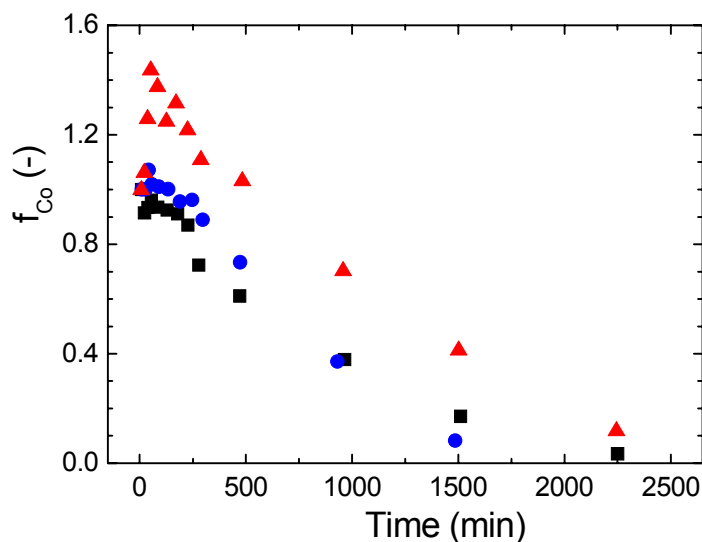

Figure 4.12 Changes in the fraction of active catalyst in time for the CCT polymerization of MMA in toluene at 60 $^{\circ}$C. ■: exp. 2, $w_{MMA} = 0.419$, [CoBF] $= 3.0 \times 10^{-6}$ mol· L^{-1}; ●: exp. 3, $w_{MMA} = 0.419$, [CoBF] $= 1.0 \times 10^{-6}$ mol· L^{-1}; ▲: exp. 4, $w_{MMA} = 0.170$, [CoBF] $= 1.0 \times 10^{-6}$ mol· L^{-1}.

Disregarding all complications, calculating a first order deactivation rate constant over the part where faster deactivation or decomposition takes place would yield $k_{dec} = 1.4 - 2.5 \times 10^{-5}$ s^{-1} for the experimental conditions used in these experiments. This corresponds to a half-life around 10 hours at 60 ^{o}C, which explains why this deactivation is not observed in short, low conversion, experiments. Unfortunately these experiments only show more complicating features and give no clear information about the origin of the effects, whether it is in solvent or monomer purity, in catalyst concentration or any other aspect of the experimental design. Although Kowollik and Davis[9] recently showed that, under presumably well chosen conditions, the decrease in M_w predicted theoretically may be achieved experimentally, the question still remains what causes the deviations observed in the present work and in the work reported by other authors. Further research is required to resolve these problems.

4.4 The effects of acid and peroxides on catalyst deactivation

4.4.1 General observations

In Chapter 3 it was shown that, to our surprise, both benzoyl peroxide at a concentration of 1×10^{-3} mol· L^{-1} and acetic acid at a concentration of 1 mol· L^{-1} do not affect the CCT polymerization of MMA at low conversions in contrast to literature reports.[25,26,27] Therefore, it was decided to perform a set of high conversion polymerizations with benzoyl peroxide and acetic acid as additives to see the effects of longer reaction times and maybe to obtain a starting-point for further research into CCT polymerization without intentionally added contaminants.

For both benzoyl peroxide and acetic acid two polymerizations were carried out at different additive concentrations. All experiments were performed at $w_{MMA} = 0.42$ and [CoBF] = 3.0×10^{-6} mol· L^{-1}. In Table 4.3 the other experimental conditions and some results are given. The radical concentrations are determined from the slope in the first five to six hours of a first order kinetic plot. The chain transfer coefficients are obtained from the second sample as explained in Section 4.3.1. The evolution of the molecular weight distributions with conversion is shown in Figure 4.13 a-d.

Table 4.3 Experimental data and results for the CCT polymerization of MMA in toluene at 60 $^{\circ}$C.

Exp.	Additive	[Add.] (mol$\cdot$ L^{-1})	[P$\bullet$] (10^{-8} mol$\cdot$ L^{-1})	C_T (10^3 -)	M_w at end (10^3 g$\cdot$ mol^{-1})
5	HAc	0.10	2.6	43.7	7.1
6	HAc	1.0	2.9	51.6	15.7
7	BPO	1.0×10^{-3}	2.9	39.2	18.1
8	BPO	4.0×10^{-3}	3.8	19.3	79.6
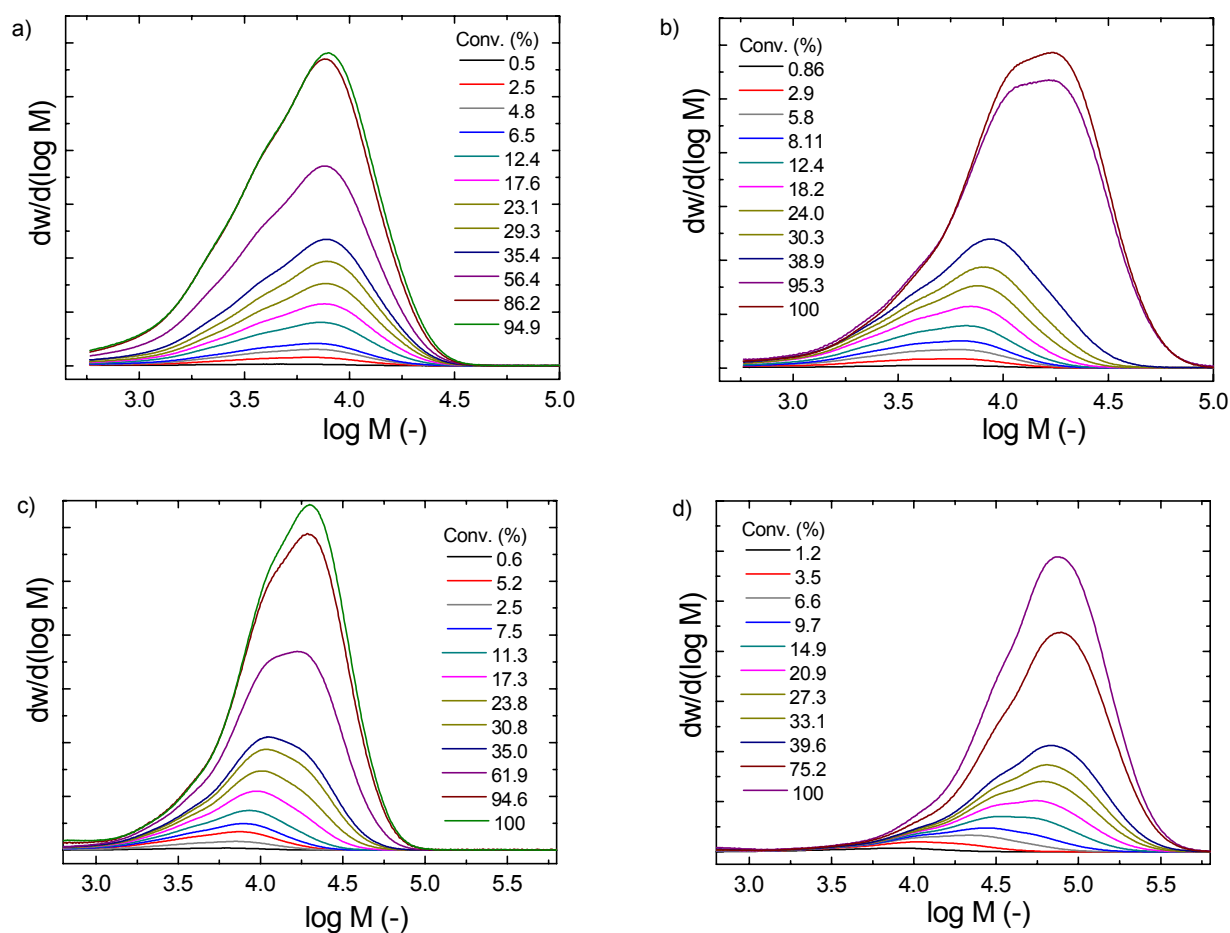
Figure 4.13 Evolution of MWD with conversion in the CCT polymerization of MMA in toluene at 60 $^{\circ}$C in the presence of acetic acid or benzoyl peroxide at $w_{MMA} = 0.419$ and [CoBF] = 3.0×10^{-6} mol$\cdot$ L^{-1}. a) [HAc] = 0.1 mol$\cdot$ L^{-1}; b) [HAc] = 1.0 mol$\cdot$ L^{-1}; c) [BPO] = 1×10^{-3} mol$\cdot$ L^{-1}; d) [BPO] = 4×10^{-3} mol$\cdot$ L^{-1}. The areas under the MWDs are proportional to conversion.

Table 4.3 and Figure 4.13 clearly demonstrate the effect of the additives. In all polymerizations M_w increases with conversion, whereas a decrease in M_w in absence of additives was observed. The M_w at the end of polymerization for experiment II, under similar conditions without additives, was 4.5×10^3 g· mol^{-1}. The increase in M_w with conversion is caused by deactivation of the Co(II) species, which, in contrast to the experiments up to low conversions, is clearly observed here. As can be seen in Figures 4.13 c and d, especially for the benzoyl peroxides the increase in M_w and thus the deactivation is very rapid, which even results in a decreased C_T as determined from the second sample. The rates of polymerization are quite similar to those in the previous experiments except for the experiment at [BPO] = 4×10^{-3} mol· L^{-1}. The increased rate for the experiment at [BPO] = 4×10^{-3} mol· L^{-1} is due both to enhanced radical formation and to a decreased termination rate constant. In addition, all four experiments show an increased polymerization rate at higher conversions due to an increase in reaction mixture viscosity, resulting in a decrease in $<k_t>$ and thus an increase in radical concentration.

4.4.2 Mechanism and modeling for BPO induced deactivation

The trends in cobalt(II) deactivation can be found in Figure 4.14 for experiments with BPO. An attempt was made to model the polymerizations using Predici. The same set of reactions and rate constants as presented in Scheme 2.4 and Table 2.2 is used. In these particular simulations inhibition was excluded and the termination rate constants for primary radicals were set to 1.5×10^8 L· mol^{-1}· s^{-1}. Additional rate constants for reactions involving BPO are shown in Table 4.4. Transfer to BPO results in termination of a growing polymer chain and in the formation of one benzoyloxy radical and must therefore be taken into account as well. It must be realized that next to deactivation induced by either of these species, deactivation observed in absence of any additives will occur simultaneously. This is accounted for by a first order decomposition reaction as defined in Table 4.4. The simulation results are shown in Figures 4.14 as well.

Table 4.4 Additional rate constants involved in BPO or HAc induced deactivation.

Description	Rate constant	Value	Reference / Remarks
- decomposition of BPO	$k_{d,BPO}$	2.8×10^{-6} s^{-1}	28
- initiation of MMA by benzoyloxy radical	$k_{i,B}$	1×10^6 L· mol^{-1}·s^{-1}	Lower limit estimated from 21
- transfer to BPO	$k_{tr,BPO}$	16.7 L· mol^{-1}· s^{-1}	16
- combination of benzoyloxy radical and CoBF	$k_{com,B}$	1×10^9 L· mol^{-1}· s^{-1}	Estimated
- spontaneous CoBF decomposition	k_{dec}	2×10^{-5} s^{-1}	Calculated from exp. 2

The solid curve in Figure 4.14 results from the simulations using the rate constants in Table 4.4. According to the simulations deactivation is not expected to be as fast as observed experimentally. The slower deactivation stemming from the simulations can be understood when the probability of a benzoyloxy radical, B•, combining with CoBF is calculated according to

$$\frac{k_{com,B}[\text{Co(II)}][\text{B}\bullet]}{k_{i,B}[\text{MMA}][\text{B}\bullet] + k_{com,B}[\text{Co(II)}][\text{B}\bullet]} = 7.5 \times 10^{-4} \qquad (4.8)$$

which means that less than 1 in every one thousand benzoyloxy radicals will combine with CoBF.

Several possible explanations can be given for the discrepancy between experimentally observed deactivation and deactivation occurring in simulations. First of all, one or more rate constants may have been incorrectly estimated or determined. The reaction steps affecting the deactivation rate most are combination and initiation. The combination rate constant $k_{com,B}$ seems to be well estimated for a radical – radical combination, but could be underestimated in view of the high reactivity of benzoyloxy radicals. The initiation rate constant $k_{i,B}$ is not expected to be overestimated by more than one order of magnitude, as it is based on several literature resources. To obtain a better agreement with the experimental data a change in the ratio of combination and initiation rate constants from 1×10^3 to 5×10^4 is required. Such a

Figure 4.14 The evolution of the fraction of cobalt(II) in the CCT polymerization of MMA in toluene at 60 $^\circ$C in the presence of benzoyl peroxide. Experimental: ● : 1.0×10^{-3} M BPO; ■ : 4.0×10^{-3} M BPO. Simulations: solid curve: $k_{com,B} / k_{i,B} = 10^3$; dashed curve: $k_{com,B} / k_{i,B} = 10^3$ and 1×10^{-3} M BPO; dotted curve: $k_{com,B} / k_{i,B} = 5 \times 10^4$ and 4×10^{-3} M BPO.

change is quite large, though not impossible. The simulation results for these input data are shown as the dashed and dotted curves for [BPO] is 1×10^{-3} mol· L^{-1} and 4×10^{-3} mol· L^{-1}, respectively.

A second explanation for the discrepancy between the initial simulations and experimental results could also be the occurrence of contaminants in BPO, as it was not purified before use. A similar effect of impurities was observed for AIBN as described in Chapter 3. These contaminants should in that case be orders of magnitude more reactive towards CoBF than the benzoyloxy radicals, which is unlikely, but can not be excluded at this point.

If deactivation occurs via combination of benzoyloxy radicals and CoBF than the peroxide induced deactivation rate equals

$$-\frac{d[\text{CoBF}]}{dt} = k_{com,B}[\text{CoBF}][\text{B}\bullet]$$

(4.9)

Assuming a steady state in benzoyloxy radicals its concentration can be calculated from

$$\frac{d[\text{B}\bullet]}{dt} = 0 = k_{\text{d,B}}[\text{BPO}] - k_{\text{i,B}}[\text{B}\bullet][\text{MMA}] - k_{\text{com,B}}[\text{B}\bullet][\text{CoBF}] - k_{\text{t}}[\text{B}\bullet][\text{P}\bullet] \qquad (4.10)$$

In expression 4.10 the termination term can be neglected compared to the other terms, as the concentration of polymeric radicals is very small with respect to monomer concentration, which results in a linear dependence of the benzoyloxy radical concentration on benzoyl peroxide concentration. Combining this with eq 4.9 gives

$$-\frac{d[\text{CoBF}]}{dt} = \frac{k_{\text{com,B}}k_{\text{d,B}}[\text{CoBF}][\text{BPO}]}{k_{\text{i,B}}[\text{MMA}] + k_{\text{com,B}}[\text{CoBF}]} \qquad (4.11)$$

For experiments 5 and 6 this would mean a factor of 4 difference in initial deactivation rate. This compares well with the 20 and 70 percent deactivations found experimentally for the second sample and supports that deactivation indeed occurs via benzoyloxy radicals.

4.4.3 Mechanism and modeling for HAc induced deactivation

The experimental trends in cobalt(II) deactivation for CCT polymerizations in presence of HAc are presented in Figure 4.15. In order to describe these polymerizations Predici simulations were performed. The same standard set of reaction steps and rate constants as in the previous section is used. In stead of the additional reaction steps for BPO, only two additional reactions are considered, *viz.* spontaneous decomposition of CoBF with a rate constant $k_{\text{dec}} = 2 \times 10^{-5}$ s^{-1} and acid induced decomposition with a rate constant $k_{\text{decH}} = 10^{-4} - 10^{-6}$ s^{-1}. The simulation results for the experiments in which acetic acid has been added to the reaction mixture are presented in Figure 4.15 as well. The rate constants for acid induced decomposition were not obtained from a statistical fitting procedure, but determined by trial and error to show reasonable agreement between experimental data and simulations, as at this stage our main interest is in describing the main trends. It is clear that with the rate constants chosen from the range $10^{-4} - 10^{-6}$ s^{-1} the experimental data can be in good agreement with the simulations. However, it is important to see whether it is possible to relate the rate constants for decomposition 1×10^{-5} s^{-1} and 4×10^{-5} s^{-1} to their respective acetic acid concentrations
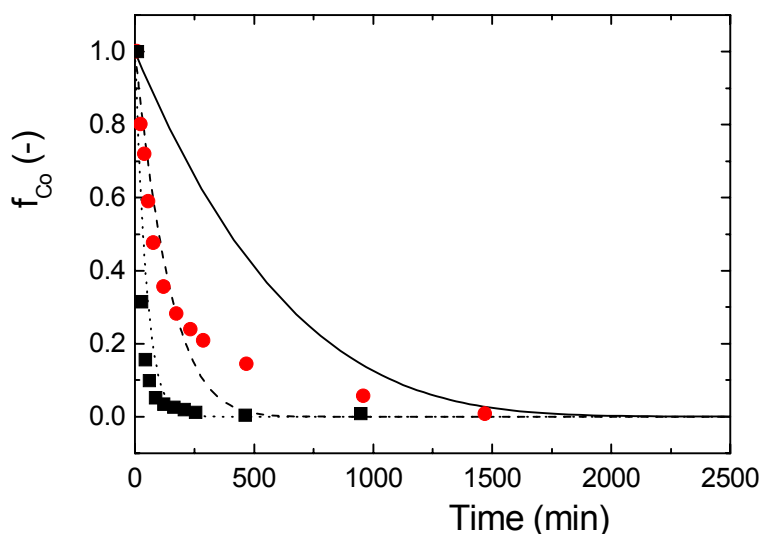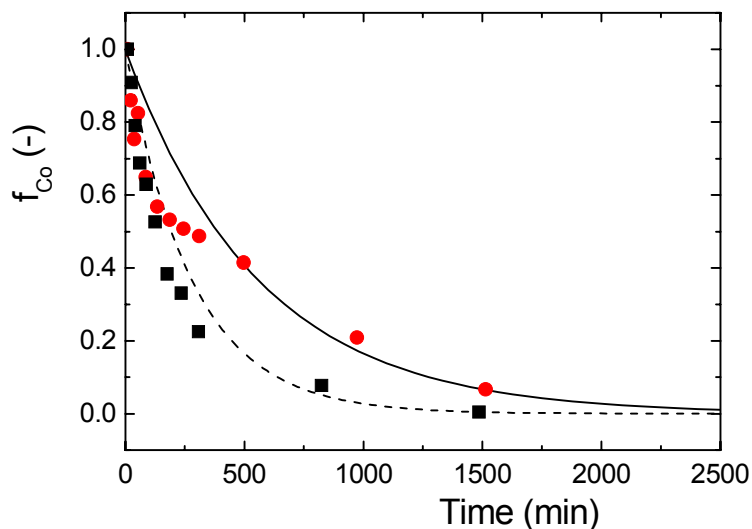
Figure 4.15 The evolution of the fraction of cobalt(II) in the CCT polymerization of MMA in toluene at 60 °C in the presence of acetic acid. Experimental: ●: 0.10 M HAc; ■: 1.0 M HAc. Simulations: solid curve: $k_{dec,H} = 1 \times 10^5$ s^{-1}; $k_{dec,H} = 4 \times 10^{-5}$ s^{-1}.

0.10 M and 1.0 M. Similar to Bakac and Espenson[13] the overall decomposition of CoBF is described as a first order process, but in order to relate rate constants to acid concentrations, a more complete description of the actual mechanism is needed. It is not unlikely that an acid – base equilibrium sets in between CoBF and acetic acid and that protonated CoBF (CoBF-H$^+$) can subsequently decompose, see Scheme 4.2. As CoBF is expected to be a very weak base, the acid – base equilibrium will be on the left hand side.

Scheme 4.2

$$CoBF + HAc \; \underset{\longleftarrow}{\overset{K_H}{\longrightarrow}} \; CoBF\text{-}H^+ + Ac^-$$

$$CoBF\text{-}H^+ \; \xrightarrow{k'_{decH}} \; \text{decomposition products}$$
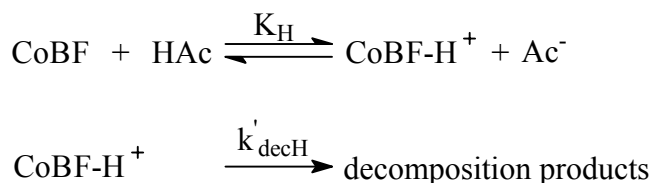
The acid induced decomposition rate can be expressed as

$$-\frac{d[CoBF]}{dt} = k'_{decH}[CoBF - H^+] \tag{4.12}$$

Using a charge balance and mass balances for both CoBF and acetic acid and the expression for the acid – base equilibrium shown in Scheme 4.2, it can be derived that the decomposition rate equals

$$-\frac{d[\text{CoBF}]}{dt} = k'_{\text{decH}} K_{\text{H}}^{\frac{1}{2}} [\text{CoBF}]_o^{\frac{1}{2}} [\text{HAc}]_o^{\frac{1}{2}}$$

(4.13)

in which $[\text{CoBF}]_o$ and $[\text{HAc}]_o$ are the initial concentrations of CoBF and HAc. This expression is valid provided that only a small part of CoBF is protonated. According to this equation a factor of 10 change in acid concentration results in a factor of $10^{\frac{1}{2}} = 3.16$ change in decomposition rate. This is in good agreement with the factor of 4 change in the estimated overall rate constants for acid induced decomposition.

The trends and expressions shown here may also be useful in modeling CCT (co)polymerization with methacrylic acid, in which CoBF decomposition is known to take place.[26]

4.5 Conclusions

In this chapter the evolution of molecular weight in the high conversion CCT polymerization of MMA in toluene has been investigated both by experiments and simulations. In contrast to most other reports in literature, recent results reported by Kowollik *et al.*[9] demonstrating that under appropriate conditions the molecular weight decreases with conversion, have now been confirmed. Simulations predict a nearly linear decrease in M_w if the CoBF concentration remains unchanged. However, in most experiments this decrease was less than expected or was reached in a non-linear way.

Simulations on various mechanisms which may explain experimental results have been performed. In general, mechanisms based on changes in intrinsic catalyst activity or on additional growth of polymer chains can be excluded. Only in experiments were a strong increase in M_w is found, diffusion control may result in an additional decrease in catalyst activity leading to a further increase in M_w. Simulations demonstrated that catalyst deactivation via solvent-derived radicals is unlikely as well. Thus, in spite of purification of all reaction components and performing the reactions inside a glovebox, catalyst deactivation is the most likely cause for the discrepancy between experimental and theoretical results. The origin of the deactivation reaction pathway remains unclear.

Under the conditions of the experiments described in this chapter a half-life for CoBF of about ten hours at 60 ^{o}C was determined. This is in agreement with the results from short, low conversion experiments where, under similar conditions, no deactivation is observed.

Finally, it can be concluded that both acetic acid and benzoyl peroxide enhance catalyst deactivation. For benzoyl peroxide the initial deactivation rate is proportional to the benzoyl peroxide concentration. For acetic acid, on the other hand, the deactivation rate is proportional to the square root of the acid concentration. This relation can also be useful in predictions of CoBF activity in the polymerization of acidic monomers.

4.6 References

[1] Suddaby, K.G.; Amin Sanayei, R.A.; Rudin, A.; O' Driscoll, K.F. *J. Appl. Pol. Sci.* **1991**, *43*, 1565

[2] Grady, M.C. *'Preparation of ω-unsaturated oligo(methyl methacrylate) macromer and its application in emulsion polymerization: Key learnings about radical desorption'* PhD Thesis, ETH Zurich, **1996**

[3] Abbey, K.J.; Carlson, G.M.; Masola, M.J.; Trumbo, D. *Polym. Mater. Sci. Eng.* **1986**, *55*, 235

[4] Yamada, B.; Tagashira, S.; Aoki, S. *J. Polym. Sci. Part A Polym. Chem.* **1994**, *32*, 2745

[5] Kukulj, D.; Davis, T.P. *Macromol. Chem. Phys.* **1998**, *199*, 1697

[6] Heuts, J.P.A.; Forster, D.J., Davis, T.P. Yamada, B.; Yamazoe, H.; Azukizawa, M. *Macromolecules* **1999**, *32*, 2511

[7] Heuts, J.P.A.; Forster, D.J., Davis, T.P. *Macromol. Rapid Commun.* **1999**, *20*, 299

[8] Heuts, J.P.A.; Forster, D.J.; Davis, T.P. In *Transition Metal Catalysis in Macromolecular Design*; Boffa, L.S.; Novak, B.M. Ed.; ACS Symposium Series, vol. 760; American Chemical Society: Washington, DC, **2000**; p. 254

[9] Kowollik, C.; Davis, T.P. *J. Polym. Sci. Part A Polym. Chem.* **2000**, *38*, 3303

[10] Muratore, L.M.; Heuts, J.P.A.; Davis, T.P. *Macromol. Chem. Phys.* **2000**, *201*, 985

[11] Heuts, J.P.A.; Muratore, L.M.; Davis, T.P. *Macromol. Chem. Phys.* **2000**, *201*, 2780

[12] Pangborn, A.B.; Giardello, M.A.; Grubbs, R.H.; Rosen, R.K.; Timmers, F.J. *Organometallics* **1996**, *15*, 1518

[13] Bakac, A.; Espenson, J.H. *J. Am. Chem. Soc.*, **1984**, *106*, 5197

[14] Hutchinson, R.A.; Paquet, D.A.; McMinn, J.H.; Beuermann, S.; Fuller, R.E.; Jackson, C. *Dechema Monographs* **1995**, *131*, 467

[15] Heuts, J.P.A. *Results presented on a poster during the SML 2001: Free radical polymerization, kinetics and mechanism*

[16] Ueda, A.; Nagai, S. in *'Polymer Handbook, 4th Edition'* (Eds. Brandrup, J.; Immergut, E.H.; Grulke, E.A.), p. II/97 Wiley: **1999**

[17] Walbiner, M.; Wu, J.Q.; Fischer, H. *Helv. Chim. Acta* **1995**, *78*, 910

[18] Bakac, A.; Espenson, J.H. *J. Am. Chem. Soc.* **1984**, *106*, 5197

[19] Cacioli, P.; Hawthorne, D.G.; Laslett, R.L.; Rizzardo, E.; Solomon, D.H. *J. Macromol. Sci.-Chem.* **1986**, *A23*, 839

[20] Moad, C.L.; Moad, G.; Rizzardo, E.; Thang, S.H. *Macromolecules* **1996**, *29*, 7717

[21] Moad, G.; Solomon, D.H.; *The Chemistry of Free Radical Polymerization*, 1st ed., Pergamon, Oxford, 1995

[22] Gridnev, A.A *J. Polym. Sci. Part A: Polym. Chem.* **2000**, *38*, 1753

[23] Suddaby, K.G.; Maloney, D.R.; Haddleton, D.M. *Macromolecules* **1997**, *30*, 702

[24] de Kock, J.B.L. *'Chain-Length Dependent Bimolecular Termination in Free-Radical Polymerization'* PhD Thesis, Eindhoven University of Technology, Eindhoven **1999**

[25] Suddaby, K.G.; Haddleton, D.M.; Hastings, J.J.; Richards, S.N.; O'Donnell, J.P. *Macromolecules*, **1996**, *29*, 8083

[26] Haddleton, D.M.; Kelly, E.J.; Kukulj, D.; Morsley, S.M.; Steward, A.G. *Pol. Preprints (ACS)*, **1999**, *40(1)*, 381

[27] Karmilova, L.V.; Ponomarev, G.V.; Smirnov, B.R.; Belgovskii, I.M. *Russian Chemical Reviews*, **1984**, *53*, 132

[28] Dixon, K.W. in *'Polymer Handbook, 4th Edition'* (Eds. Brandrup, J.; Immergut, E.H.; Grulke, E.A.), p. II/27 Wiley: **1999**

Chapter 5

Catalytic chain transfer
of non-α-methyl containing monomers

Synopsis: In this chapter the catalytic chain transfer polymerization of styrene and acrylates is discussed. For both monomers the formation of cobalt – carbon bonds between the catalyst and the polymeric radical is of major importance. For styrene this results in a strong dependence of the experimentally determined chain transfer coefficient on initiator concentration and the presence of (UV-) light. For acrylates cobalt – carbon bond formation is the predominant process, which inhibits practical use of catalytic chain transfer. However, chain transfer coefficients determined at very low conversions have the same order of magnitude as those determined for methacrylates.

5.1 Introduction

In Chapter 3 it was concluded that cobalt – carbon bond formation does not take place to any significant extent in the catalytic chain transfer polymerization of methyl methacrylate.

Scheme 5.1 Cobalt-mediated 'living' radical polymerization of methyl acrylate
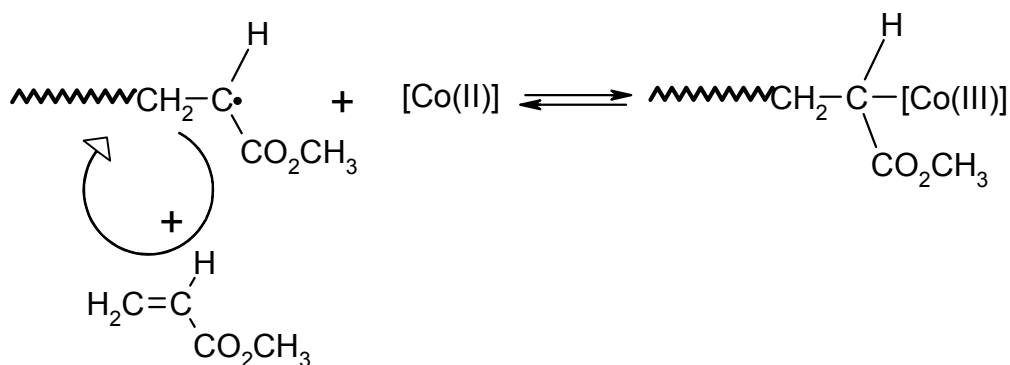
Acrylates, on the other hand, can be polymerized in a living fashion using different cobalt(II) complexes as shown in Scheme 5.1.[1,2,3] From this scheme it is clear that in the CCT polymerization of acrylates cobalt – carbon bond formation will play an important role. Furthermore, Roberts *et al.*[4] showed the occurrence of polyacrylate – cobalt bonds via MALDI-TOF mass spectrometry. Gridnev *et al.*[5] and Heuts *et al.*[6] used electron paramagnetic resonance to show that the signal from the unpaired electron in the Co(II) species disappears during polymerization of styrene. It is very likely that this is due to cobalt – carbon bond formation. However, so far the effects of cobalt – carbon bond formation in the CCT polymerization of either styrene or acrylates have not been investigated in a more quantitative way. Therefore, in this chapter it will be discussed in what way reaction conditions influence this cobalt – carbon bond formation and how this affects polymerization kinetics in the polymerization of both styrene and acrylates.

5.2 Experimental Section

Materials. Styrene (Aldrich, 99%), *n*-butyl acrylate (BA, Merck, 99%) and methyl acrylate (MA, Merck, 99 %) were all distilled under reduced pressure and stored at –10 $^{\circ}$C. Prior to use, monomers were passed over a column containing inhibitor remover and basic alumina. Toluene (Biosolve, AR) was purified using a Grubbs solvent purification set-up[7], purged with argon for at least three hours and stored over molsieves in a glovebox. Azobis(methylisobutyrate) (AIBMe, Wako Chemicals) was recrystallized from methanol and stored in a glovebox. CoBF (bis(aqua)bis((difluoroboryl)dimethylglyoximato)cobalt(II)) was prepared according to a procedure of Bakac and Espenson[8]. It was analyzed using UV-Vis spectroscopy and elemental analysis (experimental C: 23.1 %, H: 3.81 %, N: 13.3 %; calculated $C_8H_{12}N_4O_4B_2F_4Co \cdot (H_2O)_2$: C: 22.8 %, H: 3.83 %, N: 13.3 %). One single batch was used throughout all experiments.

Lamps. The emission spectra of both the UV-lamp and the fluorescent lamps in the fume-hood were measured inside the reaction vials, which were immersed in the water-bath. The spectra, shown in Figure 5.1, were recorded using a Ocean Optics spectrometer equipped with an optrode.
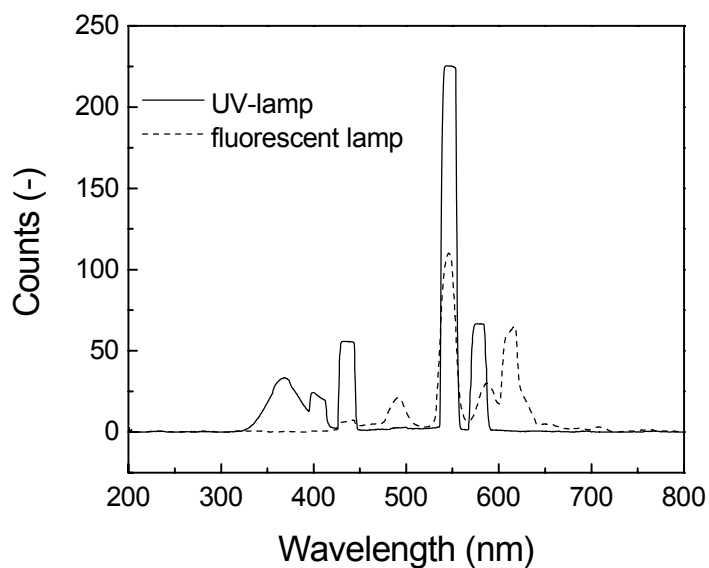
Figure 5.1 Emission spectra of both the UV-lamp and the fluorescent lamps.

General polymerization procedure. Monomers and solvents were purged with argon for at least three hours prior to transfer into a glovebox. All reaction mixtures were prepared inside a glovebox. Stock solutions of CoBF in monomer or solvent were prepared and stored for a longer period of time. AIBMe solutions in monomer were prepared immediately prior to the experiment. Reaction mixtures were made of the CoBF-solution, monomer, solvent and an AIBMe solution to a total volume of about 5 mL. Reactions were carried out at different solvent concentrations. At each set of conditions a total of eight polymerizations was done at different CoBF concentrations. Polymerizations were carried out in a water bath at a constant temperature of 60 $^{\circ}$C ($\pm$0.2 $^{\circ}$C) in the dark unless otherwise stated. Reactions were stopped by addition of hydroquinone and cooling. Monomer was evaporated and the polymer dried under vacuum at 60 $^{\circ}$C. Conversion was determined gravimetrically.

Polymerizations of methyl acrylate. These polymerizations were carried out in a similar fashion, but reaction mixtures were prepared outside a glovebox. All monomer and solvent transfer was done by gastight syringe to prevent oxygen from entering reaction vials. In these experiments the initiator concentration was kept constant and the CoBF concentration was varied. The weight fraction of monomer was about 45 %. Polymerizations were initiated by AIBN. Toluene was used as received. Samples were taken by syringe to monitor conversion.

Decomposition of AIBMe. AIBMe was dissolved in toluene in a 10 mL reaction vial and immersed in an oil-bath at the required temperature. Samples were withdrawn by a syringe at regular time intervals. Samples were diluted with toluene, cooled to room-temperature and a UV-Vis absorption spectrum was recorded. Absorption at 370 nm was chosen to monitor decomposition.

Analyses. Size exclusion chromatography (SEC) was carried out using tetrahydrofuran (THF) as an eluent at a flow rate of 1 mL· min^{-1}. Two Polymer Laboratories PLgel 5 μm Mixed-C columns (300 × 7.5 mm) and PLgel 5 μm guard column (50 × 7.5 mm) were used and calibrated with Polymer Laboratories narrow MWD polystyrene standards. The Mark-Houwink parameters used in universal calibration are: $K_{MA} = 2.61 \times 10^{-4}$ dL· g^{-1}, $a_{MA} = 0.659$, $K_S = 1.14 \times 10^{-4}$ dL· g^{-1}, $a_S = 0.716$.[9]

UV-Vis spectroscopy was carried out on a Hewlett Packard 8451A photodiode array UV-Visible system using a quartz cuvette of 1 cm optical path length. The system is equipped with both a deuterium and a tungsten lamp.

5.3 Catalytic chain transfer polymerization of styrene

5.3.1 CCT of styrene in dark, ambient light and UV-light

Experimentally determined values of C_T for the polymerization of styrene are collected in Table 5.1. In dark, C_T for the homopolymerization of styrene in the presence of CoBF was found to be around 50 which is an order of magnitude lower than found in literature[10,11,12,13], where values for C_T in between 350 and 1600 have been reported. The spread in the values reported in literature is quite remarkable, especially when it is considered that for MMA C_T is in a much smaller range from 28.000 to 40.000.

A typical Mayo-plot for a CCT polymerization of styrene in dark is shown in Figure 5.2. A very distinct feature is the enormous difference between the Mayo-plots determined from M_n and M_w. The chain transfer coefficients differ one order of magnitude, a lot more than what is normally found for methacrylates. This difference can be explained when we take a look at the differential molecular weight distribution (MWD) shown in Figure 5.3. In the lower
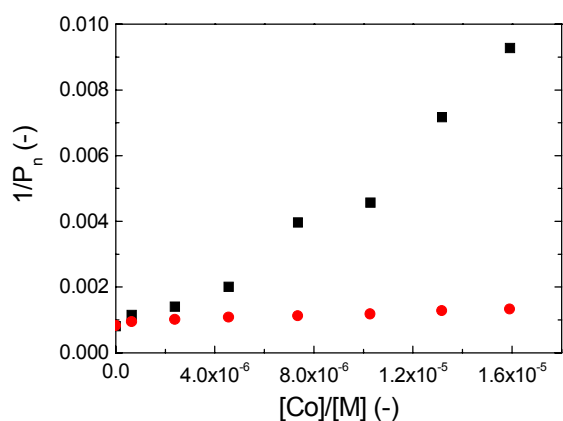
Figure 5.2 Mayo-plot for the catalytic chain transfer polymerization of styrene with CoBF at 60 ^{o}C and [AIBMe] = 6 × 10^3 mol· L^{-1}. ■: P_n calculated from M_n, ●: P_n calculated from M_w.
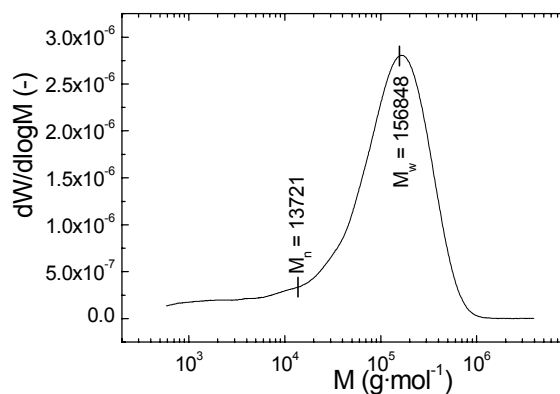
Figure 5.3 Differential log molecular weight distribution of the polymer resulting from the catalytic chain transfer polymerization of styrene in dark at 60°C. [AIBMe] = 6 × 10^{-3} mol· L^{-1}; [CoBF] = 1.4 × 10^{-4} mol· L^{-1}.

molecular weight region a long tail can be seen, resulting in a polydispersity of 11.4. Normally, for a low conversion polymerization a polydispersity of 2 would be expected. However, other authors reported the occurrence of bimodal distributions as well.[14,15]

The MWD in Figure 5.3 must be the result of more than one mode of polymerization occurring either in parallel or in series. Different modes of polymerization occurring in parallel could be due to insufficient heat transfer or mixing resulting in a temperature or concentration gradient across the reaction vial. If that were the case, polymerizations without CoBF would be expected to show broadened MWDs as well. This is not observed. Therefore, we expect that the polymerization process changes over time resulting in the formation of polymers with different chain-lengths.

Furthermore, the amount of low molecular weight material increases with increasing CoBF concentration, see Figure 5.4. For longer reaction times only additional high molecular weight polymer is formed. Our data presented so far are also in line with the observations of Heuts *et al.*[16] that the determined chain transfer coefficients depend on monomer conversion. So at the start overall catalytic activity is a lot larger than during later stages of the polymerization, pointing at some sort of catalyst deactivation. Taking into account possible cobalt – polystyryl radical bond formation and the large discrepancy between the C_T's determined in this study and those known in literature, it was considered that the absence of light might hamper
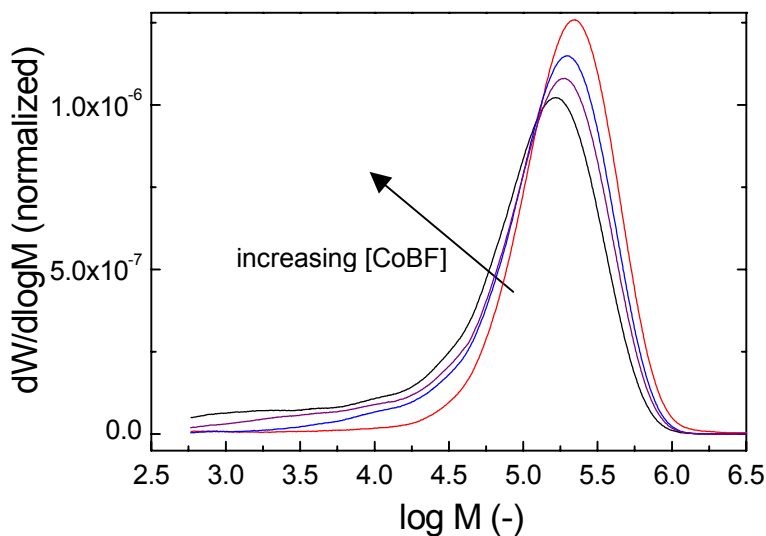
101

Figure 5.4 Differential log MWDs for polystyrene produced via catalytic chain transfer polymerization at 60 °C at CoBF concentrations ranging from 0 to 1.4×10^{-4} mol· L^{-1}.

catalytic chain transfer. Therefore, the CCT polymerizations were carried out in the presence of ambient light and UV-light as well.

The results for all these polymerizations are collected in Table 5.1. In ambient laboratory light the chain transfer coefficients increase to a level similar to that in literature reports.[10,11,12,13] When the extensive dataset reported by Kukulj *et al.*[10,13] is examined more closely it can be seen that, in general, C_T values determined via the Mayo-method from M_n are larger than the ones determined via the CLD method. The results from the CLD method usually correspond to those from the Mayo-method using M_w. A similar trend can be seen in the data presented here. For nearly all polymerizations, C_T determined from M_n-data is larger than C_T determined from M_w-data. In Figure 5.5 the chain transfer coefficients are shown for the various conditions as a function of initiator concentration.

Both light and, even more so, UV-light are able to enhance the overall catalytic activity by one to two orders of magnitude. It is very likely that the reason for this can be found in an increased dissociation rate constant for the cobalt – polystyryl radical bonds. Additionally, the chain transfer coefficients inversely depend on initiator concentration, which can be explained from the equilibrium shown in Scheme 5.1.

Table 5.1 Results for the CCT polymerization of styrene at 60 $^{\circ}$C under various conditions.

[AIBMe] (mol$\cdot$ L^{-1})	Condition	C_T (M_n)	C_T (M_w)
6.0×10^{-4}	dark	6.6×10^2	67
6.0×10^{-3}	dark	5.1×10^2	27
6.0×10^{-3}	dark	3.5×10^2	19
6.0×10^{-2}	dark	3.4×10^2	67
6.0×10^{-4}	ambient light	2.9×10^3	2.1×10^3
6.0×10^{-3}	ambient light	9.0×10^2	4.5×10^2
6.0×10^{-2}	ambient light	6.7×10^2	3.3×10^2
4.0×10^{-4}	UV-light	6.6×10^3	6.9×10^3
1.0×10^{-3}	UV-light	5.0×10^3	5.0×10^3
1.0×10^{-2}	UV-light	4.1×10^3	3.4×10^3
2.5×10^{-2}	UV-light	1.7×10^3	1.4×10^3
3.0×10^{-2}	UV-light	1.4×10^3	9.6×10^2
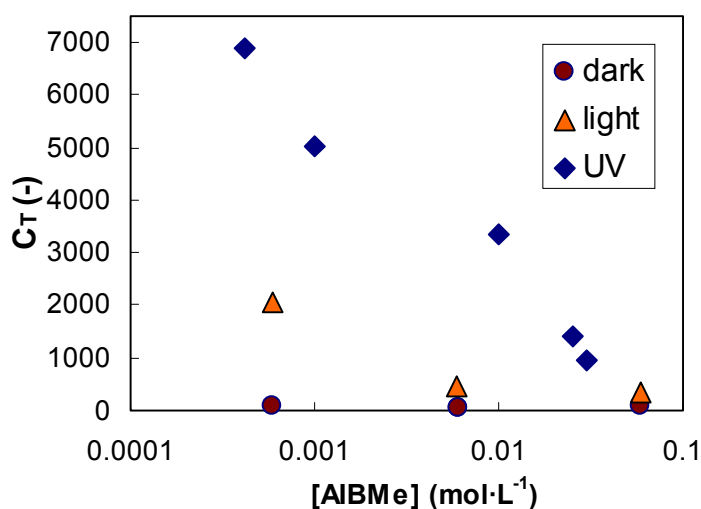
Figure 5.5 Chain transfer coefficients determined for the CCT polymerization of styrene at 60 $^{\circ}$C at different initiator concentrations in dark, light and UV-light.

In contrast, in CCT polymerizations of MMA no dependence of C_T on initiator concentration is observed. In CCT polymerizations of styrene an increase in initiator concentration results in an increase in radical concentration, which will shift the equilibrium presented in Scheme 5.1

to the right hand side. The lower concentration of cobalt(II) available results in a lower apparent chain transfer coefficient.

Temperature can strongly affect radical concentration. This may explain the negative activation energy for catalytic chain transfer in the polymerization of styrene as observed by Kukulj *et al.*[13] The chain transfer coefficients were determined in the temperature range 40 to 70 °C and found to decrease by a factor of 4, although the equilibrium for the formation of cobalt – carbon bonds is expected to be shifted to the dissociated side at higher temperatures. However, it was not taken into account by Kukulj *et al.*[13] that the initiator decomposition rate increases by two orders of magnitude,[20] resulting in a higher radical concentration, which will shift the equilibrium the other way, which may well explain the observed trends.

5.3.2 Quantitative description of CCT polymerization of styrene

It is interesting to see whether it is possible to relate the experimentally determined chain transfer coefficients to equation 3.31[*]

$$C_{\text{T}} = \frac{1}{\dfrac{k_{\text{com,overall}}}{k_{\text{dis,overall}}} \sqrt{\dfrac{fk_{\text{d}}}{<k_{\text{t}}>}} \sqrt{[\text{I}]} + 1} \frac{k_{\text{tr,overall}}}{k_{\text{p}}} \tag{3.31}$$

which relates the chain transfer coefficient to the initiator concentration in case of cobalt – carbon bond formation. When the experimentally obtained datasets are fitted to this equation two sets of parameters are obtained, which are

$$C_{\text{T,0}} = \frac{k_{\text{tr,overall}}}{k_{\text{p}}} \tag{5.1}$$

where $C_{\text{T,o}}$ is the chain transfer coefficient in absence of cobalt – carbon bond formation and

$$\kappa = \frac{k_{\text{com,overall}}}{k_{\text{dis,overall}}} \sqrt{\frac{fk_{\text{d}}}{<k_{\text{t}}>}} \tag{5.2}$$

---

[*] The overall rate coefficients for transfer, combination and dissociation in eq 3.31 combine contributions of the actual chemical reaction and diffusion and have been defined in Section 3.6.
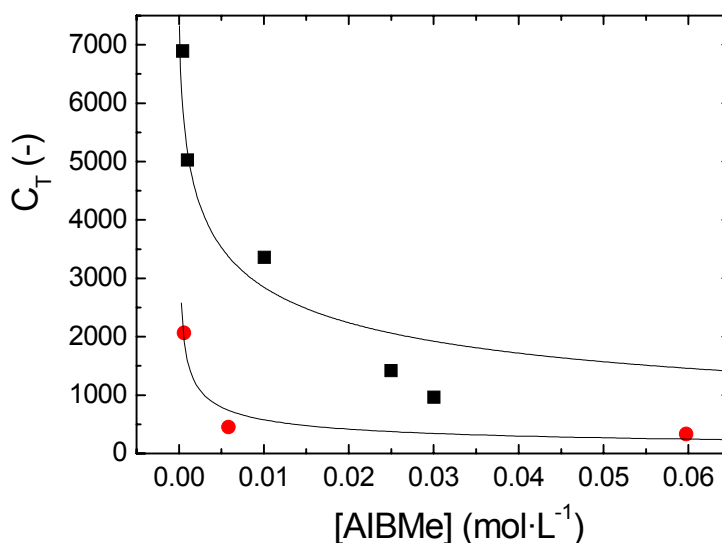
Figure 5.6 Fit of data of the CCT polymerization of styrene in light (●) and UV-light (■) to eq 3.31.

where κ is a parameter describing the cobalt – carbon bond formation equilibrium. In Figure 5.6 the fits of the chain transfer coefficients to eq 3.31 are shown.

First the data obtained in UV-light are fitted to eq 3.31 and the parameters $C_{T,o} = 8.3 \times 10^3$ and $\kappa_{UV} = 19$ $L^{\frac{1}{2}} \cdot mol^{\frac{1}{2}}$ are obtained. Assuming that $C_{T,o}$ does not depend on the wavelength and intensity of the light, this ratio was used to fit the data in normal light to eq 3.31 resulting in κ_{light} 1.3×10^2 $L^{\frac{1}{2}} \cdot mol^{\frac{1}{2}}$. It was not possible to determine the parameters independently from the data in normal light as the product of κ and the square root of initiator concentration is much larger than one. Especially at lower initiator concentrations the fit is fair. One of the main factors complicating this analysis is the fact that light and especially UV-light do not only enhance dissociation of cobalt – carbon bonds, but also initiator decomposition. Enhanced initiator decomposition leads to an increase in radical concentration and thus to a shift in the equilibrium in Scheme 5.1 to the side of Co(III). Therefore, it should be realized that enhanced initiator decomposition will partially counteract the effect of increased cobalt – carbon bond dissociation. The combined thermal and photochemical decomposition of an azo-initiator is a rather complex phenomenon that cannot be described by simple kinetics.[17] Therefore, it was decided not to adapt eq 3.31 to account for this. However, in order to get a general idea about the effect, initiator decomposition for four AIBMe solutions was monitored using UV-Vis spectroscopy both in dark and in UV-light. The results are shown in Figure 5.7. It can be seen that in the first few hours, which are relevant to these polymerizations, in UV-

light at 60 ^{0}C AIBMe decomposes about twice as fast as in dark at the same temperature. This will approximately result in a radical concentration that is about 1.4 times larger than in dark.
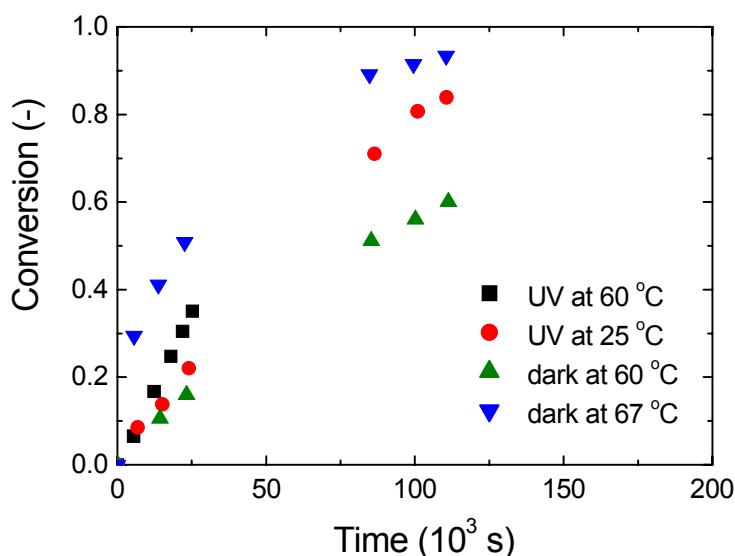

Figure. 5.7 Conversion - time profiles for AIBMe dissolved in toluene. Conversion was monitored by UV-Vis spectroscopy. Conditions are specified in the plot.

Taking a look at the parameters obtained from fitting our data to eq 3.31, we can see that the chain transfer coefficient in absence of cobalt – carbon bond formation, $C_{T,0}$ is about an order of magnitude higher than those reported so far. From κ we want to obtain an estimate of the order of magnitude of the ratio of $k_{com,overall}$ and $k_{dis,overall}$. This can be done via a combination of eq 5.2 , eq 3.28 and the following rewritten expression for the rate of polymerization

$$[P\bullet] = \frac{\dfrac{dX}{dt}}{k_p(1-X)} \tag{5.3}$$

in which X is the fractional conversion, resulting in

$$\frac{k_{com,overall}}{k_{dis,overall}} = \frac{\kappa k_p(1-X)\sqrt{[I]}}{\dfrac{dX}{dt}} \tag{5.4}$$

It is realized that the results obtained in this way will not have a high accuracy, but the order of magnitude is expected to be good. For all series of polymerizations in UV-light the

polymerization at the highest CoBF concentration was used to calculate $[P\bullet]$. The value for k_p = 341 L$\cdot$ mol$^{-1}\cdot$ s^{-1} was taken from van Herk.[18] The results are shown in Table 5.2.

Table 5.2 Determination of $k_{com,overall}/k_{dis,overall}$ from CCT polymerizations of styrene in UV-light at 60 ^{o}C.

$[I]$ (mol$\cdot$ L^{-1})	Time (s)	X (-)	$[P\bullet]$ (mol$\cdot$ L^{-1})	$k_{com,overall}/k_{dis,overall}$ (L$\cdot$ mol^{-1})
4.0×10^{-4}	1.63×10^{4}	0.028	5.2×10^{-9}	7×10^{7}
1.0×10^{-3}	1.13×10^{4}	0.031	8.3×10^{-9}	7×10^{7}
1.0×10^{-2}	1.56×10^{3}	0.013	2.5×10^{-8}	8×10^{7}
2.5×10^{-2}	1.32×10^{3}	0.024	5.5×10^{-8}	6×10^{7}
3.0×10^{-2}	1.08×10^{3}	0.019	5.0×10^{-8}	6×10^{7}

From these results it can be concluded that $k_{com,overall}$ / $k_{dis,overall}$ will be around 7×10^7 L$\cdot$ mol^{-1} under the specific conditions of the reactions carried out with UV-light. For the reactions in ambient laboratory light the same approach was used. The results are collected in Table 5.3.

Table 5.3 Determination of $k_{com,overall}/k_{dis,overall}$ from CCT polymerization of styrene in ambient laboratory light at 60 ^{o}C.

$[I]$ (mol$\cdot$ L^{-1})	Time (s)	X (-)	$[P\bullet]$ (mol$\cdot$ L^{-1})	$k_{com,overall}/k_{dis,overall}$ (L$\cdot$ mol^{-1})
6×10^{-4}	1.15×10^{4}	0.028	7.3×10^{-9}	4×10^{8}
6×10^{-3}	4.74×10^{3}	0.023	1.5×10^{-8}	6×10^{8}
6×10^{-2}	1.86×10^{3}	0.035	5.7×10^{-8}	7×10^{8}

In ambient laboratory light a value for $k_{com,overall}$ / $k_{dis,overall}$ of about 5×10^8 L$\cdot$ mol^{-1} is found. As the chain transfer coefficients obtained in dark are even an order of magnitude smaller than those obtained in laboratory light (see Table 5.1), $k_{com,overall}$ / $k_{dis,overall}$ in dark is expected to be over 10^9 L$\cdot$ mol^{-1}, which is quite a bit larger than the value of 2.4×10^7 reported by Woska et al[19] for the dissociation of a styryl(tetraanisyl)porphyrinatocobalt(III) complex.

5.3.3 Reversibility of polystyrene – cobalt bonds

The reversibility of cobalt – polystyrene radical bond formation was shown via the synthesis of polystyrene having a bimodal MWD in a one-step process. In Figure 5.8 the successive molecular weight distributions for the catalytic chain transfer polymerization of styrene are shown. During the first four hours the reaction vials were exposed to laboratory light, after which the light was turned off and the vials were protected from light during the next two hours of reaction. The molecular weight distributions shown correspond to samples taken after two, four, five and six hours. It can be clearly seen that during the first two hours polymer is formed with a M_{peak} around 25×10^3 g· mol^{-1}. After the light is turned off a shift to a M_{peak} around 200×10^3 g· mol^{-1} occurs. The opposite effect is shown in Figure 5.9. Here, the first two hours of reaction had place in dark, after which the reaction mixture was exposed to light for three hours. The first sample was taken after one hour when conversion was only 0.16 %. The molecular weight distribution was still on the low molecular weight side with a M_{peak} around 1000 g· mol^{-1}. After two hours molecular weights had shifted to 220×10^3 g· mol^{-1}. After the light is turned on, the molecular weight of the newly formed polymer decreases again. The shifts in MWD can be easily explained from the mechanisms in Scheme
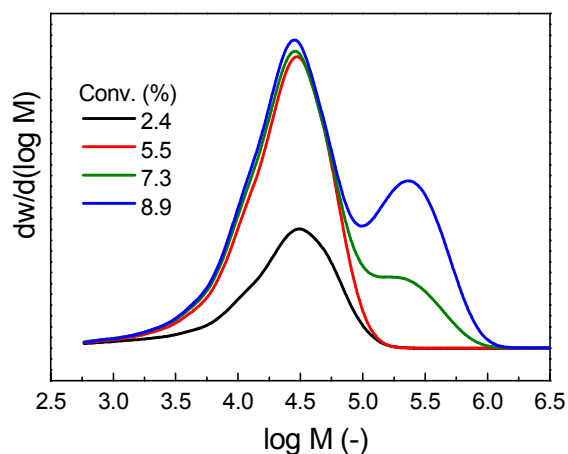
Figure 5.8 Molecular weight distributions for the catalytic chain transfer polymerization of styrene at 60 °C at successive conversions. The first four hours reaction vials were exposed to light, after which the light was turned off. Samples were taken after 2, 4, 5 and 6 hours.
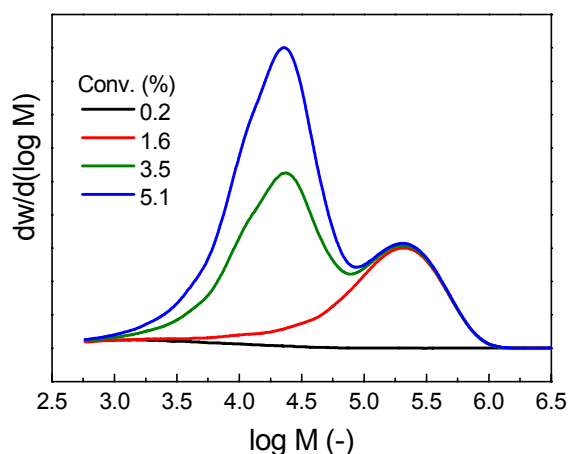
Figure 5.9 Molecular weight distributions for the catalytic chain transfer polymerization of styrene at 60 °C at successive conversions. The first two hours reaction vials were put in dark, after which they were exposed to light light for three hours. Samples were taken after 1, 2, 3.5 and 5 hours.

5.1 and Scheme 2.2. For the reaction shown in Figure 5.9 the concentration of CoBF available for transfer is still decreasing when the first sample is taken after one hour. Most newly initiated polystyrene radicals are covalently bonded to CoBF and therefore the conversion rate is low. The molecular weight of the polymer that is formed is rather low as a large part of the total amount of CoBF added to the reaction mixture is still available for transfer. When the second sample is taken after two hours an equilibrium between bound and unbound polystyrene radicals is reached. Conversion rates increase as not all freshly generated radicals will be trapped anymore and the average molecular weight increases as only a small amount of CoBF can take part in the transfer reactions. When the light is turned on the dissociation rate of the cobalt – polystyrene radicals bond goes up, resulting in a shift of the bound – unbound equilibrium to more free CoBF, which in turn gives lower molecular weights. The evolution of the MWDs in Figure 5.8 can be explained in a similar fashion. These results clearly show the reversibility of covalent bond formation between the polystyrene radical and the cobalt species.

5.4 Catalytic chain transfer polymerization of acrylates

The conversion – time history for the methyl acrylate homopolymerizations in the presence of CoBF are shown in Figure 5.10. Similar observations were recently done by Roberts *et al.*[4] The inhibition period increases with increasing ratio of [CoBF] and [AIBN]. Assuming that each growing polymer chain that is initiated by an AIBN radical fragment is captured by CoBF until CoBF has reached its equilibrium concentration, one can calculate a theoretical inhibition period t_o according to

$$t_o = \frac{-\ln(1 - \frac{(1 - f_{Co})[CoBF]_o}{2f[AIBN]_o})}{k_d} \approx \frac{(1 - f_{Co})[CoBF]_o}{2 f k_d [AIBN]_o} \tag{5.5}$$

where the AIBN dissociation rate constant $k_d = 9.7 \cdot 10^{-6}$ s^{-1} [20] and f is the initiator efficiency. For $f \approx 0.8$ and $f_{Co} \approx 0.1$ the theoretical inhibition times have the same order of magnitude as those observed experimentally. After the inhibition period polymerization starts very rapidly at a nearly constant rate, which implies that the radical concentration and thus the fraction of
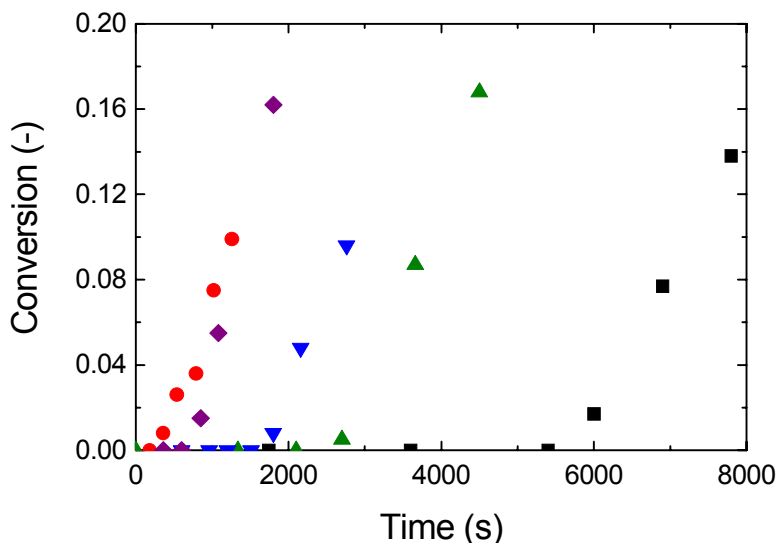
Figure 5.10 Homopolymerization of MA in presence of CoBF. [CoBF]/[AIBN]: ● = 0; ◆ = 0.012; ▼ = 0.020; ▲ = 0.047; ■ = 0.104.

free CoBF remain constant. This means that there is a steady state in the cobalt species. The molecular weight of the polymer decreases slightly with increasing CoBF-concentration resulting in an apparent $C_T = 8$ for the MA homopolymerization, which means that transfer from MA-ended polymeric radicals can indeed be neglected. The observations of Enikolopyan *et al.*[21] who reported inhibition in the homopolymerization of MA using cobalt porphyrins and of Roberts *et al.*[4] and Janowicz[22] who reported a limited chain transfer activity are both in agreement with the results presented here.

In an attempt to apply UV-light assisted catalytic chain transfer to the polymerization of butyl acrylate in a similar way as to styrene, we unfortunately still observed an inhibition time. However, the tiny amounts of polymer formed during inhibition were used in the determination of C_T. The Mayo-plot is shown in Figure 5.11. In the calculations of the CoBF concentrations it was assumed that all CoBF was available for transfer, which will mean that the obtained value $C_T = 650$ is an underestimation. This results in a transfer constant (k_{tr}) that is less than 20 % smaller than for *n*-BMA, see Table 5.4.
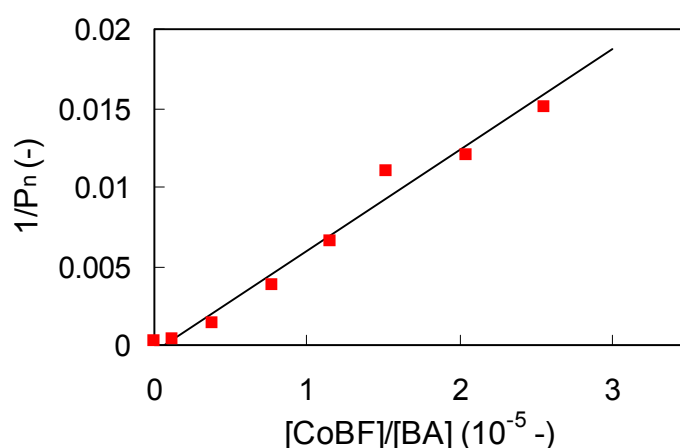
Figure 5.11 Mayo-plot of the polymer formed during the inhibition period of an attempted UV-light assisted catalytic chain transfer polymerization of *n*-butyl acrylate in toluene at 60 °C.

Table 5.4. Chain transfer coefficients, propagation and transfer rate constants for *n*-BMA, BA, styrene at 60 °C and α-methyl styrene at 50 °C.

Monomer	C_T (average)	$k_p{}^a$ (L· mol^{-1}· s^{-1})	k_{tr} (L· mol^{-1}· s^{-1})
n-BMA[b]	28.0×10^3	976	2.7×10^7
BA	0.65×10^3	33700	2.2×10^7
styrene	8.3×10^3	341	2.8×10^6
α-methyl styrene[c]	8.9×10^5	1.73	1.5×10^6

[a] All k_p-data are taken from van Herk.[18]
[b] C_T for *n*-BMA was taken from Chapter 3.
[c] Data for α-methyl styrene are taken from Kukulj *et al.*[23]

So the absence of an α-methyl group in acrylates has hardly any influence on the transfer step itself, in contrast to the general belief that hydrogen abstraction from the backbone is more difficult than from an α-methyl group.[13,23] The reduction of free cobalt by cobalt – carbon bond formation is the cause of the absence of CCT behaviour in acrylate polymerizations. A similar comparison can be made for styrene and α-methyl styrene. Using the higher values for C_T obtained from the UV-light assisted catalytic chain transfer polymerization of styrene, one calculates similar values of k_{tr} for both styrene and α-methyl styrene. This means that in this case as well the predominant effect of the α-methyl group is the prevention of cobalt – carbon bond formation and not directly facilitating hydrogen abstraction.

If in the catalytic chain transfer polymerization of acrylates the formation of cobalt – carbon bonds can be partially prevented by an increase in temperature, which may be the case in Janowicz data[22] , by using UV-light of a specific wave-length or by any other means than acrylates can be applied more easily in catalytic chain transfer polymerizations. This would result in a wider scope for application of CCT in industry.

5.5 Conclusions

From the catalytic chain transfer polymerization of styrene it appeared that it is only truly effective when the polymerization is exposed to light or even better UV-light. The obtained chain transfer coefficients have an inverse dependence on initiator concentration. This can be explained using a combination of both the catalytic chain transfer and the living polymerization mechanisms. This dependence of C_T on both light and initiator concentration may well explain the large spread in literature values for C_T. In UV-light at low initiator concentrations C_T can be increased to around 7000, an order of magnitude higher than what has been reported so far.

For both methyl and butyl acrylate an inhibition period is observed in the catalytic chain transfer polymerization. The formation of cobalt – carbon bonds dominates over the transfer process. However, for BA an intrinsic transfer rate constant has been determined. For both *n*-butyl acrylate and styrene it was shown that these intrinsic chain transfer constants differ only little from the transfer constants of their counterparts *n*-butyl methacrylate and α-methyl styrene. The absence of an α-methyl group in acrylates and styrene has hardly any influence on the transfer step itself.

5.6 References

[1] Wayland, B.B.; Poszmik, G.; Mukerjee, S.L. *J. Am. Chem. Soc.* **1994**, *116*, 7943

[2] Wayland, B.B.; Basickes, L. Mukerjee, S.; Wei, M.; Fryd, M. *Macromolecules* **1997**, *30*, 8109

[3] Arvanitopoulos, L.D.; Greuel, M.P.; King, B.M.; Shim, A.K.; Harwood, H.J. In *Controlled Radical Polymerization*; Matyjaszewski, K. Ed.; ACS Symposium Series, vol. 685; American Chemical Society: Washington, DC, **1998**; p. 316

[4] Roberts, G.E.; Heuts, J.P.A.; Davis, T.P. *Macromolecules* **2000**, *33*, 7765

[5] Gridnev, A.A.; Belgovskii, I.M.; Enikolopyan, N.S. *Dokl. Chem.* **1986**, *289*, 748

[6] Heuts, J.P.A.; Forster, D.J.; Davis, T.P.; Yamada, B.; Yamazoe, H.; Azukizawa, M. *Macromolecules* **1999**, *32*, 2511

[7] Pangborn, A.B.; Giardello, M.A.; Grubbs, R.H.; Rosen, R.K.; Timmers, F.J. *Organometallics* **1996**, *15*, 1518

[8] Bakac, A.; Espenson,, J.H. *J. Am. Chem. Soc.*, **1984**, *106*, 5197

[9] Hutchinson, R.A.; Paquet, D.A.; McMinn, J.H.; Beuermann, S.; Fuller, R.E.; Jackson, C. *Dechema Monographs* **1995**, *131*, 467

[10] Kukulj, D.; Heuts, J.P.A.; Davis, T.P. *Macromolecules* **1998**, *31*, 6034

[11] Suddaby, K.G.; Maloney, D.R.; Haddleton, D.M. *Macromolecules* **1997**, *30*, 702

[12] Haddleton, D.M.; Maloney, D.R.; Suddaby, K.G.; Muir, A.V.G.; Richards, S.N. *Macromol. Symp.* **1996**, *111*, 37

[13] Kukulj, D.; Davis, T.P. *Macromol. Chem. Phys.* **1998**, *199*, 1697

[14] Smirnov, B.R.; Plotnikov, V.D.; Ozerkovskii, B.V.; Roshchupkin, V.P.; Enikolopyan, N.S. *Pol. Sci. USSR* **1981**, *23*, 2807

[15] Plotnikov, V.D. *Pol. Sci. Ser. A* **1997**, *39*, 250

[16] Heuts, J.P.A.; Forster, D.J.; Davis, T.P. In *Transition Metal Catalysis in Macromolecular Design*; Boffa, L.S.; Novak, B.M. Ed.; ACS Symposium Series, vol. 760; American Chemical Society: Washington, DC, **2000**; p. 254

[17] Engel, P.S. *Chem. Rev.* **1980**, *80*, 99

[18] van Herk, A.M *Macromol. Theory Simul,* **2000**, *9*, 433

[19] Woska, D.C.; Xie, Z.D.; Gridnev, A.A.; Ittel, S.D.; Fryd, M.; Wayland, B.B. *J. Am. Chem. Soc.* **1996**, *118*,9102

[20] Moad, G.; Solomon, D.H. *The Chemistry of Free Radical Polymerization*, 1st ed., Pergamon, Oxford 1995, p. 59

[21] Enikolopyan, N.S.; Smirnov, B.R. Ponomarev, G.V.; Belgovskii, I.M. *J. Pol. Sci. Pol. Chem.* **1981**, *19*, 879

[22] Janowicz, A.H.*US Patent 4,694,054* **1987**

[23] Kukulj, D.; Heuts, J.P.A.; Davis, T.P. *Macromolecules* **1998**, *31*, 6034

Chapter 6

Catalytic chain transfer copolymerization
of methacrylates and acrylates

Synopsis: In this chapter it is shown that catalytic chain transfer is a very efficient way of controlling molecular weight in the copolymerization of methyl methacrylate (MMA) and methyl acrylate (MA) or n-butyl acrylate (BA). A model is developed based on copolymerization kinetics and the mechanisms for catalytic chain transfer and for cobalt-mediated living radical polymerization that can describe the observed transfer coefficients. Secondly, it is shown that the presence of a catalytic chain transfer agent does not affect the reactivity ratios within the concentration range studied. Finally, the effect of conversion and therewith composition drift on the catalytic chain transfer polymerization of MMA and BA is investigated and it is shown that under the conditions employed in the experiments a certain degree of branching is present at high partial conversions of MMA.

6.1 Introduction

In the previous chapters various aspects of CCT homopolymerizations of methacrylates, styrene and acrylates have been described and discussed. For industrial applications and especially in coatings, it is required to use combinations of various functional and non-functional monomers to obtain optimal material properties. So far, most reports on CCT copolymerization described the copolymerization of two CCT active monomers, like styrene – MMA[1,2,3,4] styrene – α-methylstyrene[5] and MMA – n-butyl methacrylate[6,7,8]. Both Bon *et al.*[9] and Heuts *et al.*[10] included the functional 2-hydroxyethyl methacrylate in their co- and terpolymerizations, respectively. However, in literature no reports on the copolymerization of

CCT active monomers and CCT inactive monomers can be found. The question is whether such a polymerization will result in inhibition[11,12], some sort of living character as is reported for acrylates[13,14,15], or CCT polymerization. Therefore, this chapter aims to focus on the copolymerization of CCT active monomers like MMA and CCT inactive monomers like methyl acrylate (MA) and *n*-butyl acrylate (BA).

6.2 Experimental Section

Materials. MMA, MA and BA (all from Merck, 99%) were distilled under reduced pressure and stored at –10 $^{\circ}$C. Prior to use, monomers were passed over a column containing inhibitor remover and basic alumina. Azobis(isobutyronitrile) (AIBN, Fluka) and toluene (Biosolve) were used as received in copolymerizations of MMA and MA. In copolymerizations of MMA and BA, toluene (Biosolve, AR) was purified using a Grubbs solvent set-up[16] and AIBN as well as azobis(methylisobutyrate) (AIBMe, Wako Chemicals) were recrystallized from methanol and stored in a glovebox.

The cobalt catalyst CoBF (bis(aqua)bis((difluoroboryl)dimethylglyoximato)cobalt(II)) was prepared according to a procedure of Bakac and Espenson[17]. It was analysed using UV-Vis spectroscopy and elemental analysis (experimental batch I: C: 23.0 %, H: 3.91 %, N: 13.5 %; batch II: C: 23.1 %, H: 3.81 %, N: 13.3 %; calculated for $C_8H_{12}N_4O_4B_2F_4Co \cdot (H_2O)_2$ C: 22.8 %, H: 3.83 %, N: 13.3 %). Batch I and II were used in the MMA – MA and MMA – BA copolymerizations, respectively.

MMA – MA copolymerizations. All monomers and solvents were purged with argon for at least one hour prior to use. CoBF and AIBN were weighed into separate vials, sealed with septa and an argon stream was passed over for more than one hour. Stock solutions of CoBF and AIBN in monomer were prepared. All monomer transfer was done by gastight syringe. For reactions at high initiator concentrations, AIBN was weighed directly into the reaction vials. Reaction mixtures were made of both monomers, CoBF solution and AIBN solution to a total volume of about 5 mL. Reactions were carried out at three different fractions of monomer in the feed and for each fraction at different initiator concentrations. At each set of

conditions a total of eight polymerizations was done at different CoBF concentrations. Before the polymerizations were started, the reaction vials were immersed in an ice/water bath and purged with argon for an additional 20 minutes. Polymerizations were carried out in a water bath at a constant temperature of 60 ^{o}C ($\pm$0.5 ^{o}C). Reactions were stopped by addition of hydroquinone and cooling. Monomer was evaporated and the polymer dried under vacuum at 40 ^{o}C. Conversion was determined gravimetrically. Polymerizations to determine the inhibition time were carried out in a similar fashion. In these experiments the initiator concentration was kept constant and the CoBF concentration was varied. The molar fraction of MMA was set at 0.46. Samples were taken by syringe to monitor conversion.

MMA – BA copolymerizations. These polymerizations were carried out in a similar fashion as the MMA – MA copolymerizations, but reaction mixture preparation was performed in a glovebox. Monomers and toluene were purged with argon for at least three hours prior to transfer into the glovebox. Stock solutions of CoBF in monomer or solvent were prepared and stored for a longer period of time. AIBMe solutions in monomer were prepared immediately prior to the experiment. Reaction mixtures were made of the CoBF solution, monomer and an AIBMe solution to a total volume of about 5 mL. The rest of the polymerization procedure is similar to what is described for the MMA – MA copolymerizations. Copolymers were dried under vacuum at 70 ^{o}C.

High conversion copolymerizations were carried out inside a glovebox in a sand bath at a constant temperature of 60 ^{o}C. The thermo-couple for temperature control was immersed into the reaction mixture for optimal control. The mixtures were stirred with a magnetic stirrer. Samples were withdrawn by syringe to monitor conversion and molecular weight distribution. Partial conversions were determined with GC.

Analyses. ^{1}H-NMR was carried out to determine the copolymer composition. Spectra were recorded with a Varian 300 MHz spectrometer at 298 K, using CDCl$_3$ as a solvent and tetramethylsilane as an internal reference. The composition was determined from the α-CH$_3$ and the total -O-CH$_3$ regions[18] for MMA – MA copolymers and from the –O-CH$_3$ and –O-CH$_2$- regions[19] for MMA – BA copolymers.

Size exclusion chromatography (SEC) was carried out using THF as an eluent at a flow rate of 1 mL· min^{-1}. Two Polymer Laboratories PLgel 5 µm Mixed-C columns (300 x 7.5 mm) and PLgel 5 µm guard column (50 x 7.5 mm) were used and calibrated with Polymer Laboratories narrow MWD polystyrene standards. For poly(MMA-co-MA) the polystyrene calibration curves were converted into copolymer composition dependent calibration curves as was done before for the system styrene-MMA[20]. Molecular weight distributions for poly(MMA-co-BA) were determined directly from the polystyrene calibration curve.
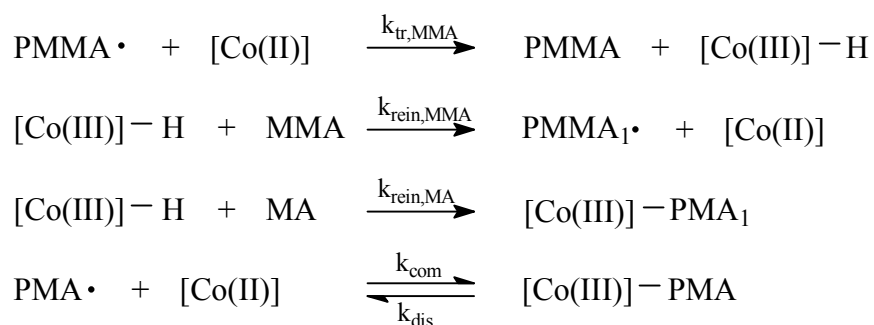
Gas chromatography was performed on a HP 5890 series II gas chromatograph equipped with an autosampler. A HP Ultra 2 column containing cross-linked 5 % Ph Me Silicone was used. Column dimensions are 25 m × 0.32 mm × 0.52 µm film thickness. Samples were diluted about ten times with THF. The solvent in which the polymerization was conducted was used as a standard for calibration.

6.3 Model for CCT copolymerization of acrylates and MMA

6.3.1 Fundamental reaction steps and basic equations

The copolymerization of acrylates and MMA in the presence of the cobalt complex is assumed to obey free-radical copolymerization kinetics. The implicit penultimate model for propagation is applied. In addition to this, the reactions as shown in Scheme 6.1 can occur. In this section MA is taken as an example. All the reactions and equations are valid for other acrylates as well.

Scheme 6.1 Reactions involving cobalt species in CCT copolymerization of MMA and MA

$$PMMA\cdot \ + \ [Co(II)] \ \xrightarrow{k_{tr,MMA}} \ PMMA \ + \ [Co(III)]-H$$

$$[Co(III)]-H \ + \ MMA \ \xrightarrow{k_{rein,MMA}} \ PMMA_1\cdot \ + \ [Co(II)]$$

$$[Co(III)]-H \ + \ MA \ \xrightarrow{k_{rein,MA}} \ [Co(III)]-PMA_1$$

$$PMA\cdot \ + \ [Co(II)] \ \underset{k_{dis}}{\overset{k_{com}}{\rightleftarrows}} \ [Co(III)]-PMA$$

PMMA• and PMA• are MMA and MA ended copolymeric radicals, respectively. $PMMA_1•$ is a polymeric MMA radical of chain-length 1. Here $k_{tr,MMA}$ is the chain transfer rate constant of the cobalt species in the MMA homopolymerization. PMA• can combine with the cobalt species to a cobalt end-capped polymer, [Co(III)]-PMA. The rate constants for combination to and dissociation of [Co(III)]-PMA are k_{com} and k_{dis}, respectively. The rate constants k_{tr}, k_{com} and k_{dis} are assumed to be independent of chain-length. The cobalt hydride formed in the chain transfer step can reinitiate either MMA resulting in a new growing chain or MA resulting in an organocobalt(III) adduct. The reinitiation constants $k_{rein,MA}$ and $k_{rein,MMA}$ are assumed to be equal. Transfer from MA ended radicals to the cobalt complex can be neglected with respect to transfer from MMA ended radicals as was shown in Chapter 5.

In the model shown in Scheme 6.1. part of the initially added cobalt(II) will be present as organocobalt(III) species, which are inactive towards chain transfer. Equation (2.1) can then be rewritten as

$$\frac{1}{P_n} = \frac{1}{P_{n0}} + <C_T> f_{Co} \frac{[Co(II)]_o}{[M]} \tag{6.1}$$

in which f_{Co} is the fraction of cobalt species present as Co(II), $<C_T>$ is the average chain transfer coefficient for copolymerization[2] and $[Co(II)]_o$ is the initial concentration of Co(II). This results in an expression for the experimentally accessible chain transfer coefficient $<C_T>$'

$$<C_T>' = <C_T> f_{Co} = \frac{<k_{tr}>}{<k_p>} f_{Co} \tag{6.2}$$

in which $<k_{tr}>$ is the average chain transfer rate constant and $<k_p>$ is the average propagation rate constant. In order to be able to predict the apparent chain transfer coefficients at different fractions of monomer in the reaction mixture, we need to express $<k_{tr}>$, $<k_p>$ and f_{Co} as a function of the fraction of MMA in the monomer mixture, f_{MMA}, and radical or more preferably initiator concentration.

6.3.2 Expressions for $<k_{tr}>$ and $<k_p>$

Assuming there is no transfer from MA-ended radicals $<k_{tr}>$ can be written as[5]

$$< k_{tr} >= \Phi_{MMA} k_{tr,MMA} \tag{6.3}$$

In this equation Φ_{MMA} is the fraction of MMA-ended polymeric radicals. Both Φ_{MMA} and $<k_p>$ can be calculated using known copolymerization equations and are expressed as[21,22]

$$\Phi_{MMA} = \frac{\bar{k}_{pMAMA} r_{MMA} f_{MMA}}{\bar{k}_{pMMAMMA} r_{MA} f_{MA} + \bar{k}_{pMAMA} r_{MMA} f_{MMA}} \tag{6.4}$$

$$< k_p >= \frac{r_{MMA} f_{MMA}^2 + 2 f_{MMA} f_{MA} + r_{MA} f_{MA}^2}{\dfrac{r_{MMA} f_{MMA}}{\bar{k}_{pMMAMMA}} + \dfrac{r_{MA} f_{MA}}{\bar{k}_{pMAMA}}} \tag{6.5}$$

$$\bar{k}_{pMMAMMA} = \frac{k_{pMMAMMAMMA} (r_{MMA} f_{MMA} + f_{MA})}{r_{MMA} f_{MMA} + \dfrac{f_{MA}}{s_{MMA}}} \tag{6.6}$$

in which $k_{pMAMAMA}$ and $k_{pMMAMMAMMA}$ are the respective homopropagation rate constants and r_{MA}, r_{MMA}, s_{MA}, s_{MMA} the implicit penultimate unit model reactivity ratios. For both monomer systems, MMA – MA and MMA – BA, $<k_p>$ and Φ_{MMA} are calculated as a function of monomer feed composition and shown in Figures 6.1 and 6.2, respectively. The homopropagation rate constants and reactivity ratios used in eqs 6.4 to 6.6 are collected in Table 6.1. For both systems the trends in $<k_p>$ and Φ_{MMA} are similar. Especially at low fractions of MMA, below 0.1, both $<k_p>$ and Φ_{MMA} change very rapidly. The fact that above $f_{MMA} = 0.1$ more than 90 % of the growing polymer chains have an MMA-end unit, is expected to be beneficial to catalytic chain transfer.

Table 6.1 Homopropagation rate constants and reactivity ratios for the monomer pairs MMA – MA[a] and MMA – BA at 60°C.

	MMA	MA	Ref.	MMA	BA	Ref.
k_p (L· mol^{-1}· s^{-1})	833	24000	23	833	33700	23
r	2.49	0.26	24	2.28	0.395	19
s	1.98	0.43	25	1.98	0.43	25

[a] No values for monomer reactivity ratios for the system MMA-MA, s_{MA} and s_{MMA}, are available. These were assumed to equal those for MMA-BA.
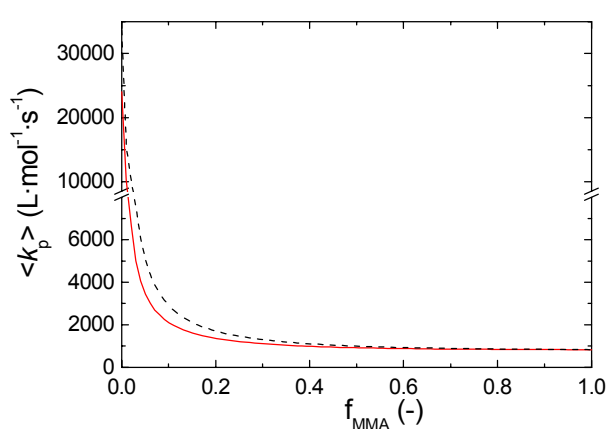

Figure 6.1 Dependence of the average propagation rate constant on the fraction of MMA in the reaction mixture for both MMA – MA (————) and MMA – BA (– – – –) at 60 ^{o}C calculated according to the implicit penultimate unit model using the data in Table 6.1.
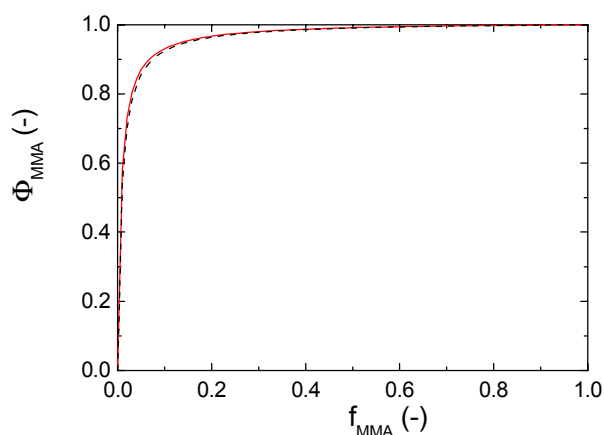
Figure 6.2 Dependence of the fraction of MMA-ended polymeric radicals on the fraction of MMA in the reaction mixture for both MMA – MA (————) and MMA – BA (– – – –) at 60 ^{o}C calculated according to the implicit penultimate unit model using the data in Table 6.1.

6.3.3 Expression for f_{Co}

Now we have found expressions for $<k_{tr}>$ and $<k_p>$, we only need to obtain an expression for f_{Co} to be able to predict $<C_T>$ as a function of f_{MMA}. As stated before f_{Co} is defined as

$$f_{Co} = \frac{[Co(II)]}{[[Co(III)] - PMA] + [Co(II)]} \qquad (6.7)$$

For MA it was shown in Chapter 5, that first cobalt – carbon bond formation takes place, after which the polymerization sets in. Therefore, it seems valid to assume a steady-state concentration of organocobalt(III) species from which a relation between [Co(II)] and [[Co(III)]-PMA] can be derived according to

$$\frac{d[[Co(III)] - PMA]}{dt} = k_{com}[Co(II)][PMA\bullet]$$
$$+ f_{MA} k_{tr,MMA}[Co(II)][PMMA\bullet] - k_{dis}[[Co(III)] - PMA] = 0 \qquad (6.8)$$

In the second term on the right hand side transfer to Co(II) and subsequent reinitiation of MA are combined. This can be explained as follows. As reinitiation constants for MA and MMA are assumed to be equal, the fraction of MA in the mixture equals the fraction of cobalt hydride that reinitiates MA. The rate of transfer equals the sum of the rates of reinitiation of MA and MMA. From eqs 6.7 and 6.8 the following can be derived

$$f_{Co} = \frac{1}{1 + \dfrac{k_{com}}{k_{dis}}[PMA\bullet] + f_{MA}\dfrac{k_{tr}}{k_{dis}}[PMMA\bullet]} \qquad (6.9)$$

When K_{cd} is the equilibrium constant for the combination to and dissociation of [Co(III)]-PMA and [P$\bullet$] is the total radical concentration, eq 6.9 can be rewritten into

$$f_{Co} = \frac{1}{1 + K_{cd}[P\bullet](1 - \Phi_{MMA} + \dfrac{k_{tr}}{k_{com}} f_{MA}\Phi_{MMA})} \qquad (6.10)$$

So according to the model, f_{Co} and therefore $<C_T>'$ are dependent on the total radical concentration and thus on initiator concentration. In Figure 6.3 f_{Co} is shown as a function of the fraction of MMA in the feed for different values of $K_{cd}[P\bullet]$. The parameters used for the calculation of Φ_{MMA} are presented in Table 6.1. The order of magnitude of the estimates for $K_{cd}[P\bullet]$ is based on a value of 2.4×10^9 L· mol^{-1} for a similar equilibrium between PMA$\bullet$ and tetramesitylporphyrinatocobalt(II) at 50 ^{o}C[14] and a radical concentration range of 10^{-7} to 10^{-9} mol· L^{-1}. Both transfer and combination are fast second order reactions with rate constants in the order 10^7 to 10^9 L· mol^{-1}· s^{-1}, but transfer is expected to be at most as fast as combination, so values for k_{tr}/k_{com} smaller than or equal to 1 are applied. As only one value for $K_{cd}[P\bullet]$ is

Figure 6.3 Fraction of cobalt(II) available for transfer as a function of the fraction of MMA in the reaction mixture calculated from eq 6.10. $k_{tr}/k_{com} = 1$. $K_{cd}[P\bullet] = 1$ (solid line); 10 (dashed line); 100 (dotted line)
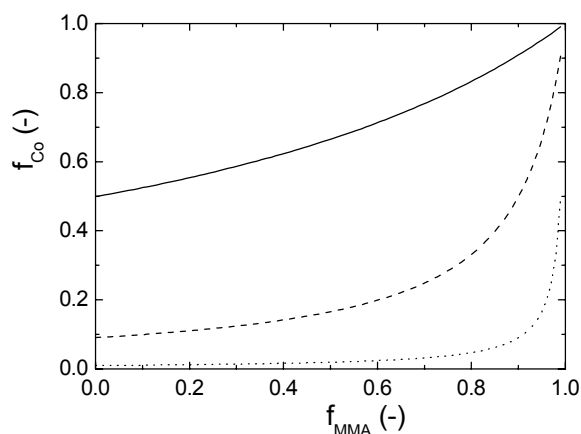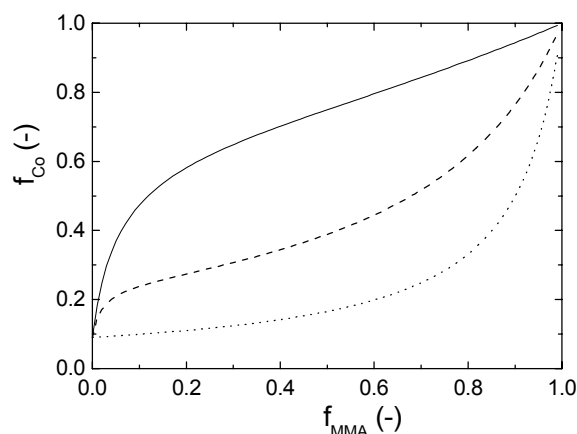
Figure 6.4 Fraction of cobalt(II) available for transfer as a function of the fraction of MMA in the reaction mixture calculated from eq 6.10. $K_{cd}[P\bullet] = 10$. $k_{tr}/k_{com} = 1$ (dotted line); 0.3 (dashed line); 0.05 (solid line).

taken for the whole composition range, this means that $[P\bullet]$ is assumed to be constant. Kowollik[26] showed that at 40 ^{o}C and 1000 bar for the system MMA – BA $<k_t>$ hardly changes with composition. For MMA – MA, $k_{t,MA}$ is only four times larger than $k_{t,MMA}$.

As Figures 6.3 and 6.4 clearly demonstrate both sets of parameters $K_{cd}[P\bullet]$ and k_{tr}/k_{com} have a large influence on f_{Co}. The first set can of course be changed most easily, by varying initiator type, initiator concentration or temperature. It can be seen that an increase in radical concentration results in a decrease in the fraction of free Co(II), which corresponds to a shift towards the covalently bonded cobalt in the equilibrium in Scheme 3.1. An increase in the transfer rate constant with respect to the combination rate constant also results in a decrease in f_{Co}. This may seem strange at first, but it can be explained from the fact that enhanced transfer will lead to enhanced reinitiation of, not only MMA, but also MA resulting in the formation of [Co(III)]-PMA.

In the following sections the model presented here will be used to study several aspects of methacrylate – acrylate copolymerizations in the presence of a catalytic chain transfer agent.

6.4 Inhibition in the copolymerization of MA and MMA with CoBF

The conversion – time histories for the MA – MMA copolymerizations in the presence of CoBF are shown in Figure 6.5. For the copolymerization, inhibition times increase with increasing [CoBF]/[AIBN] ratio. However, inhibition times are shorter as compared with the homopolymerization of MA, for which the results were presented in Section 5.4. This means that a smaller fraction of CoBF is covalently bound to MA-ended radicals as compared with the MA homopolymerization. This is in agreement with the model calculations for f_{Co} shown in Figure 6.3. Besides, it can be seen that the polymerization rate increases during the first percent of conversion, which means that during this stage f_{Co} will still be above the steady state value resulting in a higher chain transfer activity in the very first beginning of the reaction. This means that for a proper determination of chain transfer coefficients conversion must not be too low. In addition, it is observed that polymerization rates decrease with increasing ratio of CoBF and AIBN concentration. As both the initiator concentrations and initial f_{MMA} for all polymerizations are equal, this effect must have its origin in a change in $<k_t>$ with chain-length. From first order kinetic plots it can be calculated that the radical concentration decreases by a factor of 3 going from the left curve to the right curve in Figure
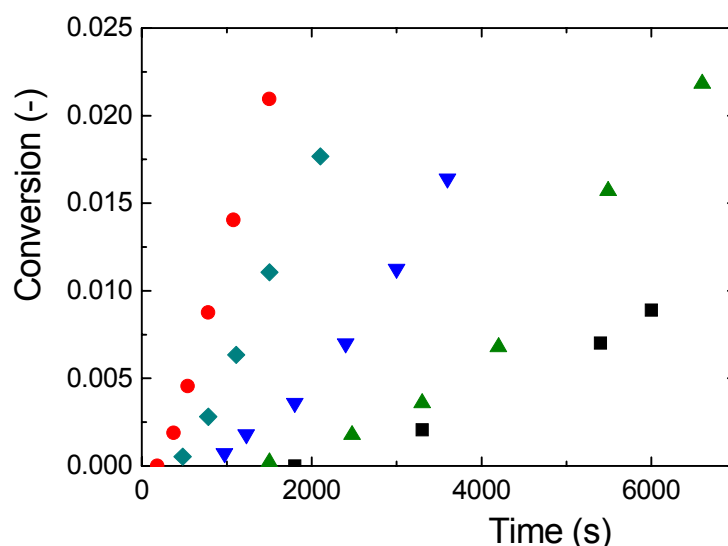

Figure 6.5 Determination of inhibition time in the CCT copolymerization of MA and MMA at 60 °C and initial f_{MMA} = 0.46. [CoBF]/[AIBN]: ● = 0; ◆ = 0.0080; ▼ = 0.020; ▲ = 0.048: ■ = 0.10

6.5, which corresponds to a factor of 9 decrease in $<k_t>$. For all polymerizations M_w was determined by SEC. In these experiments M_w changes from 1.0×10^6 for the polymerisation without CoBF to 5.0×10^3 g· mol^{-1} for the polymerisation with most CoBF. This change in M_w can explain the observed change in $<k_t>$. From eq 6.10 it is clear that the fraction of Co(II) and therewith $<C_T>$ depends on radical concentration. So for any variation in reaction conditions that, according to the model, should result in a change in molecular weight, the change in molecular weight will also affect $<k_t>$. The corresponding change in radical concentration, will enhance the effect of the change in reaction conditions on molecular weight.

6.5 CCT in MA – MMA and BA – MMA copolymerizations

In order to check the validity of the model presented in Section 6.3 for both systems, MMA – MA and MMA – BA, the CCT behaviour was investigated. Chain transfer coefficients were determined at several initial fractions of MMA in the reaction mixture and at various initiator concentrations. The results are shown in Figures 6.6 and 6.7 for the monomer pairs MMA – MA and MMA – BA, respectively. It can be seen that $<C_T>$' increases with both increasing f_{MMA} and decreasing initiator concentration. Although $<C_T>$' is in between 150 and 25000, which is lower than for the MMA homopolymerization, it is still substantially higher than for conventional chain transfer agents. Especially, at higher mole percentages of MMA the results are very good and industrial application seems promising. Furthermore, for MMA – BA apparent catalyst activity is somewhat higher than for MMA – MA.

The model predictions were calculated using equations 6.2 and 6.10 and the parameters in Table 6.1. Good agreement between experimental data and model calculations is obtained with the values for $K_{cd}[P\bullet]$ and k_{tr}/k_{com} shown in Table 6.2 for an initiator concentration, [I], of 6×10^{-3} mol· L^{-1}. For experiments at different initiator concentrations $K_{cd}[P\bullet]$ was adjusted with a factor of $[I]^{\frac{1}{2}}$. When considered separately, the parameters for both systems do not seem to be physically unrealistic. However, it is unlikely that in changing from BA to MA the combination rate constant decreases three orders of magnitude. The values for $K_{cd}[P\bullet]$ differ less than one order of magnitude, which is not in agreement with the large difference in k_{com}

Figure 6.6 Chain transfer coefficients for the CCT copolymerization of MMA and MA in bulk at 60 °C at different [AIBN]. Symbols and lines represent experimental data and model predictions, respectively. ▲, dotted line: 6×10^{-4} mol· L^{-1}; ■, dashed line: 6×10^{-3} mol· L^{-1}; ●, solid line: 6×10^{-2} mol· L^{-1}. The lines were calculated using eqs 6.2 and 6.10 and the constants in Table 6.2.
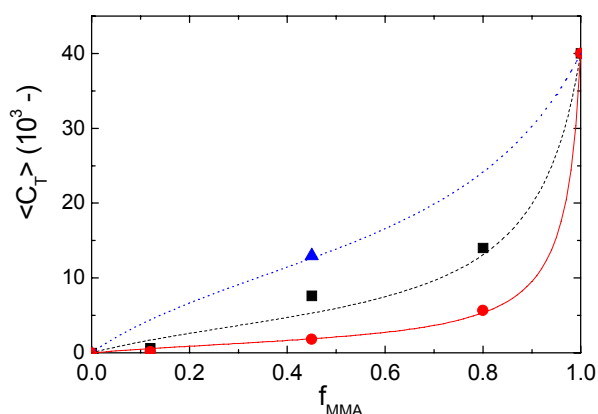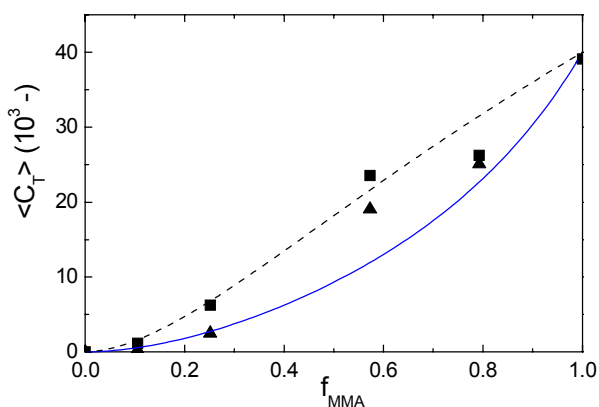
Figure 6.7 Chain transfer coefficients for the CCT copolymerization of MMA and BA in bulk at 60 °C at different [AIBMe]. Symbols and lines represent experimental data and model predictions, respectively. ■, dashed line: 6×10^{-4} mol· L^{-1}; ▲, solid line: 6×10^{-3} mol· L^{-1}. The lines were calculated using eqs 6.2 and 6.10 and the constants in Table 6.2.

found in the first parameter set. Probably the actual values for k_{tr}/k_{com} for both systems will be closer to each other and in between 0.001 and 1, but in order to obtain more accurate estimates a more extensive dataset is required. On the other hand, it is also possible to try and refine the model, but it is believed that the most important parameters have been incorporated at this point and that refining the model without independent determination of the corresponding rate constants will only lead to the introduction of more fitting parameters, whose values may lack physical meaning.

Table 6.2 Parameters used to obtain good agreement between the model and the experimental data from the CCT copolymerizations of MMA – MA and MMA – BA.

Monomer system	k_{tr} / k_{com} (-)	$K_{cd}[P\bullet]$ (-)
MMA – MA	1	10
MMA – BA	1×10^{-3}	80

Despite the apparent disagreement when both systems are compared, within each system it is well possible to give reasonable predictions of the effect of initiator concentration. Adjusting $K_{cd}[P\bullet]$ with a factor of $[I]^{\frac{1}{2}}$ results in good agreement going from one initiator concentration to the other, indicating the importance of the Co(II) – polyacrylate radical combination – dissociation equilibrium.

Two important conclusions can be drawn from these results. First, it has been demonstrated that CoBF is a very active catalytic chain transfer agent in the copolymerization of MMA and acrylates, which broadens the range of possible applications. Second, the experimental data and the model predictions show the same trends, both when changing monomer feed composition and initiator concentration. The model correctly predicts an increase in $<C_T>'$ with decreasing initiator concentration and an increase in $<C_T>'$ with increasing MMA content.

6.6 Effect of CCT on reactivity ratios

6.6.1 Introduction

Haddleton *et al.*[7] determined reactivity ratios for MMA – *n*-butyl methacrylate (BMA) for six different polymerization mechanisms, varying from anionic to various radical type polymerizations. The different reactivity ratios that were found are indicative of differences in the mechanism. Chambard[27] recently showed that for ATRP and conventional free-radical polymerization variations in observed reactivity ratios do not necessarily reflect differences in intrinsic reactivities. In ATRP copolymerizations monomer consumption in the beginning of the reaction, when the activation – deactivation equilibria for both radical species have not yet been reached, may deviate from what is expected in conventional free-radical polymerization. This can affect monomer consumption over the whole conversion range and therefore the observed reactivity ratios.

In CCT copolymerizations, in which at least one of the monomer ended polymeric radicals can form a covalent bond to the cobalt species, similar effects may be observable. However, as the catalyst concentrations are generally low, the equilibrium sets in at very low

conversions. When the target molecular weight is low, *e.g.* below 1000 g· mol^{-1} and therefore higher concentrations of Co(II) are required, PMA – [Co(III)] formation may start to affect radical concentration ratios and therefore apparent reactivity ratios.

As stated by other authors[6,7] another reason for deviations in observed reactivity ratios may be that the long chain assumption[28] required in the derivation of the copolymer composition equation is no longer valid. This can be caused by *e.g.* a chain-length dependence of k_p, which has been reported by several authors.[29,30] A second reason can be that the ratio of addition rate constants for MMA and BA to an MMA-ended polymeric radical differs from the ratio of reinitiation rate constants of MMA and BA by cobalt hydride. In that case each chain transfer step will result in a deviation from the monomer consumption that would be observed in absence of chain transfer agent. Especially at lower chain lengths this can contribute to deviations in the apparent reactivity ratios as well. In addition, the ratio of reinitiation rate constants can influence the apparent chain transfer coefficients, but this will not be dealt with here.

6.6.2 Computer simulations on possible effects

Computer simulations using Predici software were performed to gain more insight into the influence of the ratio of reinitiation rate constants on copolymer composition. A bulk copolymerization with equal mole fractions of MMA and BA with an initiator concentration of 6×10^{-3} mol· L^{-1} was monitored over 5000 s. For simplicity the terminal model for copolymerization was applied. Reaction rate constants can be found in Tables 2.2 and 6.1. In addition the following rate constants were assumed $k_{com} = 3.3 \times 10^8$ L· mol^{-1}· s^{-1} and $k_{dis} = 0.1$ s^{-1} which fall in the range obtained from the experiments described in the previous section.

In Figure 6.8 the effect of initial concentration of Co(II)-species on F_{MMA} is shown for equal reinitiation rate constants. The curves for 0 and 1×10^{-6} mol· L^{-1} of CoBF overlap, whereas at 1×10^{-4} mol· L^{-1} a significant deviation is observed. In Figure 6.9 the effect of different ratios of reinitiation rate constants is shown for [CoBF] = 1×10^{-4} mol· L^{-1}. The ratio of $k_{rein,MMA}$ and $k_{rein,MA}$ was varied from 0.01 to 100. Copolymer compositions differ by more than 10 percent. For the dashed curve this ratio was set equal to r_{MMA}. This curve is also shown in Figure 6.8 and completely overlaps with the curves where no effect on Co(II) concentration is
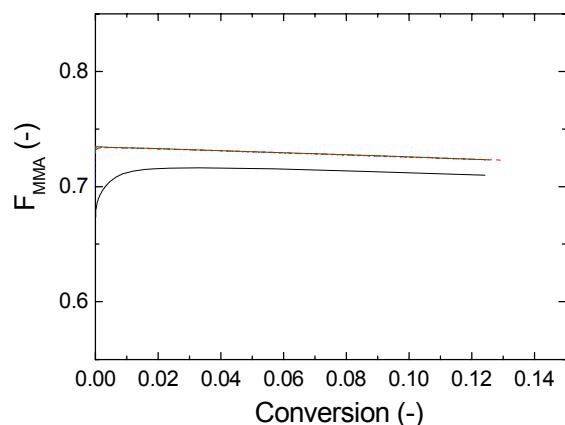
Figure 6.8 Effect of cobalt concentration on copolymer composition in the CCT copolymerization of MMA and BA according to Predici computer simulations. Reaction time is 5000 s. $k_{rein,MMA}/k_{rein,MA}$ =1. [CoBF] = 10^{-4} (solid line); 10^{-6} (dotted line); 0 mol· L^{-1}(dashed line). (The dotted and dashed curves overlap.)

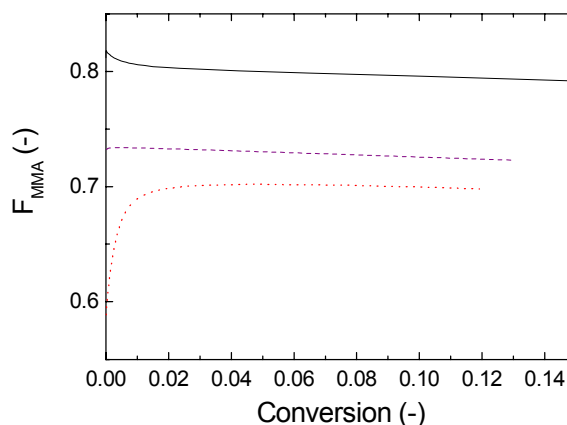**Figure 6.9** Effect of $k_{rein,MMA}/k_{rein,MA}$ on copolymer composition in the CCT copolymerization of MMA and BA according to Predici computer simulations. Reaction time is 5000 s. [CoBF] = 10^{-4} mol· L^{-1}. $k_{rein,MMA}/k_{rein,MA}$ = 100 (solid line); 2.28 (dashed line); 0.01 (dotted line).

observed. So it is demonstrated clearly that, when the ratio of reinitiation rate constants deviates from the reactivity ratio, a large effect on copolymer composition may be observed.

6.6.3 Determination of MMA – BA reactivity ratios

In order to study the effect of CCT on reactivity ratios, three sets of eight copolymerizations of MMA and BA were conducted at cobalt concentrations of 0, 1×10^{-6} and 1×10^{-5} mol· L^{-1}, respectively. The monomer system MMA – BA was preferred over MMA – MA, as the determination of copolymer composition for MMA – BA is more straightforward and accurate. This is due to the fact that in a ^{1}H-NMR spectrum of a MMA – BA copolymer the –O-CH$_3$ and –O-CH$_2$- peaks are well separated[19] in contrast to the corresponding peaks in a MMA – MA copolymer.[31] The fractions of monomer in the reaction mixture for optimal determination of the reactivity ratios were determined using the Tidwell and Mortimer criterion.[32] Initial estimates for the reactivity ratios were taken from Aerdts *et al.*[19] The copolymer compositions for all experiments are shown in Table 6.3. Conversions were around 3,5 %.

Table 6.3 Experimental copolymer compositions for the determination of reactivity ratios for different [CoBF].

[CoBF] = 0 mol·L^{-1}		[CoBF] = 1 × 10^{-6} mol·L^{-1}		[CoBF] = 1 × 10^{-5} mol·L^{-1}	
f_{MMA}	F_{MMA}	f_{MMA}	F_{MMA}	f_{MMA}	F_{MMA}
0.467	0.679	0.466	0.672	*0.468*	*0.627*
0.468	0.675	0.467	0.671	0.467	0.671
0.467	0.676	0.467	0.674	0.467	0.656
0.466	0.665	0.468	0.678	0.467	0.676
0.165	0.346	0.165	0.343	0.164	0.342
0.166	0.347	0.165	0.346	0.164	0.341
0.166	0.347	0.166	0.347	0.164	0.340
0.164	0.338	0.166	0.346	0.166	0.342

Reactivity ratios and 95 % joint confidence intervals were calculated using Contour,[33] a computer program based on a non-linear least squares fitting procedure. The results are presented in Figure 6.10. In Table 6.4 the point estimates are collected, together with data from other authors.

The reactivity ratios presented in this work are in good agreement with data collected from other authors. Although the point estimate for the highest concentration of CoBF deviates somewhat from the point estimates at lower concentrations of CoBF, the joint confidence intervals completely overlap. In addition, this deviation is mainly caused by one data-point, which is written in italics in Table 6.3. If this data-point is regarded as an outlier and not taken into account, the point estimate becomes r_{MMA} = 2.03 and r_{BA} = 0.335 which is much closer to the other point estimates. In addition, the joint confidence interval decreases in size. Therefore, it can be concluded that under the conditions employed in this study the presence of CoBF does not affect the apparent reactivity ratios in the bulk copolymerization of MMA and BA to any significant extent. Therefore, the reinitiation rate constants are expected to have the same order of magnitude. In the model to describe the dependence of $<C_T>$ on f_{MMA} it was assumed that apparent reactivity ratios did not depend on CoBF concentration. With these results it has been shown that this is indeed a valid assumption.
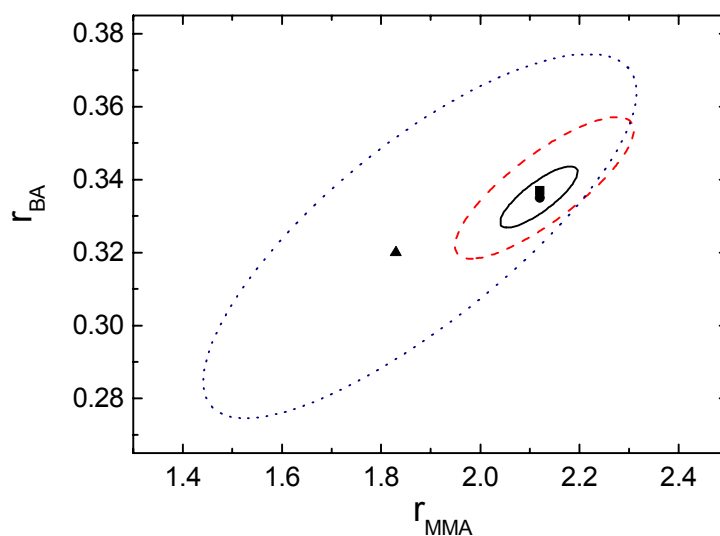
Figure 6.10 Reactivity ratios and 95 % joint confidence intervals for the copolymerization of MMA and BA in bulk at 60 $^{\circ}$C for different [CoBF]. ■, solid line: [CoBF] = 0 mol· L^{-1}; ●, dashed line: [CoBF] = 1 × 10^{-6} mol· L^{-1}; ▲, dotted line: [CoBF] = 1 × 10^{-5} mol· L^{-1}

Table 6.4 Collected reactivity ratios for MMA – BA.

r_{MMA} (-)	r_{BA} (-)	Temperature ($^{\circ}$C)	References / Remarks
2.12	0.337	60	this work, [CoBF] = 0 mol· L^{-1}
2.12	0.335	60	this work, [CoBF] = 1 × 10^{-6} mol· L^{-1}
1.83	0.32	60	this work, [CoBF] = 1 × 10^{-5} mol· L^{-1}
2.28	0.395	50	Aerdts *et al.*[19]
2.56	0.47	60	Han and Wu[25]
1.98	0.355	60	Dubé *et al.*[34]
2.51	0.357	50	Hutchinson *et al.*[25]

6.7 Effect of conversion on CCT copolymerization of MMA and BA

6.7.1 Introduction

When a CCT copolymerization of MMA and BA is performed up to high conversion, several additional aspects can play a role. First of all, like in most copolymerizations, composition drift is likely to occur. In Figure 6.11 the *F-f* curve is shown for MMA – BA, which is calculated using eq 6.11.

$$F_{\text{MMA}} = \frac{r_{\text{MMA}} f_{\text{MMA}}^2 + f_{\text{MMA}} f_{BA}}{r_{\text{MMA}} f_{\text{MMA}}^2 + 2 f_{\text{MMA}} f_{BA} + r_{BA} f_{BA}^2} \tag{6.11}$$

It is clear that for all compositions MMA is the more reactive monomer. For a reaction starting at 50 % MMA in the reaction mixture the instantaneous copolymer composition will be around 70 %. The fraction of MMA in the reaction mixture will continue to decrease until all MMA is consumed and only BA is left. It is not hard to imagine that this will drastically affect the catalytic chain transfer reactions. Another aspect that may play a role is the
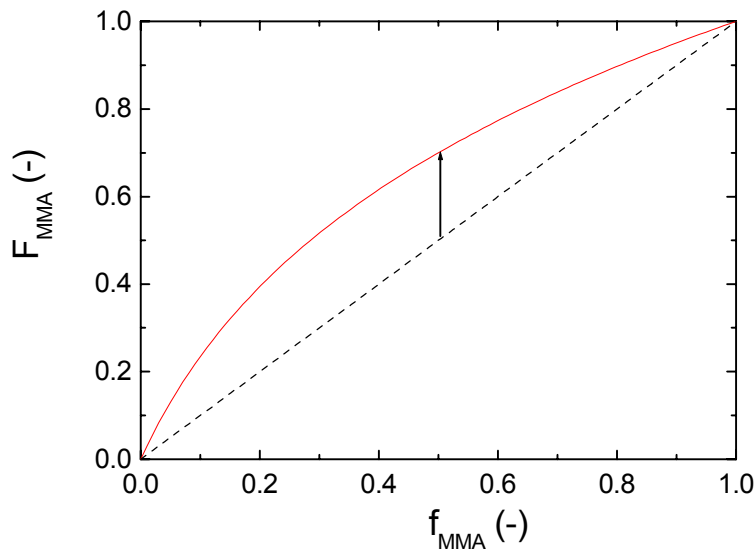

Figure 6.11 Dependence of instantaneous copolymer composition on the fractions of both monomers in the reaction mixture for the system MMA – BA calculated from the Mayo-Lewis equation according to the implicit penultimate unit model using reactivity ratios determined in Section 6.6.

copolymerization of MMA ended macromonomers, which has been briefly discussed in Section 2.4. Although it is known that these macromonomers do not copolymerize with MMA,[35,36,37] copolymerization with ethyl acrylate does occur.[35,38] Therefore, copolymerization with BA is expected to occur as well. Finally, cobalt(II) catalyst deactivation, as discussed in Chapter 4 for the CCT homopolymerization of MMA, is likely to occur in the copolymerization as well.

6.7.2 General aspects of high conversion CCT copolymerization

Two high conversion CCT copolymerizations of MMA and BA were performed to investigate which of the above effects are of importance. The experimental conditions for both experiments have been collected in Table 6.5. The copolymerizations were run in 70 w% toluene to prevent an excessive viscosity increase.

Table 6.5 Reaction conditions for high conversion CCT solution copolymerizations of MMA and BA in toluene.

	Experiment I	Experiment II
w% toluene (%)	70	70
initial f_{MMA} (-)	0.500	0.500
temperature (^{o}C)	60	60
[CoBF] (mol· L^{-1})	1.0×10^{-4}	1.0×10^{-4}
[AIBN] (mol· L^{-1})	6.0×10^{-3}	3.0×10^{-2}
Total reaction time (hrs)	96	48

The evolution of the molecular weight distributions (MWD) with conversion is presented in Figures 6.12 a and b for experiment I and II, respectively. In Figures 6.13 a and b partial and total conversions are shown. The number of polymer chains and f_{MMA} versus total conversion can be found in 6.14 a and b.
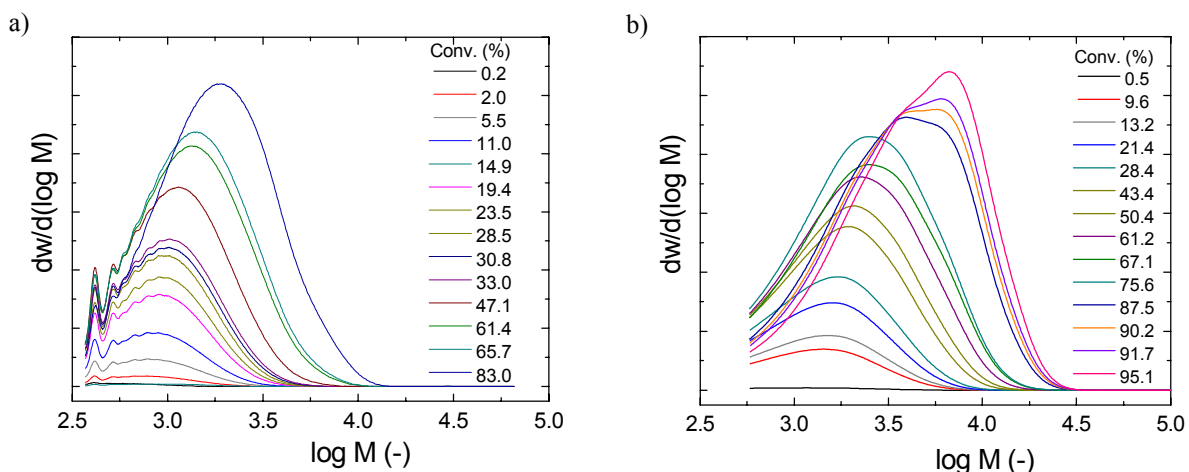
a)

b)

Figure 6.12 Evolution of MWDs with conversion for the CCT copolymerization of MMA and BA in toluene at 60 ^{o}C. a) [AIBN] = 6×10^{-3} mol· L^{-1}; b) [AIBN] = 3×10^{-2} mol· L^{-1}.
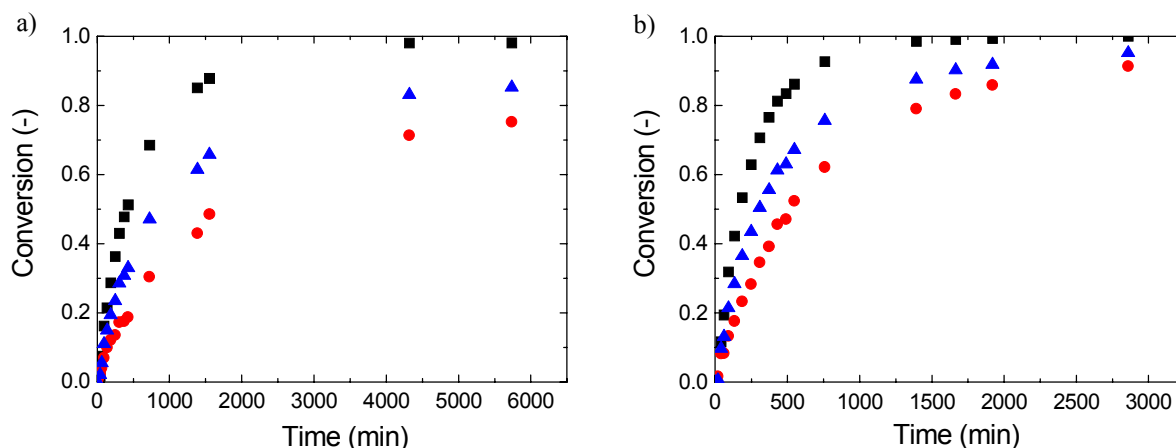
a)

b)

Figure 6.13 Partial conversions for MMA (■) and BA (●) and total conversion (▲) as determined from GC measurements for the CCT copolymerization of MMA and BA in toluene at 60 ^{o}C. a) [AIBN] = 6×10^{-3} mol· L^{-1}; b) [AIBN] = 3×10^{-2} mol· L^{-1}.

First of all, some straightforward observations are given. From Figures 6.13 a and b it is clear that the rate of polymerization for experiment II is higher than for experiment I, as is expected from initiator concentrations. Final conversions reach 85 % and 95 % for experiments I and II, respectively. As was predicted in Figure 6.11 strong composition drift occurs as MMA is consumed at higher rates than BA. This leads to a steady decrease in the fraction of MMA with total conversion, which is presented in Figures 6.14. Near the end of the reaction practically all MMA has been consumed.

Each MWD in Figures 6.12 a and b corresponds to a data point in Figures 6.13 a and b. Initially, for both copolymerizations a gradual shift to higher molecular weights occurs. This
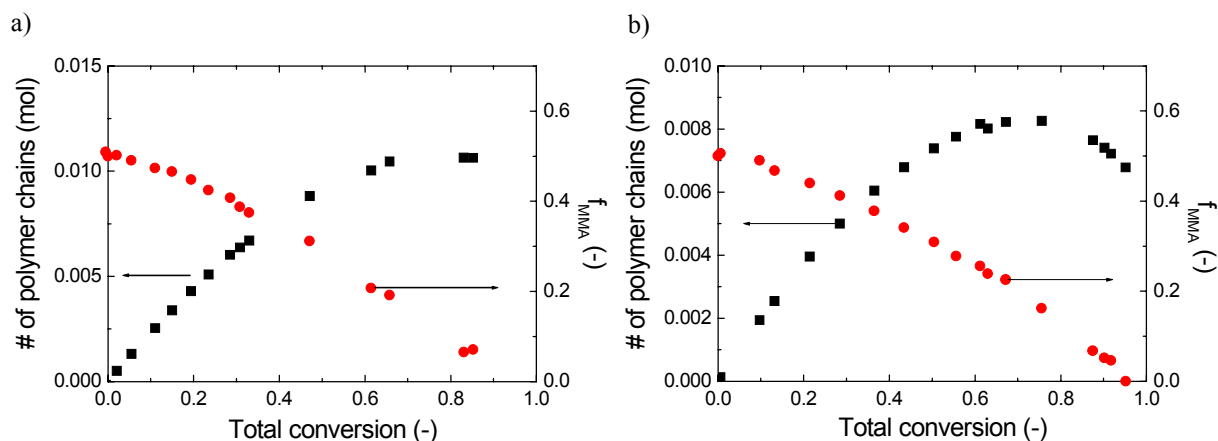
Figure 6.14 The number of polymer chains (■) and the fraction of MMA with respect to total monomer content (●) as a function of overall conversion for the CCT copolymerization of MMA and BA in toluene at 60 °C. a) [AIBN] = 6×10^{-3} mol· L^{-1}; b) [AIBN] = 3×10^{-2} mol· L^{-1}.

can be explained when it is realized that a lower f_{MMA} results in a lower apparent C_T and therefore an increase in molecular weight. The effect of composition drift on $<k_p>$ is incorporated in $<C_T>$'. In addition, cobalt(II) deactivation may take place, as discussed in Chapter 4. The differences in molecular weight between both experiments stem from the difference in initiator concentration. As is demonstrated in Figure 6.7, an increase in initiator concentration results in a decrease in $<C_T>$'.

6.7.3 Macromer incorporation

A more striking feature is that, for both copolymerizations, at approximately 98 % conversion of MMA, low molecular weight material starts to disappear and relatively higher molecular weight material is formed. This can also be observed from the total number of polymer chains present, that can be calculated from M_n^* and conversion data and which is shown in Figures 6.14 a and b. It is demonstrated that at high conversions the number of chains decreases. This can only mean that incorporation of macromonomers in the growing polymer chain occurs, as was also reported for MMA-homomacromer – ethyl acrylate copolymerization.[35,38] Although it is obvious that macromer copolymerization takes place at high conversions, it is expected to occur right from the start of the polymerization as well.

---

* It is realized that M_n for heterogeneous copolymers cannot be determined accurately from SEC-data and that this will affect the calculations of the number of chains. However, it is believed that the curves reflect correct trends.

Scheme 6.2 Chain transfer to macromer
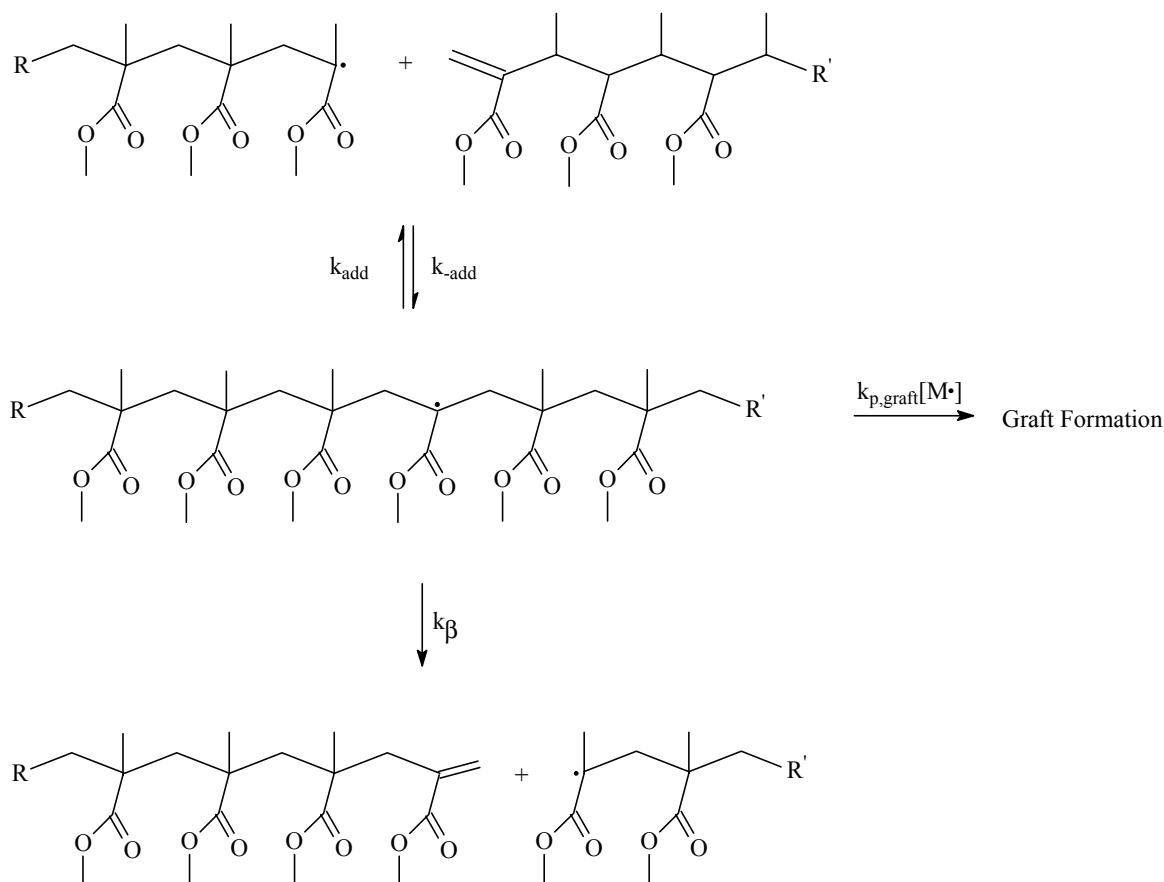
Moad *et al.*[39] studied the chain transfer activity of MMA macromers and reported that the chain transfer constant depends on the partitioning of the radical resulting from macromer addition over reverse addition and β-scission as expressed in

$$k_{tr} = k_{add} \frac{k_\beta}{k_{-add} + k_\beta}$$

(6.12)

This process is presented in Scheme 6.2. For completeness also propagation of the intermediate radical is shown. In the CCT copolymerization of MMA and BA some complexity is added to the model in Scheme 6.2. In this copolymerization four distinct intermediate radicals, shown in Scheme 6.3, play a role. As noted earlier, propagation of the intermediate radical with MMA has not been observed. However, propagation of all radicals

Scheme 6.3 Intermediate radicals after addition of macromer to the radical chain end in the CCT copolymerization of MMA and BA.
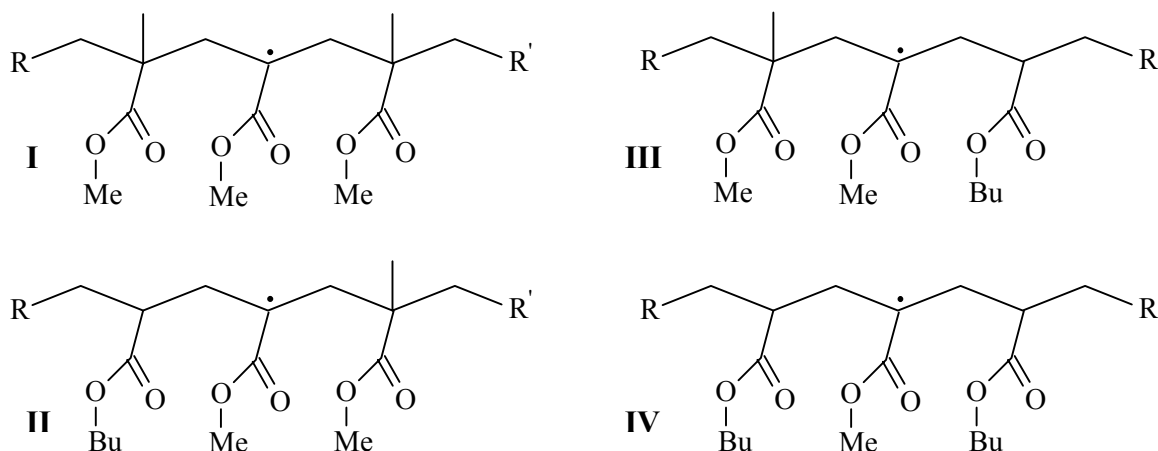
with BA seems possible[35,38] and may occur in competition with reverse addition and β-scission. When a BA-ended radical adds macromer, resulting in radical II, reverse addition will be less likely as the BA-ended radical is not expected to be a good leaving group. If the penultimate unit in the macromer is a BA unit, as in radical III and V, the rate constant for β-scission will also be reduced for the same reason as given above. When both units next to the radical are BA units (radical IV) the dominant pathway for the intermediate radical will be propagation, resulting in the formation of grafts.

In summary , the rate of graft formation will increase with conversion due to

1) an increasing macromer concentration as compared with monomer concentration,

2) an increasing ratio of BA and MMA,

3) an increasing ratio of BA and MMA ended polymeric radicals,

4) an increasing incorporation of BA in macromers, resulting in more BA penultimate units.

Moad *et al.*[39] also showed that in the MMA − MMA macromer copolymerization no retardation occurs. However, the calculated radical concentrations[*] in the experiments presented in Figure 6.15 decrease more rapidly than could be expected from regular initiator

---

[*] Radical concentrations were calculated according to $[P\bullet] = \dfrac{1}{<k_p>}\dfrac{d(-\ln(1-X))}{dt}$

consumption. An increase in $<k_t>$ is unlikely to be the reason , as both molecular weight and conversion increase. Furthermore, changes in f_{MMA} have been taken into account in the calculation of $<k_p>$. An explanation may be found in the formation of less reactive intermediate radicals, resulting from macromer addition. Especially the radical IV, presented in Scheme 6.3, may have reduced reactivity. Tanaka *et al.*[40] actually observed similar radicals by ESR spectroscopy. When these less reactive radicals are present to a significant extent, $<k_p>$ will be overestimated giving an underestimation of the radical concentration. In that case the experimentally determined radical concentrations are apparent concentrations. So macromer incorporation may also explain reduced polymerization rates.
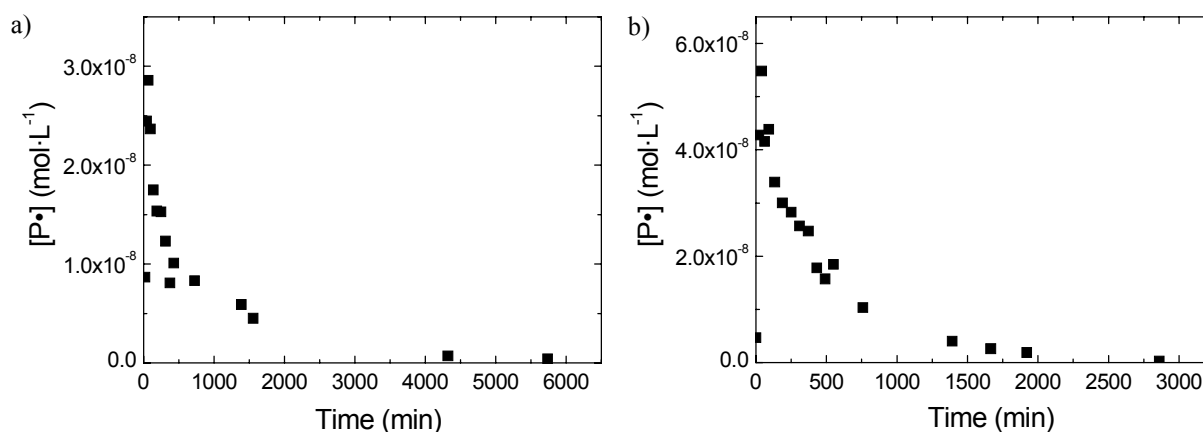
Figure 6.15 The evolution of radical concentration calculated from the derivative of the first order kinetic plot and the copolymerization propagation rate constant for the CCT copolymerization of MMA and BA in toluene at 60 ^{o}C. a) [AIBN] = 6 × 10^{-3} mol· L^{-1}; b) [AIBN] = 3 × 10^{-2} mol· L^{-1}.

6.7.4 Summary

In short, it can be said that high conversion CCT copolymerization of MMA and BA can be used to prepare low molecular weight copolymers. At high conversions of MMA significant macromer incorporation occurs, but molecular weights remain relatively low. It will probably depend on the type of application whether this graft formation is considered to be an advantage or disadvantage. All observations can be explained qualitatively using a combination of copolymerization kinetics, the CCT copolymerization model and macromer chemistry.

6.8 Conclusions

In this work it was shown that CoBF is a very active catalytic chain transfer agent in the copolymerization of MMA and MA as well as BA. The chain transfer coefficient appears to be dependent on monomer feed composition and on initiator concentration. In some cases an inhibition period is observed. A model, combining features of both catalytic chain transfer polymerization of methacrylates and cobalt-mediated controlled radical polymerization, was developed which can describe these effects. The model predicts that part of the CoBF is covalently bonded to acrylate-ended polymeric radicals and that therefore the apparent chain transfer coefficient is lowered as compared with the chain transfer coefficient for MMA homopolymerizations.

Furthermore, it has been shown that the presence of a catalytic chain transfer agent does not affect the observed reactivity ratios in the investigated CoBF concentration range. Finally, it was demonstrated that at high conversion incorporation of previously formed macromers in the growing polymer chain occurs to a significant extent. The evolution of the MWD has been explained via a combination of copolymerization kinetics, cobalt chemistry and macromer chemistry. The understanding gained in this chapter on the various aspects of CCT copolymerizations may facilitate the production of pre-defined low molecular weight copolymers with or without grafts.

6.9 References

[1] Greuel, M.P.; Harwood, H.J. *Polym. Prepr. (Am. Chem. Soc. Div. Polym. Chem.)* **1990**, *32(1)*, 545

[2] Heuts, J.P.A; Kukulj, D.; Forster, D.J.; Davis, T.P. *Macromolecules* **1998**, *31*, 2894

[3] Suddaby, K.G.; Haddleton, D.M.; Hastings, J.J.; Richards, S.N.; O' Donnell, J.P. **1996**, *29*, 8083

[4] Heuts, J.P.A.; Coote, M.L.; Davis, T.P.; Johnston, L.P.M. In *Controlled Radical Polymerization*; Matyjaszewski, K. Ed.; ACS Symposium Series, vol. 685; American Chemical Society: Washington, DC, **1998**; p.120

[5] Kukulj, D.; Heuts, J.P.A.; Davis, T.P. *Macromolecules* **1998**, *31*, 6034

[6] Suddaby, K.G.; Hunt, K.H.; Haddleton, D.M. *Macromolecules* **1996**, *29*, 8642

[7] Haddleton, D.M.; Crossman, M.C.; Hunt, K.H.; Topping, C.; Waterson, C.; Suddaby, K.G. *Macromolecules* **1997**, *30*, 3992

[8] Kukulj, D.; Davis, T.P.; Suddaby, K.G.; Haddleton, D.M.; Gilbert, R.G. *J. Pol. Sci. Pol. Chem.* **1997**, *35*, 859

[9] Bon, S.A.F.; Morsley, D.R.; Waterson, J.; Haddleton, D.M. *Macromol. Symp.* **2001**, *165*, 29

[10] Heuts, J.P.A.; Muratore, L.M.; Davis, T.P. *Macromol. Chem. Phys.* **2000**, *201*, 2780

[11] Enikolopyan, N.S.; Smirnov, B.R.; Ponomarev, G.V.; Belgovskii, I.M. *J. Pol. Sci. Pol. Chem. Ed.* **1981**, *19*, 879

[12] Roberts, G.E.; Heuts, J.P.A.; Davis, T.P. *Macromolecules* **2000**, *33*, 7765

[13] Wayland, B.B.; Poszmik, G.; Mukerjee, S.L. *J. Am. Chem. Soc.* **1994**, *116*, 7943

[14] Wayland, B.B.; Basickes, L. Mukerjee, S.; Wei, M.; Fryd, M. *Macromolecules* **1997**, *30*, 8109

[15] Arvanitopoulos, L.D.; Greuel, M.P.; King, B.M.; Shim, A.K.; Harwood, H.J. In *Controlled Radical Polymerization*; Matyjaszewski, K. Ed.; ACS Symposium Series, vol. 685; American Chemical Society: Washington, DC, **1998**; p. 316

[16] Pangborn, A.B.; Giardello, M.A.; Grubbs, R.H.; Rosen, R.K.; Timmers, F.J. *Organometallics* **1996**, *15*, 1518

[17] Bakac, A.; Espenson,, J.H. *J. Am. Chem. Soc.*, **106**, 5197 (1984)

[18] López-González, M.M.C.; Fernández-García, M.; Barrales-Rienda, J.M., Madruga, E.L.; Arias, E. *Polymer* **1993**, *34*, 3123

[19] Aerdts, A.M.; German, A.L.; van der Velden, G.P.M. *Magn. Res. Chem.* **1994**, *32*, S80

[20] Schoonbrood, H.A.S.; Pierik, S.C.J.;. van den Reijen, B; Heuts, J.P.A.; German, A.L. *Macromolecules*, **1996**, *29*, 6717

[21] Schoonbrood, H.A.S.; German, A.L.; Gilbert, R.G. *Macromolecules* **1995**, *28*, 34

[22] Fukuda, T.; Kubo, K.; Ma, Y.D. *Prog. Polym. Sci.* **1992**, *17*, 875

[23] van Herk, A.M. *Macromol. Theory Simul.* **2000**, *9*, 433

[24] Schoonbrood, H.A.S. *Emulsion Co- and Terpolymerization, Monomer Partitioning, Kinetics and Control of Microstructure and Mechanical Properties* Ph.D. Thesis, Eindhoven University of Technology, The Netherlands 1994

[25] Hutchinson, R.A.; McMinn, J.H.; Paquet Jr., D.A.; Beuermann, S.; Jackson, C. *Ind. Eng. Chem. Res.* **36**, 1103 (1997)

[26] Kowollik, C. In *'Free-Radical Bulk Copolymerization Kinetic of Acrylate and Methacrylate Monomers Studied by Pulsed Laser Techniques'* Ph.D. Thesis, Georg-August-Universität zu Göttingen, Germany, Cuvillier Verlag, **1999**

[27] Chambard, G. In *'Control of Monomer Sequence Distribution'* PhD. Thesis, Eindhoven University of Technology, The Netherlands, **2000**

[28] Mayo, F.R.; Lewis, F.M. *J. Am. Chem. Soc.* **1944**, *66*, 1594

[29] Gridnev, A.A.; Ittel, S.D *Macromolecules* **1996**, *29*, 5864

[30] Krstina, J.; Moad, G.; Willing, R.I.; Daner, S.K.; Kelly, D.P.; Jones, S.L.; Solomon, D.H. *Eur. Pol. J.* **1993**, *29*, 379

[31] Grassie, N.; Torrance, B.J.D.; Fortune, J.D.; Gemmell, J.D. *Polymer* **1965**, *6*, 653

[32] Tidwell, P.W.; Mortimer, G.A. *J. Polym. Sci. Part A* **1965**, *3*, 369

[33] van Herk, A.M. *J. Chem. Ed.* **1995**, *72*, 138

[34] Dubé, M.A.; Penlidis, A. *Polymer* **1995**, *36*, 587

[35] Cacioli, P.; Hawthorne, D.G.; Laslett, R.L.; Rizzardo, E.; Solomon, D.H. *J. Macromol. Sci.-Chem.* **1986**, *A23*, 839

[36] Krstina, J.; Moad, G.; Rizzardo, E.; Winzor, C.L.; Berge, C.T.; Fryd, M. *Macromolecules* **1995**, *28*, 5381

[37] Krstina, J. Moad, C.L.; Moad, G.; Rizzardo, E.; Berge, C.T.; Fryd, M. *Macromol. Symp.* **1996**, *111*, 13

[38] Abbey, K.J.; Carlson, G.M.; Masola, M.J.; Trumbo, D. *Polym. Mater. Sci. Eng.* **1986**, *55*, 235

[39] Moad, C.L.; Moad, G.; Rizzardo, E.; Thang, S.H. *Macromolecules* **1996**, *29*, 7717

[40] Tanaka, H.; Kawai, H.; Sato, T.; Ota, T. *J. Polym. Sci. Polym. Chem.* **1989**, *27*, 1741

Chapter 7

Catalytic chain transfer polymerization
in emulsion systems

Synopsis: In this chapter a brief outlook on the application of catalytic chain transfer in emulsion systems is presented. Three different glyoximes, *viz.* dimethyl-, diethyl-, and diphenylglyoxime are used in catalyst synthesis, resulting in cobaloximes with varying partitioning over the water phase and the organic phase. The application of these catalysts in semi-batch emulsion polymerization of methyl methacrylate (MMA) is discussed and especially the catalyst having the diethylglyoximato ligands ($Co(Et)_4BF$) appears to have well-balanced properties for application in emulsion polymerization. In addition, results on the application of CCT to the MMA – *n*-butyl acrylate (BA) copolymerization in miniemulsion are presented. Low molecular weight macromers are formed during the early stages of the polymerization, which are incorporated at higher conversions. Nevertheless, fifty-fold reductions in molecular weight are achieved compared with polymerizations without catalyst.

7.1 Introduction

The previous chapters focused on application of catalytic chain transfer agents in both bulk and solution polymerization, in other words homogeneous systems. However, many polymerization processes are carried out in heterogeneous systems, like suspensions or emulsions. Emulsion polymerization has the benefit of a good heat-exchange and generally high polymerization rates. Often the resulting dispersions can be used without separating the

polymer from the water phase. This makes emulsion polymerization an attractive process for industry.

In an emulsion polymerization three different phases can be present, a continuous aqueous phase, dispersed monomer droplets and colloidally stable latex or polymer particles.[1] Both monomer droplets and latex particles are stabilized by surfactant. Polymerization takes place in the particles, which are an order of magnitude smaller than the monomer droplets (50 – 300 nm versus 1 – 10 µm). Due to the compartmentalization of the free radicals in the polymerization loci and partitioning of monomer over the three phases, emulsion polymerization kinetics differ from homogeneous polymerization kinetics. Most importantly, molecular weight and polymerization rate can be varied independently within certain limits. When compared with homogeneous systems, many additional aspects play a role in emulsion (co)polymerization, like particle nucleation, monomer partitioning and colloidal stability. This results in rather complex kinetics.[1,2,3] It is not hard to imagine that addition of a CCT agent will affect and further complicate this process. The application of CCT in emulsion polymerization is disclosed in several patents by Janowicz[4,5] and Haddleton *et al.*[6,7,8] In a few papers, most of Haddleton *et al.*, the process is described and explained in more detail.[9,10,11,12,13] Their findings will be discussed in Section 7.4 and compared to new preliminary results.

In the second part of this chapter the application of CCT in miniemulsion will be investigated. The main difference between emulsion and miniemulsion polymerization is that in the latter, polymerization takes place in the monomer droplets, which have about the same size as polymer particles in emulsion polymerization. In order to be able to produce such small monomer droplets larger amounts of surfactant and cosurfactant are required. This is generally considered to be a disadvantage. However, controlled radical polymerizations in miniemulsions usually give better defined polymers than in regular emulsion polymerization.[14,15,16,17] Kukulj *et al.* published some interesting results on CCT in miniemulsion.[18] In Section 7.5 these will be elaborated upon with the application of CCT copolymerization of MMA and BA in miniemulsion.

7.2 Experimental Section

Materials. MMA (Merck, 99%) and BA (Merck, 99%) were distilled under reduced pressure, and stored at −10 °C. Prior to use, monomers were passed over a column, containing inhibitor remover and basic alumina. 2,2'-Azobis(isobutyronitrile) (AIBN), 1,1'-azobis(cyclohexanecarbonitrile) (ACHN) and 4,4'-azobis(4-cyanovaleric acid) (ACVA) were used as received, except for the miniemulsion polymerizations where AIBN and ACHN were recrystallized once from methanol and stored inside a glovebox at room temperature. All other chemicals were used without further purification.

Synthesis of 3,4-hexanedione dioxime. A modification of the procedures of Lance *et al.*[19] and Cervera *et al.*[20] was followed. 7.629 g pyridine and 6.42 g NH$_2$OH.HCl were added to a solution of 7.025 g 3,4-hexanedione in 100 mL ethanol. The slurry was stirred for 4 hours under reflux. After cooling to room temperature the solvent was evaporated on a rotary evaporator. The solid was washed thoroughly with cold water, filtrated and dried. The product was analysed by elemental analysis. C$_6$H$_{12}$N$_2$O$_2$ experimental: C: 50.5 %; H: 8.4 %; N: 19.1 %, calculated: C: 50.0 %; H: 8.39 %; N: 19.4 %.

Synthesis of cobaloximes. Three different cobaloxime boron fluorides were synthesized according to a procedure of Bakac and Espenson[21] modified for the different ligands. The general structure is shown in Figure 7.1. R is either methyl (CoBF), ethyl (Co(Et)$_4$BF), or phenyl (Co(Ph)$_4$BF). All products were analysed by elemental analysis. The results are collected in Table 7.1. It can be seen that the purity of both CoBF and Co(Et)$_4$BF is good. The Co(Ph)$_4$BF is not very pure. For C, H and N the measured weight percentages are higher than calculated. Therefore, it is expected that the sample is contaminated with unreacted ligand.
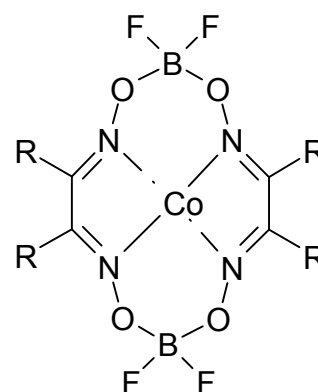
Figure 7.1 Cobaloxime boron fluoride

Table 7.1 Elemental analysis results for cobaloxime catalysts

Catalyst	Formula	Measured w%			Calculated w%		
		C	H	N	C	H	N
CoBF	$C_8H_{12}N_4O_4B_2F_4Co \cdot 2H_2O$	23.1	3.8	13.3	22.8	3.8	13.3
Co(Et)$_4$BF	$C_{12}H_{20}N_4O_4B_2F_4Co \cdot 2H_2O$	30.3	4.9	11.6	30.2	5.1	11.7
Co(Ph)$_4$BF	$C_{28}H_{20}N_4O_4B_2F_4Co \cdot 2H_2O$	56.7	4.2	9.0	50.3	3.6	8.4

Catalyst partitioning experiments. Samples were prepared by dissolving a known amount of catalyst, about 2 mg, in 25 mL MMA and adding an equal amount of water. The mixture was shaken vigorously and after that the phases were allowed to separate. The concentration in the MMA phase was determined via UV-Vis spectroscopy using a calibration curve. The concentration in the water phase was determined from a mass balance.

Determination of chain transfer coefficient. The determination of chain transfer coefficients was carried out according to the procedure described in Section 3.2 for Co(Et)$_4$BF. For CoBF and Co(Ph)$_4$BF a procedure similar to the one described in Section 6.2 for the MA − MMA copolymerizations was applied.

Emulsion polymerizations. The emulsion polymerizations were carried out in an *ab initio* semi-batch mode. A typical recipe consisted of 217 mL demineralised water, 50 mL MMA, either 0.45 g or 2.0 g sodium dodecyl sulphate (SDS), 5.0 mg of catalyst and 1.0 g of ACVA. The reactor was equipped with a turbine impeller. No baffles were used. During all steps care was taken to exclude oxygen. SDS was dissolved in water and brought into the reactor. The reactor was heated to 80 ^{o}C and initiator was added. Catalyst was dissolved in monomer and the solution was fed to the reactor over one hour. Samples were withdrawn by syringe to monitor both conversion and molecular weight distributions. Samples were dried on a hotplate and in a vacuum oven at 50 ^{0}C. Conversion was determined gravimetrically.

Miniemulsion polymerizations. The recipe for the miniemulsion polymerizations was similar to the one presented by Kukulj *et al.*[18] The polymerizations were carried out in batch

mode in a conically shaped, double-walled reactor, which is especially designed for the preparation of monomer miniemulsions. A magnetic stirrer bar is used to provide sufficient mixing. A typical recipe consisted of 80 g water, in total 20 g of BA and / or MMA, 0.50 g hexadecane, 0.80 g SDS, 0.20 g AIBN or 0.28 g ACHN and a varying amount of Co(Et)$_4$BF. Inside a glovebox a mixture of catalyst, monomer, hexadecane and initiator was prepared. This phase was stirred until all components had dissolved. SDS was added to the reactor in the required amount. Subsequently the reactor was purged with argon. Demineralised water was heated and evacuated to remove all oxygen. The water was added to the reactor under a continuous flow of argon. After that, the monomer phase was added drop wise to the reactor while stirring vigorously. Monomer phase transfer was performed by gastight syringe. After 15 more minutes of stirring, an ultrasound probe (750 W Sonics Vibra cell) was immersed into the reaction mixture. During sonication the reactor was cooled using a cryostat set at 5 $^{\circ}$C. Sonication was carried out for 4 minutes at 60 % amplitude. Subsequently the mixture was stirred for an additional 15 minutes. The reactor was connected to a pre-heated thermostated water bath set at 75 $^{\circ}$C unless stated otherwise. Before and during the reaction samples were withdrawn by syringe to monitor conversion, MWD and particle size. During all steps care was taken to exclude oxygen.

Analyses. Size exclusion chromatography (SEC) was carried out using tetrahydrofuran (THF) as an eluent at a flow rate of 1 mL min^{-1}. Two Polymer Laboratories PLgel 5 μm Mixed-C columns (300 × 7.5 mm) and PLgel 5 μm guard column (50 × 7.5 mm) were used and calibrated with Polymer Laboratories narrow MWD polystyrene standards. Mark-Houwink constants used in universal calibration are: $K_{MMA} = 9.44 \times 10^{-5}$ dL· g^{-1}, a$_{MMA} = 0.719$, $K_S = 1.14 \times 10^{-4}$ dL· g^{-1}, a$_S = 0.716$.[22] UV-Vis spectroscopy was carried out on a Hewlett Packard 8451A photodiode array UV-Visible system using a quartz cuvette of 1 cm optical path length. The system was equipped with both a deuterium and a tungsten lamp.

Dynamic light scattering was performed on a Malvern 4700 light scattering apparatus equipped with a Malvern 7032 correlator at a scattering angle of 90° at a temperature of 25 $^{\circ}$C. Results were based on an average of ten measurements. In order to obtain accurate results samples were diluted with demineralised water. Monomer miniemulsions were diluted with monomer saturated water to prevent dissolution of the monomer droplets on dilution.

7.3 Catalyst properties

When CCT catalysts are applied in emulsion or miniemulsion not only the intrinsic activity is of importance. The partitioning of the catalyst over the different phases will influence various aspects of the reaction, like *e.g.* nucleation and colloidal stability. Therefore, both activity in bulk and partitioning over water and monomer were determined for all complexes before applying them in emulsion. These three complexes were selected to differ in their partitioning behaviour and span a large range of water solubility.

7.3.1 Determination of catalyst activity

For all three complexes the activity was determined in the bulk polymerization of MMA. The results are presented in Table 7.2. The activity of Co(Ph)$_4$BF is slightly lower as compared with literature reports. This is probably due to the limited purity as stated in Section 7.2. On the other hand, the activity of Co(Et)$_4$BF is higher than reported earlier and almost equals the chain transfer coefficient of CoBF.

Table 7.2 Chain transfer coefficients for three different cobaloxime boron fluorides

Complex	C_T (10^3 -) measured	C_T (10^3 -) literature	Reference
CoBF	33 (50 ^{o}C)	24 – 40 (60 ^{o}C)	18, 23
Co(Et)$_4$BF	32 (60 ^{o}C)	18 (60 ^{o}C)	24
Co(Ph)$_4$BF	13 (50 ^{o}C)	14 - 20 (60 ^{o}C)	18, 25, 26

7.3.2 Catalyst partitioning

Experiments were performed to determine the partitioning of the three catalyst types over the water and the monomer phase. The results are collected in Table 7.3 together with literature data. The data presented here are in line with earlier reports. CoBF partitions more or less equally over both phases. Co(Et)$_4$BF is predominantly present in the monomer phase. The solubility of Co(Ph)$_4$BF in the water phase is limited and only a small part partitions into the

water phase. According to Kukulj *et al.*[9] even virtually no $Co(Ph)_4BF$ is expected to be present in the water phase. Kukulj *et al.* also reported on the partitioning of CoBF between the water phase and the polymer phase. For PMMA particles CoBF partitioned equally over both phases. So, similar to monomer partitioning[27], the partitioning of the Co(II) complexes over monomer and water phase is very similar to that over polymer particle and water phase.

Table 7.3 Percentage of catalyst present in water phase in a biphasic water – monomer system.

Complex	in water phase (%) (measured)	in water phase (%) (literature)	Reference
CoBF	31.4	28.5 – 60	9, 10, 24
$Co(Et)_4BF$	4.7	4.83	24
$Co(Ph)_4BF$	2.3	-	9

7.3.3 Summary

The catalysts CoBF and $Co(Et)_4BF$ have about the same activity in bulk polymerization. However, nearly 95 % of $Co(Et)_4BF$ is present in the monomer, whereas only 70 % of CoBF resides in the monomer phase. The partitioning between the polymer particle and the water phase is expected to be similar to the monomer – water phase partitioning. Therefore, $Co(Et)_4BF$ is expected to show highest overall activity. When compared to $Co(Ph)_4BF$, $Co(Et)_4BF$ still has a reasonable water solubility. From studies on emulsion polymerization[28,29] it is known that compounds of which the water solubility is too low are not transported across the water phase and their effectiveness in emulsion polymerization is therefore restricted. This can affect not only incorporation of monomer[28,29,30], but also radical entry rate[31] and effectiveness of chain transfer agents.[32] Restricted transport from droplets to polymer particles may also play a role for these catalysts and might favour the use of $Co(Et)_4BF$ over $Co(Ph)_4BF$.

7.4 CCT in emulsion polymerization

7.4.1 Introduction

Janowicz was the first to report on the application of CCT in emulsion.[4] CoBF was used as catalyst in a batch process. Both anionic an cationic emulsifiers were employed. A large reduction in molecular weight was observed, but no data on conversion, particle size or emulsion stability were presented. Suddaby *et al.*[10] observed coagulation during a batch emulsion polymerization. Therefore, both Suddaby *et al.*[10] and Kukulj *et al.*[9] introduced a semi-batch process, in which both catalyst and monomer are fed to the reactor over a one hour period. In a patent Haddleton *et al.*[6] also describe a semi-batch process in which a pre-emulsion of both catalyst and monomer is introduced into the reactor. Best results were obtained when the polymerizations were run under monomer flooded conditions.[9,10] Under monomer starved conditions, PMMA latex particles become glassy[9] and diffusion of catalyst is restricted, resulting in an increase in molecular weight.[9] Furthermore, it was demonstrated that the rates of polymerization were reduced, due to the enhanced formation and subsequent exit of small radicals.

Overall apparent chain transfer coefficients were around 1000 under optimal conditions, which is one order of magnitude less than in bulk or solution, but still much higher than for conventional chain transfer agents. This decrease in catalyst effectiveness is ascribed to both partitioning and catalyst hydrolysis. Another remarkable feature is the occurrence of a threshold level of catalyst, below which apparent catalyst activity drops by a factor of two and polydispersity increases to values above 6. [9] This is due to the fact that below the threshold level the average number of catalyst molecules per particle is around 1 and due to the higher instantaneous conversions compared with experiments at higher catalyst levels. These high instantaneous conversions make the particles glassy and restrict diffusion of the catalyst. In practice this means that it is not possible to produce macromers of intermediate molecular weight via this semi-batch procedure introduced by Suddaby *et al.*[10] and Kukulj *et al.*[9] This again is a typical effect related to compartmentalization in the emulsion polymerization process. Haddleton *et al.*[11] and Bon *et al.*[12] circumvented the problem of high instantaneous conversions by adding the first 20 % of the feed in one shot and the remainder over 48

minutes. This results in reduced instantaneous conversions and therefore higher apparent chain transfer coefficients, also at low catalyst levels.

Kukulj *et al.*[9] also compared the chain transfer behaviour of CoBF and Co(Ph)$_4$BF. The latter appeared to be more than a factor of ten less active than CoBF, whereas bulk polymerization activities generally only differ a factor of two. This was explained from the fact that transport of Co(Ph)$_4$BF across the water phase to the polymer particles is the limiting factor, because of its low water solubility. Waterson *et al.*[24] suggested the use of some other cobaloxime boron fluorides in emulsion polymerization, but they did not report on the actual application. In the next subsection some initial results on the comparison of CoBF, Co(Et)$_4$BF and Co(Ph)$_4$BF in emulsion polymerization will be presented.

7.4.2 Application of CoBF, Co(Et)$_4$BF and Co(Ph)$_4$BF in emulsion polymerization

All these complexes, CoBF, Co(Et)$_4$BF and Co(Ph)$_4$BF, were applied in an *ab initio* semi-batch emulsion polymerization, in which a solution of catalyst in monomer was added to the reactor over one hour. SDS was used as an emulsifier at concentrations both below and above the critical micelle concentration. An overview of experimental data for all six polymerizations is given in Table 7.4. An overview of results is presented in Table 7.5.

Table 7.4 Overview of experimental data for all six CCT semi-batch emulsion polymerizations.

Exp.	Catalyst	[Cat.] (ppm)[a]	[SDS][b] (10^{-2} mol·L^{-1})	Marker
1	CoBF	31	0.71	▼
2	Co(Et)$_4$BF	21	0.64	●
3	Co(Ph)$_4$BF	20	0.74	◀
4	CoBF	31	3.6	◆
5	Co(Et)$_4$BF	22	3.7	▲
6	Co(Ph)$_4$BF	18	3.3	■

[a] Here 1 ppm is defined as 10^{-6} moles of catalyst per mole of monomer.

[b] Total concentration of SDS with respect to the aqueous phase.

Table 7.5 Overview of results for all six CCT semi-batch emulsion polymerizations.

Exp.	Final M_n $(10^3$ g· mol$^{-1})$	Final PDI (-)	D_n (nm)	catalyst per particle[a] (-)
1	9.59	2.78	86	62.8
2	0.836	1.45	412	4600
3	43.4	2.00	17	0.3
4	7.36	1.91	36	4.7
5	1.27	1.87	66	21
6	47.9	2.03	9	0.04

[a] In the calculation of the number of catalyst molecules per particle both partitioning and catalyst deactivation are not taken into account.

In Figures 7.2 a and b the evolution of M_n and polydispersity (PDI) with time is presented for the polymerizations below CMC (exp. 1 – 3). The results for the experiments above CMC (exp. 4 – 6) are shown in Figures 7.3 a and b. It can be clearly seen that both polymerizations containing Co(Et)$_4$BF, *i.e.* experiments 2 and 5, produce the lowest molecular weight material, around 1000 g· mol^{-1}. Although the overall concentration of CoBF is higher than the concentration of Co(Et)$_4$BF, molecular weights in the presence of CoBF are substantially larger with $M_n \sim 8000$ g· mol^{-1}. For Co(Ph)$_4$BF M_n is in between 40×10^3 and 50×10^3 g· mol^{-1}, showing the smallest molecular weight effect.
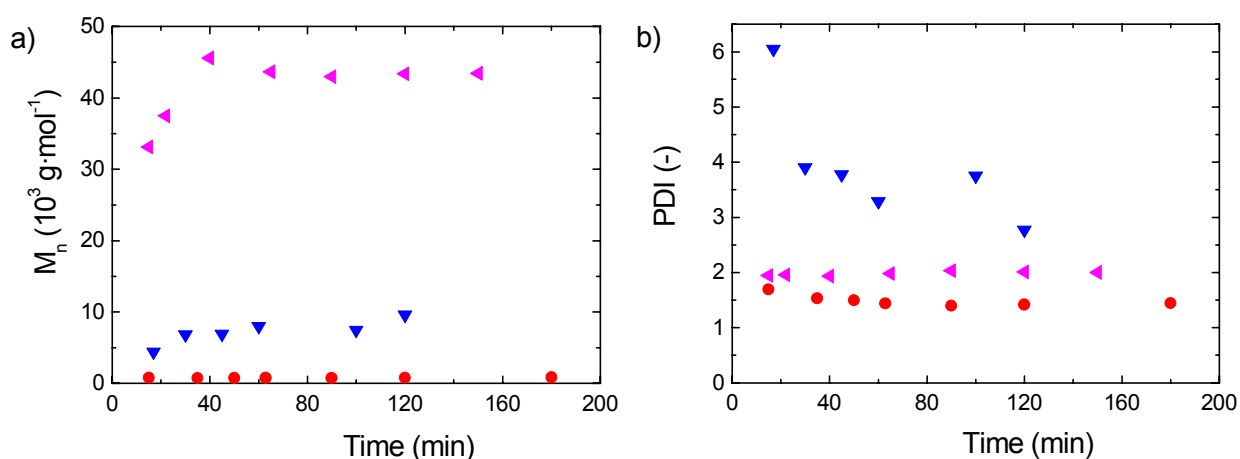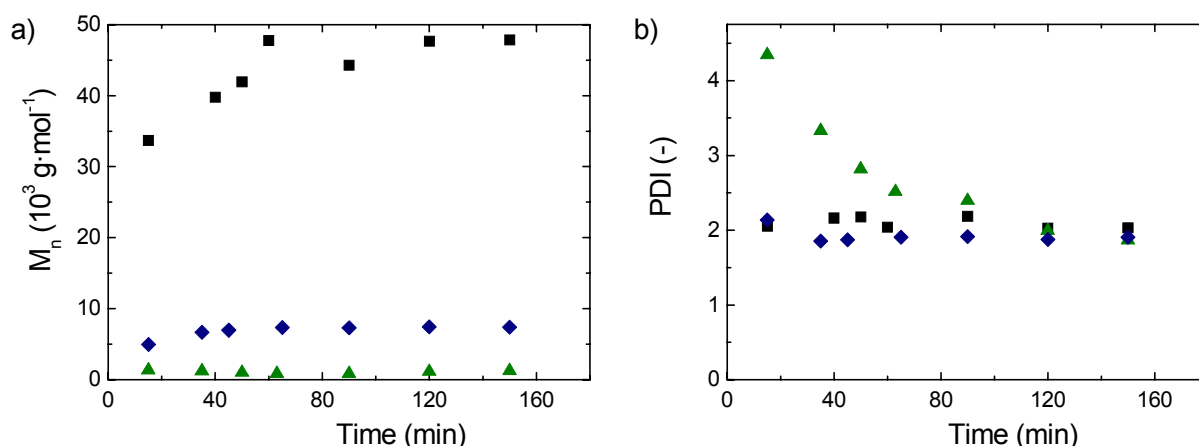

Figure 7.2 The evolution of M_n (a) and polydispersity (b) with time for the semi-batch CCT emulsion polymerizations of MMA below CMC at 80°C. Different Co(II) complexes were used as catalyst.
▼: CoBF; ●: Co(Et)$_4$BF; ◀: Co(Ph)$_4$BF.

Figure 7.3 The evolution of M_n (a) and polydispersity (b) with time for the semi-batch CCT emulsion polymerizations of MMA above CMC at 80°C. Different Co(II) complexes were used as catalyst.

◆ : CoBF; ▲: Co(Et)$_4$BF; ■: Co(Ph)$_4$BF.

7.4.2.1 Effects of catalyst type on molecular weight

Both Kukulj *et al.*[9] and Suddaby *et al.*[10] demonstrated that the instantaneous conversion in a semi-batch emulsion polymerization is the most important parameter in explaining the effects of CCT agents, as at high instantaneous conversions PMMA latex particles become glassy resulting in restricted diffusion of the catalyst and, therefore, lower overall activity. Instantaneous conversion is defined as the conversion of the amount of monomer that has already been added to the reactor. For all six polymerizations the instantaneous conversions are shown in Figure 7.4. In this figure, a very clear distinction is observed between both polymerizations containing Co(Et)$_4$BF, on one hand, and the other polymerizations, on the other hand. Whereas instantaneous conversions are around 50 % during the first hour of polymerization for the Co(Et)$_4$BF mediated reactions, instantaneous conversions over 80 % are observed for all other experiments. These Co(Et)$_4$BF runs also produced the lowest molecular weights. This parallel between instantaneous conversion and molecular weight was also noted by Kukulj *et al.*[9] and Suddaby *et al.*[10] This relation bears similarity to the "chicken and egg" dilemma. Which one was first? Low instantaneous conversions are required for the catalyst to be very active and, on the other hand, an active catalyst is required to lower the reaction rate and obtain lower instantaneous conversions.

The question now is, why in presence of Co(Et)$_4$BF molecular weights are successfully reduced, where in presence of other catalysts this reduction is not achieved. When comparing Co(Et)$_4$BF and CoBF the most important difference is, that CoBF is partitioned more or less equally over the aqueous phase and the polymer phase, whereas Co(Et)$_4$BF is predominantly present in the polymer phase. So, the average amount of molecules of Co(Et)$_4$BF per particle will be larger than for CoBF, as is shown in Table 7.5. Additionally, as the average time CoBF is present in the water phase is larger than for Co(Et)$_4$BF, CoBF will decompose at higher rates. As the bulk chain transfer coefficients are nearly equal, the overall activity of Co(Et)$_4$BF is higher, giving more transfer to monomer, followed by exit of monomeric radicals and increased termination. This results in a lower instantaneous conversion, which creates the right conditions for Co(Et)$_4$BF to remain more active.
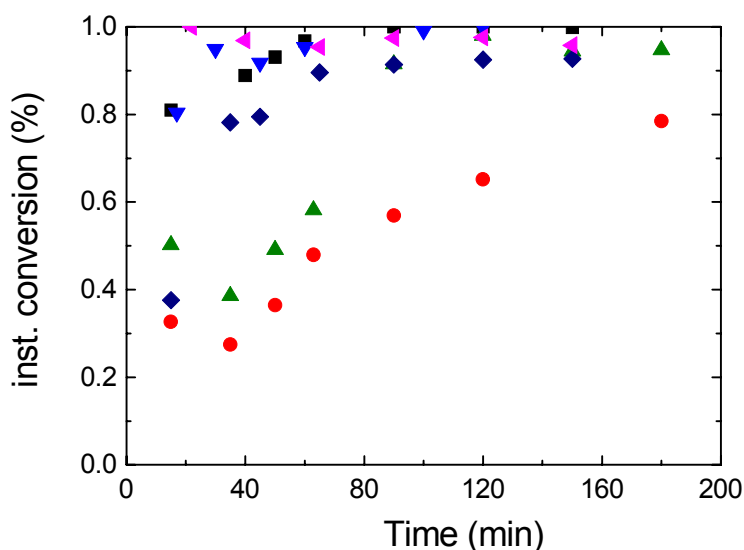

Figure 7.4 The instantaneous conversion with time for the semi-batch CCT emulsion polymerizations of MMA both below and above CMC at 80°C. Different Co(II) complexes were used as catalyst. ▼: CoBF, below CMC; ●: Co(Et)$_4$BF, below CMC; ◄: Co(Ph)$_4$BF, below CMC; ◆: CoBF, above CMC; ▲: Co(Et)$_4$BF, above CMC; ■: Co(Ph)$_4$BF, above CMC.

When comparing Co(Et)$_4$BF and Co(Ph)$_4$BF two other aspects play a role. Co(Ph)$_4$BF is much less water soluble than Co(Et)$_4$BF, which may reduce the rate of transport of Co(Ph)$_4$BF from monomer droplets to polymer particles,[10] as discussed in Section 7.3.2.

When transport of Co(Ph)$_4$BF across the water phase is not required, as *e.g.* in miniemulsion polymerization, Co(Ph)$_4$BF does show a high overall activity, as was reported by Kukulj *et al.*[18] Furthermore, bulk activity for Co(Ph)$_4$BF is smaller. So, both concentration and activity of Co(Ph)$_4$BF in the particles are smaller as compared with Co(Et)$_4$BF. This results in high instantaneous conversions, which will cause the overall activity to remain very low.

In Figure 7.4 it is demonstrated that for both CoBF and Co(Ph)$_4$BF polymerizations run at high instantaneous conversions. However, M_n for CoBF is about a factor of five lower than for Co(Ph)$_4$BF. A reason for this may be that the average particle size for the emulsion polymerizations in presence of Co(Ph)$_4$BF is so small, that the average number of catalyst molecules per particle is less than one. In addition, CoBF has a higher intrinsic reactivity than Co(Ph)$_4$BF.

7.4.2.2 Effects of emulsifier concentration and catalyst type on nucleation and particle size

When we focus on particle size as collected in Table 7.5, two trends can be observed. First of all for the polymerizations in presence of the same catalyst an increase in emulsifier concentration results in smaller and thus more particles. This behaviour is fully in line with emulsion polymerization theory.[1] For both Co(Et)$_4$BF and Co(Ph)$_4$BF a decrease in particle size is accompanied by an increase in molecular weight. For CoBF the opposite is observed. Thus, there is no general correlation between particle size and molecular weight, which is independent of catalyst type. However, when all complexes are considered separately, some additional remarks can be made.

For Co(Ph)$_4$BF the average amount of catalyst molecules per particle is in both cases significantly lower than one. Especially for such small particles, this means that the entry rate will strongly influence molecular weight. The emulsion polymerization below CMC results in the largest particles and thus the smallest number of particles. This means that the time interval between entry of two radicals for the polymerization below CMC is smaller than for the polymerization above CMC. This explains the smaller molecular weights in the polymerization below CMC.

For both CoBF and Co(Et)$_4$BF the amount of catalyst molecules per particle is larger than one. Therefore, the entry rate will not determine molecular weight. A correlation that is observed is that, for both CoBF and Co(Et)$_4$BF, in the polymerization which runs at lower instantaneous conversions, lower molecular weights are produced. However, for CoBF this is the polymerization above CMC and for Co(Et)$_4$BF this is the polymerization below CMC.

For Co(Et)$_4$BF an explanation may be that the larger number of particles above CMC results in a higher polymerization rate, resulting in a higher instantaneous conversion and therefore higher molecular weights than in the polymerization below CMC. For CoBF, on the other hand, a decrease in polymerization rate is observed when the number of particles increases, pointing to a strong decrease in the average number of radicals per particle. The main difference between CoBF and Co(Et)$_4$BF is in their water solubilities. Radicals that exit from a polymer particle into the water phase, are more likely to react with the Co(II) catalyst in the water phase in the CoBF emulsion polymerization than in the Co(Et)$_4$BF emulsion polymerization. Chain transfer in the water phase may result in termination. As smaller particles give more exit[1], more water phase termination will occur for the emulsion polymerization with CoBF above CMC than below CMC. This may explain the lower instantaneous conversion and therefore the lower molecular weight in the emulsion polymerization with CoBF above CMC compared with the emulsion polymerization below CMC.

The second trend is that, for equal emulsifier concentrations, the polymerizations showing the highest overall activity, have the largest particles. A similar correlation can be found in the work of Suddaby *et al.*[10] In their experiments catalyst concentrations are varied and higher catalyst concentrations are accompanied by larger particles. Unfortunately, the authors do not explain this trend. In the work of Kukulj *et al.*[9] CoBF and Co(Ph)$_4$BF are compared and the results display the same trend, though less strongly.

So, in the emulsion polymerizations where effective CCT occurs, less particles are nucleated. In the work of Suddaby *et al.*[10] on emulsion polymerizations with CoBF, it can be argued that chain transfer in the water phase, resulting in the formation of water soluble oligomers, may account for decreased particle nucleation with increasing catalyst concentration. However, it is unlikely that water phase chain transfer can explain decreased nucleation for Co(Et)$_4$BF

compared with CoBF. It could be that when a radical enters a monomer swollen micelle and initiates polymerization that chain transfer occurs after a few propagation steps. If chain transfer is followed by exit of the radical, it may be that the monomer swollen micelle is not transformed into a polymer particle, but still behaves like a monomer swollen micelle that can eventually disappear. This may account for a decrease in nucleation rate.

Another important question to be answered is whether a decrease in nucleation rate is beneficial to efficient chain transfer or that a decrease in nucleation rate is only a consequence of efficient chain transfer. In addition, this may be another "chicken and egg" dilemma as was also observed for efficient chain transfer and lower instantaneous conversions. Unfortunately, from these preliminary experiments it seems not possible to come up with a satisfactory answer. Additional experiments will be required to solve the questions relating to nucleation in CCT.

7.4.3 Summary

It was shown that the level of Co(Et)$_4$BF required to produce low molecular weight polymer in an emulsion polymerization is significantly lower than the level of either CoBF or Co(Ph)$_4$BF. When the instantaneous conversions are maintained at an intermediate level, efficient CCT is observed. However, to obtain intermediate instantaneous conversions, sufficient CCT is required. This relation has also been observed in previous work by other authors.[9,10] The effect of emulsifier concentration on molecular weight seems to depend on catalyst type and can not be explained in a straightforward manner. Every combination of catalyst type and emulsifier concentration probably requires a different explanation.

7.5 CCT in miniemulsion polymerization

7.5.1 Introduction

Kukulj *et al.*[18] have demonstrated that CCT can be readily applied in miniemulsion polymerization. Apparent C_T's were in good agreement with results from bulk polymerization

experiments. Due to the fact that the catalyst is already present in the locus of polymerization before the reaction starts, there is no need for sufficient transport of catalyst through the water phase. In addition, sparsely water soluble catalysts, such as $Co(Ph)_4BF$, have the advantage, over better water soluble catalysts, such as CoBF, that no water phase deactivation occurs. So, especially for $Co(Ph)_4BF$ good results were obtained.

In emulsion systems a certain threshold level of catalyst was observed, below which CCT was less effective. Due to this threshold, in emulsion polymerization it is difficult to produce intermediate molecular weights, above 5000 g· mol^{-1}.[9] This problem was solved via the initial shot method. Miniemulsion polymerization may provide an alternative route. However, in the polymerizations presented by Kukulj *et al.*[18] at low $Co(Ph)_4BF$ concentrations, broader MWDs were obtained than at high $Co(Ph)_4BF$ concentrations. This may be caused by the low number of catalyst molecules per particle, which is around 5. Depending on the distribution, there may also be particles with 2 or 8 catalyst molecules, which may explain the observed broadening of the MWD. Furthermore, it was demonstrated that miniemulsions containing $Co(Ph)_4BF$ can be initiated with potassium persulphate without loss of catalytic activity. All in all CCT in miniemulsion seems to be a promising method to produce macromers in an aqueous dispersion.

Over the years there have been several reports on miniemulsion copolymerization as well, *e.g.* on styrene – MMA[33], vinyl acetate – BA[34,35,36] and vinyl acetate – vinyl 2-ethylhexanoate.[37] One of the problems occurring in these copolymerizations is that only part of the original droplets is nucleated. This problem may be at least partially resolved via the addition of polymer[38] or by using an oil-soluble initiator.[39] When we wish to prepare an aqueous dispersion of an MMA – BA macromer, this can, in principle, be achieved via either emulsion or miniemulsion polymerization. As was reported by Kukulj *et al.*[18] in miniemulsion polymerization smaller amounts of catalyst are required. This is important, as it was shown in the previous chapter that in the homogeneous MMA – BA copolymerization already an increased amount of catalyst is necessary to obtain low molecular weight polymers with respect to the amount of catalyst required in MMA homopolymerizations. Therefore, miniemulsion polymerization was used in the preparation of aqueous dispersions of MMA – BA macromers.

7.5.2 AIBN-initiated miniemulsion homo- and copolymerization

In the miniemulsion polymerizations, a recipe similar to that of Kukulj *et al.*[18] is applied. A total of four polymerizations is performed, two MMA homopolymerizations and two MMA – BA copolymerizations at f_{MMA} = 0.5. One homopolymerization and one copolymerization are carried out in presence of Co(Et)$_4$BF. The experimental data and results are collected in Table 7.6.

Table 7.6 Experimental data and results for Co(Et)$_4$BF mediated homo- and copolymerizations.

Exp.	f_{MMA}	[Co(Et)$_4$BF]	Conv.[b]	M_n[b]	PDI[b]	initial D_z	final D_z	Marker
	(-)	(ppm)[a]	(%)	(10^3 g· mol^{-1})		(nm)	(nm)	
1	1	0	99.0	546	2.43	148	125	▼
2	1	4.7	95.6	2.39	1.72	151	188	▲
3	0.5	0	100	358	3.00	238	92.7	●
4	0.5	68	88.1	14.6	3.13	445	180	■

[a] Here 1 ppm is defined as 10^{-6} moles of catalyst per mole of monomer
[b] Final latex properties

It appeared to be rather difficult to produce a monomodal particle size distribution (PSD). In general, over 90 % particles of small size, less than 100 nm, and a small amount of larger particles, in between 300 to 500 nm, are produced. Final PSDs are generally more narrow having D_z in between 100 and 200 nm. This change in PSD means that not all particles were nucleated. The effects of incomplete nucleation are unclear, and require further research. However, incomplete nucleation may well affect apparent catalyst activity.

The effect of Co(Et)$_4$BF on molecular weight can be seen readily from the results in Table 7.6 and from Figure 7.5, in which the evolution of M_n with conversion is presented for all four experiments. In the MMA polymerizations M_n is reduced by more than two orders of magnitude, whereas in the copolymerization a 25-fold reduction is observed. From these results an apparent C_T of 8.9×10^3 for MMA and of 1.1×10^2 for MMA – BA is calculated. C_T for MMA is in line with results obtained by Kukulj *et al.*[18] for CoBF and Co(Ph)$_4$BF. However, it is expected, that when both the formation of the monomer miniemulsion by

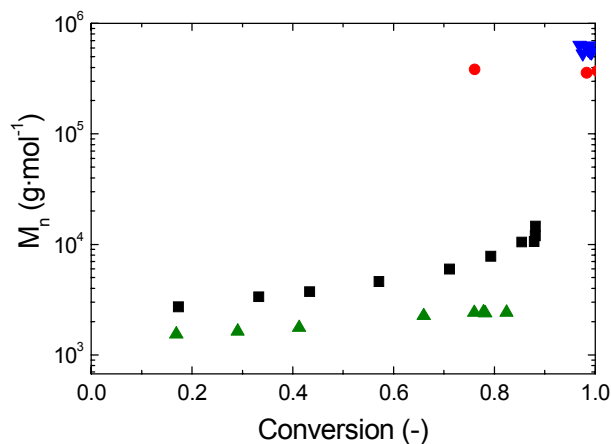ultrasound and the nucleation of particles are better controlled more effective CCT can be achieved.

Figure 7.5 Evolution of M_n with conversion for 4 miniemulsion polymerizations initiated by AIBN. ▼: MMA, no Co(Et)$_4$BF; ▲: MMA, 4.7 ppm Co(Et)$_4$BF; ●: MMA-BA, no Co(Et)$_4$BF; ■: MMA-BA, 67 ppm Co(Et)$_4$BF
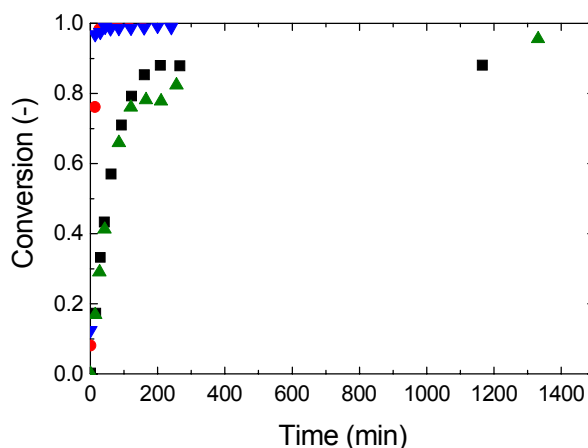
Figure 7.6 Conversion – time plots for 4 miniemulsion polymerization initiated by AIBN. ▼: MMA, no Co(Et)$_4$BF; ▲ : MMA, 4.7 ppm Co(Et)$_4$BF; ●: MMA-BA, no Co(Et)$_4$BF; ■: MMA-BA, 67 ppm Co(Et)$_4$BF

In Figure 7.6 conversion – time histories are presented. The polymerizations without Co(II) catalyst present reach nearly full conversion within half an hour. The rate of the CCT mediated miniemulsion polymerizations is lower, which is to be expected from the increased generation of small radicals, followed by exit and finally termination. In between 80 and 90 % conversion, the rate of polymerization drops considerably and both polymerizations do not reach full conversion. Kukulj *et al.*[18] observed similar behaviour.

The polymerizations in absence of catalyst proceeded so fast that for all but one sample conversions over 90 % were determined. At these conversions no change in the MWDs was observed and therefore these are not shown. The MWDs for the polymerizations in the presence of Co(Et)$_4$BF are presented in Figures 7.7 and 7.8 for the MMA homopolymerization and for the MMA – BA copolymerization, respectively. In the MMA homopolymerization a slight shift to higher molecular weights is observed, which is in agreement with data reported by Kukulj *et al.*[18] In Chapter 4 several possible reasons for such
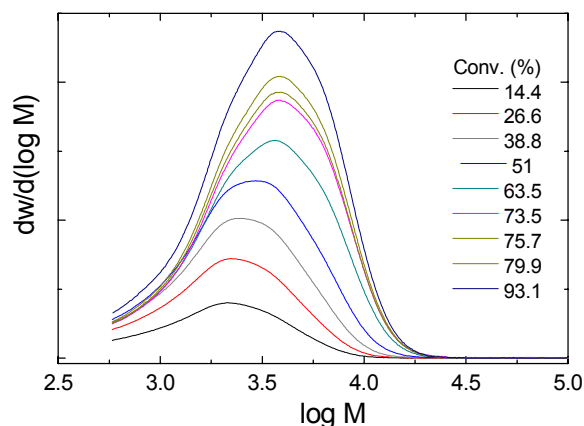
Figure 7.7 Molecular weight distributions measured at different conversions for the CCT miniemulsion polymerization of MMA at 75 °C. The area under the distributions is proportional to the corresponding conversions.
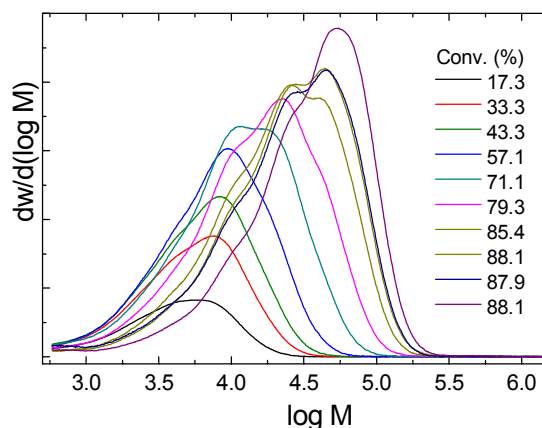
Figure 7.8 Molecular weight distributions measured at different conversions for the CCT miniemulsion polymerization of MMA – BA at 75 °C. The area under the distributions is proportional to the corresponding conversions.

an increase have been discussed. In this case, hydrolysis of the Co(II) in the water phase is a plausible explanation.

In the MMA − BA copolymerization an increase in molecular weights similar to that in the MMA homopolymerization is observed initially, but starting around 70 % conversion low molecular weight material starts disappearing and high molecular weight material is formed. After three and a half hours, 88.1 % conversion has been reached. During the next 16 hours no additional conversion could be determined, but a significant shift in the MWD to higher molecular weights was observed. Similar behaviour has been reported in Chapter 6 for the corresponding solution polymerization. This is explained by the incorporation of macromers into the growing polymer chain. However, in the miniemulsion polymerization the observed shift in molecular weight is more pronounced than in solution polymerization as can be seen when Figures 7.8 and 6.12 b are compared.

As can be seen in Figure 7.9 the number of polymer chains in the MMA − BA copolymerization decreases nearly 50 percent when going from 57 to 88 percent monomer conversion. The number of chains in the MMA homopolymerization, on the other hand, shows a steady increase. A reason for the differences between miniemulsion and solution polymerization may be the different water solubilities of MMA, *viz.* 0.15 g· mol^{-1} and BA, *viz.* 0.01 g· mol^{-1}.[3] For this particular reaction this means that about 1.2 g of MMA can maximally

be dissolved in the water phase. As only about 8.8 g of MMA is present in total, this has a significant effect on the ratio of MMA and BA in the particles, where the polymerization takes place. A smaller ratio of MMA and BA will favour macromer incorporation, as discussed in Chapter 6.
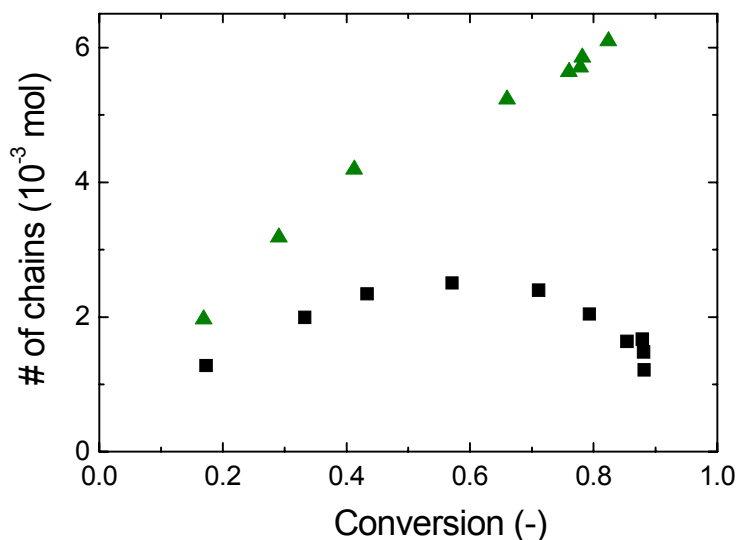

Figure 7.9 The evolution of the number of polymer chains with conversion in the CCT miniemulsion polymerizations of MMA (▲) and MMA – BA (■).

However, in spite of enhanced macromer incorporation, a significant reduction in molecular weight has been achieved, which clearly demonstrates the applicability of CCT in the miniemulsion copolymerization of MMA and BA.

7.6 Conclusions

It has been found that Co(Et)$_4$BF has a similar chain transfer activity in bulk as CoBF. However, the partitioning between water phase and monomer phase is very different for both complexes. Whereas CoBF partitions nearly equally over both phases, Co(Et)$_4$BF is predominantly present in the monomer phase. This strongly affects overall catalyst activity in emulsion polymerization. Compared to CoBF, lower amounts of Co(Et)$_4$BF are required to obtain similar reductions in molecular weight. Findings from other authors that highest catalyst activity is obtained at intermediate conversions have been confirmed.

The second part of this chapter focused on the application of Co(Et)$_4$BF as CCT agent in miniemulsion polymerization. For MMA homopolymerizations, results of Kukulj *et al.* that catalysts display higher activities in miniemulsion than in emulsion polymerization have been confirmed. More importantly, it has been demonstrated that CCT copolymerizations of MMA and BA can be performed in miniemulsion. In presence of Co(Et)$_4$BF large molecular weight reductions are achieved, but at high conversions significant macromer incorporation occurs.

7.7 References

[1] Gilbert, R.G. *'Emulsion Polymerization: a Mechanistic Approach'* Academic Press, London **1995**

[2] van Herk, A.M.; German, A.L. *Macromol. Theory Simul.* **1998**, *7*, 557

[3] Schoonbrood, H.A.S. *'Emulsion co- and Terpolymerization. Monomer partitioning, kinetics and control of microstructure and mechanical properties.'* PhD Thesis, Eindhoven University of Technology, Eindhoven, **1994**

[4] Janowicz, A.H. *US Patent 4,694,054*, **1987**

[5] Janowicz, A.H. *US Patent 5,028,677*, **1991**

[6] Haddleton, D.M.; Muir, A.V.G. *US Patent 5,602,220*, **1997**

[7] Haddleton, D.M., Padget, J.C., Overbeek, G.C. *WO Patent 95/04767*, **1995**

[8] Haddleton, D.M.; Muir, A.V.G.; Leeming, S.W.; O'Donnell, J.P.; Richards, S.N. *WO Patent 96/13527*, **1996**

[9] Kukulj, D.; Davis, T.P.; Suddaby, K.G.; Haddleton, D.M.; Gilbert, R.G. *J. Pol. Sci. A: Polym. Chem.* **1997**, *35*, 859

[10] Suddaby, K.G.; Haddleton, D.M.; Hastings, J.J.; Richards, S.N.; O'Donnell, J.P. *Macromolecules* **1996**, *29*, 8083

[11] Haddleton, D.M.; Morsley, D.R.; O'Donnell, J.P.; Richards, S.N. *J. Pol. Sci. A: Polym. Chem.* **1999**, *37*, 3549

[12] Bon, S.A.F.; Morsley, D.R.; Waterson, J.; Haddleton, D.M. *Macromol. Symp.* **2001**, *165*, 29

[13] Krstina, J.; Moad, C.L., Moad, G.; Rizzardo, E.; Berge, C.T.; Fryd, M. *Macromol. Symp.* **1996**, *111*, 13

[14] de Brouwer, H. *'RAFT memorabilia, living radical polymerization in homogeneous and heterogeneous media'* PhD Thesis, Eindhoven University of Technology, Eindhoven, **2001**

[15] Matyjaszewski, K.; Shipp, D.A.; Qiu, J.; Gaynor, S.G. *Macromolecules* **2000**, *33*, 2296

[16] Prodpran, T.; Dimonie, V.L.; Sudol, E.D.; El-Aasser, M.S. *Macromol. Symp.* **2000**, *155*, 1

[17] MacLeod, P.J.; Barber, R.; Odell, P.G.; Keoshkerian, B.; Georges, M.K. *Macromol. Symp.* **2000**, *155*, 31

[18] Kukulj, D.; Davis, T.P.; Gilbert, R.G. *Macromolecules* **1997**, *30*, 7661

[19] Lance, K.A.; Goldsby, K.A.; Busch, D.H. *Inorg. Chem.* **1990**, *29*, 4537

[20] Cervera, B.; Ruiz, R.; Lloret, F.; Julve, M.; Cano, J.; Faus, J.; Bois, C.; Mrozinsko, J. *J. Chem. Soc., Dalton Trans.* **1997**, 395

[21] Bakac, A.; Espenson, J.H. *J. Am. Chem. Soc.* **1984**, *106*, 5197

[22] Hutchinson, R.A.; Paquet, D.A.; McMinn, J.H.; Beuermann, S.; Fuller, R.E.; Jackson, C. *Dechema Monographs* **1995**, *131*, 467

[23] Haddleton, D.M.; Maloney, D.R.; Suddaby, K.G.; Muir, A.V.G.; Richards, S.N. *Macromol. Symp.* **1996**, *111*, 37

[24] Waterson, J.L.; Haddleton, D.M.; Harrison, R.J.; Richards, S.N. *Pol. Preprints (ACS)* **1998**, *39(2)*, 457

[25] Heuts, J.P.A.; Forster, D.J.; Davis, T.P. *Macromolecules* **1999**, *32*, 3907

[26] Forster, D.J.; Heuts, J.P.A.; Lucien, F.P.; Davis, T.P. *Macromolecules* **1999**, *32*, 5514

[27] Maxwell, I.A.; Kurja, J.; van Doremaele, G.H.J.; German, A.L. *Makromol. Chem.* **1992**, *193*, 2049

[28] Kitzmiller, E.L.; Miller, C.M.; Sudol, E.D.; El-Aasser, M.S. *Macromol. Symp.* **1995**, *92*, 157

[29] Lau, W. *Cyclodextrin: Basic Res. Mark., 10th Int. Cyclodextrin Symp.* **2000**, 60

[30] Wang, S.T.; Schork, F.J.; Poehlein, G.W.; Gooch, J.W. *J. Appl. Pol. Sci.* **1996**, *60*, 2069

[31] De Burbuaga, A.S.; De la Cal, J.G.; Asua, J.M. *Polymer* **2000**, *41*, 1269

[32] Cunningham, M.F.; Ma, J.W. *J. Appl. Pol. Sci.* **2000**, *78*, 217

[33] Rodriguez, V.S.; El-Aasser, M.S.; Asua, J.M.; Silebi, C.A. *J. Pol. Sci: Part A Pol. Chem.* **1989**, *27*, 3659

[34] Delgado, J.; El-Aasser, M.S.; Silebi, C.A.; Vanderhoff, J.W. *J. Pol. Sci: Part A Pol. Chem.* **1989**, *27*, 193

[35] Delgado, J.; El-Aasser, M.S.; Silebi, C.A.; Vanderhoff, J.W. *J. Pol. Sci: Part A Pol. Chem.* **1990**, *28*, 777

[36] Delgado, J.; El-Aasser, M.S.; Silebi, C.A.; Vanderhoff, J.W.; Guillot, J. *J. Pol. Sci: Part A Pol. Chem.* **1988**, *26*, 1495

[37] Kitzmiller, E.L.; Miller, C.M.; Sudol, E.D.; El-Aasser, M.S. *Macromol. Symp.* **1995**, *92*, 157

[38] Reimers, J.; Schork, F.J. *J. Appl. Pol. Sci.* **1996**, *59*, 1833

[39] Alduncin, J.A.; Forcada, J.; Asua, J.M. *Macromolecules* **1994**, *27*, 2256

Chapter 8

Epilogue

Synopsis: In this chapter the aims and results of the work described in this thesis are evaluated briefly. Promising directions for future research are set out.

8.1 Evaluation

Due to more strict environmental legislation, the coatings industry is forced to look for ways to produce coatings with a lower solvent content, the so-called high-solid coatings. In order to ensure good processability of these coatings, the polymeric binder material needs to consist of low molecular weight polymers. More traditional ways of producing low molecular weight polymers, like the use of thiols, suffer from drawbacks with respect to the properties of the end-product. Catalytic chain transfer can be a good alternative polymerization technique, that has the additional advantage of producing polymers with a vinyl end functionality. However, although CCT is very effective in polymerizations of methacrylates, for *e.g.* polymerizations of acrylates inhibition has been reported, which may limit the applicability of CCT.

So far, most research on CCT has been focused on the development of new catalysts and on the application of CCT to both functional and non-functional methacrylates and to styrene. Only a few groups have conducted more quantitative research in the area of CCT. One of the major challenges in this field is to obtain a good understanding of the CCT homopolymerizations of monomers that, in contrast to methacrylates, do not contain an α-methyl group, and of the copolymerizations of these monomers with methacrylates. This has been the main focus of this thesis.

The first part of the investigations has resulted in a better insight in the conditions required to obtain quantitative information on CCT. In addition, the results presented in this thesis have led to the interpretation that the transfer step is not diffusion controlled, which is in contrast to

reports of other authors. More importantly, for both acrylates and styrene a more quantitative description of the CCT process has been given. The described dependence of the overall catalyst activity in the polymerization of styrene on exposure to light and on initiator concentration most probably explains the spread in results reported in literature.

In the second part of the investigations it has been demonstrated that CCT is an effective tool in controlling the molecular weight in copolymerizations of methacrylates and acrylates up to high conversion, which opens up a much wider range of applications. The model developed to describe the overall transfer activity may assist in selecting the right conditions to obtain a copolymer of a specific average molecular weight. The results of these investigations clearly fill a gap in the knowledge on CCT.

In the third and last part of the investigations the CCT homo- and copolymerizations have been applied in (mini)emulsion polymerization. In the emulsion polymerizations of methyl methacrylate an alternative catalyst with a well-balanced water solubility showed good overall activity. Successful application of this catalyst in the miniemulsion copolymerization of methyl methacrylate and butyl acrylate has opened up new possibilities for the production of low molecular weight acrylate – methacrylate copolymers in water based systems.

8.2 Future research

There are several promising lines of research, some of which are interesting from a more scientific point of view and others because of their orientation towards useful applications. Four have been selected and will be presented briefly.

Comparison of the chain transfer activity for fully protonated and fully deuterated methyl methacrylate will give additional information with respect to diffusion control.

Another important question to be answered is whether the bond dissociation rate of polyacrylate – cobalt bonds can be enhanced, so that it will be possible to produce polyacrylate oligomers. An answer may be found in changing temperature, intensity and wavelength of UV-light, or in using ultrasound.

Thirdly, the methacrylate – acrylate oligomers synthesized in high conversion polymerizations are heterogeneous in composition and in the extent of branching. In a semi-batch polymerization it is possible to control the reaction mixture composition using Raman spectroscopy. In this way control over oligomer molecular weight, composition and branching can be exerted, resulting in a better control over properties.

A fourth important line of research is CCT in emulsion polymerization. It is now known how to achieve efficient CCT in emulsion polymerization, but there is no thorough understanding of the effects of CCT on important aspects such as *e.g.* nucleation, water phase polymerization and colloidal stability.

8.3 Conclusion

The investigations in this thesis have contributed to a better understanding of catalytic chain transfer, especially in the area of the homopolymerizations of styrene and acrylates and in the area of the copolymerization of acrylates and methacrylates. It has been shown that the use of CCT need not be limited to methacrylates and styrene, but that it can be extended to other monomers as well, which increases its potential for industrial application. Future research is expected to lead to methods to further increase overall catalyst activity for acrylate monomers.

Glossary

Symbol	Description
$a_{monomer}$	Mark-Houwink constant for a specific monomer (-)
C_T	chain transfer coefficient (-)
$C_{T,o}$	chain transfer coefficient in absence of Co – C bond formation (-)
C_T^{bulk}	chain transfer coefficient for bulk polymerization (-)
$\langle C_T \rangle$	average chain transfer coefficient for copolymerization (-)
$\langle C_T \rangle'$	apparent average chain transfer coefficient for copolymerization (-)
D	diffusion coefficient (m$^2 \cdot$ s^{-1})
d	length scale for diffusion (m)
Da	Damköhler number (-)
D_{Co}	diffusion coefficient of cobalt species (m$^2 \cdot$ s^{-1})
D_n	number average particle diameter (nm)
$D_{P\bullet}$	diffusion coefficient for a polymeric radical (m$^2 \cdot$ s^{-1})
D_z	z-average particle (nm)
f	efficiency factor for initiator decomposition (-)
f_{Co}	fraction of total amount of Co complex present as Co(II) (-)
$f_{monomer}$	molar fraction of a specific monomer with respect to total monomer (-)
$F_{monomer}$	molar fraction of a specific monomer in a copolymer (-)
G	Gibbs energy (J)
k	Boltzmann constant (J$\cdot$ K^{-1})
k_β	rate constant for β-scission of a polymeric radical – macromer adduct (s^{-1})
K_1	equilibrium constant for the formation of paired reactants (L$\cdot$ mol^{-1})
k_1	rate constant for diffusive encounter (L$\cdot$ mol$^{-1} \cdot$ s^{-1})
k_{-1}	rate constant for diffusive separation (s^{-1})
k_1'	constant for diffusive encounter excluding viscosity contributions (Pa$\cdot$ L$^{-1} \cdot$ mol^{-1})
k_{-1}'	constant for diffusive separation excluding viscosity contributions (Pa)
K_a	acid dissociation constant (-)
k_{add}	rate constant for addition of a polymeric radical to macromer (L$\cdot$ mol$^{-1} \cdot$ s^{-1})
k_{-add}	rate constant for reverse addition of a polymeric radical – macromer adduct (s^{-1})
K_{cd}	equilibrium constant for combination of and dissociation into CoBF and a polyacrylate radical (L$\cdot$ mol^{-1})
k_{com}	bimolecular combination rate constant (L$\cdot$ mol$^{-1} \cdot$ s^{-1})

k_{com}	unimolecular combination rate constant (when diffusion is taken into account in the reaction mechanism) (s^{-1})
$k_{com,B}$	rate constant for combination of CoBF and benzoyloxy radicals ($L \cdot mol^{-1} \cdot s^{-1}$)
$k_{com,ben}$	rate constant for combination of CoBF and a benzylic radical ($L \cdot mol^{-1} \cdot s^{-1}$)
$k_{com,overall}$	overall combination rate constant ($L \cdot mol^{-1} \cdot s^{-1}$)
k_d	initiator decomposition rate constant (s^{-1})
$k_{d,BPO}$	decomposition rate constant of BPO (s^{-1})
k_{dec}	rate constant for spontaneous decomposition of CoBF (s^{-1})
k_{decH}	rate constant for acid induced decomposition of CoBF (s^{-1})
k_{decH}'	rate constant for decomposition of CoBF-H$^+$ (s^{-1})
k_{dis}	dissociation rate constant (s^{-1})
$k_{dis,ben}$	rate constant for dissociation of benzyl – Co(III) complex (s^{-1})
$k_{dis,overall}$	overall dissociation rate constant (s^{-1})
K_H	equilibrium constant for the protonation of CoBF by HAc (-)
k_i	initiation rate constant ($L \cdot mol^{-1} \cdot s^{-1}$)
$k_{i,B}$	rate constant for initiation of MMA by benzoyloxy radicals ($L \cdot mol^{-1} \cdot s^{-1}$)
$k_{i,ben}$	rate constant for initiation of MMA by benzylic radicals ($L \cdot mol^{-1} \cdot s^{-1}$)
k_{in}	inhibition rate constant ($L \cdot mol^{-1} \cdot s^{-1}$)
k_{macro}	rate constant for reinitiation of macromer ($L \cdot mol^{-1} \cdot s^{-1}$)
$K_{monomer}$	Mark-Houwink constant for a specific monomer ($dL \cdot g^{-1}$)
$K_{overall}$	overall equilibrium constant for combination – dissociation ($L \cdot mol^{-1}$)
k_p	propagation rate constant ($L \cdot mol^{-1} \cdot s^{-1}$)
$k_{p,graft}$	rate constant for propagation of a polymeric radical – macromer adduct ($L \cdot mol^{-1} \cdot s^{-1}$)
$<k_p>$	average propagation rate constant for copolymerization ($L \cdot mol^{-1} \cdot s^{-1}$)
k_{rein}	reinitiation rate constant ($L \cdot mol^{-1} \cdot s^{-1}$)
$k_{rein,monomer}$	rate constant for reinitiation of a specific monomer ($L \cdot mol^{-1} \cdot s^{-1}$)
k_t	termination rate constant ($L \cdot mol^{-1} \cdot s^{-1}$)
$<k_t>$	average termination rate constant ($L \cdot mol^{-1} \cdot s^{-1}$)
$k_{t,ben}$	rate constant for termination involving a benzylic radical ($L \cdot mol^{-1} \cdot s^{-1}$)
$k_{t,monomer}$	termination rate constant for a specific monomer ($L \cdot mol^{-1} \cdot s^{-1}$)
k_{tc}	termination rate constant for combination ($L \cdot mol^{-1} \cdot s^{-1}$)
k_{tc1}	termination rate constant for combination involving at least one radical of chain length 1 ($L \cdot mol^{-1} \cdot s^{-1}$)

k_{td}	termination rate constant for disproportionation (L· mol^{-1}· s^{-1})
k_{td1}	termination rate constant for disproportionation involving at least one radical of chain length 1 (L· mol^{-1}· s^{-1})
k_{tr}	bimolecular chain transfer rate constant (L· mol^{-1}· s^{-1})
k_{tr}	unimolecular chain transfer rate constant (when diffusion is taken into account in the reaction mechanism) (s^{-1})
$<k_{tr}>$	average chain transfer rate constant for copolymerization (L· mol^{-1}· s^{-1})
$k_{tr,BPO}$	rate constant for chain transfer to benzoyl peroxide (L· mol^{-1}· s^{-1})
$k_{tr,overall}$	overall chain transfer rate coefficient (L· mol^{-1}· s^{-1})
$k_{tr,tol}$	chain transfer rate constant to toluene (L· mol^{-1}· s^{-1})
$M_{i,\Delta t}$	molecular weight of chain with length i formed in time period Δt (g· mol^{-1})
M_n	number average molecular weight (g· mol^{-1})
m_o	initial amount of monomer (g)
M_o	molar mass of 1 monomer unit (g· mol^{-1})
M_{peak}	molecular weight at the top of the MWD (g· mol^{-1})
M_w	weight average molecular weight (g· mol^{-1})
$M_{w,\Delta t}$	weight average molecular weight of polymer formed in time period Δt (g· mol^{-1})
$M_{w,cum}$	cumulative weight average molecular weight (g· mol^{-1})
$M_{w,in}$	instantaneous weight average molecular weight (g· mol^{-1})
N_A	Avogadro number (mol^{-1})
p	statistical spin factor (-)
$P(M)$	number molecular weight distribution (-)
P_n	number average chain-length (-)
P_{n0}	number average chain-length in a polymerization without chain transfer agent (-)
$r_{monomer}$	radical reactivity ratio (-)
R_p	rate of propagation (mol· L^{-1}· s^{-1})
R_{tr}	rate of transfer (mol· L^{-1}· s^{-1})
$s_{monomer}$	monomer reactivity ratio (-)
T	absolute temperature (K)
t_o	inhibition time (s)
V_1	volume available to 1 catalyst molecule (m^3)
$W_{i,\Delta t}$	mass of polymer chains of chain-length i formed in time period Δt (g)
X	conversion (-)

168

Greek symbol	Description
α	coefficient for chain-length dependence of $<k_t>$ (-)
Δt	time period (s)
η	dynamic viscosity (Pa· s)
η_{sol}	dynamic viscosity of a solution (Pa· s)
η_{bulk}	dynamic viscosity of bulk monomer (Pa· s)
Φ_{MMA}	molar fraction of MMA ended radicals (-)
κ	cobalt – carbon bond formation equilibrium parameter ($L^{1/2}$· $mol^{1/2}$)
λ	diffusion control parameter (-)
σ_r	radius of solute (m)
χ	ratio of k_1 and k_{-1} (L· mol^{-1})

Abbreviation	Meaning
Ac^-	acetate anion
ACHN	1,1'-azobis(cyclohexanenitrile)
ACVA	4,4'-azobis(4-cyanovaleric acid)
AIBMe	2,2'-azobis(methylisobutyrate)
AIBN	2,2'-azobis(isobutyronitrile)
ATRP	atom transfer radical polymerization
B·	benzoyloxy radical
BA	*n*-butyl acrylate
BMA	*n*-butyl methacrylate
BPO	benzoyl peroxide
BuAc	*n*-butyl acetate
CCT	catalytic chain transfer
CLD	chain-length distribution
CMC	critical micelle concentration
$Co(Et)_4BF$	tetraethyl cobaloxime boron fluoride
Co(II)	cobalt(II) species
[Co(III)]-H	cobalt(III) hydride

[Co(III)]-P_n	cobalt end capped polymer
Co(III)-R	organocobalt(III) complex
Co(Ph)$_4$BF	tetraphenyl cobaloxime boron fluoride
CoBF	cobaloxime boron fluoride
CoBF-H$^+$	protonated CoBF
D_n	dead polymer of chain length n
2-EHMA	2-ethylhexyl methacrylate
ESR	electron spin resonance
HAc	acetic acid
I	initiator
M	monomer
MA	methyl acrylate
MALDI-TOF	matrix assisted laser desorption ionization - time of flight
MMA	methyl methacrylate
MWD	molecular weight distribution
NMP	nitroxide mediated polymerization
P·	polymeric radical
P_1·	polymeric radical of chain-length one
PMMA	polymethyl methacrylate
P_n·	polymeric radical of chain-length n
[P_n· Co(II)]	diffusion encounter pair of a polymeric radical and Co(II) complex
PSD	particle size distribution
RAFT	reversible addition fragmentation chain transfer
SDS	sodium dodecyl sulfate
SEC	size exclusion chromatography
THF	tetrahydofuran
Tol	toluene

170

Summary

In the past two decades there has been a tremendous growth of interest in research aimed at controlling polymer microstructure in free-radical polymerization. One of the newly developed techniques is catalytic chain transfer (CCT). In CCT only a ppm amount of catalyst is required to reduce polymer molecular weight by orders of magnitude, resulting in macromonomers with a vinyl end-group.

So far, investigations on CCT have been limited to polymerizations of methacrylates, styrene and α-methyl styrene. The investigations in this thesis were aimed at acquiring sufficient mechanistic knowledge to be able to produce macromonomers consisting of CCT active and CCT inactive monomers in both homogeneous and heterogeneous systems. In order to be able to understand and control these copolymerizations, it is necessary to obtain a good understanding of the homopolymerizations first.

Initially, previous studies have been reviewed and the results of these studies have been compared to Predici computer simulations. It has been shown that chain-length dependent termination can account for a decrease in polymerization rate with increasing catalyst concentration. Curvature of the Mayo-plot at high catalyst concentrations has been shown to be due to transfer of monomeric radicals resulting in reformation of monomer.

The CCT homopolymerization of MMA in presence of CoBF has been chosen as a model system to study the mechanism of CCT and the effects of reaction components on the catalyst. It has been demonstrated that the presence of oxygen or impurities in either solvent or initiator can have a strong effect on catalyst activity. Thorough purification of all reactants has revealed the absence of solvent effects in CCT polymerizations of MMA. Both calculations and experimental results have indicated the absence of diffusion control, which is in contrast to results reported by other authors. In addition, no effect of cobalt – carbon bond formation on the CCT polymerization of MMA has been observed.

In CCT polymerizations of MMA up to full conversion, catalyst deactivation has been shown to be the most likely explanation for differences in experimentally determined and theoretically predicted molecular weights. This deactivation occurred in spite of thorough solvent purification. It has been demonstrated that deactivation is enhanced when benzoyl peroxide or acetic acid are added to the polymerization system. The rate of deactivation has

been described by taking into account benzoyloxy radical – CoBF combination and decomposition of protonated CoBF, respectively.

Next, CCT polymerizations of monomers that lack an α-methyl group, from which CoBF can abstract hydrogen, have been studied. For both styrene and acrylates it has been demonstrated that the polymeric radicals form covalent bonds to the cobalt catalyst. For polystyryl radicals this cobalt – carbon bond is rather weak, which is reflected in a dependence of the chain transfer coefficient on the presence of light, the wavelength of that light and on initiator concentration. This dependence has not been demonstrated before. For acrylate radicals on the other hand, cobalt – carbon bonds are stronger, resulting in nearly complete catalyst consumption. However, it has been shown that before all CoBF is consumed, it does take part in chain transfer reactions. The corresponding chain transfer constant nearly equals the chain transfer constant of its methacrylate analogue. Therefore, it has been argued that the α-methyl group only prevents cobalt – carbon bond formation and does not facilitate hydrogen abstraction.

After this knowledge on the homopolymerizations of MMA and of acrylates had been gathered, it was demonstrated that CCT is a very effective way of controlling molecular weight in copolymerizations of methacrylates and acrylates as well. A model to predict the chain transfer coefficients has been developed that incorporates chain transfer from MMA ended polymeric radicals and cobalt – carbon bond formation for acrylate ended radicals. The chain transfer coefficient can be described as a function of monomer composition and radical concentration. The model also includes the reactivity ratios for both monomers. It has been shown that the reactivity ratios are not influenced by the presence of CoBF. At higher conversions, copolymeric macromonomers formed at lower conversions are incorporated in growing polymer chains. However, the final molecular weight reduction is still considerable compared with polymerizations without catalyst.

Next, the application of CCT in emulsion polymerization has been studied. A different, less water soluble catalyst, $Co(Et)_4BF$, has appeared to display more efficient CCT in emulsion polymerization than CoBF. $Co(Et)_4BF$ has been applied in the miniemulsion polymerization of MMA and of MMA – BA as well. It has been shown that the overall activity in miniemulsion polymerization is higher than in emulsion polymerization. So, it has been

demonstrated to be possible to obtain efficient CCT in methacrylate – acrylate copolymerizations in a heterogeneous system as well.

Finally, the overall results have been evaluated and promising directions for future research have been indicated.

Samenvatting

Het onderzoek aan de controle van de microstructuur van met behulp van vrije radicaal polymerisatie gemaakte polymeren, heeft de afgelopen twintig jaar volop in de belangstelling gestaan. Een van de nieuw ontwikkelde technieken is katalytische ketenoverdracht (KKO). In KKO is slechts ongeveer 1 ppm katalysator nodig om het molecuulgewicht van het polymeer een paar ordes van grootte te reduceren, waarbij macromonomeren met een vinyl eindgroep gevormd worden.

Tot nu toe heeft het onderzoek naar KKO zich vooral gericht op polymerisaties van methacrylaten, styreen en α-methylstyreen. Het doel van het onderzoek beschreven in dit proefschrift was om voldoende mechanistische kennis over KKO te vergaren om uiteindelijk macromonomeren, die bestaan uit monomeren die wel en monomeren die geen KKO ondergaan, te kunnen produceren in zowel homogene als heterogene systemen. Teneinde deze copolymerisatie te begrijpen en te kunnen controleren, is het noodzakelijk allereerst een goed begrip van de homopolymerisaties te ontwikkelen.

In eerste instantie zijn de resultaten van eerder onderzoek bestudeerd en vergeleken met Predici computer simulaties. Hiermee is duidelijk geworden dat ketenlengte-afhankelijke terminatie een verklaring vormt voor het feit dat de polymerisatiesnelheid afneemt bij toenemende katalysatorconcentratie. Het feit dat de helling van een Mayo grafiek afneemt bij hoge katalysatorconcentraties wordt veroorzaakt doordat monomere radicalen KKO ondergaan, waarbij monomeer wordt teruggevormd.

De KKO-polymerisatie van MMA in aanwezigheid van CoBF is gekozen als modelsysteem om het mechanisme en de effecten van de verschillende componenten in het reactiemengsel op de katalysator te kunnen bestuderen. Er is aangetoond dat de aanwezigheid van zuurstof, dan wel van verontreinigingen in oplosmiddel of initiator een sterke daling van de activiteit van de katalysator tot gevolg kunnen hebben. Na gedegen zuivering is gebleken, dat er geen oplosmiddeleffecten in KKO-polymerisaties van MMA optreden. Zowel berekeningen als experimentele resultaten wijzen op de afwezigheid van diffusielimitering, dit in tegenstelling tot resultaten van andere auteurs. Bovendien zijn er geen effecten van de vorming van kobalt – koolstof bindingen op de KKO-polymerisatie van MMA waargenomen.

In KKO-polymerisaties van MMA tot volledige conversie is gebleken dat deactivering van de katalysator de meest waarschijnlijke verklaring is voor het verschil tussen experimenteel bepaalde en theoretisch voorspelde molecuulgewichten. Deze deactivering vindt plaats ondanks de grondige zuivering van het oplosmiddel. Er is verder aangetoond dat deactivering versterkt wordt in aanwezigheid van benzoyl peroxide en azijnzuur. De deactiveringssnelheid kan in het eerste geval beschreven worden met een combinatie van benzoyloxy radicalen en CoBF en in het tweede geval met decompositie van geprotoneerd CoBF.

Vervolgens zijn polymerisaties bestudeerd van monomeren, die geen α-methyl groep bezitten waarvan CoBF een waterstof kan abstraheren. Voor zowel styreen als acrylaten is vastgesteld, dat de polymere radicalen covalente bindingen vormen met de kobaltkatalysator. In het geval van polystyreenradicalen is deze binding vrij zwak, hetgeen blijkt uit een afhankelijkheid van de ketenoverdrachtscoëfficiënt van de aanwezigheid van licht, de golflengte van dit licht en de initiatorconcentratie. Deze afhankelijkheid is niet eerder aangetoond. In het geval van polyacrylaatradicalen is deze binding dusdanig sterk dat bijna alle katalysatormoleculen aan polyacrylaatradicalen gebonden worden. Er is echter gebleken dat, voordat alle CoBF moleculen aan radicalen gebonden zijn, CoBF ook ketenoverdracht katalyseert. Zeer verrassend is dat de bijbehorende ketenoverdrachtsconstante zo goed als gelijk is aan de ketenoverdrachtsconstante van het corresponderende methacrylaat. Hieruit is dan ook geconcludeerd dat de α-methyl groep slechts de vorming van kobalt − koolstof bindingen verhindert en dat zij niet de abstractie van waterstof vergemakkelijkt.

Nadat deze kennis met betrekking tot de KKO-homopolymerisaties van methacrylaten en acrylaten was opgedaan, is aangetoond dat ook in copolymerisaties van beide typen monomeren, KKO een zeer efficiënte wijze is om het molecuulgewicht te controleren. Er is een model ontwikkeld om de ketenoverdrachtsconstanten te kunnen berekenen als functie van de monomere samenstelling en van de radicaalconcentratie. Dit model omvat ketenoverdracht van radicalen met een methacrylaateindgroep en de vorming van kobalt − koolstof bindingen voor radicalen met een acrylaateindgroep. De copolymere reactiviteitsverhoudingen zijn in het model opgenomen. Er is gebleken dat deze reactiviteitsverhoudingen niet beïnvloed worden door de aanwezigheid van CoBF. Bij hogere monomeerconversies worden de macromonomeren die bij lagere conversie zijn gevormd, ingebouwd in de groeiende

176

polymeerketens. De reductie in molecuulgewicht ten opzichte van polymerisatie zonder KKO-katalysator is echter nog steeds aanzienlijk.

Vervolgens is de toepassing van KKO in emulsiepolymerisatie bestudeerd. Er is gebleken dat een andere, minder wateroplosbare, katalysator, Co(Et)$_4$BF, een hogere activiteit in emulsie vertoont dan CoBF. Co(Et)$_4$BF is ook toegepast in de KKO-mini-emulsiepolymerisatie van MMA en van MMA – BA. Dit bevestigde dat de totale activiteit in mini-emulsiepolymerisatie hoger ligt dan in emulsiepolymerisatie. Hiermee is aangetoond dat het mogelijk is om op effectieve wijze KKO-copolymerisaties van methacrylaten en acrylaten ook in heterogene systemen uit te voeren.

Tenslotte zijn de resultaten geëvalueerd en veelbelovende richtingen voor toekomstig onderzoek aangegeven.

steeds bereid zijn om van alles en nog wat uit te lenen, Wouter voor het maken van tijd om binnen en buiten de TUE mee te helpen, Jos voor de viscositeitsmetingen en Henk Eding voor de elementanalyses. Helly en Caroline wil ik bedanken voor hun hulp en goede raad. Mijn kamergenoten Camiel, Martine, Adil, Greg, Michel en Davy en al mijn andere SPC-collega's, ook de al eerder genoemde, voor de goede sfeer binnen en buiten de TUE en de onderlinge steun. In short, thanks. I really enjoyed working with you.

Zonder anderen te kort te doen, wil ik met name Margreta, Jeroen, Hilde en Raymond (2×) bedanken voor hun vriendschap, het lekkere eten en de vele hulp bij van alles en nog wat. Raymond, bedankt dat je `s nachts in de vrieskou mee wilde helpen om de foto voor de omslag te maken. Agnieszka, bedankt voor de vele gesprekken over de leuke en minder leuke kanten van promoveren en het leven in het algemeen. Het heeft mij vaak weer goede moed gegeven. Ik ben er trots op dat je mijn paranimf wil zijn. Mijn familie en vrienden wil ik bedanken voor hun interesse, steun en verhelderende inzichten over het dagelijks leven op de TUE.

Tenslotte wil ik Sandra bedanken. Sandra, bedankt voor je bedrijfskundige, taalkundige en scheikundige inbreng, het maken van de tekeningen in mijn proefschrift, de positieve kritiek op mijn presentaties, het mij doen nadenken en je vele geduld. Ik houd van je, nu en in de toekomst. Als jij promoveert, wil ik met liefde aan jouw zijde staan.

Bedankt,

Bas

Curriculum Vitae

Bas Pierik was born on 11 September 1973 in Spaubeek, The Netherlands. In 1991, he completed his secondary education at Scholengemeenschap Sint Michiel in Geleen. Shortly after, he moved to Eindhoven to study Chemical Engineering at Eindhoven University of Technology. In January 1997 he graduated with distinction. A few days later he accepted a temporary job as a lecturer in a College for Laboratory Education in Etten-Leur. He enjoyed lecturing a lot. In August of the same year he started a Ph.D. project with prof.dr.ir. A.L. German and (at that time) dr. A.M. van Herk in the Polymer Chemistry group at Eindhoven University of Technology. In March 2002 he will start working as a Research Associate at Eindhoven University of Technology. Research topics include science education and emulsion polymerization.

STELLINGEN

behorende bij het proefschrift

Shining a Light on Catalytic Chain Transfer

van

Sebastianus Christoffel Josephus Pierik

1. De vaak waargenomen afname van de ketenoverdrachtscoëfficiënt in niet-coördinerende oplosmiddelen in een katalytische ketenoverdrachtspolymerisatie is niet het gevolg van een oplosmiddeleffect, maar hoogstens van een effect van verontreinigingen in het oplosmiddel.

    Hoofdstuk 3 van dit proefschrift

2. De ketenoverdrachtsstap in katalytische ketenoverdracht is niet diffusiegecontroleerd.

    Hoofdstuk 3 van dit proefschrift

3. De afwezigheid van een α-methyl groep in styreen en acrylaten heeft geen effect op de daadwerkelijke chemie van de transferstap. De α-methyl groep voorkomt slechts dat er kobalt – koolstof bindingen gevormd worden.

    Hoofdstuk 5 van dit proefschrift

4. Voor een effectieve katalytische ketenoverdrachtspolymerisatie van styreen is (UV)-licht noodzakelijk.

    Hoofdstuk 5 van dit proefschrift

5. Combinatie van katalytische ketenoverdrachtspolymerisatie en on-line processturing biedt goede mogelijkheden om tot daadwerkelijke controle over de copolymere microstructuur te komen.

    Hoofdstuk 8 van dit proefschrift

6. Om het niveau van het universitair onderwijs op peil te houden, is regelmatige bijscholing op onderwijsgebied van alle wetenschappelijk medewerkers van groot belang.

7. Het idee dat voor de maatschappij belangrijke publieke organisaties betere kwaliteit zouden leveren onder het juk van de markt dan onder directe verantwoordelijkheid van de overheid, zou niet noodzakelijkerwijs tot privatisering van die organisaties moeten leiden, maar wel tot een grondige reflectie over het functioneren van die overheid.

8. Na een jarenlang focus op *shareholdervalue* is er binnen de top van het bedrijfsleven gelukkig ook weer aandacht voor de werknemer, wat blijkt uit het feit dat ABN-AMRO topman Groenink, na 6000 arbeidsplaatsen geschrapt te hebben, toegeeft persoonlijk moeite te hebben met het inkrimpen van de Raad van Bestuur.

    de Volkskrant, 17 augustus 2001

9. Het door de overheid in de campagne "Huren, dat kan natuurlijk ook!" geschetste idyllische beeld van de huurwoning staat haaks op de praktijk van lange wachttijden, huurverhogingen, dunne muren en te korte schroeven.

    Persoonlijke ervaringen

10. Het geheugen van de meeste politici over het functioneren van overheidsinstanties wordt gewist op het moment van privatiseren van deze instanties.

11. Bij toenemende welvaart, gedefinieerd als het bruto nationaal product, gaat het welzijn door een maximum. Aangezien dit punt in het Westen veelal gepasseerd is, zal een betere verdeling van welvaart over de hele wereld dan ook tot een algehele stijging van het welzijn leiden.

12. Er is geen weg naar vrede, vrede is de weg.

    Gandhi

13. Het verhogen van de drempels om voor een WAO-uitkering in aanmerking te komen, waardoor veel aanvragers op een WW- of bijstandsuitkering terug zullen moeten vallen, lost het werkelijke WAO-probleem niet op en is klassiek voorbeeld van symptoombestrijding.

14. Het feit dat de VVD, om de lage inkomens te ontzien, pleit voor het behoud van de hypotheekrenteaftrek, terwijl GroenLinks streeft naar de afschaffing hiervan, zou mij bijna doen geloven dat vele Nederlanders jarenlang op de verkeerde partij gestemd hebben.

15. Gezien de recente ontwikkelingen in onderwijsland, ligt het in de lijn der verwachtingen dat de Onderwijsraad binnen tien jaar voorstelt om naast Science ook Dutch verplicht te stellen voor het middelbaar onderwijs.

de Volkskrant, 17 oktober 2001